MC 70 - 3001 - R2 (BNY)

FINAL REPORT

THE AERODYNAMIC CHARACTERISTICS OF LARGE ANGLED CONES WITH RETROROCKETS

Contract No. NAS 7 - 576

By
Philip O. Jarvinen
Richard H. Adams

Prepared For

NATIONAL AERONAUTICS AND SPACE ADMINISTRATION
Liquid Rocket Research and Technology Code RPL
Washington, D.C.

FEBRUARY 1970

Prepared By
MITHRAS
A DIVISION OF SANDERS ASSOCIATES, INC.
701 Concord Ave. , Cambridge, Mass. 02138

*T.M. Sanders Associates, Inc.

MC 70 - 3001 - R2 (BNY)

FINAL REPORT

THE AERODYNAMIC CHARACTERISTICS OF LARGE ANGLED CONES WITH RETROROCKETS

Contract No. NAS 7 - 576

By
Philip O. Jarvinen
Richard H. Adams

Prepared For

NATIONAL AERONAUTICS AND SPACE ADMINISTRATION
Liquid Rocket Research and Technology Code RPL
Washington, D.C.

FEBRUARY 1970

Prepared By

MITHRAS
A DIVISION OF SANDERS ASSOCIATES, INC.
701 Concord Ave., Cambridge, Mass. 02138

*T.M. Sanders Associates, Inc.

FOREWORD

This report was prepared by MITHRAS, a division of sanders associates inc., for the National Aeronautics and Space Administration, Liquid Rocket Research and Technology Branch, Washington, D. C. Mr. Hartwell Long of the Jet Propulsion Laboratory, California Institute of Technology was the Technical Manager.

The investigations whose results are reported here represent the work accomplished during Phase II of Contract NAS 7-576 during the period 1 June 1968 to 1 February 1970. Phase I of this contract was completed on 1 June 1968 and is documented in the report entitled "Propulsive Re-Entry Aerodynamics"[1] by P. O. Jarvinen, R. W. Luce and E. Wachsler. Analytical methods were developed during Phase I to predict the flow field in the immediate vicinity of a planetary entry system composed of an aeroshell with a single retrorocket which exhausts into a subsonic or supersonic counter-flowing planetary atmosphere. In Phase II, a digital computer program was developed for the analytical solutions, and an experimental wind tunnel test program was conducted to explore, in a general manner, single and multiple retrorocket-free stream interactions and to obtain, in particular, experimental results to test the analytical model developed in Phase I.

The research reported here was performed in the Aeroscience Department of MITHRAS under the direction of the department manager, Mr. J. A. F. Hill. Mr. P. O. Jarvinen was project engineer and wrote the final report. The authors would like to acknowledge the valuable suggestions and comments made by J. A.F. Hill, Head of the AeroSciences Department of MITHRAS, during the planning and performance of this work. The authors would like to thank Mr. J. Wilson for designing the wind tunnel models, Dr. H. Dyner for implementing the theoretical analysis for the computer and Mr. E. Wachsler for generating the computer program.

The experimental wind tunnel test program was performed in the NASA Ames 6' x 6' supersonic wind tunnel which was operated by ARO Inc. personnel. We would like especially to acknowledge the assistance of Mr. T. Barrington, the ARO project engineer, during the test program.

ABSTRACT

Analytical and experimental phases of the subject investigation are described. The analytical program for the single jet determines the terminal shock location, the jet boundary, the interface profile, the bow shock profile, the shear layer growth and the dead air region pressure. The experimental program described was conducted over the range of $M_\infty = 0.4$ to $M_\infty = 2.0$ at angles-of-attack up to 18^o and at thrusting coefficients up to $C_T = T/q_\infty A_m = 30$. Variables investigated included aeroshell angle, number of nozzles, engine thrust, size of nozzles, nozzle throttling and gas composition. The influence of these variables on the aeroshell stability, drag, and loads was determined by integrating pressure measurements on the aeroshell. The total system forces consist of components due to pure thrust and components due to pressures on the aeroshell arising from the jet-free stream interaction. Shadowgraphs provided flow field geometries which proved to be within 10% of those predicted analytically.

TABLE OF CONTENTS

TABLE OF CONTENTS (CONTINUED)

NOMENCLATURE

SYMBOL	DESCRIPTION	PAGE
A^*	Nozzle throat area	7
A_{e_j}, A_e	Nozzle exit area	4
A_B, A_m	Aeroshell base area and model base area respectively	ii
C_{A_F}	Forebody axial force coefficient = $X/q_\infty A_m$	68
$C_{A_{total}}$	Sum of forebody axial force coefficient and engine thrusting coefficient, $C_{A_{total}} = C_{A_F} + C_T$	81
C_D	Drag coefficient	28
C_m	Pitching moment coefficient, $M/q_\infty A_m d_m$	59
$dC_m/d\alpha$	Pitching moment slope-per degree	59
C_{M_f}	Pitching moment due to pressure forces	123
C_{M_E}	Pitching moment due to unbalanced thrust	123
ΔC_M	Change in pitching moment coefficient	123
C_n	Yawing moment coefficient	109
C_N	Normal force coefficient = $Y/q_\infty A_m$	60
$dC_N/d\alpha$	Normal force slope ~ per degree	60

C_P	Pressure coefficient, $P-P_\infty / q_\infty$	40
$C_{P_{BASE}}$, C_{P_B}	Base pressure coefficient	47
$(C_{P_{FRONT}})_{Average}$	Average forebody pressure coefficient	45
C_T	Thrusting coefficient, $T/q_\infty A_m$	ii
C_Y	Side force coefficient	110
d*	Nozzle throat diameter	5
d_m	Model base diameter	5
M	Pitching moment (about apparent cone vertex, positive nose up)	10
M_{e_j}, M_e	Nozzle exit Mach number	5
M_∞	Free stream Mach number	ii
P_{e_j}, P_e	Nozzle exit pressure	4
P_d	Dead air region pressure	6
P_f	Pressure on front surface of aeroshell	
P_∞	Free stream static pressure	4
q_∞	Free stream dynamic pressure	ii
r	Radial distance from model centerline	14
r_b	Aeroshell base radius	28
r_c	Model shoulder radius	25
r_e	Radial distance to multiple engine circle	18
r_{e_j}	Nozzle exit plane radius	144

r_m	Model base radius	14
r_n	Model nose radius	15
T	Engine thrust	ii
x	Longitudinal distance along model centerline measured from model base	33
x_{ac}/d_m	Longitudinal location of aerodynamic center measured rearward from aeroshell virtual nose, in model base diameters	61
α	Angle-of-attack, positive up	21
γ_e	Nozzle specific heat ratio	4
γ_∞	Free stream specific heat ratio	4
ν	Flow direction at nozzle exit plane	6
ϕ	Sting roll angle, positive "left wing" down	14

Subscripts

E1, E2, E3	Engines one, two and three respectively	71
$( )_{eff}$	Equivalent single nozzle value	5
TOTAL	Sum of individual engine contributions	71

LIST OF FIGURES

LIST OF FIGURES (CONTINUED)

LIST OF FIGURES (CONTINUED)

LIST OF FIGURES (CONTINUED)

LIST OF FIGURES (CONTINUED)

LIST OF FIGURES (CONTINUED)

LIST OF FIGURES (CONTINUED)

LIST OF TABLES

1. INTRODUCTION AND SUMMARY

Intense interest has been generated recently in various techniques for the aerodynamic and propulsive deceleration of planetary lander vehicles. One of the more promising systems that has been proposed consists of a large-angled conical aeroshell augmented with a retrorocket(s). This system operates in supersonic, transonic and subsonic flight regimes during landing and has a retrorocket(s) which furnishes high thrusting coefficients (i.e., $C_T > 1.0$ at $M_\infty = 2.0$, increasing to $C_T > 40$ at $M_\infty = 0.3$) for deceleration and operates in the presence of a large angle conical aeroshell shape.

The advancement of such a system, however, has been stymied due to the lack of an adequate definition of the interaction of the retrorocket exhaust(s) with the counterflowing atmosphere and the subsequent effects on the aerodynamic characteristics of the aeroshell. Specifically the effects of aeroshell angle, number of nozzles, engine thrust, size of nozzles, nozzle throttling and exhaust gas composition on the aerodynamic loads, stability and drag are required.

To define this interaction, NASA Office of Advanced Research and Technology sponsored an analytical and experimental investigation of the flow field about aeroshell-retrorocket systems in a counterflowing atmosphere. Analytical methods[1] were developed during the first year to predict the flow field in the immediate vicinity of an aeroshell with a single retrorocket exhausting into an oncoming supersonic flow. In the second year a digital computer program was developed for the analytical solution and a general experimental investigation of the interaction was undertaken which recovered both subsonic and supersonic free stream conditions. Comparisons were made between experimental and analytical results. These results provide a basis for understanding the flow field about planetary lander vehicles with retrorocket systems.

In this report, the results of an exploratory experimental wind tunnel test program, performed in the NASA Ames 6' x 6' supersonic wind tunnel, are described. This test program has provided, for the first time, many of the

answers necessary to determine the effects of various retrorocket configurations on the system stability and drag. In addition, a comparison is made between the theoretical predictions of Reference 1 and the experimental results for the locations of the jet terminal shock, jet boundary, interface and bow shock wave in the flow field of a single centrally mounted engine.

The existing literature on the effects of retrorockets projected upstream from the nose of bodies in supersonic flows is considerable, dating back at least 15 years. However, not all previous work has been dedicated to the use of forward facing jets for deceleration and the bulk of the material published is limited to supersonic free stream Mach numbers, single jets centrally mounted, low thrusting coefficients ($C_T < 0.5$) and to flow exhausting from tubes or flat faced cylindrical bodies. A review of previous work is contained in Reference 1.

Only a limited amount of experimental data is available on multiple engine-aeroshell combinations. Keyes and Hefner[2] tested a three jet configuration on a sixty degree half angle cone and a flat faced model at thrusting coefficients up to $C_T = 1.2$ and a free stream Mach number of six, $M_\infty = 6.0$. Peterson and McKenzie[3] made experimental measurements of the forces and moments on a semi-ellipsoid body shape which had four simulated retrorockets on the forward flat face which operated countercurrent to subsonic and supersonic airstreams. Experiments were performed at free stream Mach numbers ranging from 0.25 to 1.90 and total thrusting coefficients up to 10.

The present experiments were performed over a free stream Mach number range from $M_\infty = 0.4$ to $M_\infty = 2.0$. The wind tunnel models consisted of a single jet 45° aeroshell pressure model and single and three jet 60° aeroshell pressure models (Figure 1) and air and helium were used to simulate the exhaust gas. Three air nozzle sizes and one helium nozzle size were tested in conjunction with the single engine aeroshell models. A single air nozzle size and a single helium nozzle size were tested on the three engine aeroshell. The three engine, 60° aeroshell-air nozzle combination as well as one of the single air nozzle- 45° and 60° aeroshell combinations simulated a representative Mars lander vehicle. A brief summary of the experimental results were published previously in Reference 15. A theory for jets exhausting counter to subsonic free streams may be found in Reference 16.

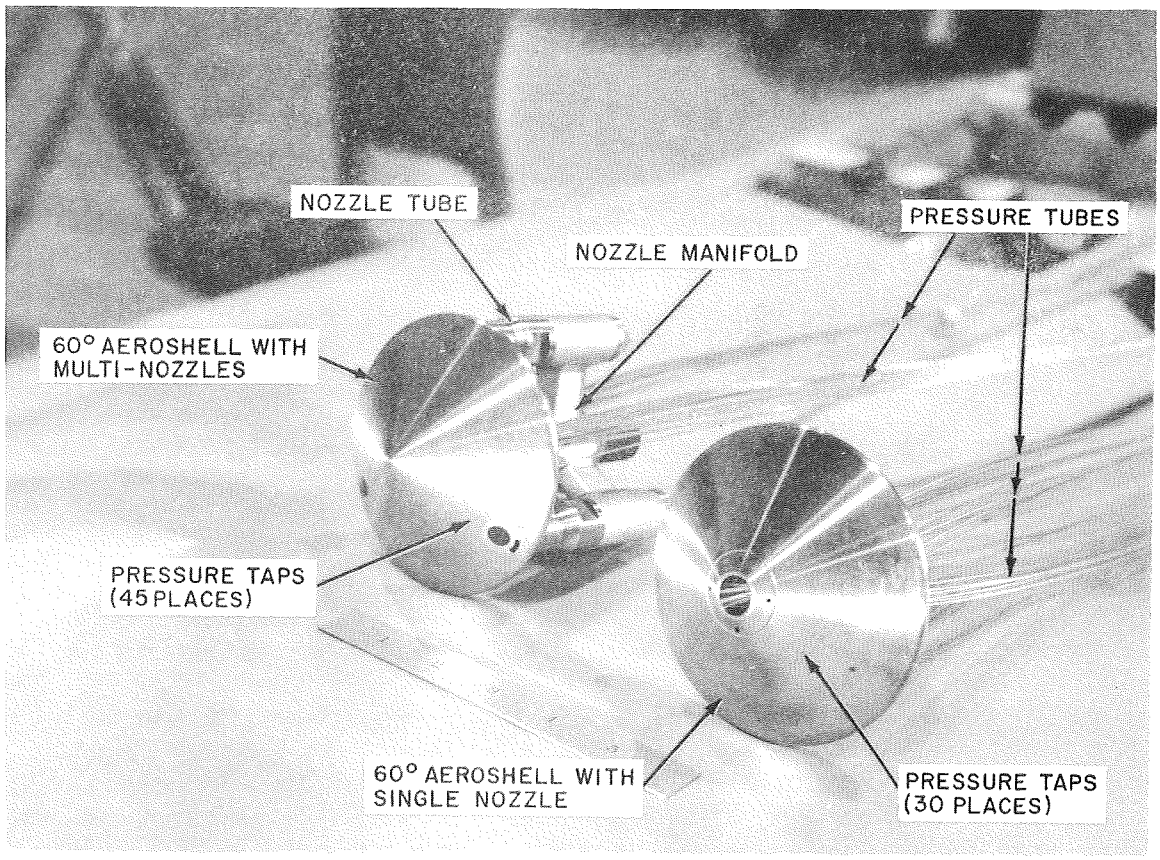

Figure 1 60° Aeroshell Wind Tunnel Models.

2. EXPERIMENTAL METHOD

2.1 Scaling Parameters

One of the considerations in the wind tunnel test program was to simulate the retrorocket-free stream interaction of representative Mars lander vehicle (Table 1, p. 5) using different fluids for the retrorocket exhaust and atmosphere in the simulation. It has been shown before[4,5] that proper simulation of the exhaust flow may be accomplished if the nozzle exit to ambient pressure ratio, P_{e_j} / P_d, as well as the pressure sensitivity of the exhaust flow with respect to flow direction $P^{-1} \frac{dP}{d\nu}$ are matched. In the present investigation total simulation is accomplished by matching the engine scaling parameter, free stream Mach number, thrusting coefficient and plume sensitivity parameter.

The primary parameter which characterizes the interaction of a retrojet with a countercurrent stream is the thrusting coefficient

$$C_T = \frac{T}{q_\infty A_B} = \frac{2T}{\gamma_\infty M_\infty^2 P_\infty A_B} \tag{1}$$

The thrust, T, may be written as

$$T = P_e A_e (1+ \gamma_e M_e^2) \tag{2}$$

therefore,

$$C_T = \frac{2}{\gamma_\infty M_\infty^2} \cdot \frac{Pe}{P_\infty} \frac{Ae}{A_B} (1 + \gamma_e M_e^2) \tag{3}$$

TABLE I. NOZZLE DESIGN PARAMETERS

Nozzle	γ_∞	Jet Fluid	γ_e	A_e/A^*	M_e	$\left(\frac{d^*}{d_m}\right)_{eff}$	Nozzle Scaling Parameter
Mars Lander	1.304	Combustion products	1.28	40	4.73	0.0182	1.664
Air Nozzle 1	1.4	Air	1.4	13.95	4.3	0.0236	3.328
Air Nozzle 2	1.4	Air	1.4	13.95	4.3	0.0334	1.664
Air Nozzle 3	1.4	Air	1.4	13.95	4.3	0.0472	0.832
Helium	1.4	Helium	1.67	3.41	3.2	0.0825	1.664

It also follows that the flow geometry will depend on the ratio of the nozzle exit pressure to the local dead air region pressure, P_e/P_d, since this parameter controls the expansion of the exhaust gases and the location of the jet boundary. Since $P_d \propto P_\infty$, the expansion of the jet gases and location of the jet boundary will be simulated if the ratio of P_e/P_∞ is matched. From equation (3) we see that P_e/P_∞ varies lineraly with $M_\infty^2 C_T$ for a given nozzle configuration.

Rewriting equation (3) in the form

$$\frac{P_e}{M_\infty^2 P_\infty C_T} = \frac{\gamma_\infty A_B}{2A_e (1 + \gamma_e M_e^2)} \tag{4}$$

we see that the right hand of the above expression is only dependent on the nozzle paramters and γ_∞. This will be termed the engine scaling parameter.

Finally, the difference in ratios of specific heats must be accounted for in order to properly simulate the rocket retro-plume with a model utilizing air. In particular, compensation is required for the differences in the variation of flow turning angle with pressure ratio. This may be done by matching the vehicle and model exhaust gas pressure sensitivity with respect to flow direction, $1/P \frac{dP}{d\nu}$. Rewriting this condition, we obtain $dP/P \propto d\nu$, so that we plot P vs. ν on semilog paper for the hot rocket exhaust ($\gamma_e = 1.28$) and the cold air jet ($\gamma_e = 1.4$), overlay the curves and translate the axes until a best fit is found. The point at which the model curve is superimposed upon the one for the hot rocket exhaust will yield the optimum model exit Mach number, M_e. This procedure was also followed for the helium nozzle.

In summary, the scaling parameters which were matched in the tests are

$$\begin{aligned} &M_\infty \\ &C_T \\ &\frac{\gamma_\infty A_B}{2A_e (1 + \gamma_e M_e^2)} \quad \text{(Engine Scaling Parameter)} \\ &P_e/P_\infty \\ &1/P \; dP/d\nu \end{aligned} \tag{5}$$

2.2 Model Nozzle Design

The model nozzle design was based upon a hypothetical Mars lander consisting of an aeroshell with retrorockets (Reference 1). This lander was assumed to have the following engine characteristics.

$$A^*/A_B = 3.31 \times 10^{-4} \quad \text{(total for three engines)}$$

$$A_e/A^* = 40$$

$$M_e = 4.73$$

$$\gamma_e = 1.28$$

The specific heat ratio of the Martian atmosphere was taken as 1.304.

To simulate this engine the first procedure was to match $1/P\ dP/d\nu$. This resulted in an air nozzle exit Mach number of $M_e = 4.30$ ($A_e/A^* = 13.95$) and a helium nozzle exit Mach number of 3.2 ($A_e/A^* = 3.41$) to achieve a good turning angle match up to pressure ratios of 1000.

The Mars lander nozzle scaling parameter is

$$\frac{\gamma_\infty A_B}{2A_e\ (1 + \gamma_e M_e^2)} = 1.664 \qquad (6)$$

From this, the ratio of the model base area to the nozzle exit area, A_m/A_e, and thus the throat area to model base area ratio A^*/A_m of the model could be determined. For instance, for air nozzle 2 which simulates the representative Mars lander vehicle, it was found that the model throat area ratio was $A^*/A_m = 11.16 \times 10^{-4}$ (Total for three engines) which fixed the basic scaled model nozzle design.

In addition to the basic scaled model air nozzle, two other air nozzle sizes were selected such that the nozzle scaling parameter could be made a factor of two larger and smaller. The purpose of this was to provide information as to the influence of the engine size on the retro flow field.

A helium nozzle was also selected which simulated the representative Mars lander vehicle. Helium nozzle flow was utilized to determine if changes in exhaust gas composition, which effect the mixing between the free stream and exhaust gases, cause changes in the aerodynamic characteristics of aeroshell vehicles with retrorockets.

The model nozzle configurations used in the test are summarized in Table I along with the Mars lander nozzle. Note that the nozzle designated air nozzle 2 simulates the Mars lander nozzle. This nozzle was the only air nozzle tested on the three engine 60^{o} aeroshell. The column labeled $(d^*/d_m)_{eff}$ is the diameter ratio of a single equivalent nozzle. The diameter ratio for each nozzle of the three engine configuration is equal to $(d^*/d_m)_{eff}/\sqrt{3}$.

2.3 Wind Tunnel Models

The configurations tested in the Ames 6' x 6' Supersonic Wind Tunnel were

a) a forty five degree (45^{o}) half angle conical aeroshell with a single engine,

b) a sixty degree (60^{o}) half angle conical aeroshell with a single engine,

c) a sixty degree (60^{o}) half angle conical aeroshell with three engines, spaced 120^{o} apart (Figure 1).

The models were 4.0 inches in diameter and were sting mounted in the wind tunnel. The retrorockets were supplied by a high pressure source of dry air and helium which was piped to the model plenum chamber through a hollow streamlined strut and sting. The nose radius and corner radius of all aeroshells were twenty percent and six percent respectively of the model base radius. Three air engine sizes and one helium engine size were tested in the single jet model and one air and one helium size were tested in the three engine configuration. All nozzles used had conical diverging sections with semivertex angles of fifteen (15^{o}) degrees.

Details of the single engine models are shown in Figures 2 through 5. Pitching moment data is referenced to the virtual nose of the aeroshell vehicles. The single engine 60° and 45° aeroshells were instrumented with thirty (30) pressure taps of .028 inch inside diameter installed flush with the model surface. The locations of the pressure taps are noted in Figures 3 and 4 and pressure taps numbered 129 and 130 were used to measure the base pressure. The pressure taps on the forward surface of the aeroshell were located on seven concentric circles. The aximuthal angle, ϕ, and the radius ratio for each pressure tap are noted in Table II, P. 14. The geometric features of the three air nozzles and the helium nozzle tested with the single engine aeroshell vehicles are noted in Figure 5.

The three nozzle 60° aeroshell model was instrumented (Figure 6) with forty five (45) pressure taps of which there was one edge tap (343) and two base pressure taps (344 and 345). The geometric features of the three engine air and helium nozzles are shown in Figure 7. Each engine was scarfed at an angle of thirty degrees (30°) so the nozzle exit plane would be flush with the aeroshell surface. The aximuthal angle, ϕ, and the radius ratio for each of the three engine aeroshell pressure taps are noted in Table III, P. 17.

In the three engine case, all nozzles were connected to a common manifold located behind the aeroshell (Figure 8). The gas was then conducted to each engine through spearate engine tubes. Uniform flow properties were preserved by placing a flow straightener in each engine tube. The engine circle was at .8 of the aeroshell radius for the multiple jet configuration. The multiple engines were scarfed at an angle of thirty degrees (30°) so their exit planes would be flush with the aeroshell surface. The retrorockets, designated air nozzle 2 ($d^*/d_m = 0.0334$) and helium nozzle, simulated the Mars lander vehicle retrorocket and were tested on the three engine aeroshell model as well as on both the 45° and 60° single engine aeroshell models. Engine throttling on the multiple engine model was accomplished by placing the proper orifice plug in each engine tube on the supply side of the flow straightener. A photograph of the three engine model installed ($\phi = 30^{\circ}$) in the Ames 6' x 6' Wind Tunnel is shown in Figure 9.

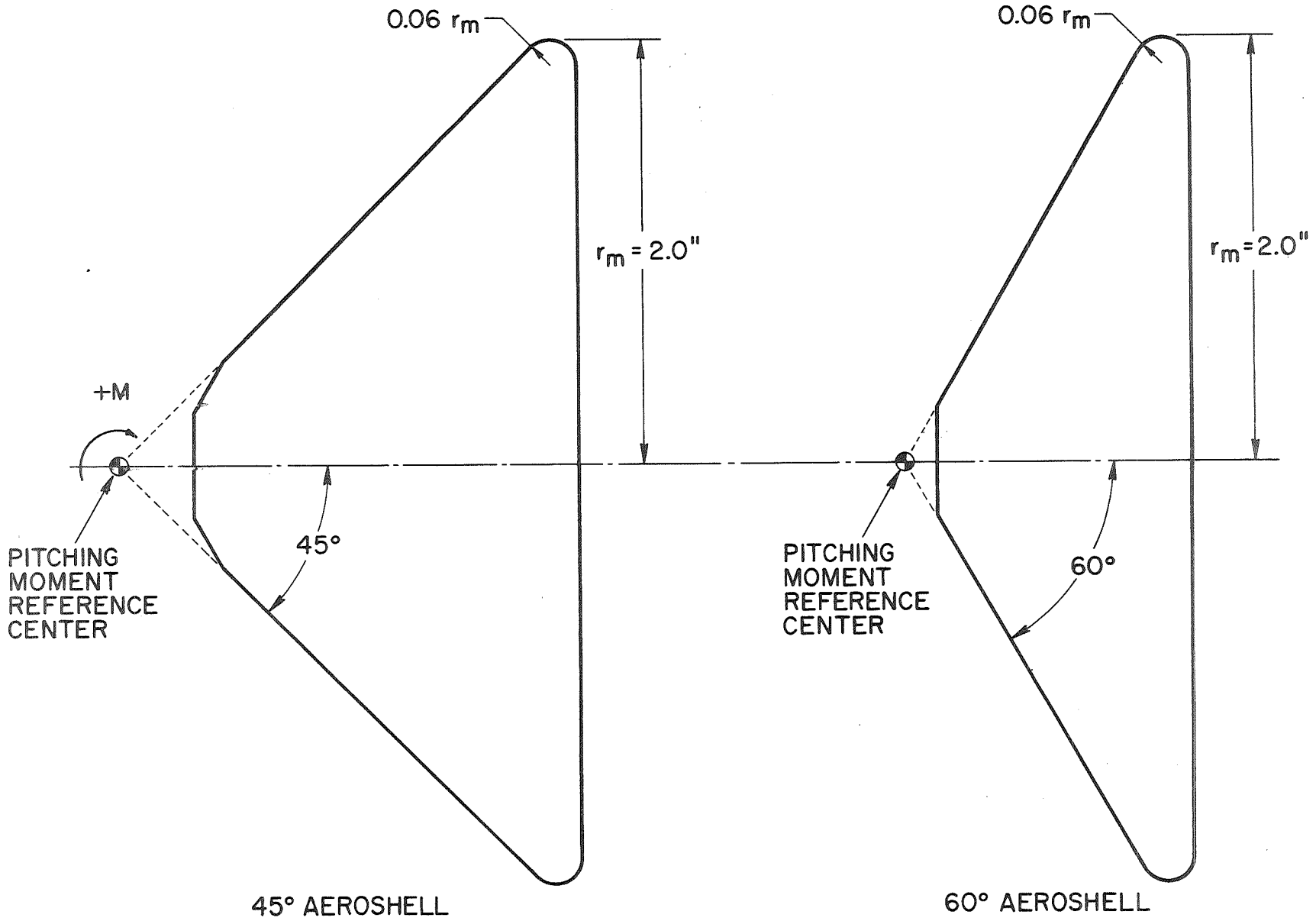

Figure 2 Model Details.

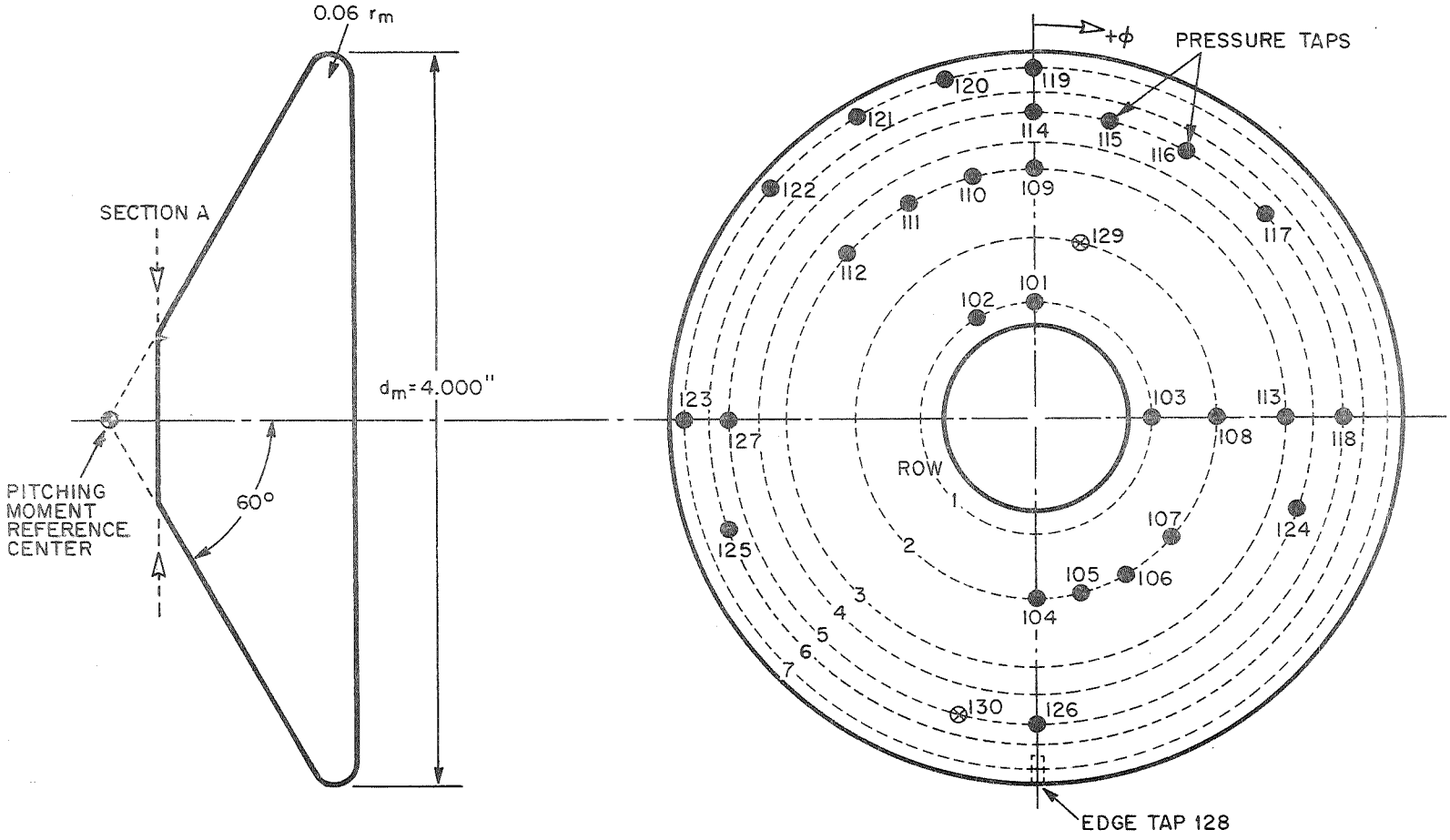

Figure 3 Pressure Tap Locations - 60° Single Engine Aeroshell.

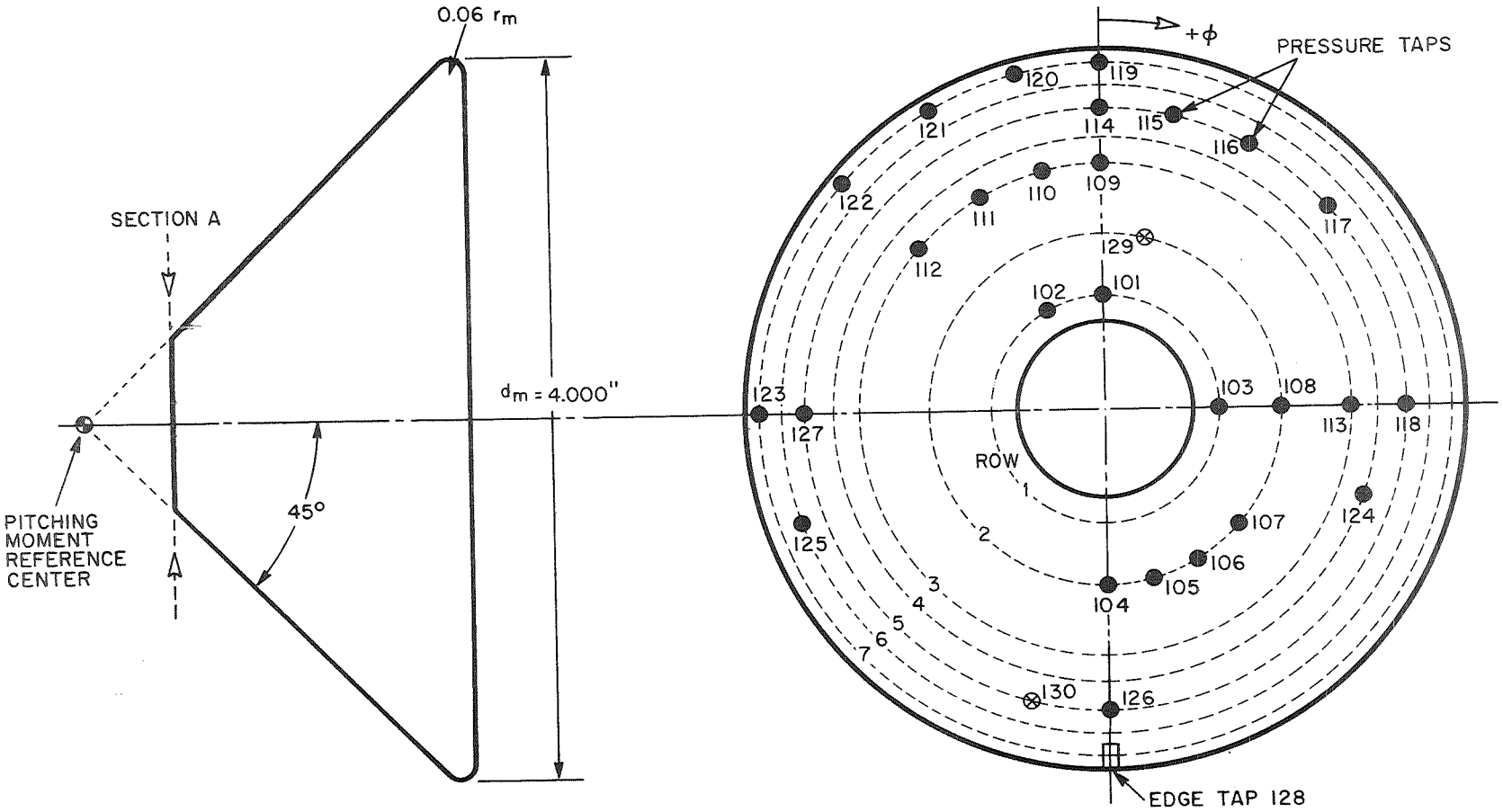

Figure 4 Pressure Tap Locations - 45° Single Engine Aeroshell.

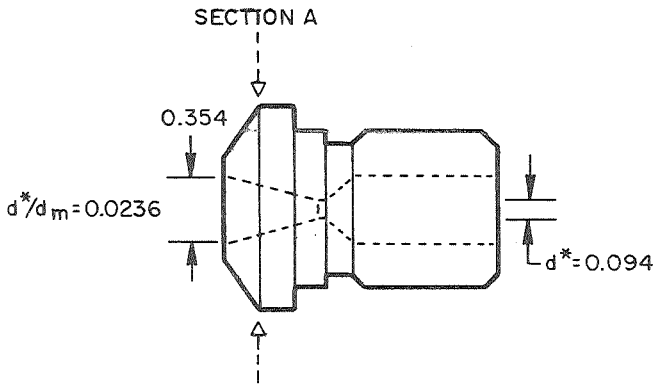

AIR NOZZLE 1

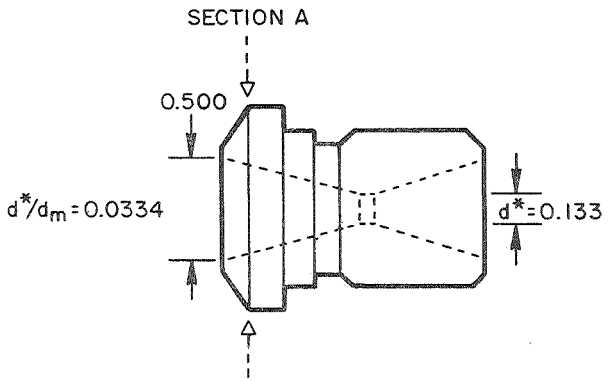

AIR NOZZLE 2

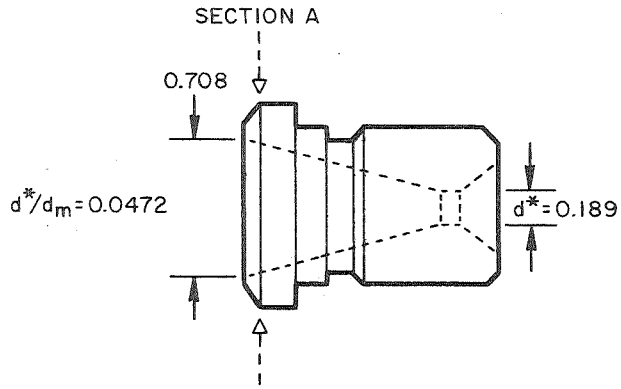

AIR NOZZLE 3

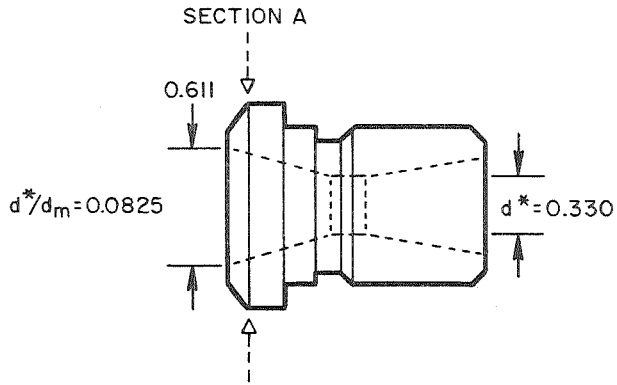

HELIUM NOZZLE

Figure 5 Single Engine Nozzles.

TABLE II. PRESSURE TAP LOCATIONS - SINGLE ENGINE MODELS

ϕ	r/r_m						
	Row 1 .3125	Row 2 .4850	Row 3 .6860	Row 4 .7515	Row 5 .840	Row 6 .9075	Row 7 .970
0	101		109		114		117
14° - 30'		129 (Base)			115		
30° - 0'					116		
48° - 30'					117		
90° - 0'	103	108	113		118		
110° - 0'				124			
131° - 30'		107					
150° - 0'		106					
165° - 30'		105					
180° - 0'		104			126		
194° - 30'					130 (Base)		
250° - 0'						125	
270° - 0'					127		123
311° - 30'			112				122
330° - 0'	102		111				121
345° - 30'			110				120

Note: Tap 128 located on model shoulder $\phi = 180^\circ$, $r/r_m = 1.0$

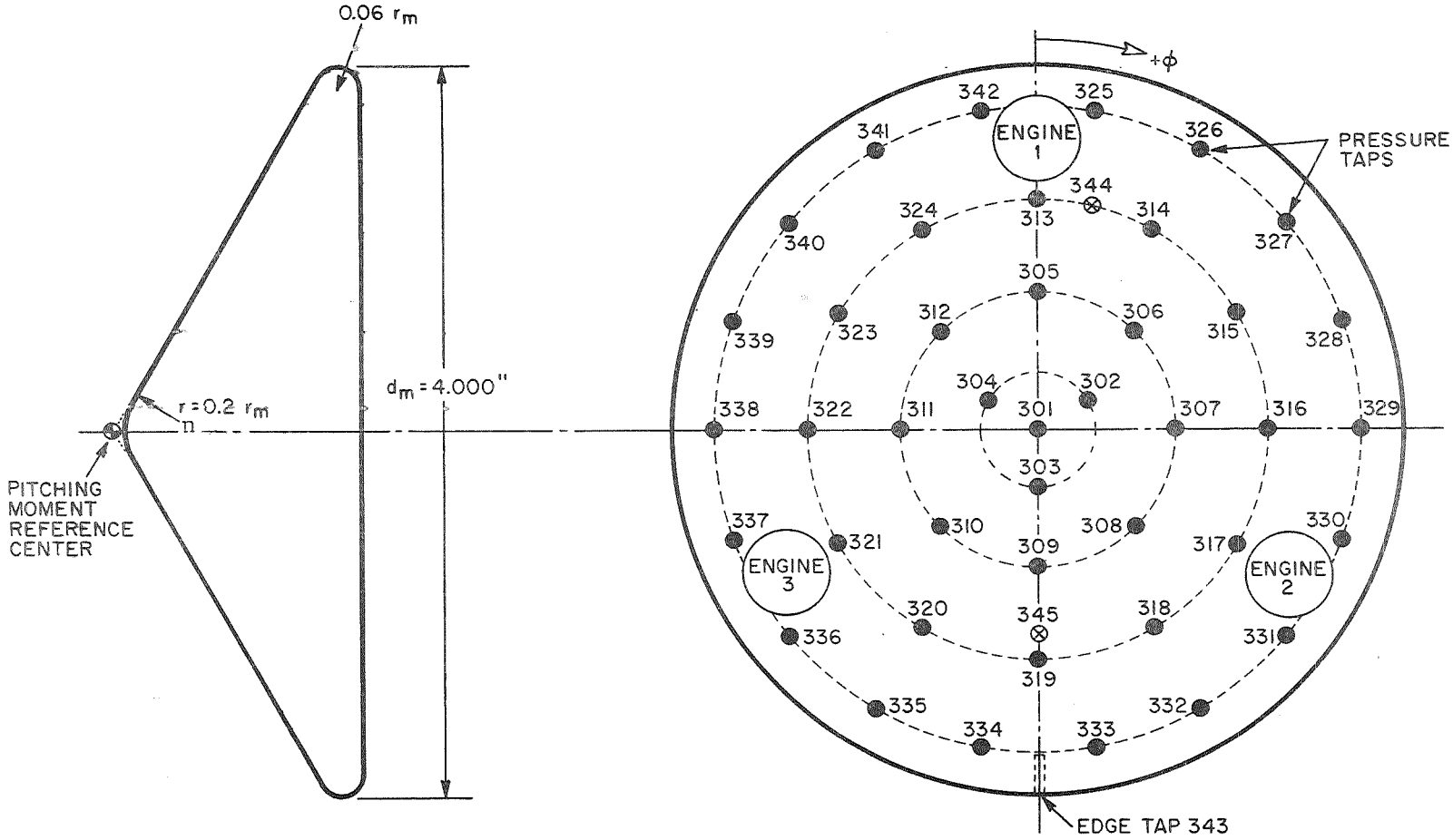

Figure 6 Pressure Tap Locations - 60° Three Engine Aeroshell.

Note:
NOZZLES MOUNTED FLUSH
WITH MODEL SURFACE

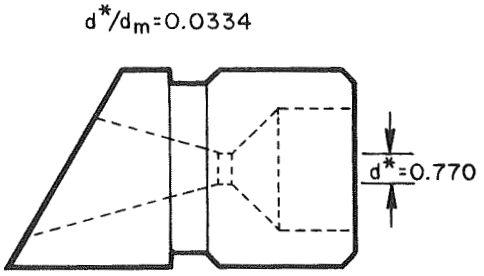

AIR NOZZLE 2

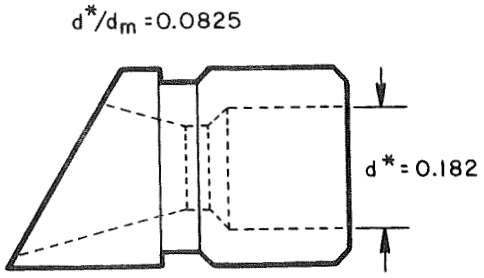

HELIUM NOZZLE 4

Figure 7 Three Engine 60° Aeroshell Nozzles.

TABLE III. PRESSURE TAP LOCATIONS - THREE ENGINE MODELS

	r/r_m				
ϕ	0	.1535	.3780	.6250	.8750
0	301		305	313	
10					325
30				314	326
45			306		
50					327
60		302		315	
70					328
90			307	316	329
110					330
120				317	
130					331
135			308		
150				318	332
170					333
180		303	309	319	
190					334
210				320	335
225			310		
230					336
240				321	
250					337
270			311	322	338
290					339
300		304		323	
310					340
315			312		
330				324	341
350					342

Note: Tap 343 located on model shoulder $\phi=180^{\circ}$, $r/r_m=1.0$
Tap 344 located on model base $\phi=14^{\circ}-30'$, $r/r_m=.6375$
Tap 345 located on model base $\phi=180^{\circ}$, $r/r_m=.5750$

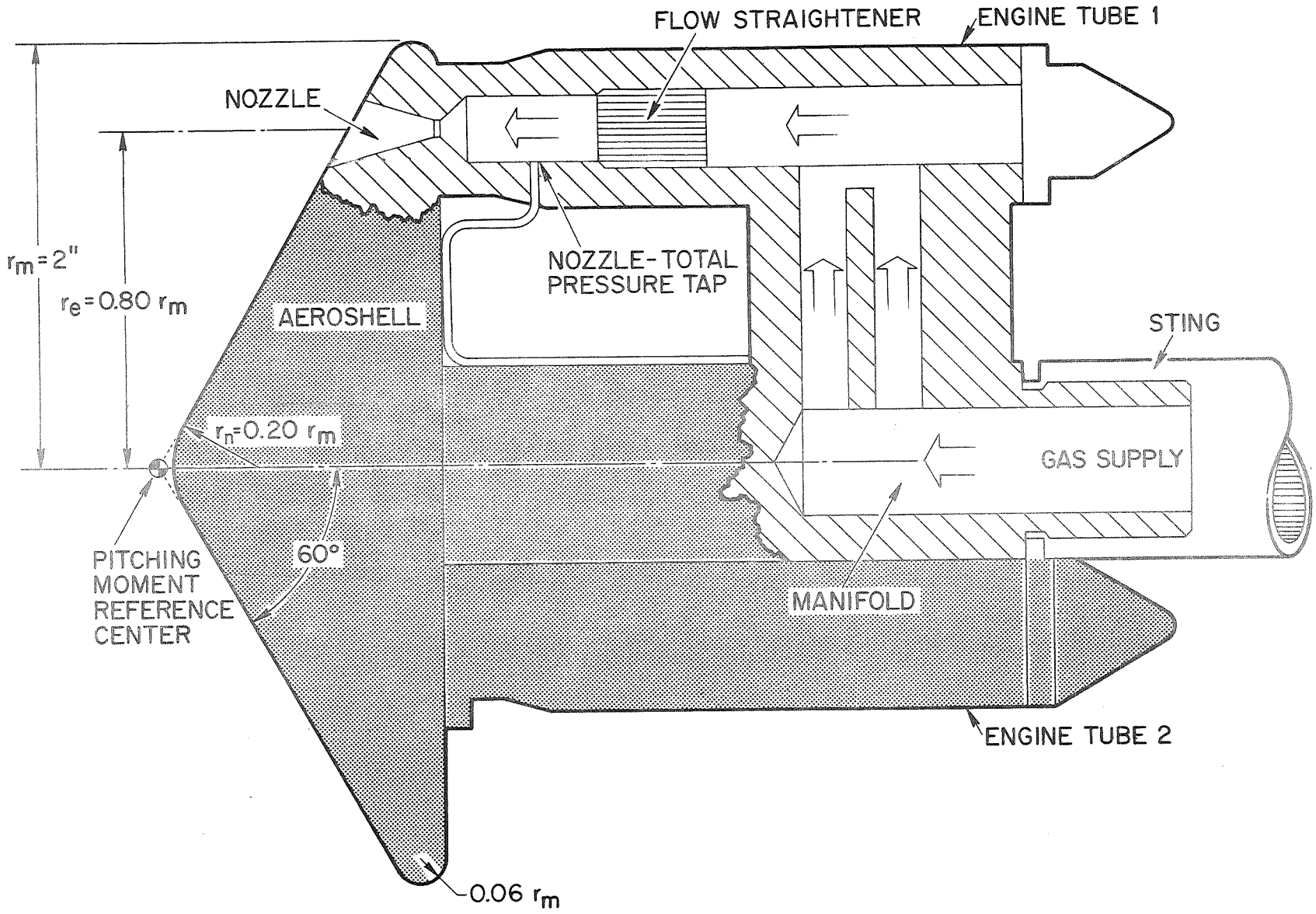

Figure 8 - 60° Three Engine Aeroshell Model.

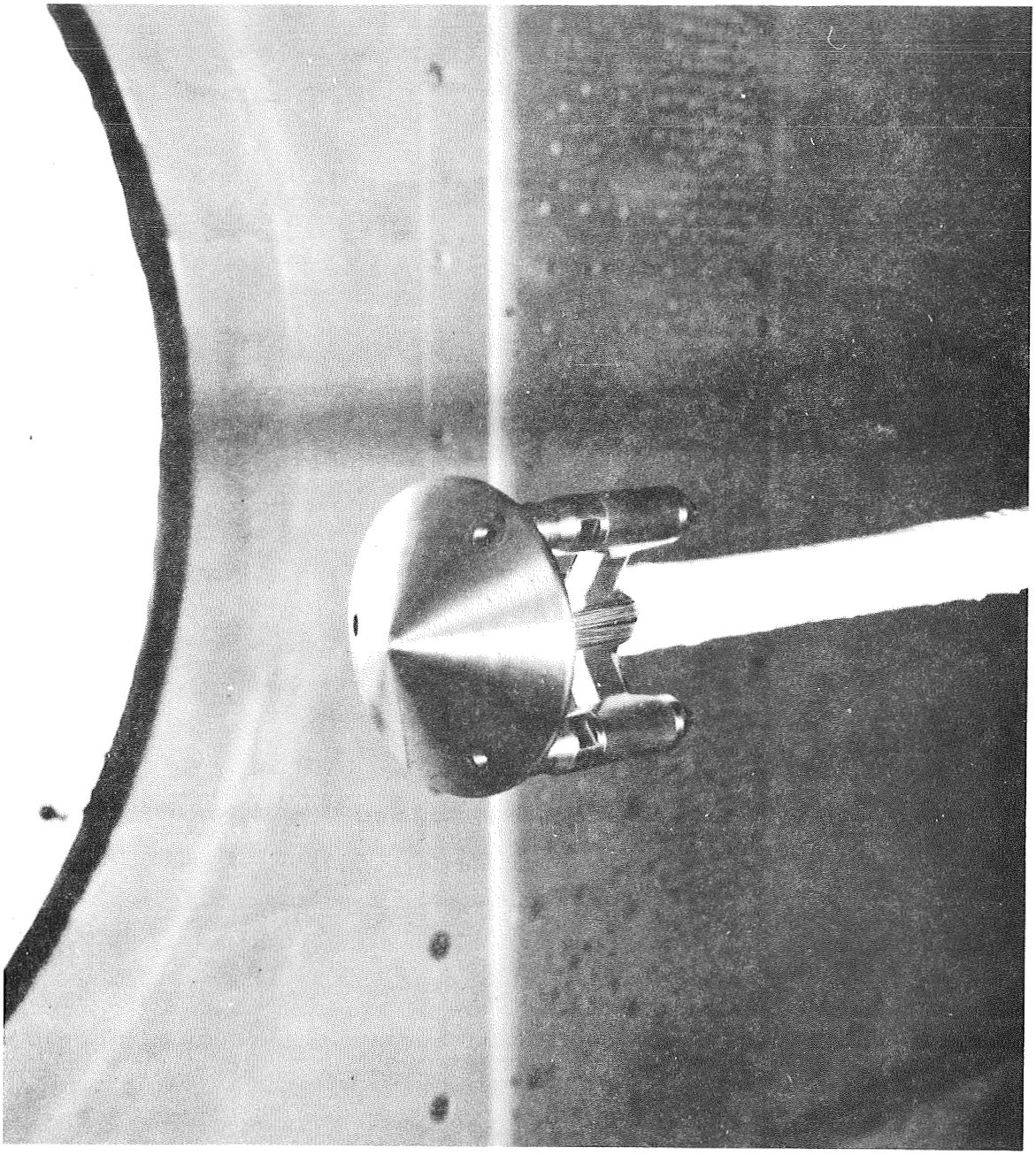

Figure 9 Three-Nozzle Model Installed in Wind Tunnel $\phi = 30^{\circ}$.

2.4 Instrumentation

The single nozzle 45^{o} and 60^{o} aeroshell models were instrumented with thirty (30) pressure taps of .028 inch inside diameter installed flush with the model surface. The thirty pressure taps included one edge tap on the shoulder of the model and two base pressure taps. The three nozzle 60^{o} aeroshell model was instrumented with forty five (45) pressure taps of which there was one edge tap and two base pressure taps. Surface pressures were measured with one bank of 3-24 port scanivalve modules. Model surface pressure taps were connected to the scanivalve ports with stainless steel tubing.

The total plenum chamber pressure and total temperature were measured on single nozzle models. For the three jet case, the plenum chamber total pressure for each nozzle was measured in addition to the main supply variables. The engine and supply pressures were measured with high pressure transducers.

Shadowgraphs were taken at each data point.

2.5 Range of Test Variables

The tests were conducted at free-stream Mach Number of 0.40, 0.60, 0.80, 1.05, 1.5 and 2.0. Free stream total pressure was set at 2 psia for all free stream Mach numbers. Angle of attack data was taken at free stream Mach numbers of 0.6, 1.05 and 2.0 with an angle-of-attack range from $+9^{o}$ to -18^{o}. The plenum air chamber pressure was varied up to 2700 psia. A summary run schedule of the experimental investigation is presented in Table IV, Pages 21-22.

The range of thrusting coefficients obtained during the wind tunnel test is shown in Figure 10. Air nozzle 3 covered the same range of thrusting coefficients as air nozzle 2 as well as the shaded areas. The variation of thrusting coefficient with free stream Mach number, M_{∞} , for the typical terminal lander of Reference 1 is noted. This lander is assumed to have a vehicle ballistic coefficient β of 0.5 slugs/ft^2 down to a retrorocket ignition altitude of 5 kilometers. Adequate simulation of the representative Mars lander vehicle was achieved in the present experiment.

TABLE IV. SUMMARY RUN SCHEDULE

Model Configuration	Nozzle Configuration	Mach Number	Angle-of-Attack Range - α	C_T Range
45° single jet	Air-2	0.4	0	0-25
		0.6	-18° to $+9^\circ$	0-10
		0.8	0	0-6
		1.05	-18° to $+9^\circ$	0-5
		1.5	0	0-4
		2.0	-18° to $+9^\circ$	0-4
60° single jet	Air-2	0.4	0	0-20
		0.6	-18° to $+9^\circ$	0-12
		0.8	0	0-8
		1.05	-18° to $+9^\circ$	0-6
		1.5	0	0-6
		2.0	-18° to $+9^\circ$	0-6
60° single jet	Air-1	0.6	0	1-6
		1.05	0	1-4
		2.0	0	0.1-4
60° single jet	Air-3	0.6	0	1-27
		1.05	0	1-14
		1.5	0	1-14
		2.0	0	0.1-14

TABLE IV. SUMMARY RUN SCHEDULE (CONTINUED)

Model Configuration	Nozzle Configuration	Mach Number	Angle-of-Attack Range - α	C_T Range
60° single jet	Helium	0.4	0	4-40
		0.6	0	2-30
		0.8	0	1-10
		1.05	0	1-5
		1.5	0	0.5-4
		2.0	0	0.5-4
60° three jet	Air-2	0.4	0	0-20
		0.6	-18° to $+9^\circ$	0-12
		0.8	0	0-8
		1.05	-18° to $+9^\circ$	0-6
		1.5	0	0-6
		2.0	-18° to $+9^\circ$	0-6
60° three jet	Air-2 with one engine throttled 1/2	0.6	0 to 13°	2-12
		1.05	0 to 13°	1-6
		2.0	0 to 13°	1-6
60° three jet	Air-2 with one engine throttled 1/4	2.0	0 to 13°	1-6
60° three jet rolled 30°	Air-2 with two engines throttled 1/2	0.6	0 to -13°	2-4
		1.05	0 to -13°	1-2
		2.0	0 to -13°	1-2
60° three jet rolled 30°	Air-2 with two engines throttled 1/4	0.6	0 to -13°	2-4
		1.05	0 to -13°	1-2
		2.0	0 to -13°	1-2
60° three jet	Helium	0.6	0	2-8
		1.5	0	1-4
		2.0	0	1-4

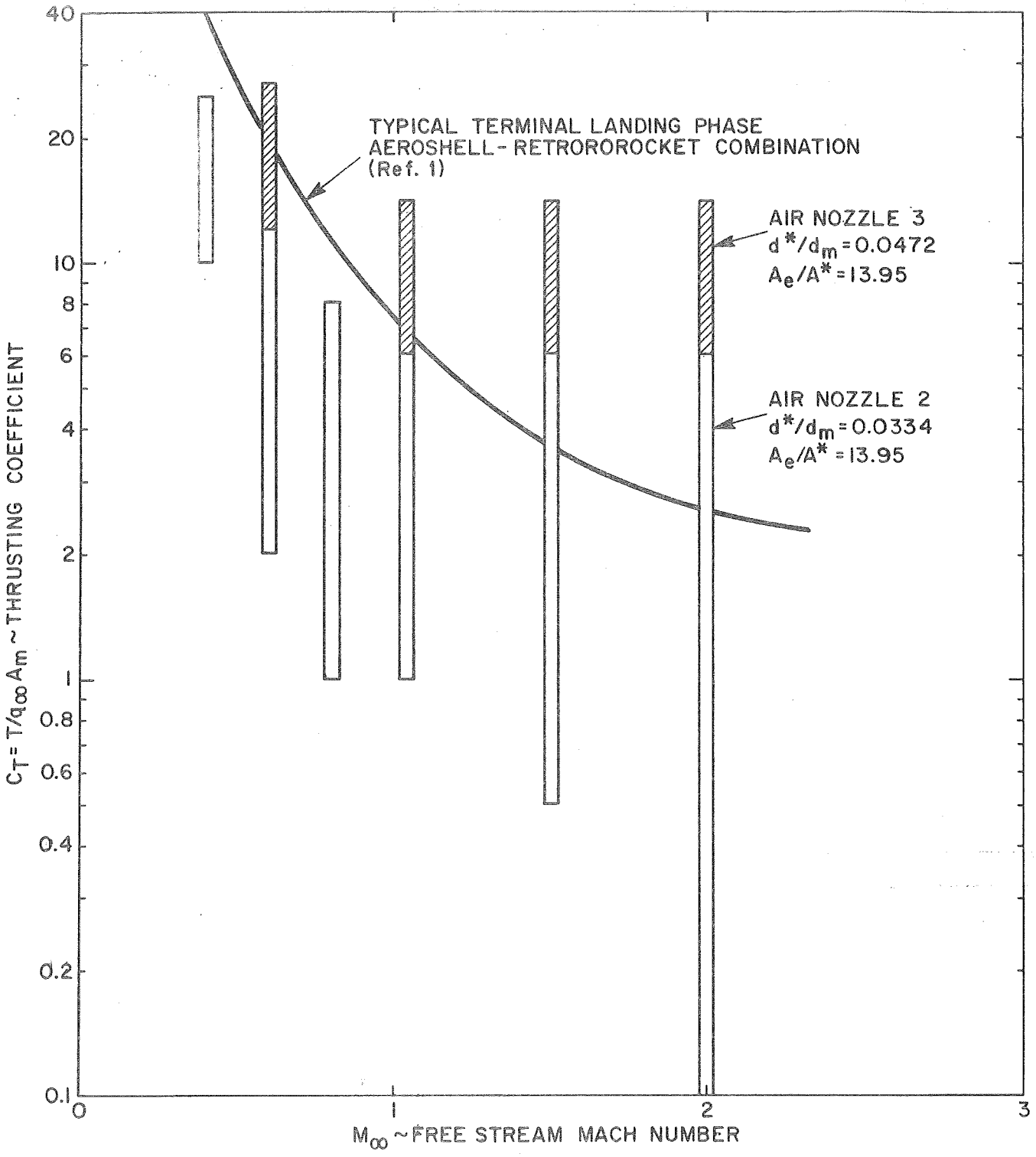

Figure 10 Thrusting Coefficients Obtained During Wind Tunnel Tests.

2.6 Data Reduction

Pressure coefficients were computed from the individual pressure measurements made on the model surface. Force and moment coefficients for the aeroshell models were obtained from integrations of the pressure coefficients over the model face excluding the nozzle exits. The total axial force coefficients were obtained from a summation of the model forebody axial force coefficient and the nozzle thrusting coefficients. The pitching moment coefficients for all aeroshells are referenced to the aeroshell virtual nose and are based on the model base area and diameter and the retrothrust (thrusting) coefficient is based on free stream dynamic pressure and model base area.

PRESSURE COEFFICIENT

$$C_P = P - P_\infty / q_\infty$$

FOREBODY AXIAL FORCE COEFFICIENT

$$C_{A_f} = X/q_\infty A_m = \int\int (P_f - P_\infty) \sin\theta \, dA/q_\infty A_m$$

THRUSTING COEFFICIENT

$$C_T = T/q_\infty A_m$$

TOTAL AXIAL FORCE COEFFICIENT

$$C_{A_{TOTAL}} = C_{A_f} + C_T \text{ (THREE ENGINES)}$$

PITCHING MOMENT COEFFICIENT

$$C_M = m/q_\infty A_m d_m$$

The pressure coefficients and the forebody axial force coefficients are evaluated assuming that free stream static pressure acts on the model base. No corrections have been made to the experimental data to reflect actual measured base pressures. With this assumption, pressure coefficients will be negative when the measured pressure falls below free stream static pressure. Negative axial force coefficients may also occur.

3. RESULTS

3.1 Single Engine Aeroshell Models

3.1.1 Forebody Axial Force Coefficient Without Retrothrust

The variation of the forebody axial force coefficient with Mach number for the forty-five degree and sixty degree aeroshell models without retrothrust ($C_T = 0$) was compared with experimental data from previous wind tunnel tests performed by NASA[6-8] and JPL[9] and was in very close agreement over the complete range of Mach Numbers investigated (Figure 11). The use of a corner to base radius ratio of $r_c/r_m = 0.06$ in the present test caused a reduction in the axial force coefficient of about five (5) percent below the sharp cornered cone data. A similar effect was observed previously[10] at $M_\infty = 3.0$ (Figure 12).

3.1.2 Shadowgraphs of Retrorocket-Freestream Interaction

A series of shadowgraphs of the flow field about the single nozzle 60^o aeroshell, as the thrusting coefficient is increased, is shown in Figures 13 through 15. This series shows the typical behavior that is observed for supersonic free stream Mach numbers. At low thrusting coefficients, the jet penetrates into the oncoming flow, the flow is unsteady and the bow shock is far upstream from the model (Figure 13). Line drawings are shown in Figures 13 through 15 to aid in interpretation of the photos. For this case, the total head of exhaust flow decays by mixing. The flow field collapses when the thrusting coefficient is increased further (Figure 14) and a steady blunt

flow interaction forms closer to the aeroshell. The geometrical features of the flow field such as the terminal shock, jet boundary, interface and bow shock wave are discernible. The features in the flow field grow in size as the thrusting coefficient is increased still furthur but the geometry stays nearly similar (Figure 15). In Figures 14 and 15, the total head of the exhaust flow decays by passing through the terminal shock wave. The aeroshell surface pressure data corresponding to the conditions illustrated in Figure 14 indicates that flow reattachment to the forward surface of the aeroshell is occurring. At M = 1.5 and C_T = 6.0 (Figure 15), the pressure data indicates that the aeroshell is immersed in a constant pressure region which is typical of a wake type flow region.

In both Figure 14 and 15, the retrojet issues into a region of separated flow and expands laterally to a maximum diameter determined by the ratio of the jet exit pressure to separated (dead air) flow pressure. The upstream extent of the retrojet is bounded by a terminal or jet shock which adjusts its pitot pressure to balance that of the free stream. The free stagnation point at which the pitot pressures are actually balanced is somewhat upstream of the terminal shock, and defines the apex of the interface between the jet and atmospheric gases. The location of the jet boundary is dependent on the ratio of the jet exit pressure P_e to the dead air pressure P_d. An interface separates the free stream gas from the jet gases. The free stream gas which passes through the bow shock wave turns and flows outward between the bow shock wave and interface while the jet flow which passes through the jet terminal shock flows outward between the jet terminal shock and interface. Mixing between the free stream gases and the jet gases may occur along the interface if properties such as the velocity and density of the two fluids are different. Mixing may occur in the region which separates the free stream-jet layer from the dead air region (recirculation region) as well as along the jet boundary.

At subsonic speeds and for all thrusting coefficients tested, the single engine exhaust flow penetrates far upstream into the oncoming flow and the flow is unsteady. The flow field is much like that shown in Figure 13, without the bow shock wave. The total head of the jet decays through a mixing process and the penetration of the jet ceases when the jet and the free stream total heads become equal.

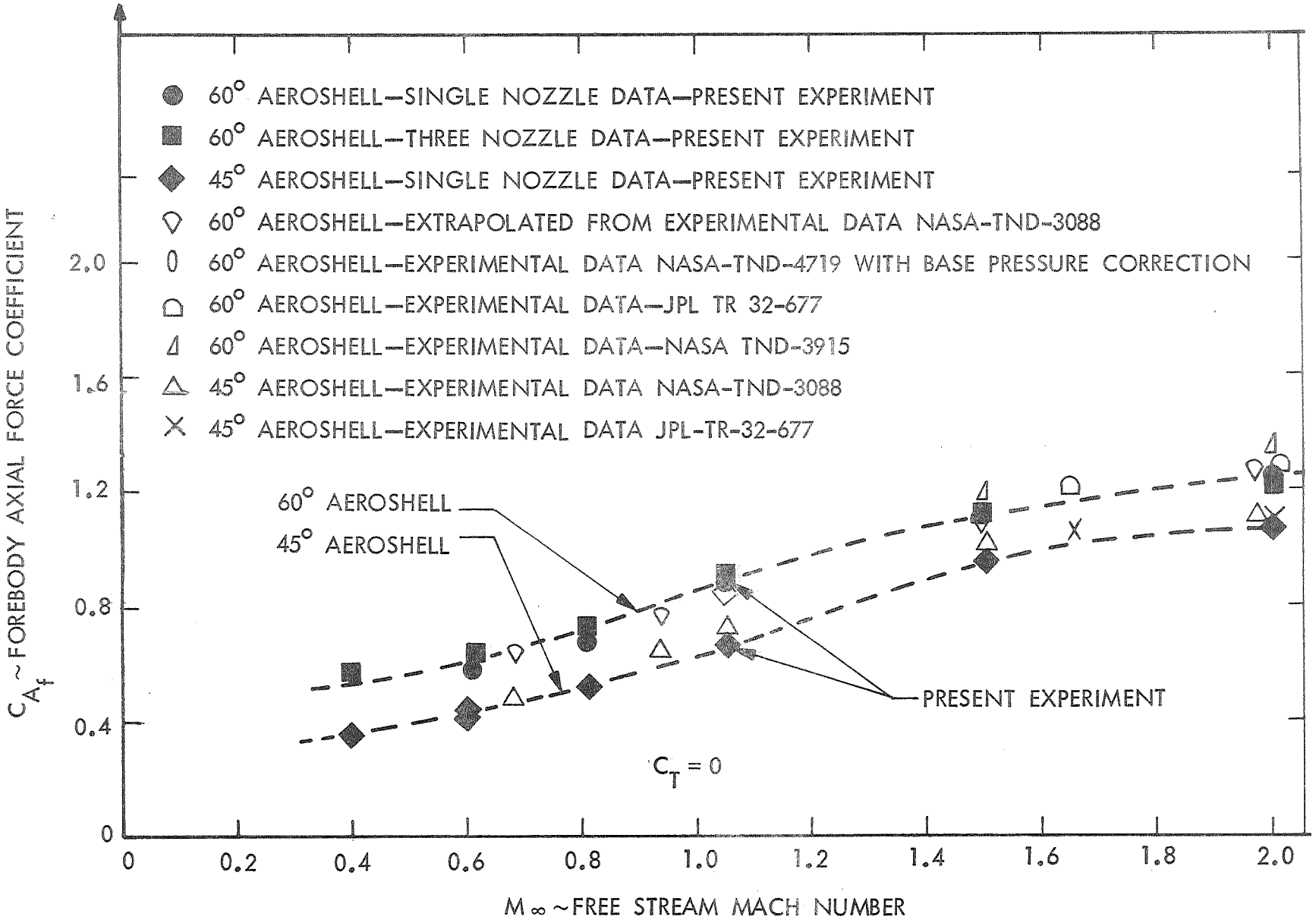

Figure 11 Forebody Axial Force Coefficient, $C_T = 0$.

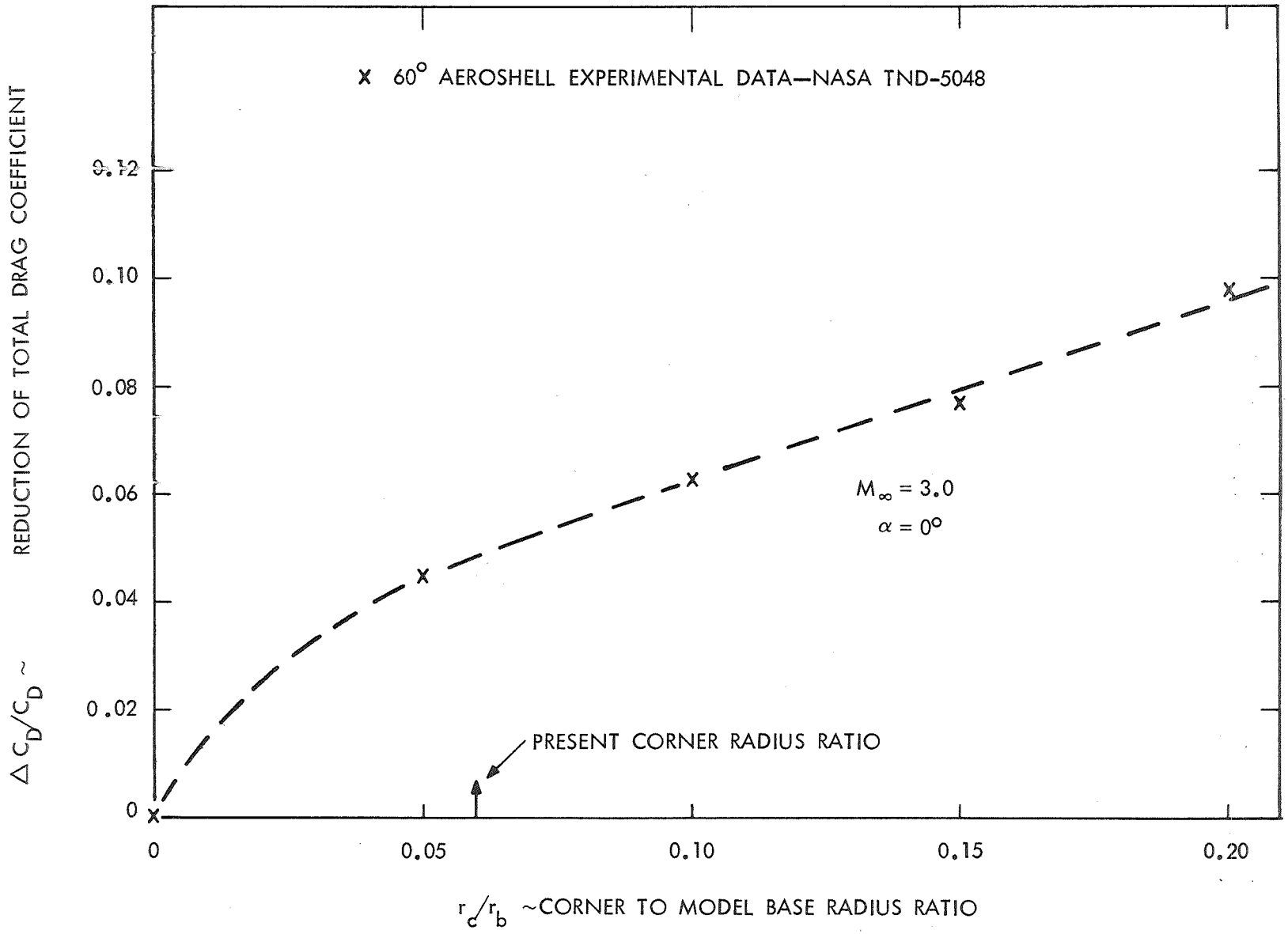

Figure 12 Reduction of Total Drag Coefficient with Variations in Corner to Model Base Radius Ratio, $M_\infty = 3.0$.

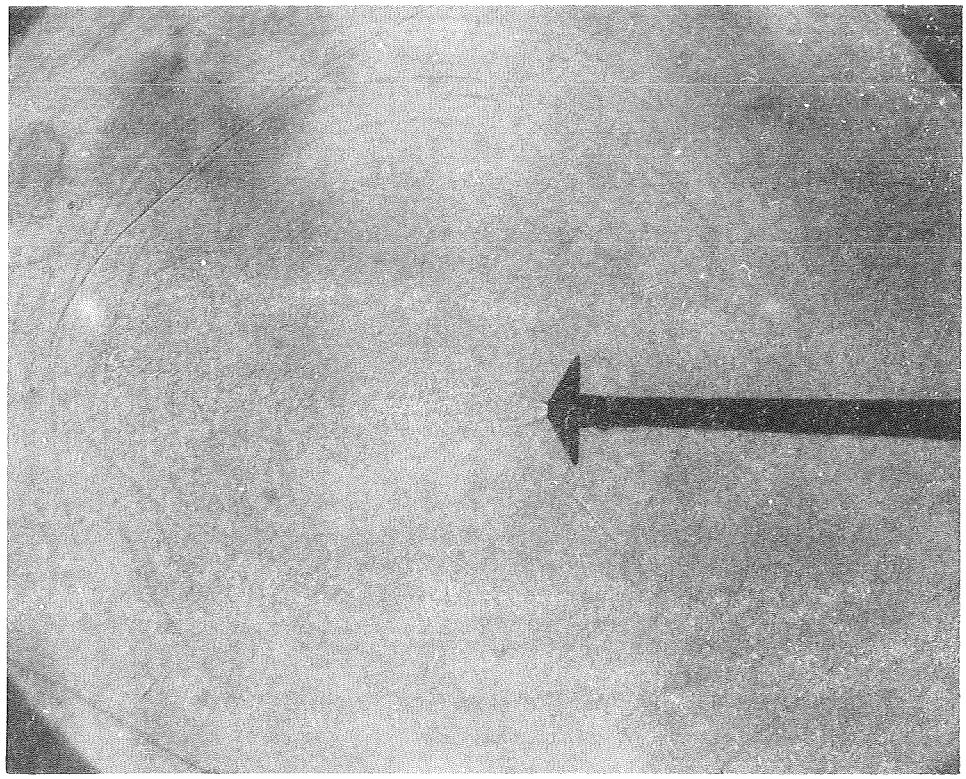

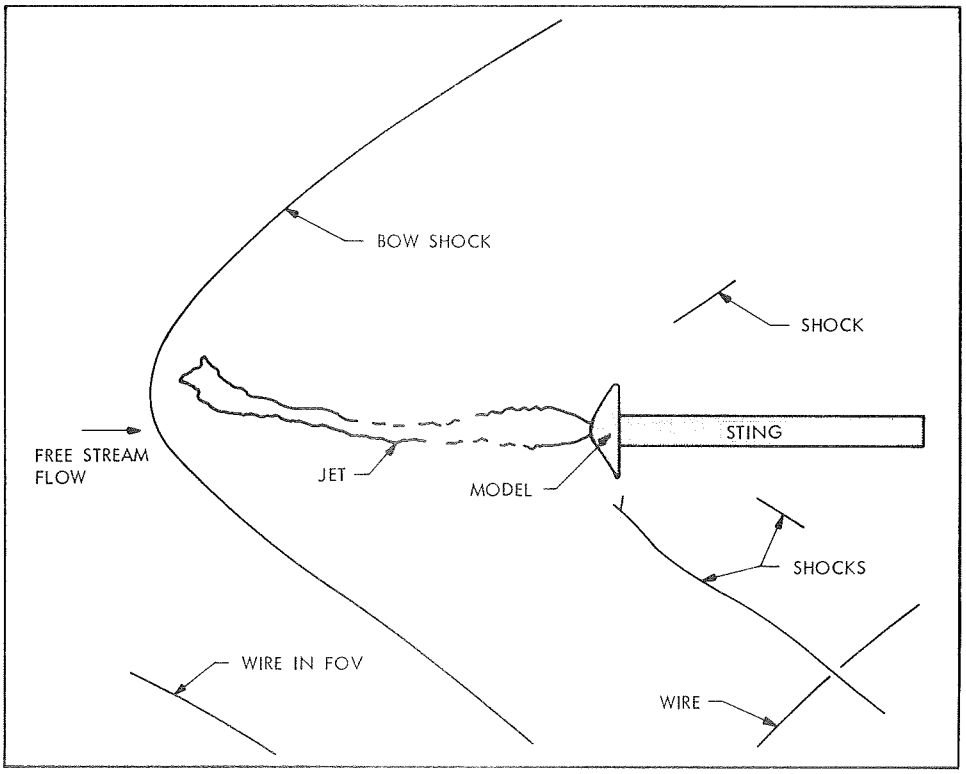

Figure 13 Single-Nozzle 60° Aeroshell Model with Large Jet Penetration
$M = 2.0,\ C_T = 0.7.$

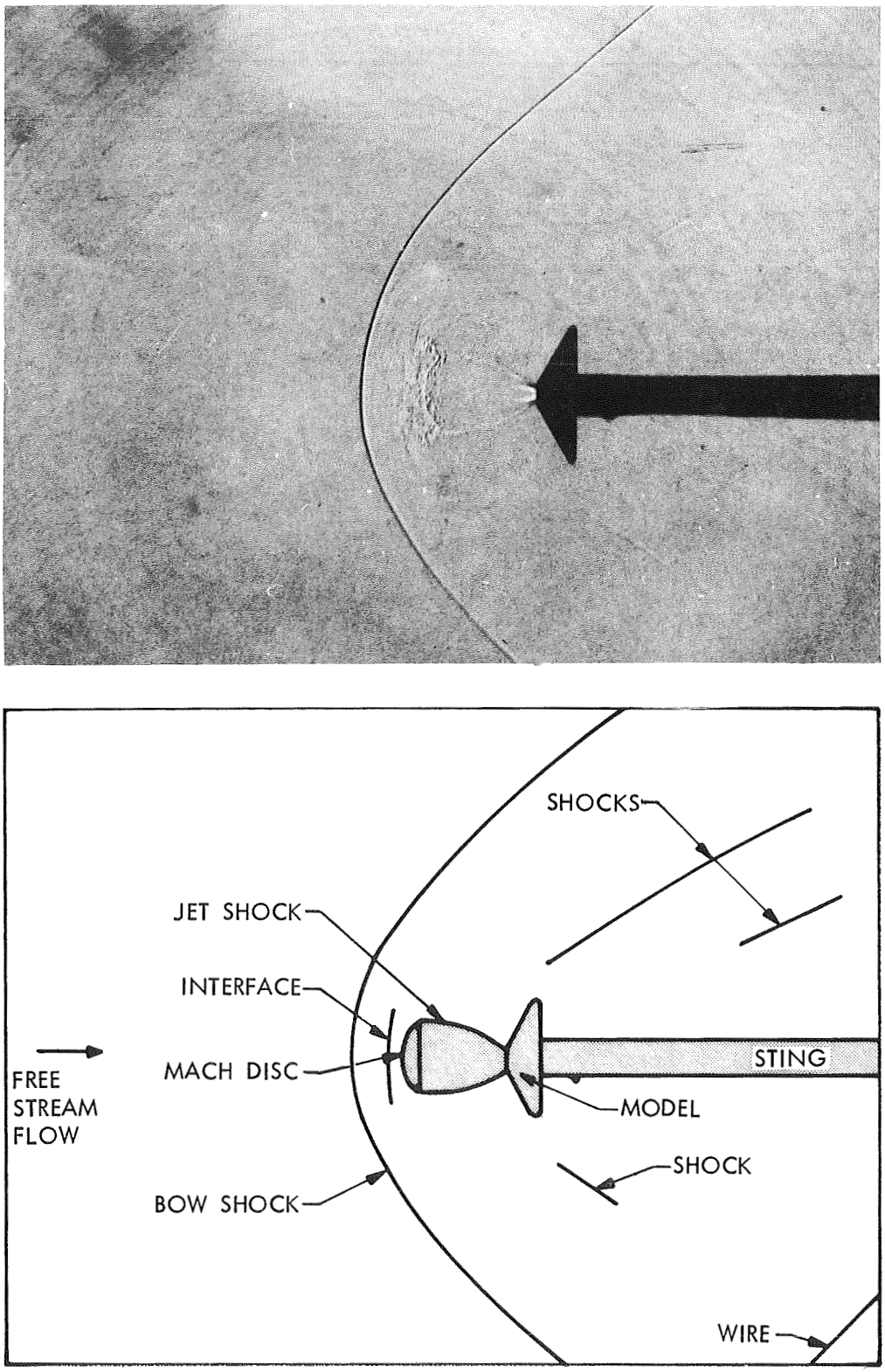

Figure 14 Single Nozzle 60° Aeroshell Model with Blunt Flow Interaction, $M_{\infty} = 2.0$, $C_T = 1.1$.

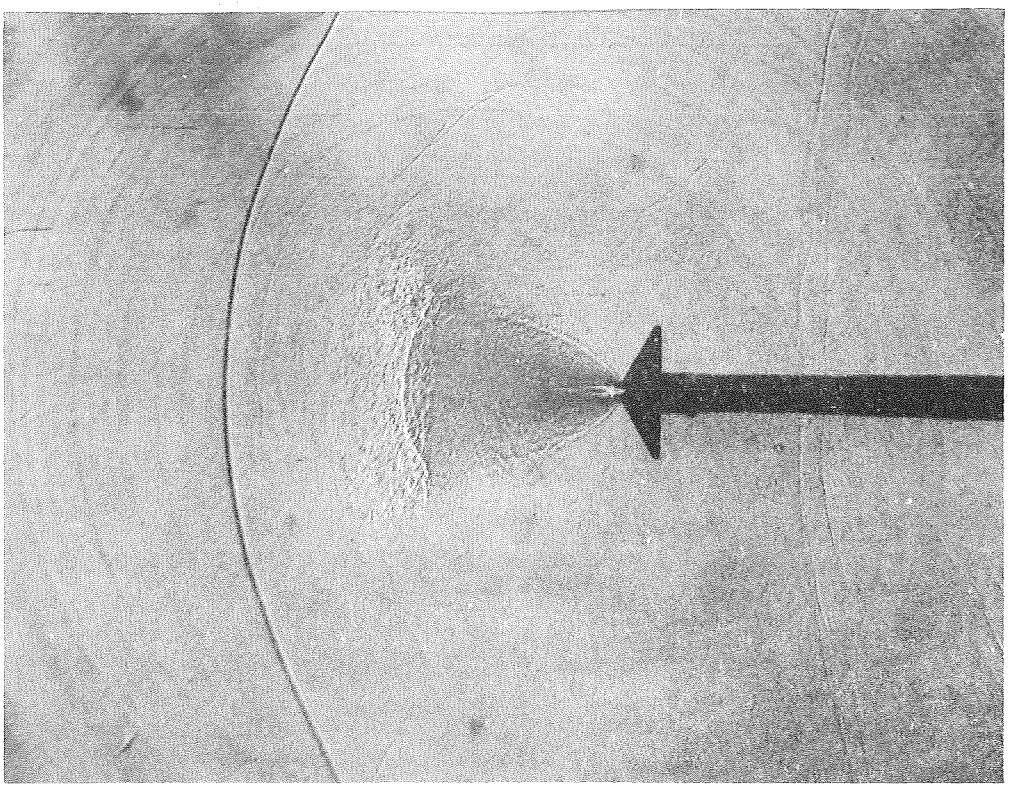

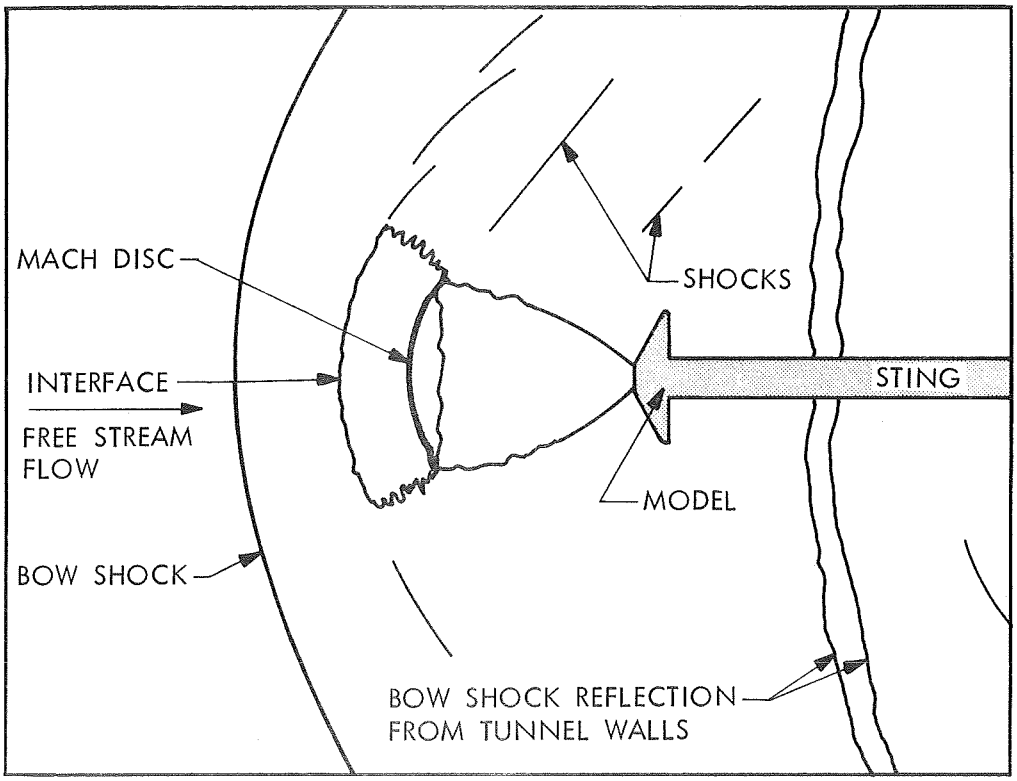

Figure 15 Single Nozzle 60° Aeroshell Flow Field - $M_\infty = 1.5$, $C_T = 6.0$, Air Nozzle.

3.1.3 Bow Shock Location

Shadowgraphs such as those shown in Figures 13 through 15 were analyzed to determine the location of the bow shock wave as a function of thrusting coefficient. The bow shock location for single engine aeroshells is shown in Figure 16 for $M_\infty = 2.0$ and the nozzle simulating the Mars lander. Data is shown for both the 45^o and 60^o single engine aeroshells. The transition from jet penetration to blunt flow regimes occurs sharply at a thrusting coefficient near unity (1). The bow shock location is independent of aeroshell shape. At thrusting coefficients below one, the jet shock may be as many as six body diameters forward of the model. The flow field is of the blunt flow interaction type at thrusting coefficients above one. In this region, the scale of the jet-free stream interaction increases with increases in thrusting coefficient but the geometric features of the interaction remain invariant.

At lower supersonic Mach numbers, the transition from jet penetration to blunt flow interaction occurs at a higher thrusting coefficient (Figure 17).

3.1.4 Transition from Jet Penetration to Blunt Flow Interaction

Transition from jet penetration to blunt flow was found to occur at the same nozzle exit to free stream pressure ratio independent of engine scaling parameter (Figure 18). Data for three air nozzle sizes and two supersonic free stream Mach numbers are shown. It should be noted that, since transition occurs at the same pressure ratio, a change in engine size will cause transition to occur at a different thrusting coefficient. Transition occurs at lower thrusting coefficients for smaller nozzles and at larger coefficients for bigger nozzles.

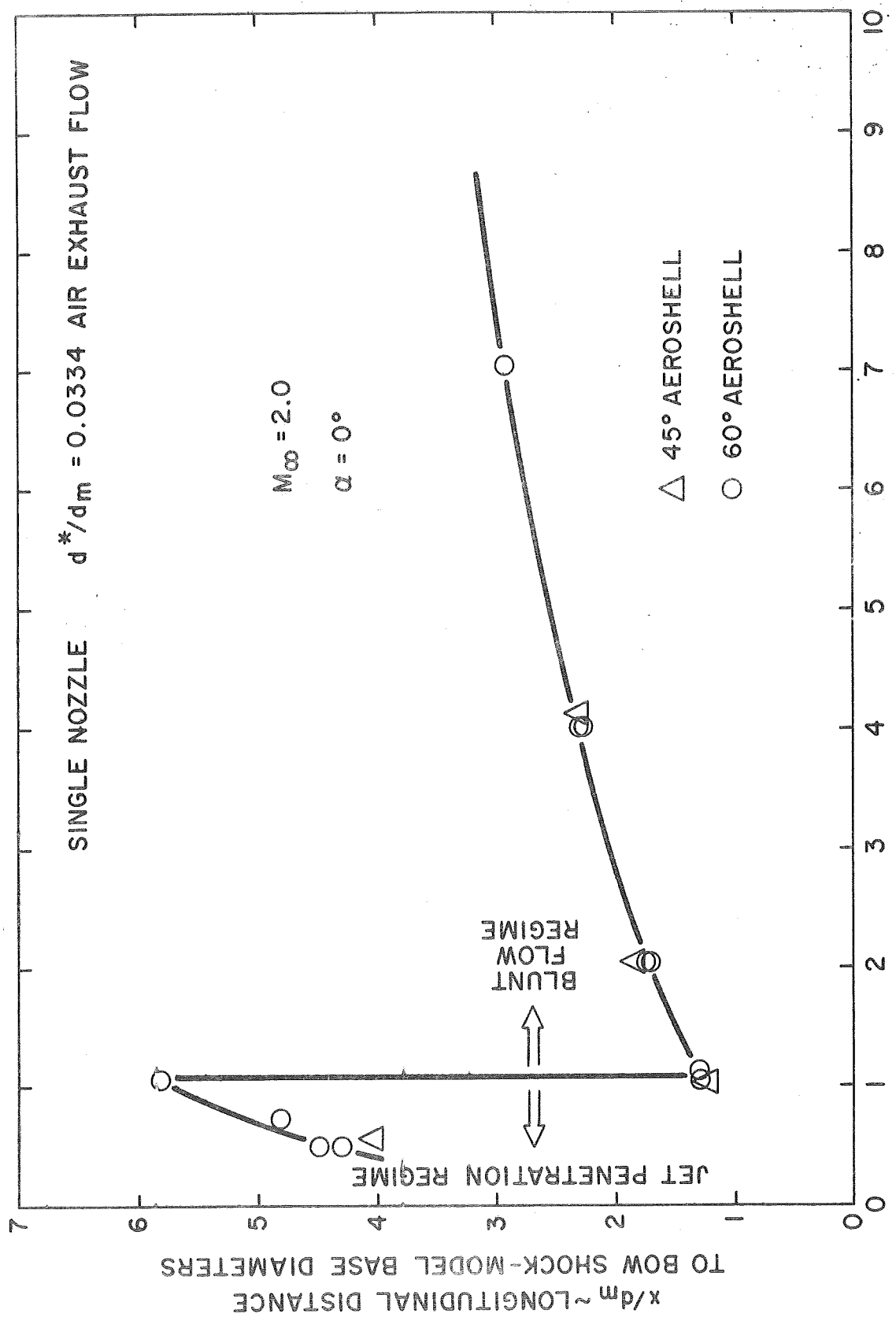

Figure 16 Bow Shock Location for Single Engine Aeroshells M_∞ = 2.0.

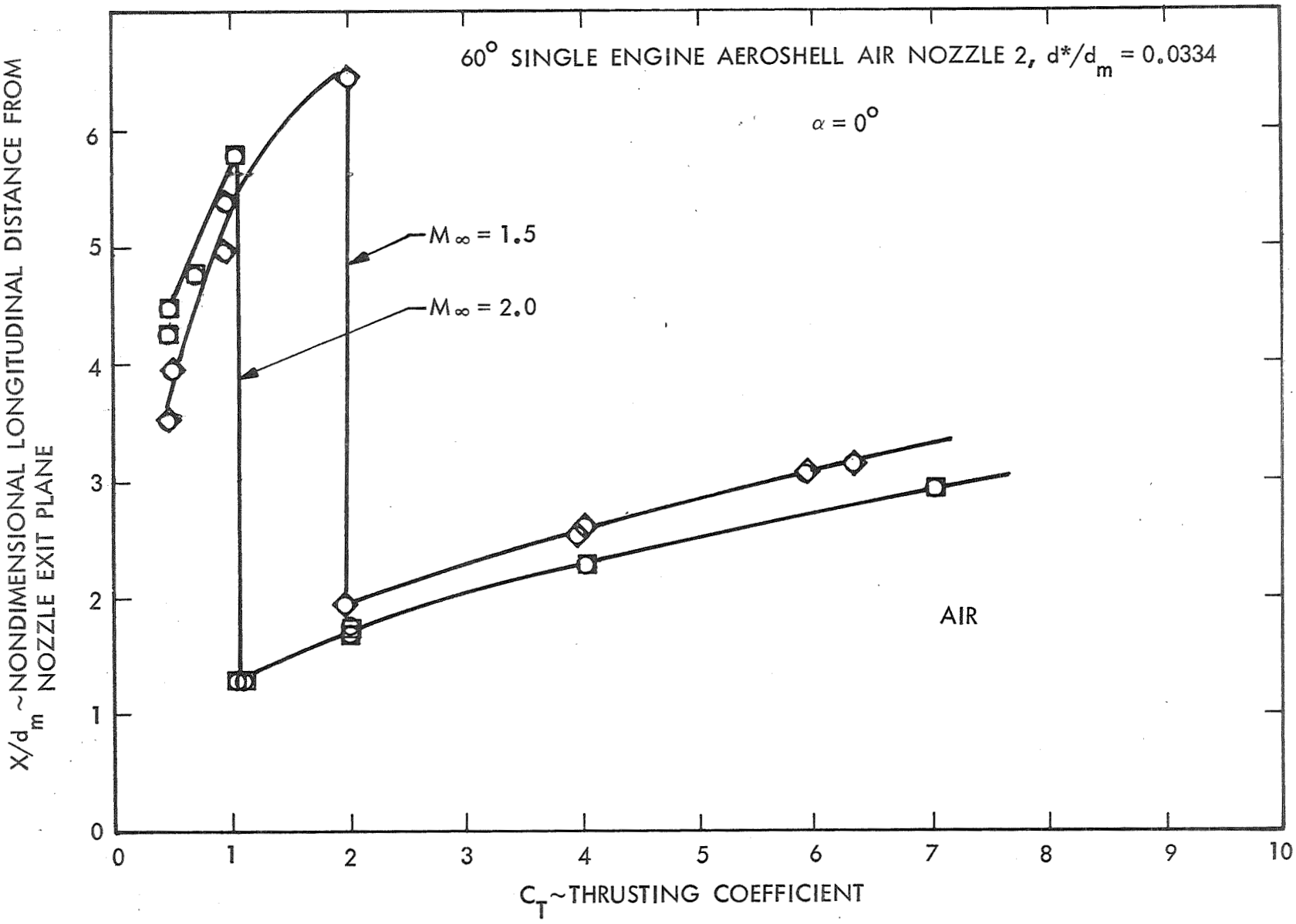

Figure 17 Variation of Bow Shock Location with Mach Number - Single Engine 60° Aeroshell - M_∞ = 1.5 and 2.0.

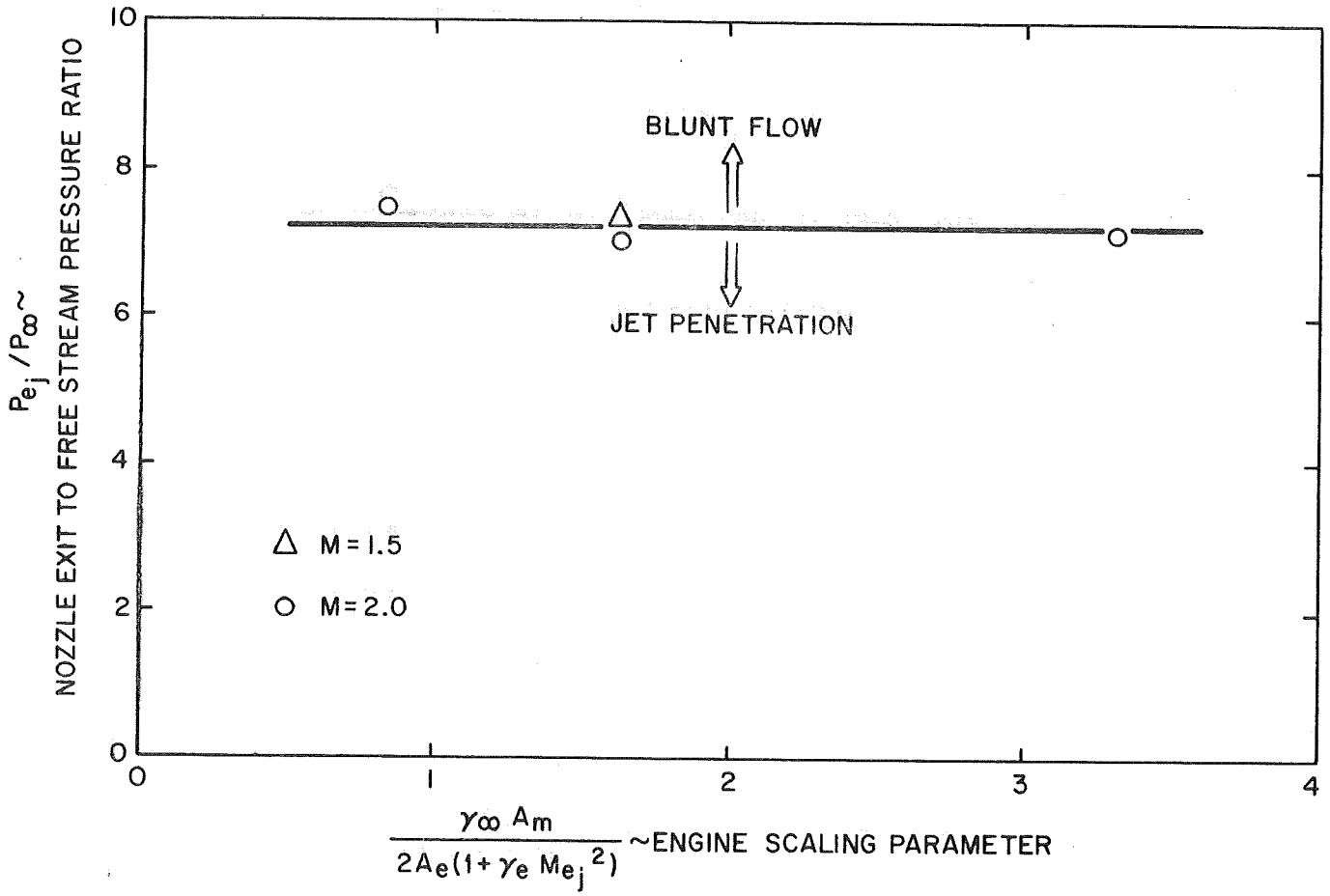

Figure 18 Pressure Ratio for Transition From Jet Penetration to Blunt Flow.

3.1.5 Flow Field Geometry

The shadowgraph pictures of the flow field in the blunt flow regime were analyzed for the locations of the bow shock, interface and terminal shock wave. Flow field geometry for air nozzle 2, which simulates the representative Mars lander vehicle, is shown in Figures 19 and 20 for free stream Mach numbers of $M_\infty = 1.5$ and $M_\infty = 2.0$ respectively. The interaction geometry is independent of aeroshell angle (Figure 20). Data for air nozzle 1 at $M_\infty = 2.0$ is shown in Figure 21. A comparison of this data with that for air nozzle 2 (Figure 20) indicates that the distances to the flow field features are less for the smaller nozzle as was expected. The experimental data indicates that the distance to the terminal shock wave varies as $(C_T)^{\frac{1}{2}}$ in agreement with the theoretical predictions of Reference 1. (See equation 42, page 39).

3.1.6 Aeroshell Surface Pressure Distributions

The change in surface pressure distribution on the forebody of the sixty degree single engine aeroshell as the retrorocket thrusting coefficient is increased is noted in Figures 22 through 25. Retrothrust coefficients of $C_T = 0$, 3.8, and 12.7 are considered at $M_\infty = 0.60$ in Figure 22. Data at $M_\infty = 0.60$ and thrusting coefficients of $C_T = 1.96$, 5.59 and 9.02 is shown in Figure 23. The pressure acting on the aeroshell forebody decreases with increasing thrusting coefficients. Pressure distributions at $M_\infty = 2.0$ are shown in Figures 24 and 25. This data indicates that at high thrusting coefficients, $C_T = 4.04$ (Figure 25) and $C_T = 7.0$ (Figure 24), the pressure acting on the outer portion of the forebody surface is constant. Base pressure measurements, for these cases, show that the base pressure is also equal to the pressure acting on the forebody surface. We conclude from these facts that the aeroshell is immersed in a constant pressure region and wake type flow exists. The increase in surface pressure near the aeroshell shoulder, $C_T = 2.0$ (Figure 24), is interpreted as indicating that reattachment of the interface shear layer to the aeroshell is occurring at this thrusting coefficient.

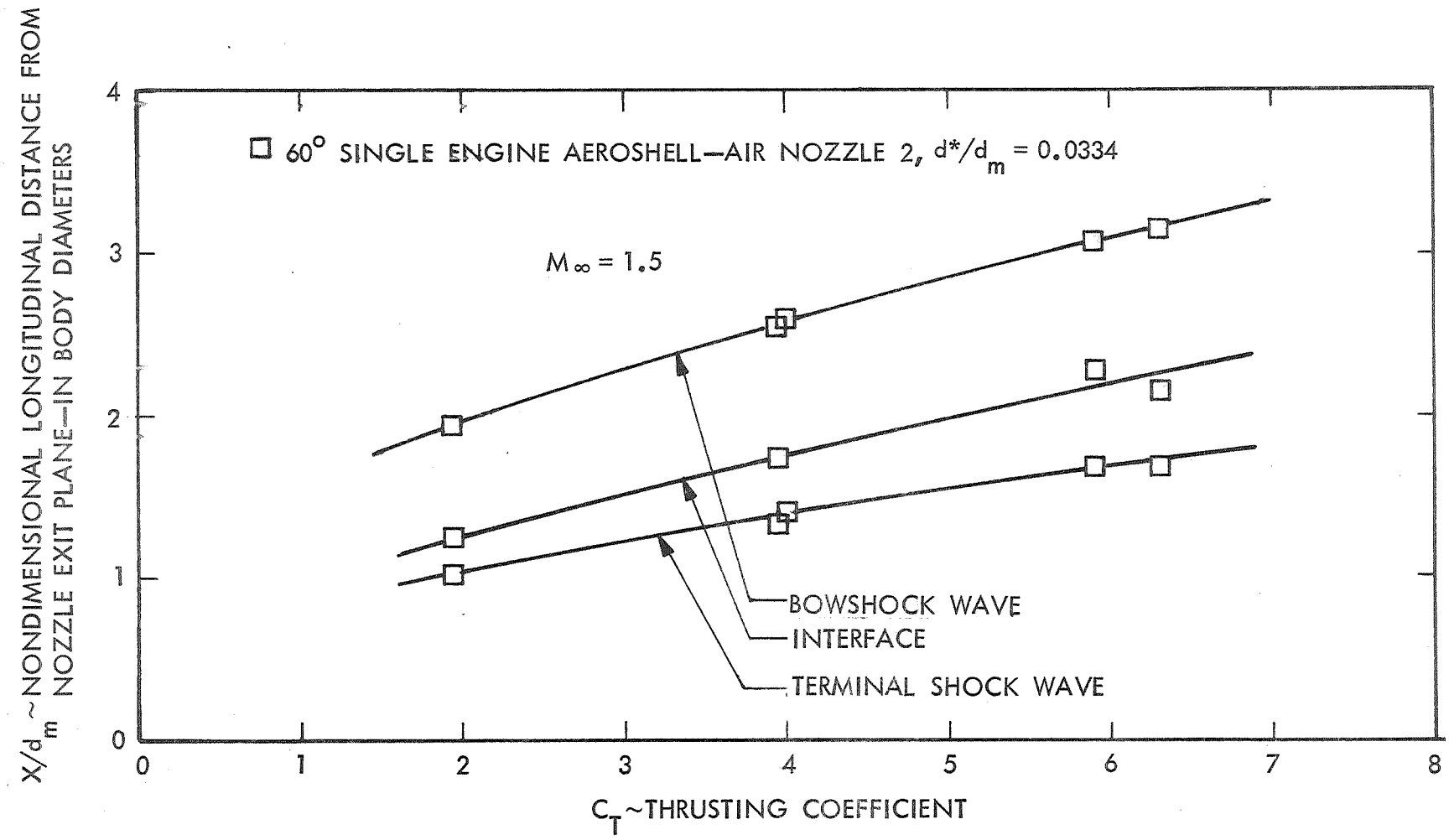

Figure 19 Retrorocket Plume Geometry - 60° Aeroshell - Air Nozzle 2, $M_\infty = 1.5$.

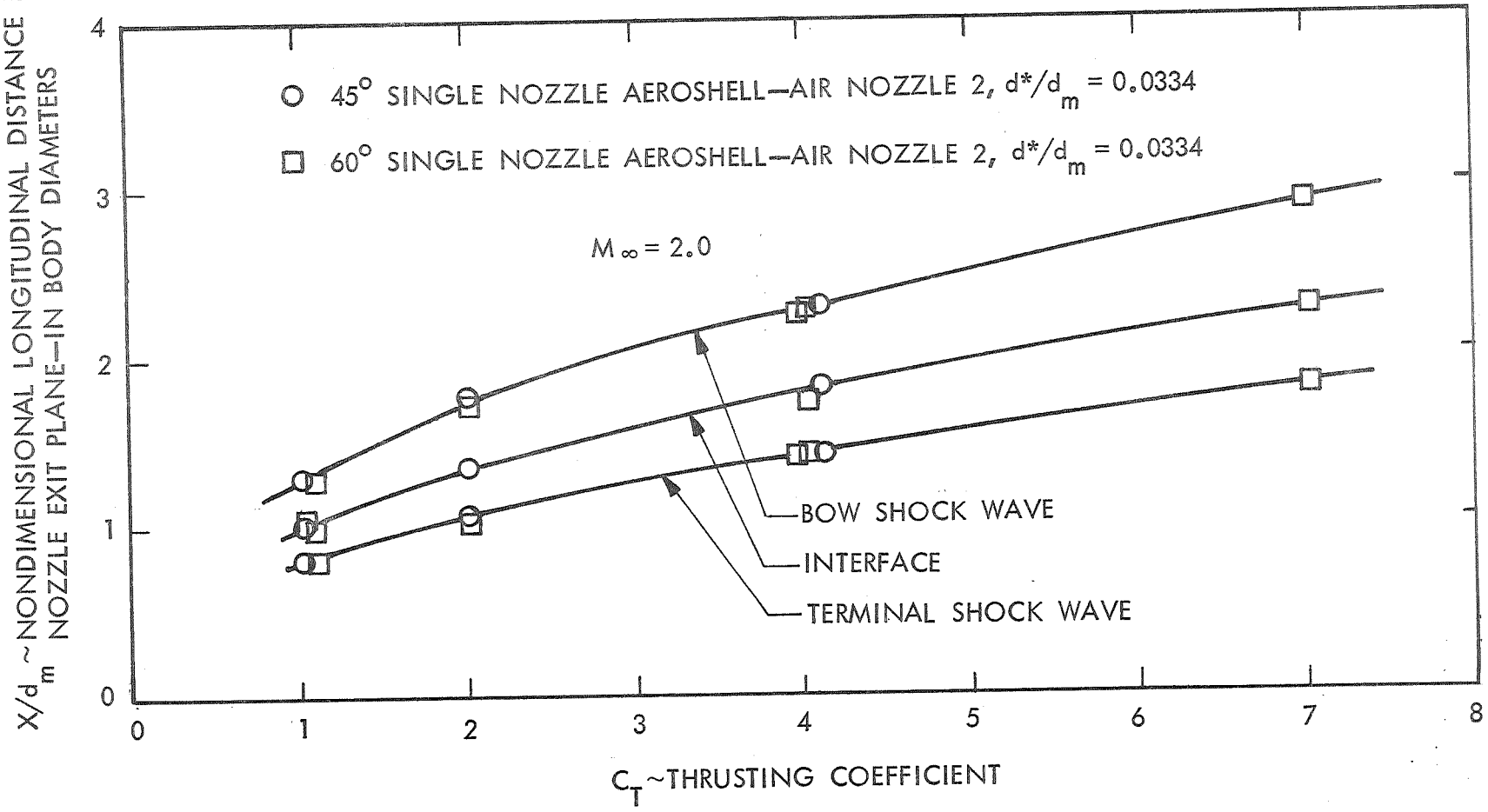

Figure 20 Flow Field Geometry - Air Nozzle 2, $M_\infty = 2.0$.

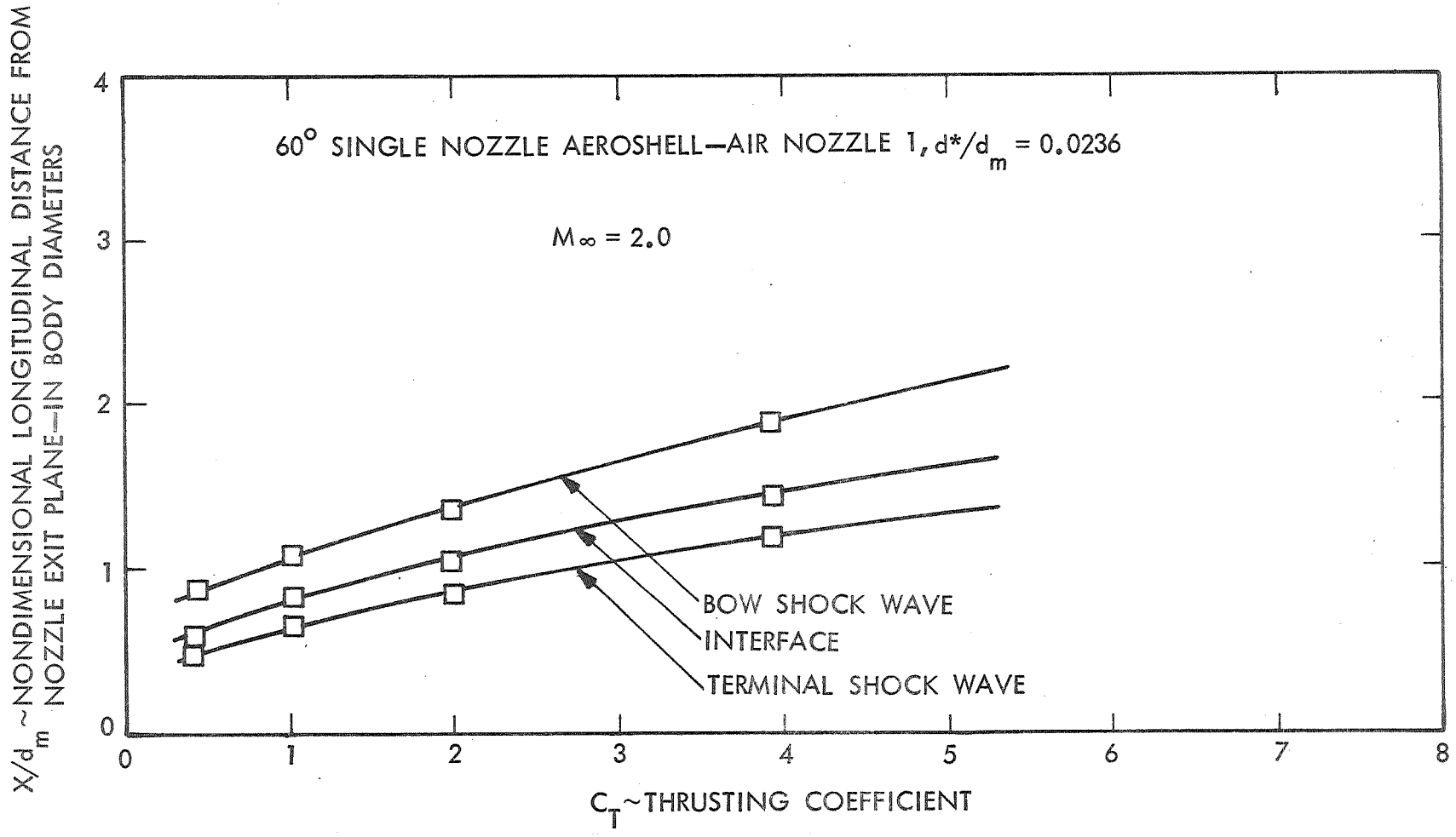

Figure 21 Location of Bow Shock, Interface and Terminal Shock Wave Air Nozzle 1, $M_\infty = 2.0$.

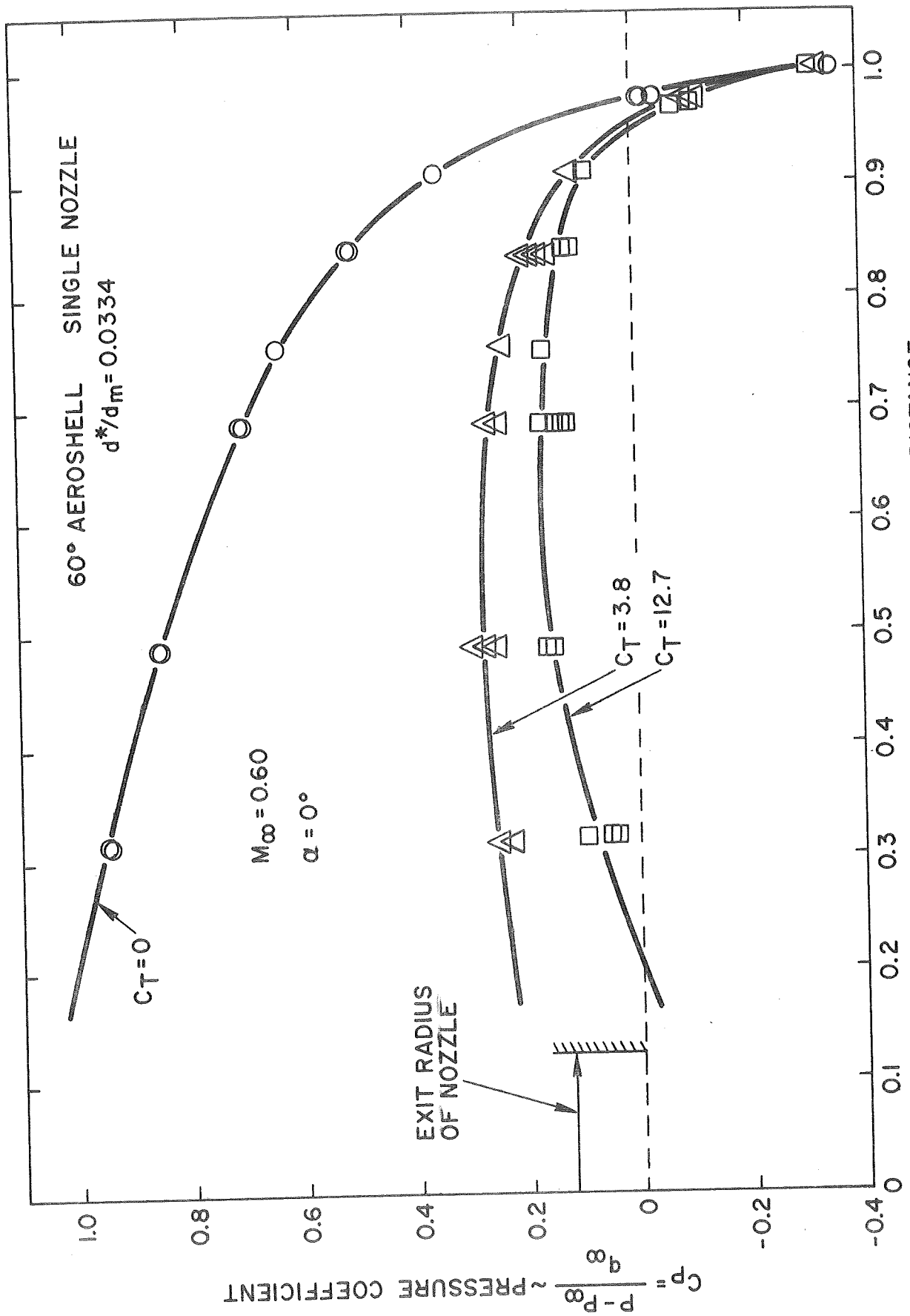

Figure 22 Variation of 60° Single Engine Aeroshell Surface Pressure Distribution with Retrothrust $M_\infty = 0.60$, $C_T = 0$, 3.8 and 12.7.

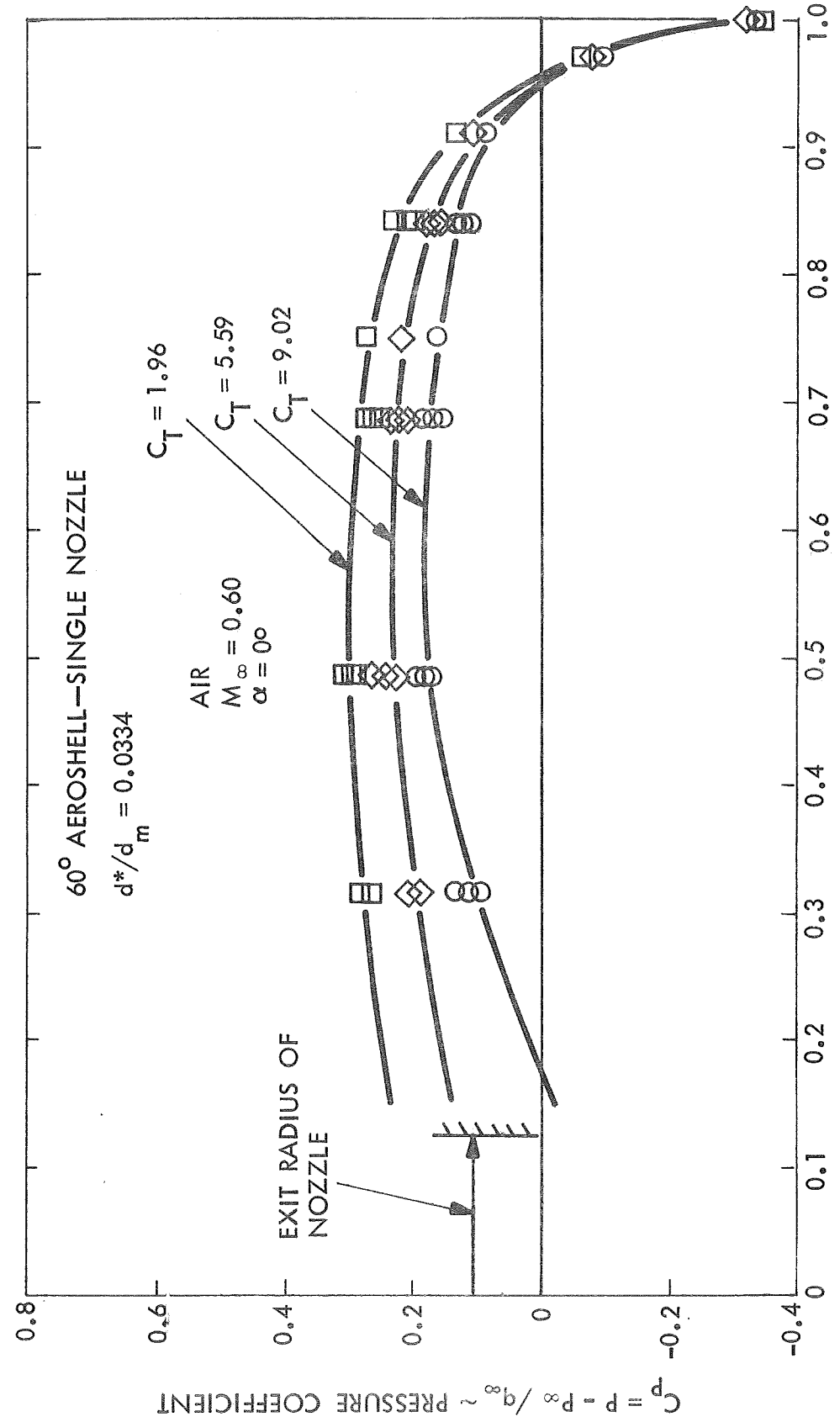

Figure 23 Aeroshell Pressure Distribution with Retrothrust, $M_\infty = 0.60$, $C_T = 1.96$, 5.59 and 9.02.

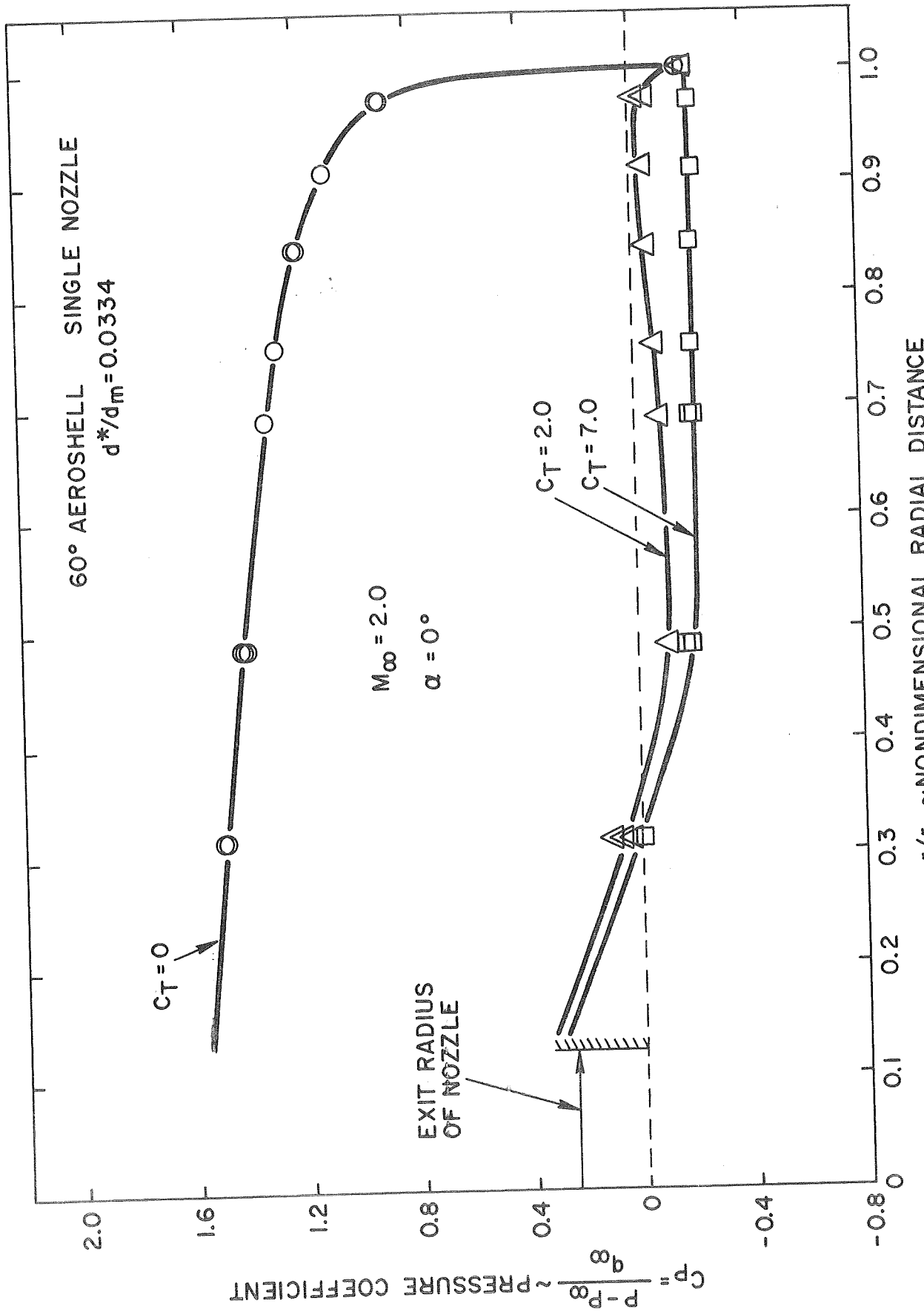

Figure 24 Variation of 60° Single Engine Aeroshell Surface Pressure Distribution With Retrothrust - M_∞ = 2.0.

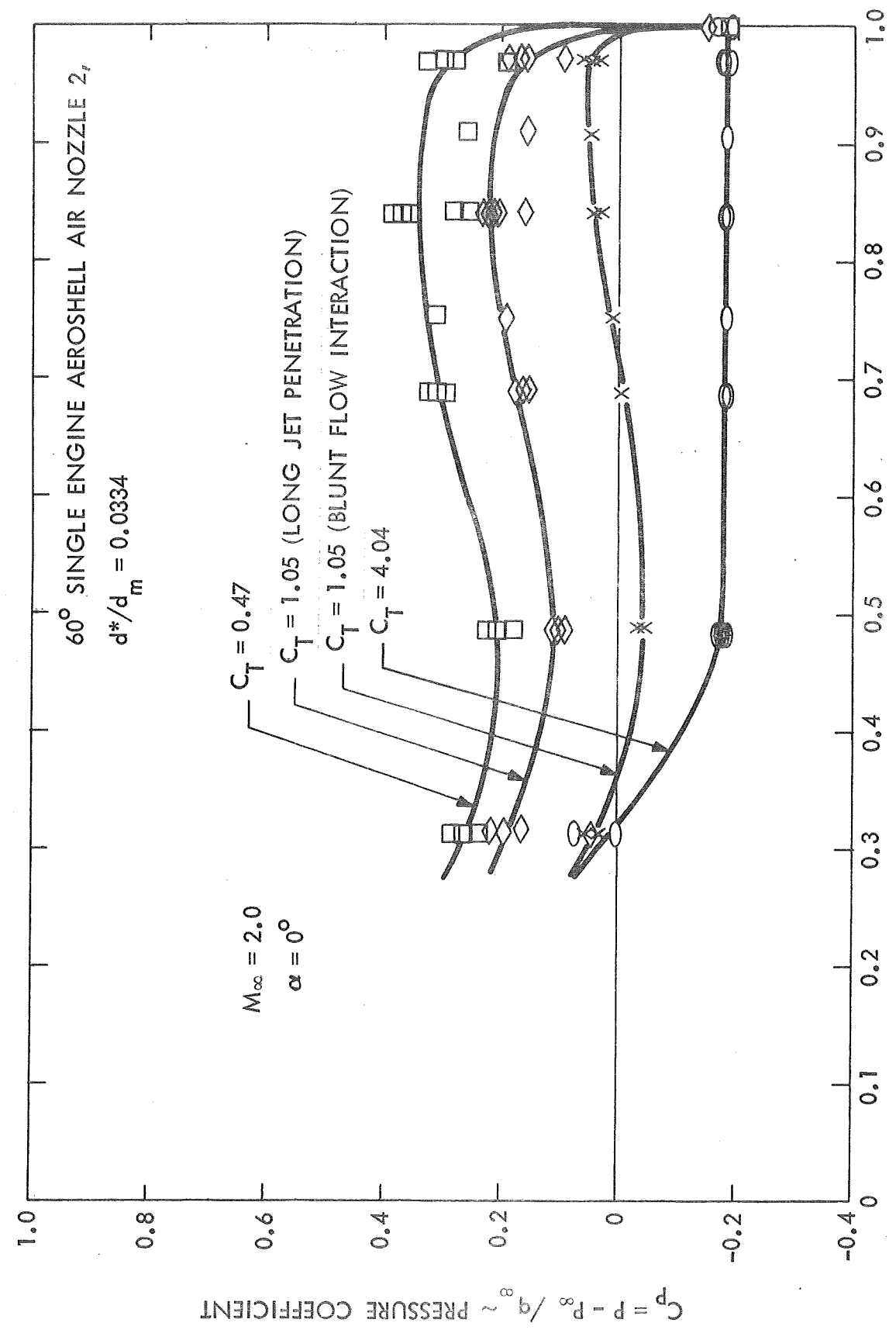

Figure 25 Single Engine Aeroshell Pressure Distribution with Retrothrust - $M_\infty = 2.0$, $C_T = 0.47$, 1.05 and 4.04.

3.1.7 Forebody and Base Pressure Variations with Thrusting Coefficient

The average aeroshell frontal surface and base pressures are plotted as a function of thrusting coefficient in Figures 26 through 29. Data for 45^{o} and 60^{o} aeroshell vehicles are superimposed and indicates little effect of aeroshell angle on the resulting pressures. At $M_{\infty} = 0.60$ (Figure 26) and $M_{\infty} = 1.05$ (Figure 27), the average frontal pressure remains higher than the base pressure, for thrusting coefficients considered in the present experiment. At supersonic speeds of $M_{\infty} = 1.5$ (Figure 28) and $M_{\infty} = 2.0$ (Figure 29), the average frontal pressure decreases with increases in thrusting coefficient and becomes equal to the base pressure at the larger thrusting coefficients.

3.1.8 Transition from Flow Reattachment to Wake Type Flow

Transition from shear layer reattachment type flow to wake type flow is assumed to occur at supersonic speeds when the average frontal surface pressure becomes equal to the base pressure. The thrusting coefficient magnitude for transition from flow reattachment to wake type flow is noted in Figure 30 for free stream Mach numbers of $M_{\infty} = 1.5$ and 2.0.

3.1.9 Universal Base Pressure Correlation

The universal base pressure correlation shown in Figure 31 is based on the experimental data recorded for all single engine aeroshell models utilizing air exhaust flow and provides results within 10% of any of the experimental data.

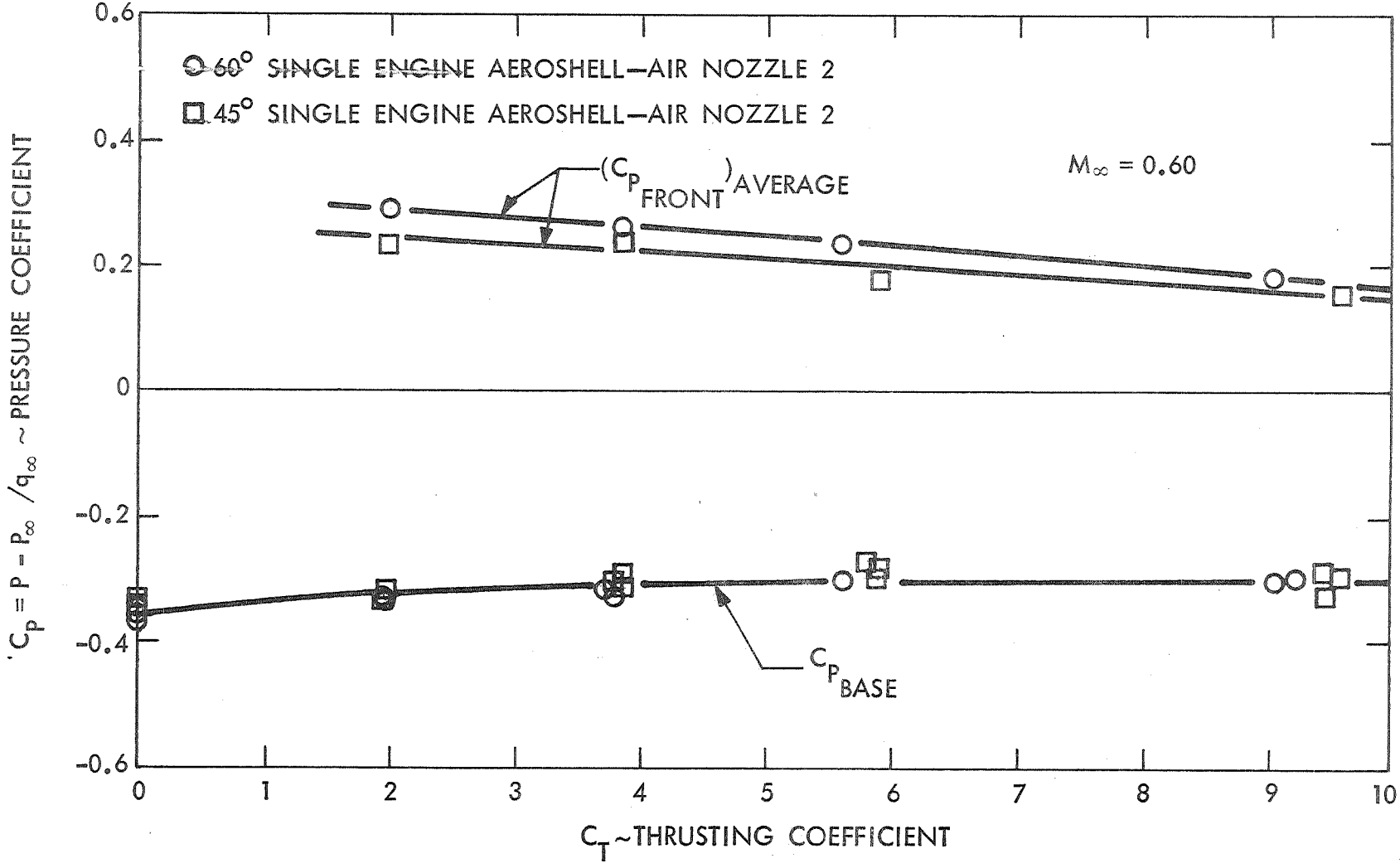

Figure 26 Average Frontal and Base Pressures - Single Engine Aeroshells, $M_\infty = 0.60$.

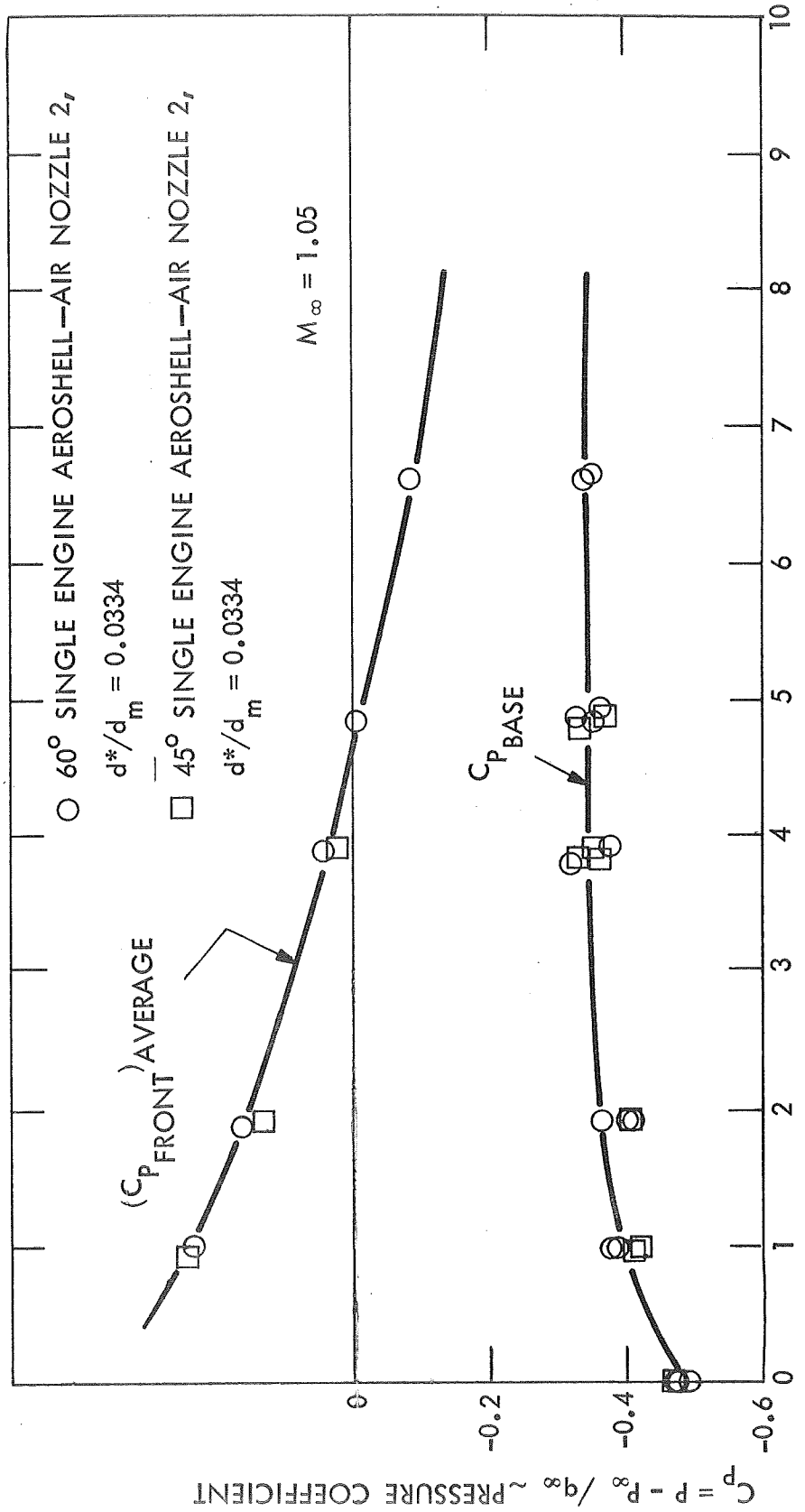

Figure 27 Average Frontal and Base Pressures - Single Engine Aeroshells, $M_\infty = 1.05$.

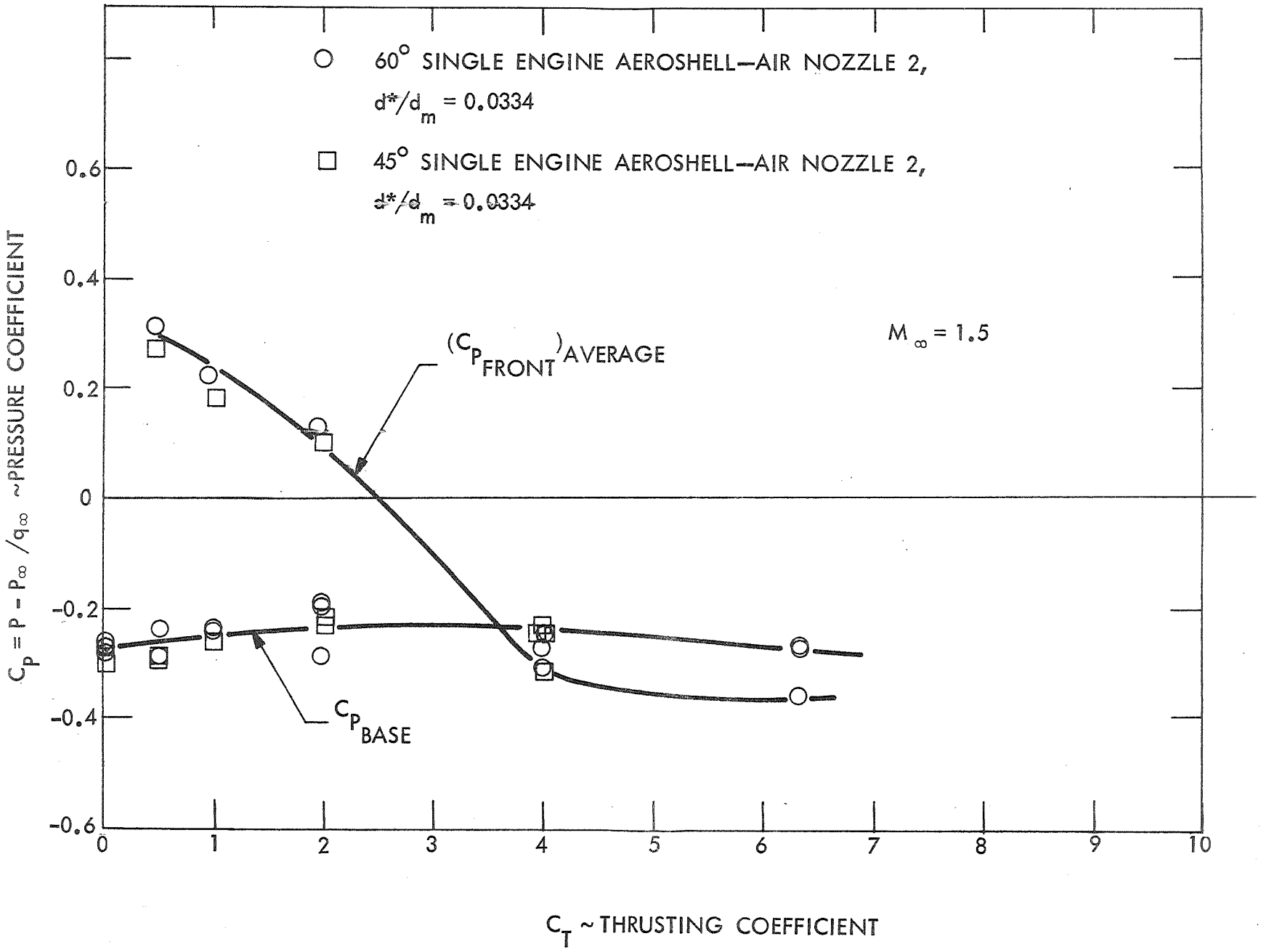

Figure 28 Average Frontal and Base Pressures - Single Engine Aeroshells, $M_\infty = 1.5$.

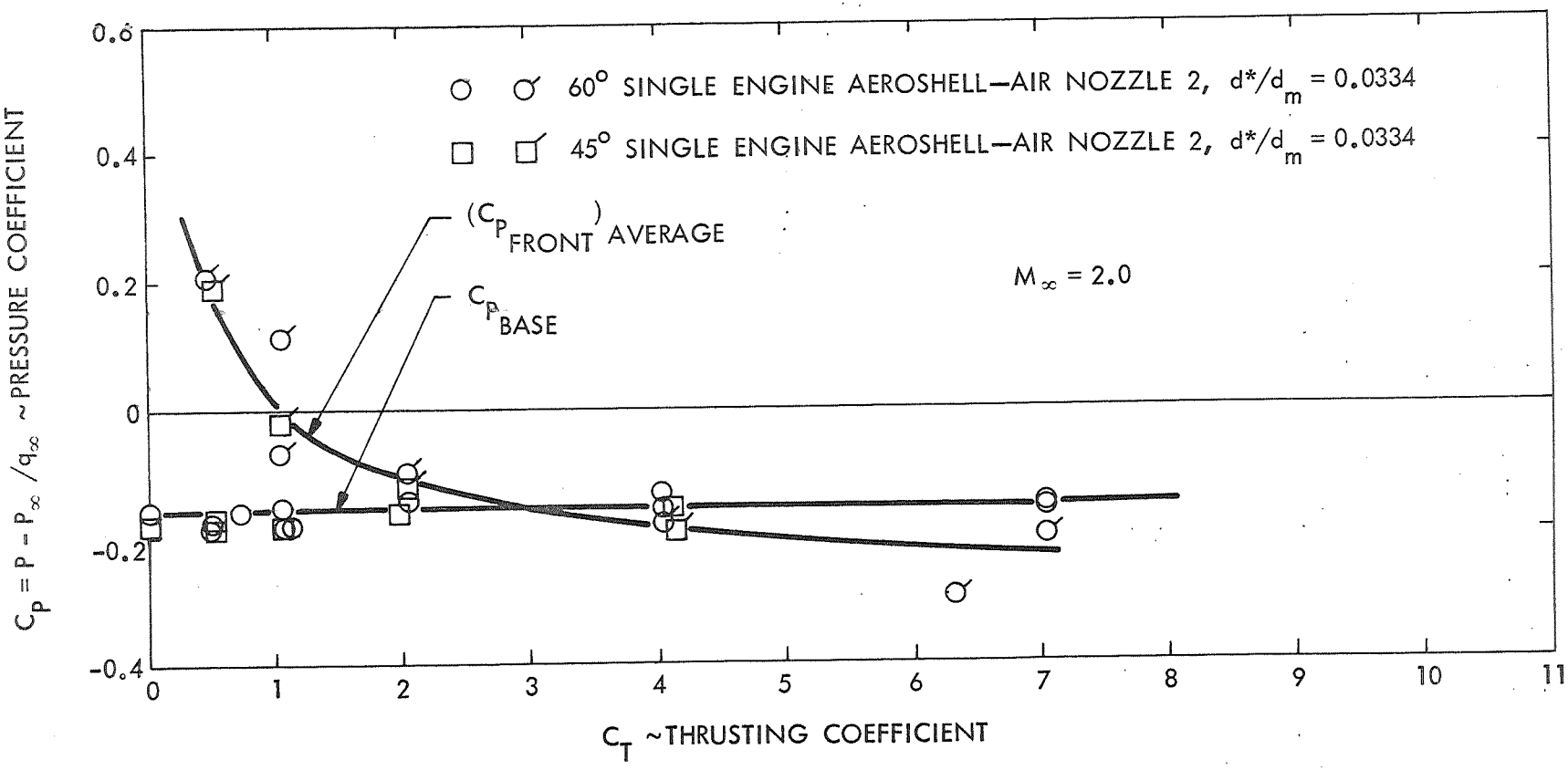

Figure 29 Average Frontal and Base Pressures - Single Engine Aeroshell, $M_\infty = 2.0$.

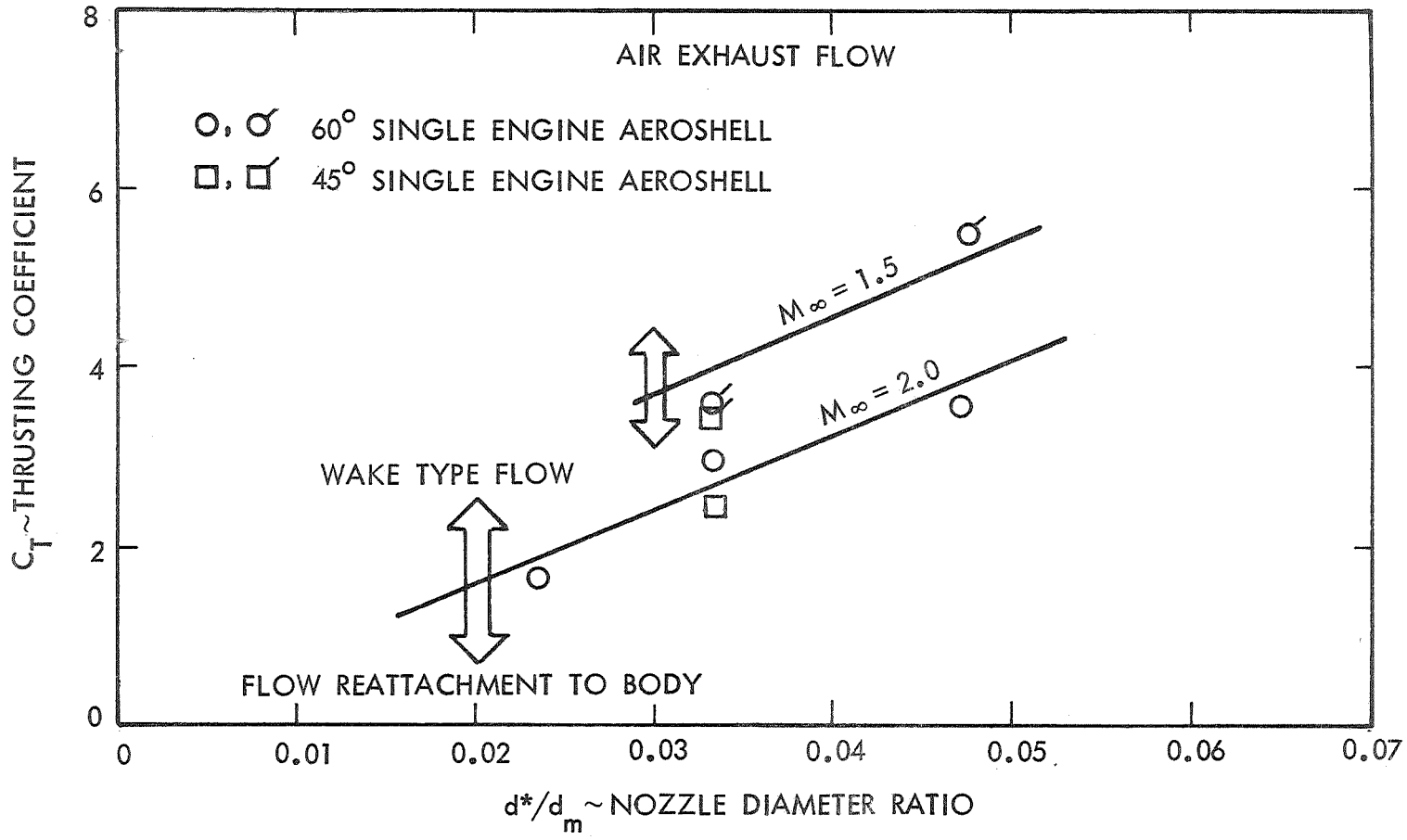

Figure 30 Thrusting Coefficient Magnitude for Transition from Flow Reattachment to Wake Type Flow.

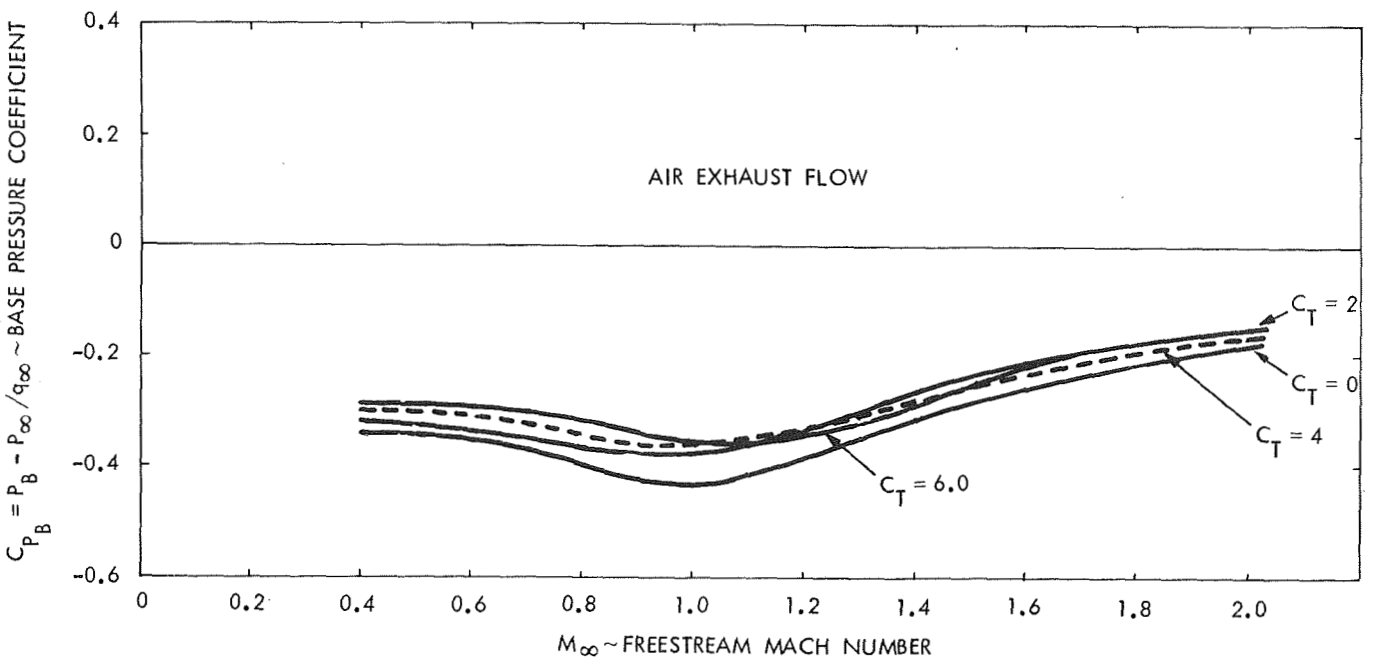

Figure 31 Average Base Pressure Correlation, Single Nozzle Aeroshell Models with Retorthrust.

3.1.10 Forebody Axial Force Coefficient with Retrothrust

The application of retrothrust from a single centrally mounted engine was shown to cause the pressure on the forebody surface to decrease substantially below the no retrothrust case, (Figures 22 through 25). The corresponding decreases in forebody axial force coefficient with increases in retrothrust coefficient are shown in Figures 32 through 36. Application of retrothrust results in a sharp decrease in forebody axial force coefficient at all Mach numbers (Figure 32). The axial force coefficients for the 60^{o} single aeroshell, utilizing air nozzle 2 which simulates the representative Mars lander vehicle are shown in Figures 32 and 33. For thrusting coefficients above two, there is little difference between the total axial force coefficient (i.e. sum of forebody axial force coefficient and thrusting coefficient) and the thrusting coefficient of the retrorocket alone. The forebody axial force coefficients were obtained by integrating the pressure data over the surface of the aeroshell and assume that the base pressure acting on the aeroshell is the free stream static pressure. No correction was made to the data to account for the actual, experimentally measured base pressures.

Forebody axial force coefficients for 60^{o} single engine aeroshells utilizing air nozzle 1 and air nozzle 3 are shown in Figures 34 and 35 respectively. Data for the 45^{o} single engine aeroshell using air nozzle 2 is noted in Figure 36.

3.1.11 Aeroshell Stability

The variation of pitching moment and normal force coefficients with angle-of-attack for the 45^{o} and 60^{o} single engine aeroshells is linear to six degrees angle-of-attack for all Mach numbers tested, with and without retrothurs. The magnitude of the pitching moment and normal force slopes agree quite well with other NASA and JPL experiments for the case of no retrothrust ($C_{T} = 0$). The change of pitching moment slope, normal force slope and aerodynamic center location with application of retrothrust is shown in Figures 37 through 39 for the 60^{o} aeroshell and Figures 40 through 42 for the

45^{o} aeroshell. The pitching moment coefficient is referred to the virtual nose of the aeroshell. The pitching moment slope increases substantially as the thrusting coefficient is increased to unity (Figure 37). The pitching moment slope decreases from this level with further increases in thrusting coefficient. The pitching moment slope with retrothrust is greater than the no retrothrust case at all Mach numbers for thrusting coefficients up to $C_T = 2.5$. The normal force slope shows the same variation with thrusting coefficient as the pitching moment slope (Figure 38). The aerodynamic center location remains essentially unchanged (Figure 39) with application of retrothrust. The aerodynamic center is about one half a base diameter behind the base of the 60^{o} aeroshell (Figure 39). The variation of pitching moment slope, normal force slope and aerodynamic center location with retrothrust for the 45^{o} aeroshell (Figures 40, 41, and 42 respectively) is quite similar to that observed for the 60^{o} single engine aeroshell. However, the aerodynamic center of this configuration is located nearer to the vehicle base (Figure 42).

3.1.12 Aerodynamic Characteristics with Helium Exhaust Flow

A portion of the experimental testing was performed with helium retrorocket exhaust flow. A previous theoretical analysis[1] indicated that the speed of sound ratio across the interface, which separates the shocked free stream gases from the retrorocket exhaust gases, has an important effect on mixing in the interface shear layer. (See Figure 15). In the case of the representative Mars lander vehicle, the speed of sound ratio arises from the substantial difference in temperature between the shocked free stream and exhaust gases and differences in specific heat ratio and gas constant of the two streams. The exhaust gases are about nine times hotter than the free stream gases. The helium exhaust flow was used to test experimentally the effect of changing the speed of sound ratio on the mixing and its subsequent effect on the aeroshell aerodynamic characteristics.

Tests were performed at helium thrusting coefficients up to about $C_T = 11.0$ at subsonic ($M_\infty = 0.80$) and transonic ($M_\infty = 1.05$) speeds and up to about $C_T = 4.0$ at supersonic speeds. The location of the bow shock wave at supersonic free stream velocities, for the single engine 60^o aeroshell with the helium nozzle, is shown in Figure 43. The characteristics of the helium nozzle are noted in Table 1 and were chosen to simulate the representative Mars lander vehicle. The helium jet penetrated further forward into the oncoming air free stream flow than the air jet from air nozzle 2, when both nozzles operated at the same thrusting coefficient. The bow shock wave location for the helium jet could not be photographed above thrusting coefficients of $C_T = 0.6$ because it passed from the field of view of the shadowgraph system. The aeroshell-wind tunnel window geometry was such that the window edge was about six and one half base diameters upstream from the aeroshell nozzle exit plane. Shadowgraph pictures were taken of the exhaust plume in field of view of shadowgraph at thrusting coefficients up to $C_T = 4.0$ at $M_\infty = 2.0$. The flow pattern observed was always that of long jet penetration. Tests were not performed at higher thrusting coefficients in order to minimize the amount of helium consumed and therefore, it is not possible to say whether transition to a blunt flow interaction would have occurred, as with air exhaust flow, when the nozzle to free stream pressure ratio reached $P_{e_j} / P_\infty \approx 7.0$.

The pressure distributions with retrothrust and helium exhaust flow are shown in Figure 44 for $M_\infty = 0.60$ and $C_T = 1.68$, 6.76 and 13.91. Pressure distributions for $M_\infty = 2.0$ and thrusting coefficients up to 3.6 are shown in Figure 45.

The effect of retrothrust on the forebody axial force coefficient for helium exhaust flow is noted in Figure 46. A comparison of the helium data with air nozzle 2 data (Figures 32 and 33) indicates that the forebody axial force coefficients with helium flow are significantly different than those with air nozzle flow at all Mach numbers tested.

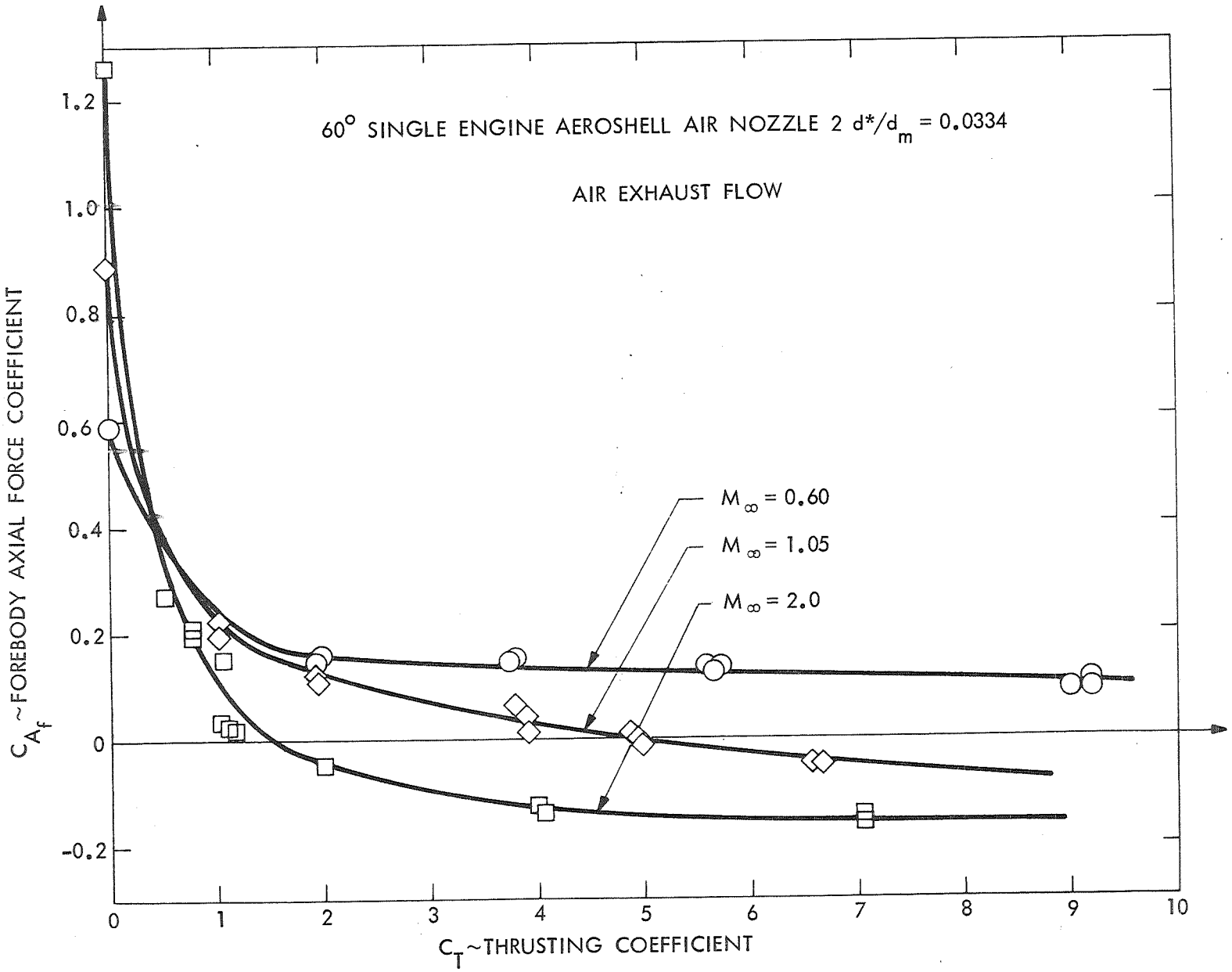

Figure 32 Effect of Retrothrust on the Forebody Axial Force Coefficient - 60° Single Engine Aeroshell - M_∞ = 0.6, 1.05, and 2.0.

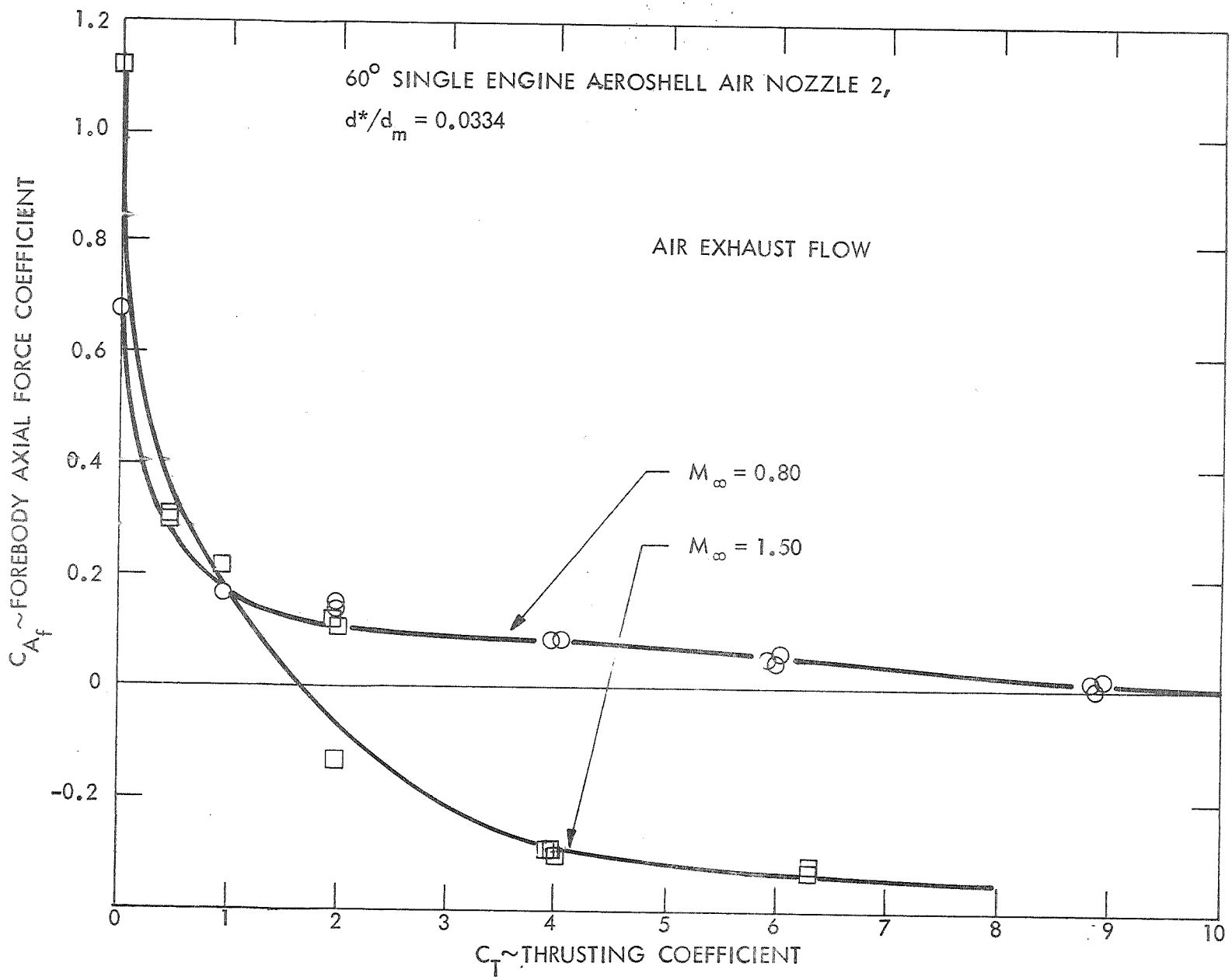

Figure 33 Effect of Retrothrust on the Forebody Axial Force Coefficient - 60° Single Engine Aeroshell - M_∞ = 0.80 and 1.5, Air Nozzle 2.

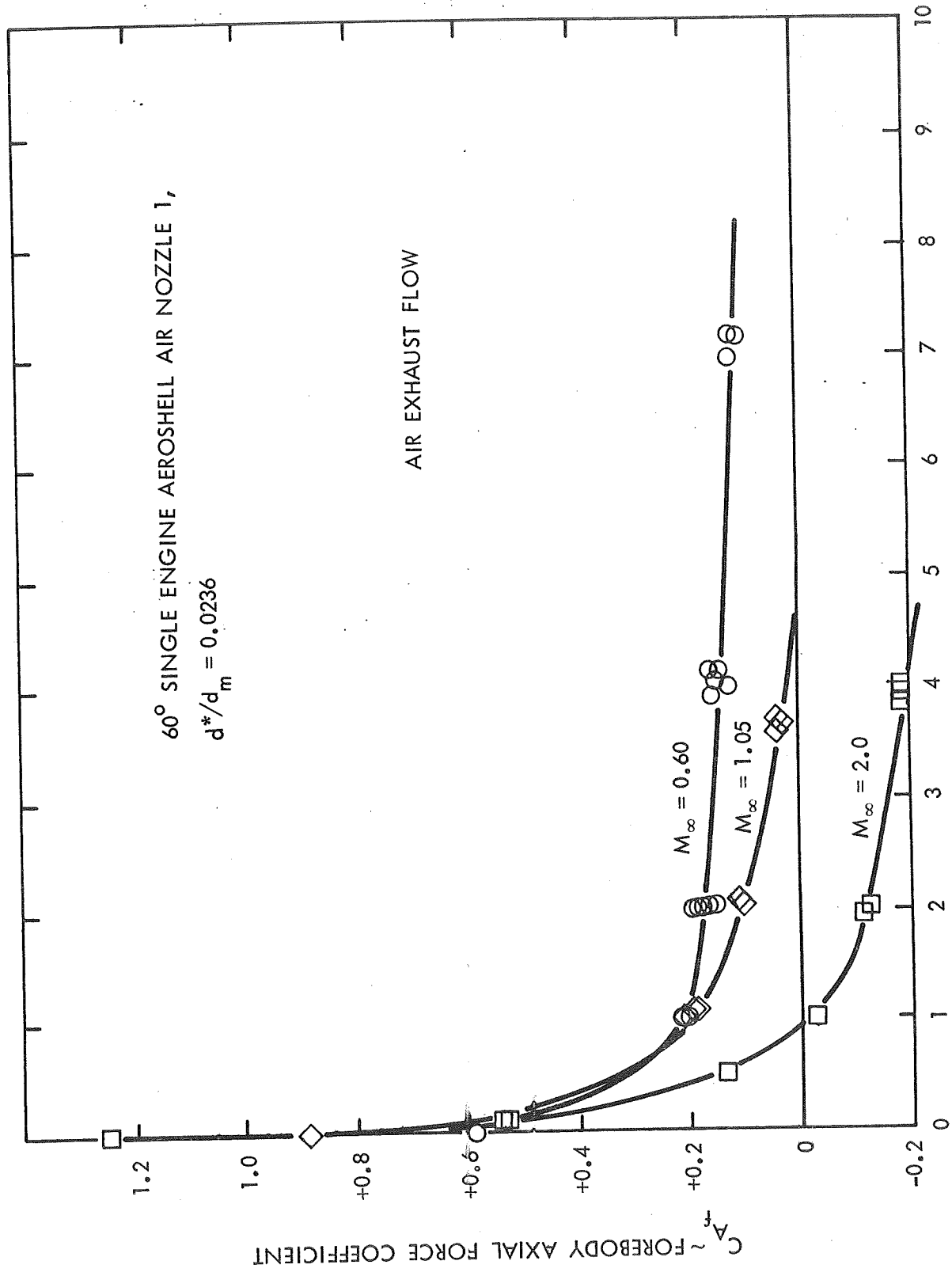

Figure 34 Effect of Retrothrust on the Forebody Axial Force Coefficient - 60° Single Engine Aeroshell - M_∞ = 0.60, 1.05 and 2.0, Air Nozzle 1.

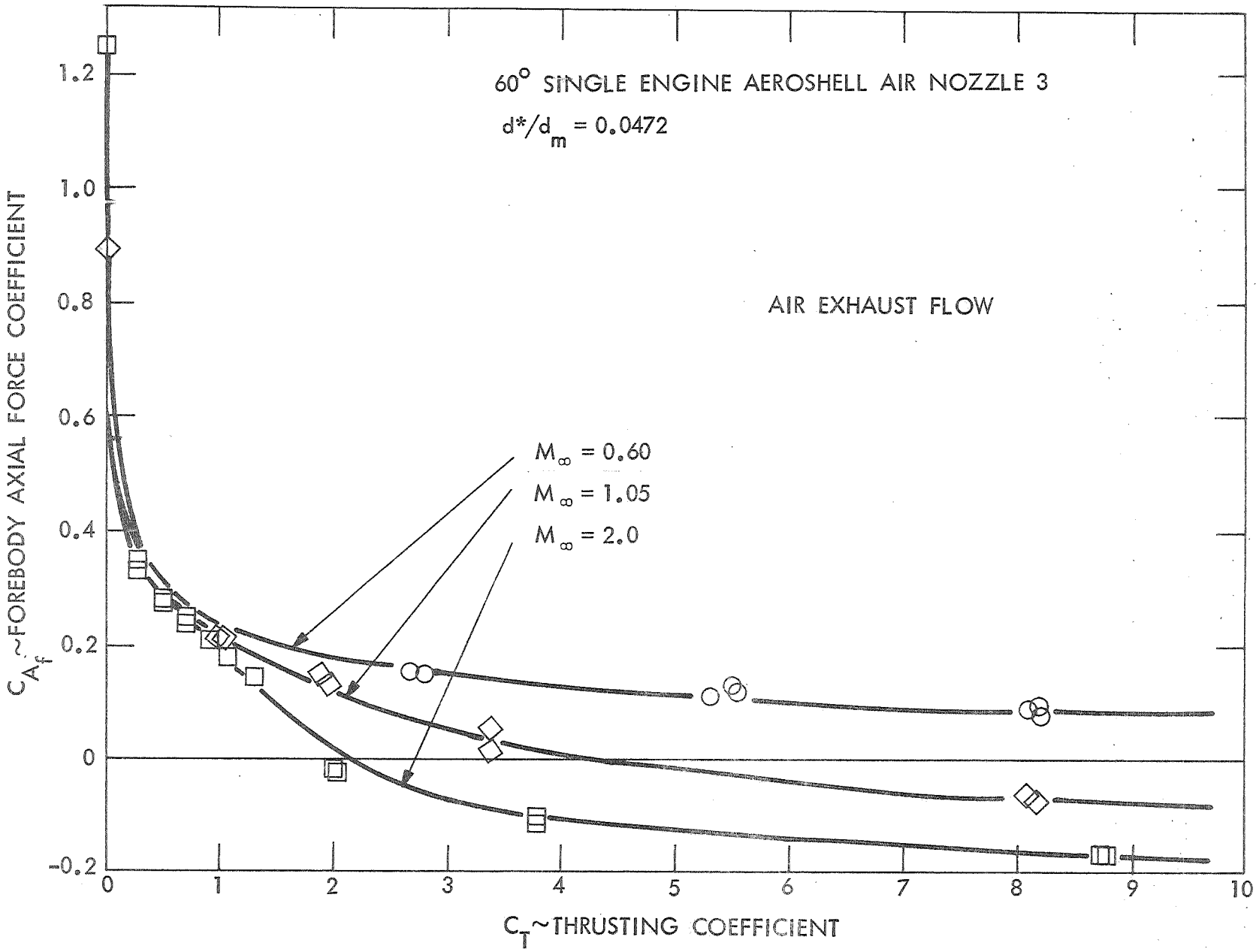

Figure 35 Effect of Retrothrust on the Forebody Axial Force Coefficient - 60° Single Engine Aeroshell - M_∞ = 0.60, 1.05 and 2.0, Air Nozzle 3.

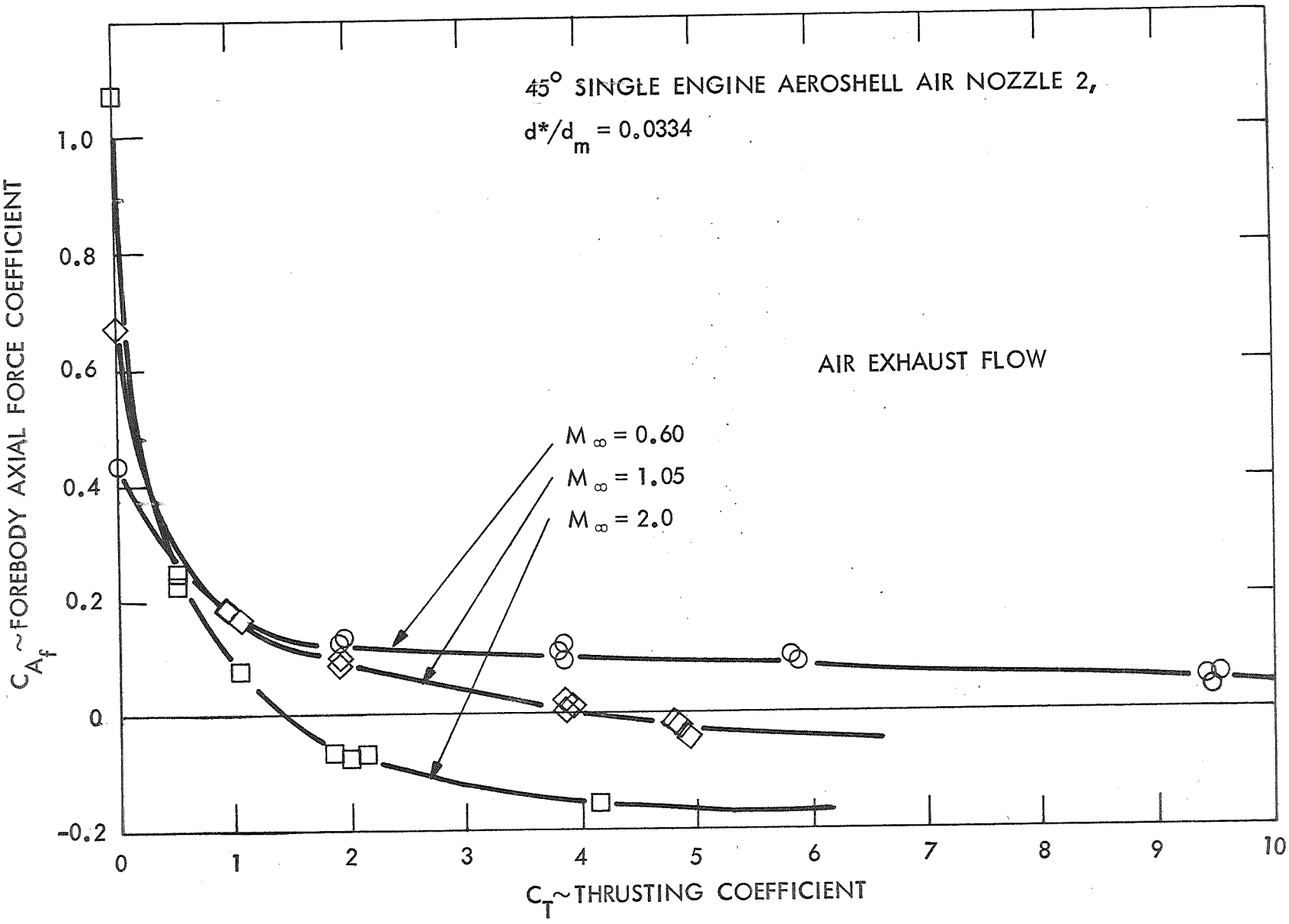

Figure 36 Effect of Retrothrust on the Forebody Axial Force Coefficient - 45° Single Engine Aeroshell - M_∞ = 0.60, 1.05 and 2.0, Air Nozzle 2.

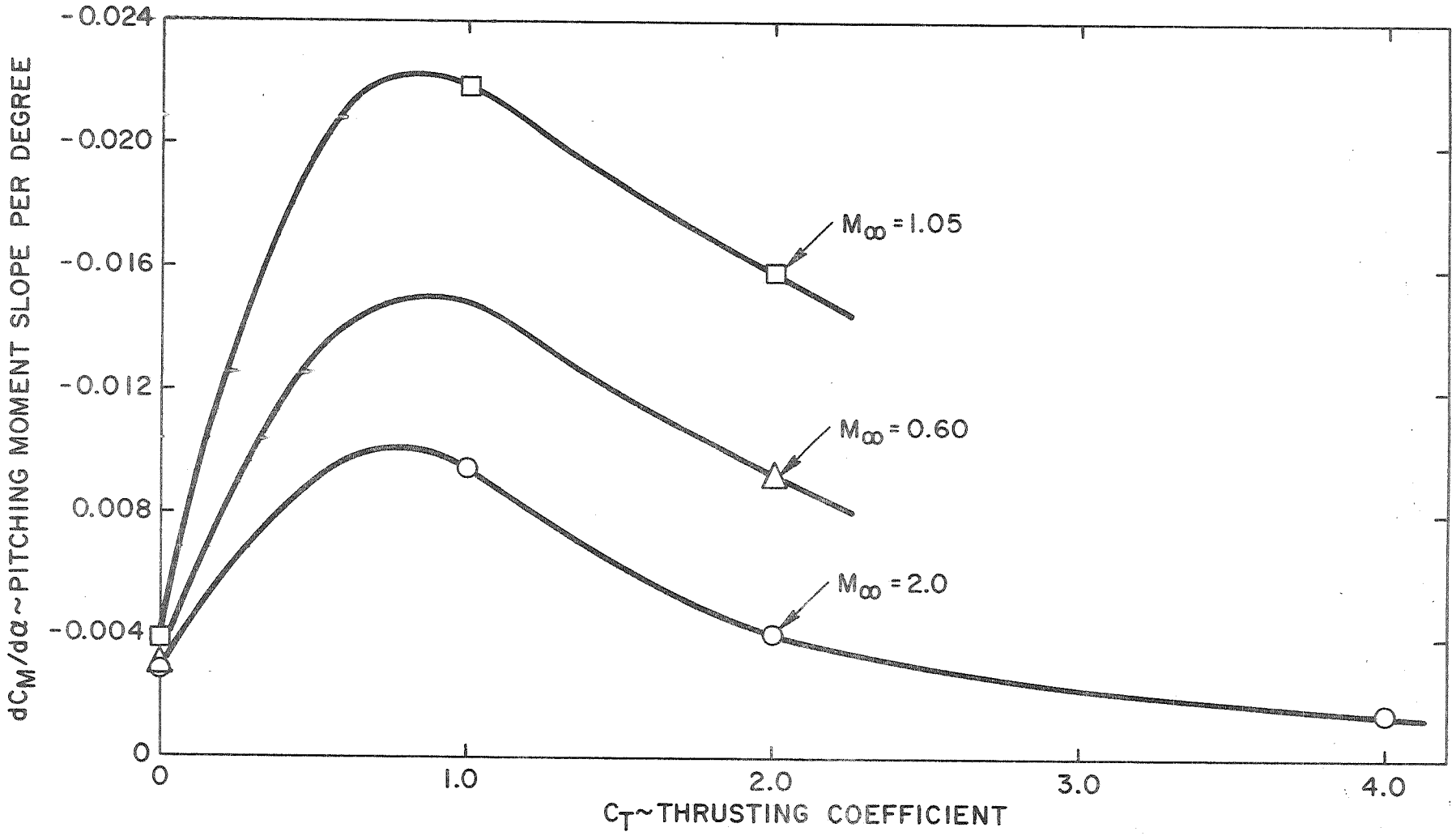

Figure 37 Variation of Pitching Moment Slope with Thrusting Coefficient - 60° Single Engine Aeroshell.

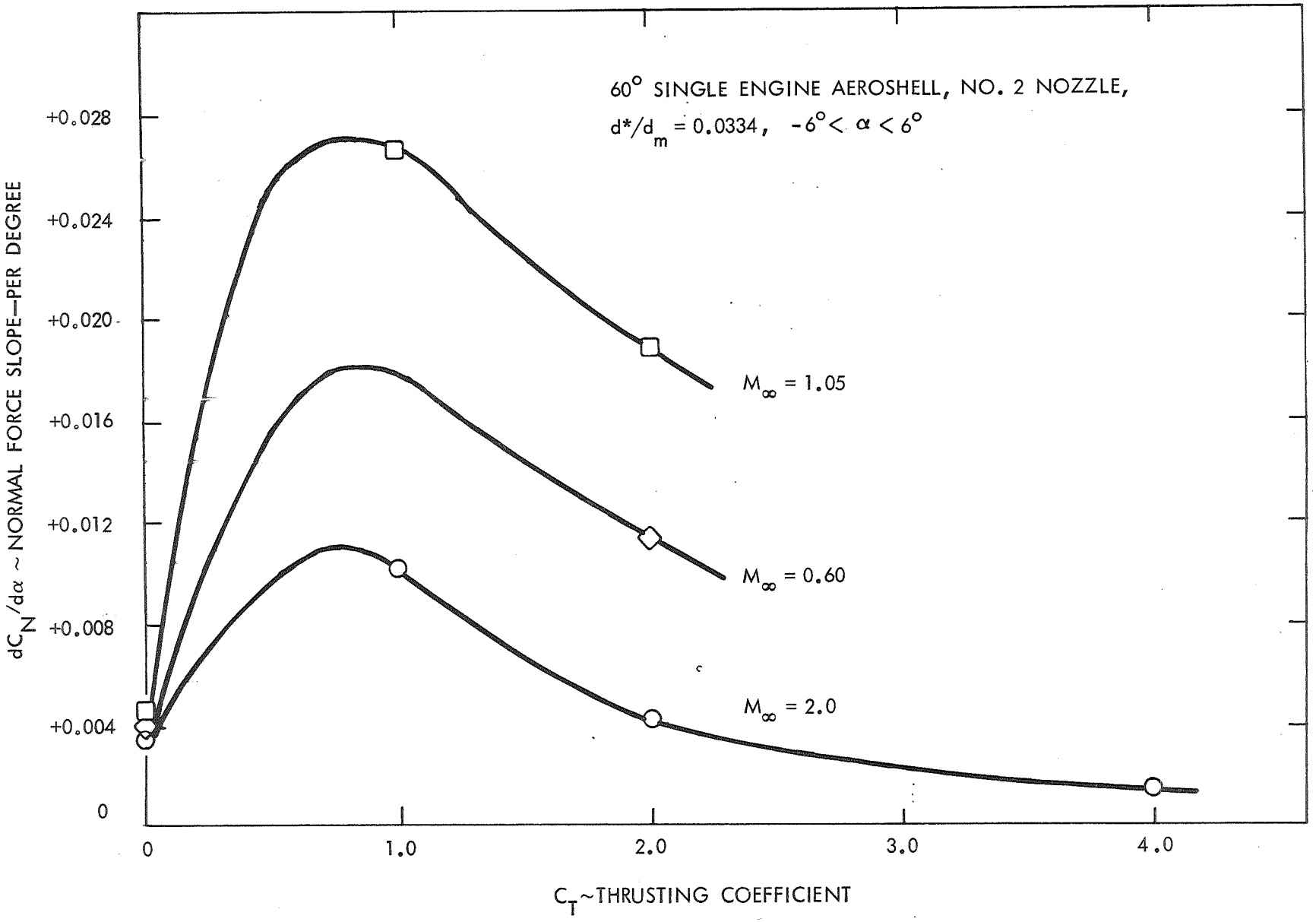

Figure 38 Variation of Normal Force Slope with Thrusting Coefficient 60° Single Engine Aeroshell.

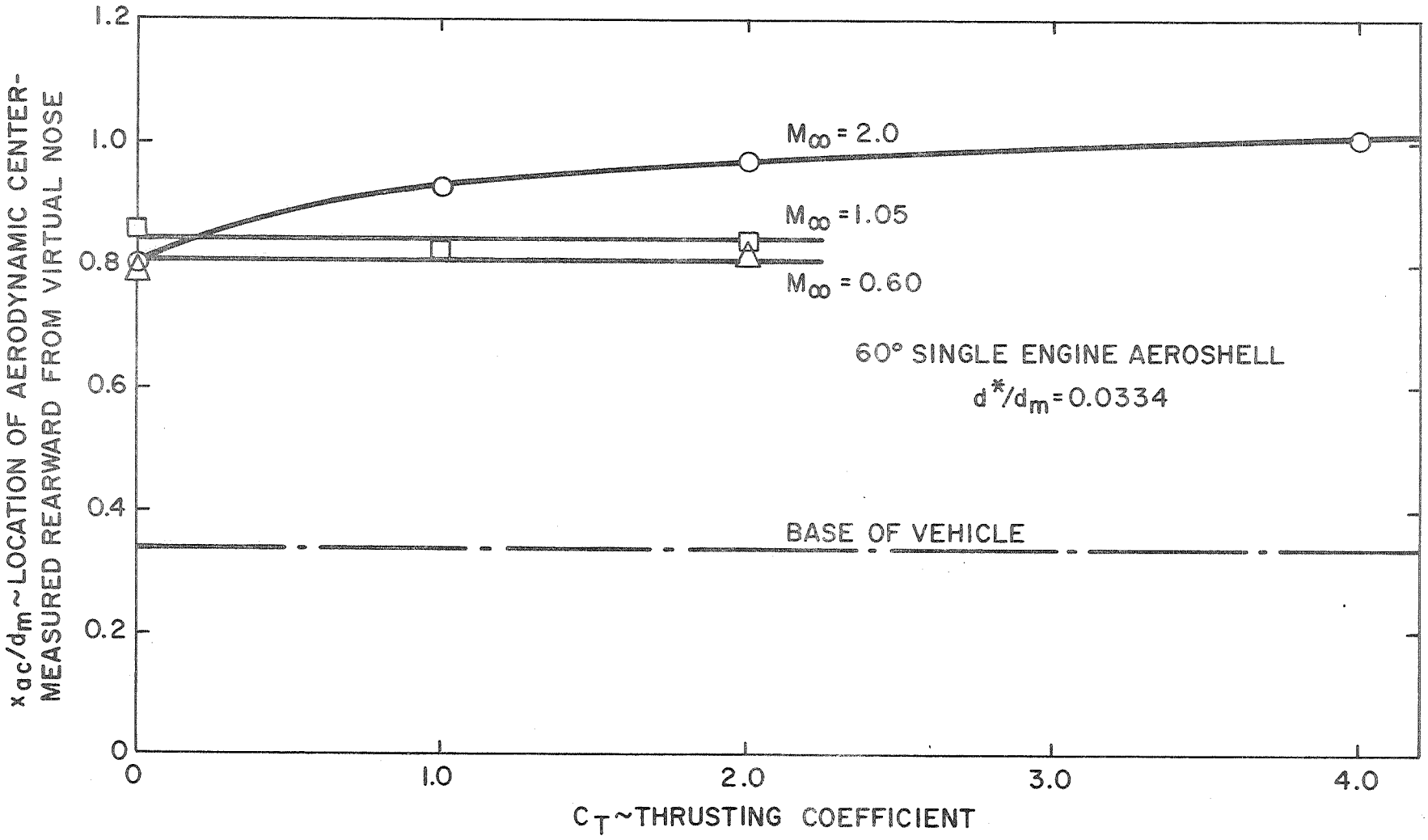

Figure 39 Effect of Retrothrust on Aerodynamic Center Location - 60° Single Engine Aeroshell.

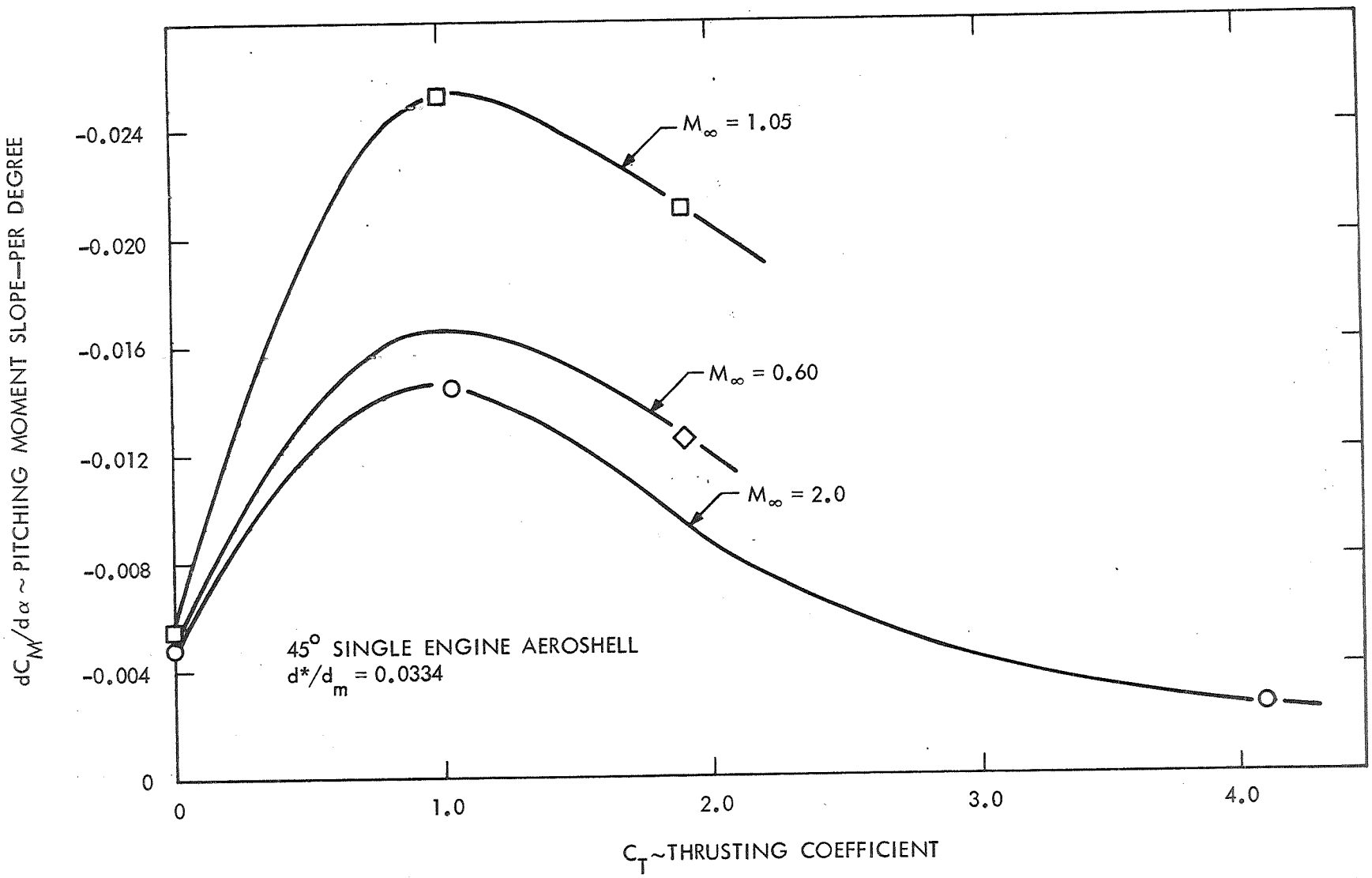

Figure 40 Variation of Pitching Moment Slope with Thrusting Coefficient - 45° Single Engine Aeroshell.

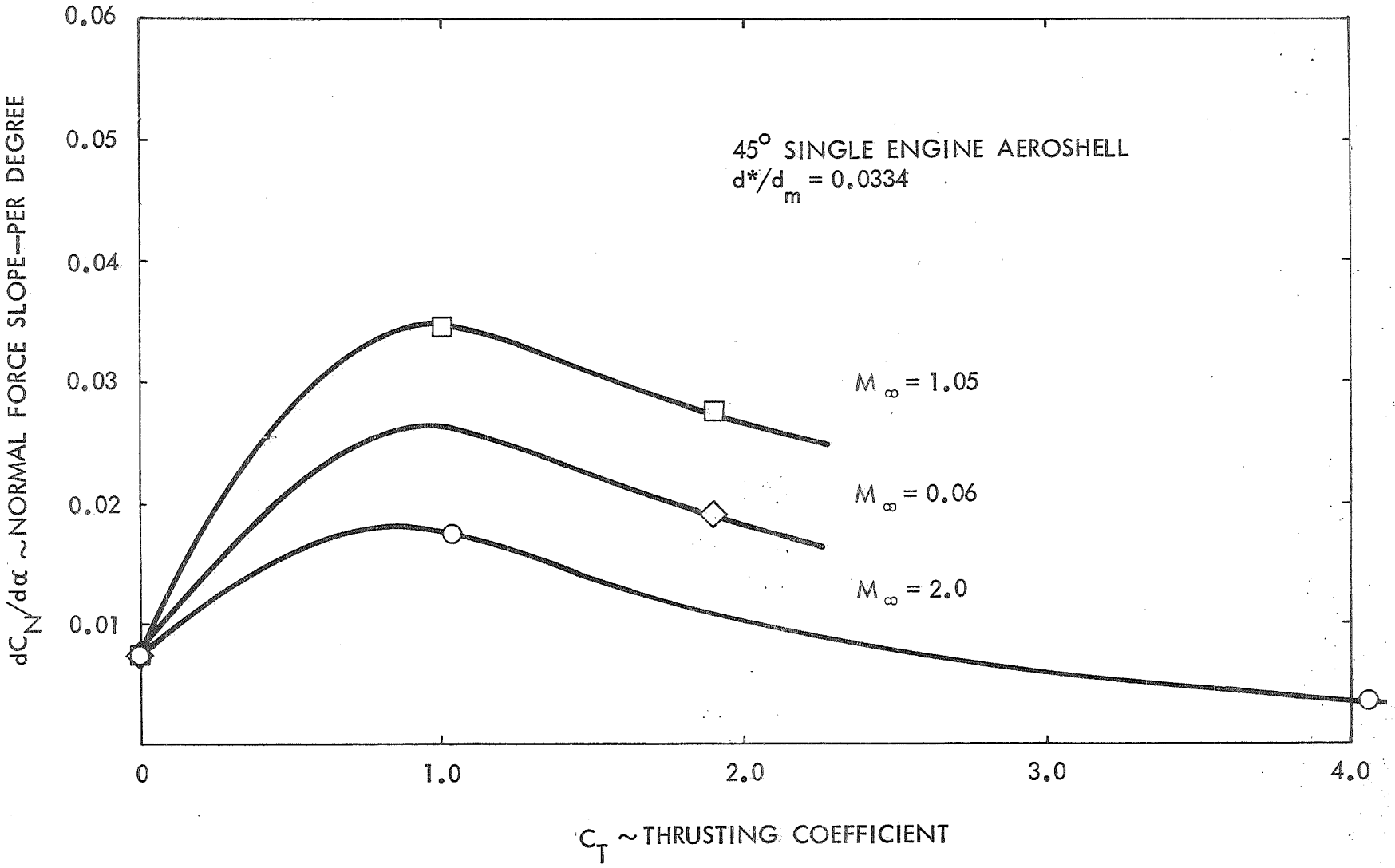

Figure 41 Variation of Normal Force Slope with Thrusting Coefficient - 45° Single Engine Aeroshell.

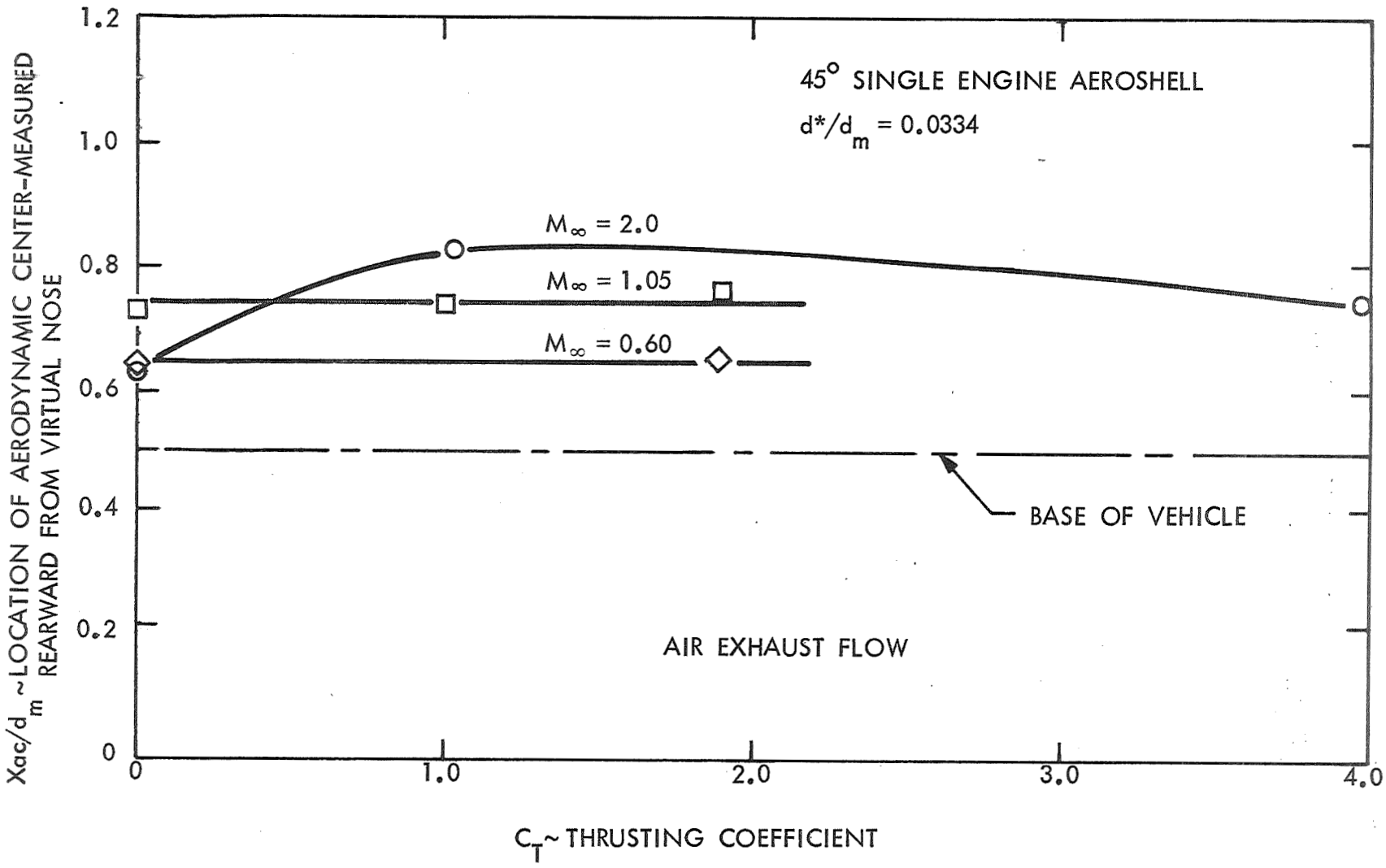

Figure 42 Effect of Retrothrust on Aerodynamic Center Location - 45° Single Engine Aeroshell.

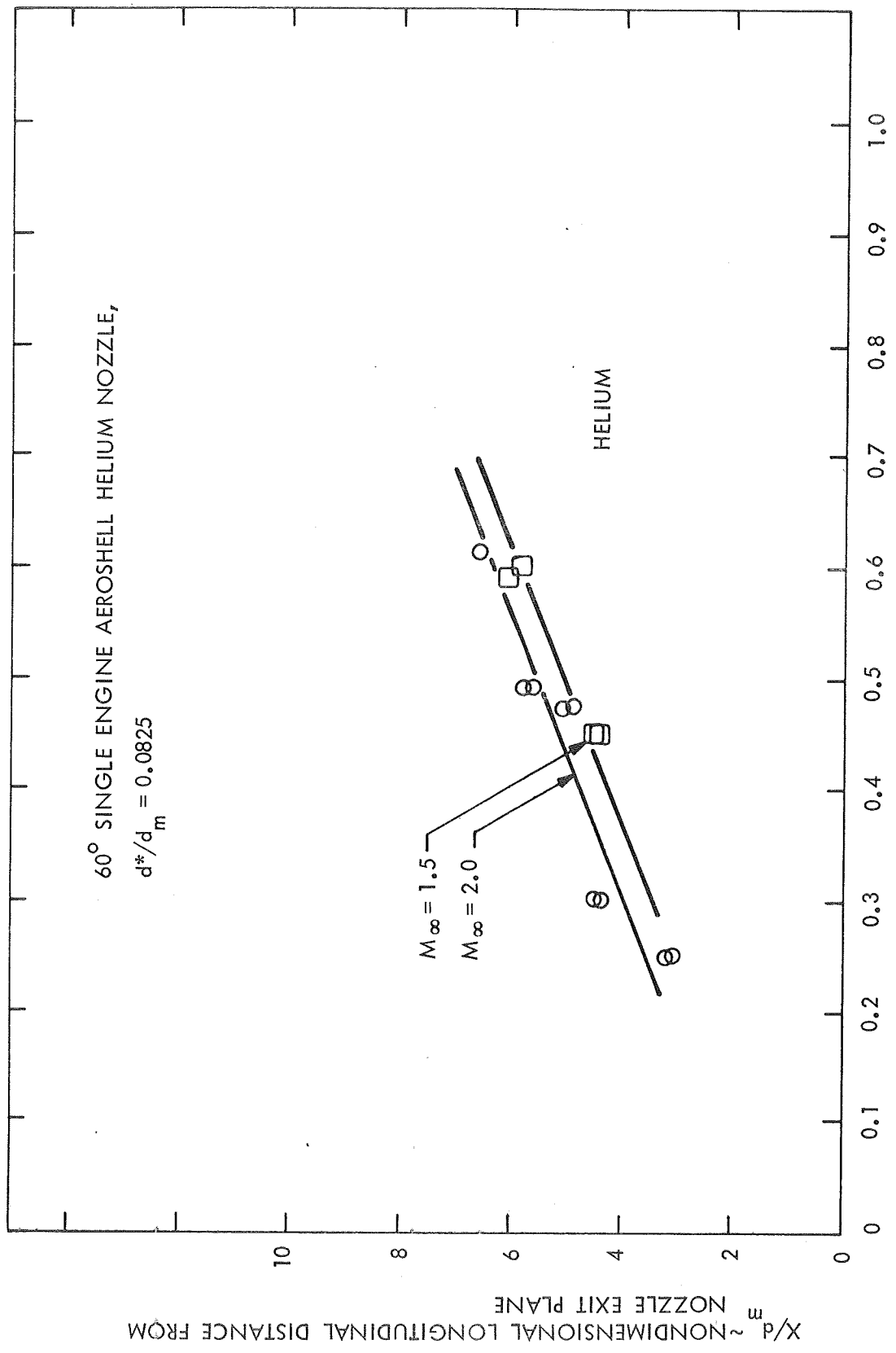

Figure 43 Location of Bow Shock Wave - 60° Single Engine Aeroshell, Helium Nozzle.

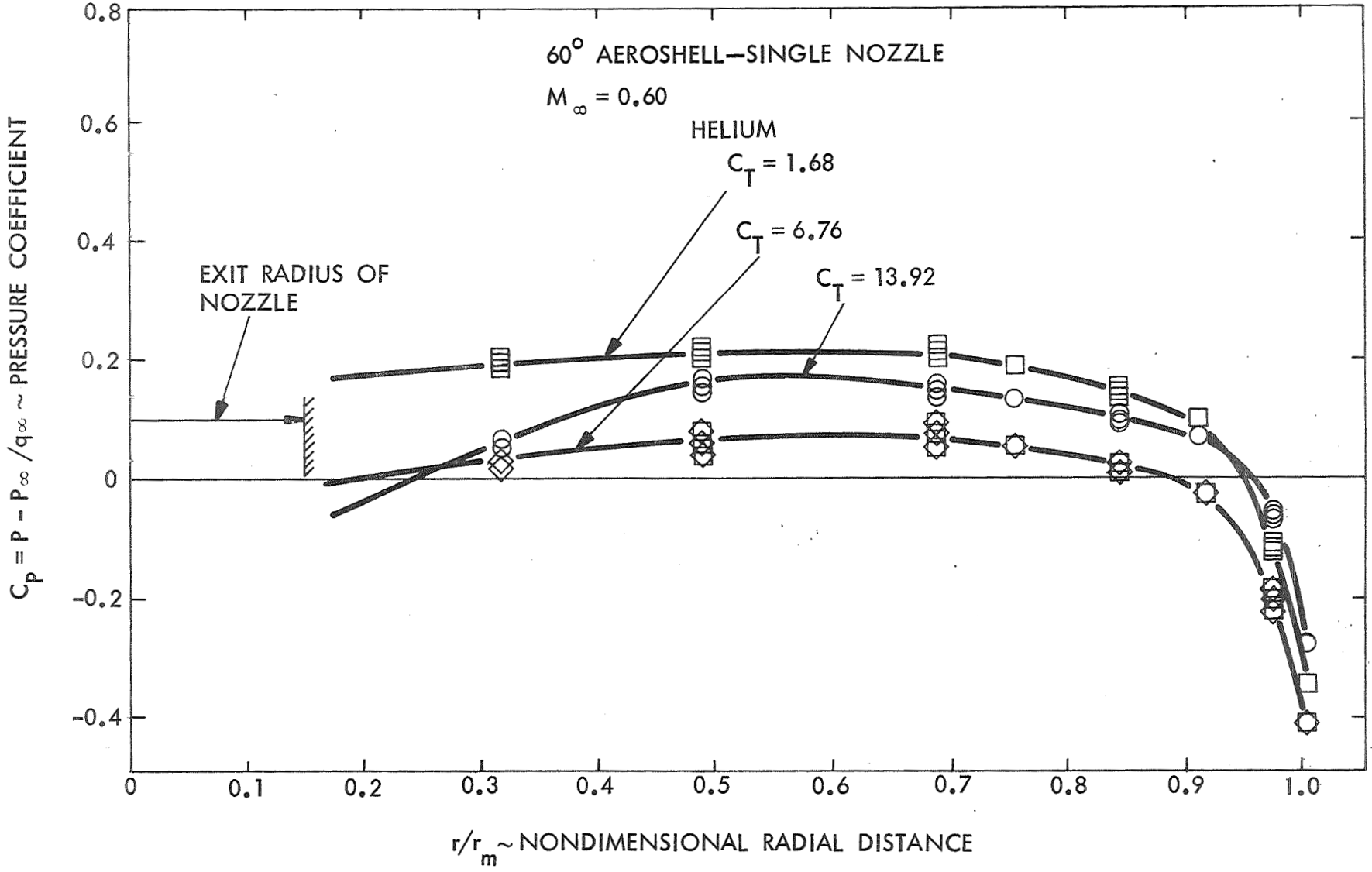

Figure 44 Pressure Distribution with Retrothrust - Helium Nozzle - 60° Single Engine Aeroshell - $M_\infty = 0.60$.

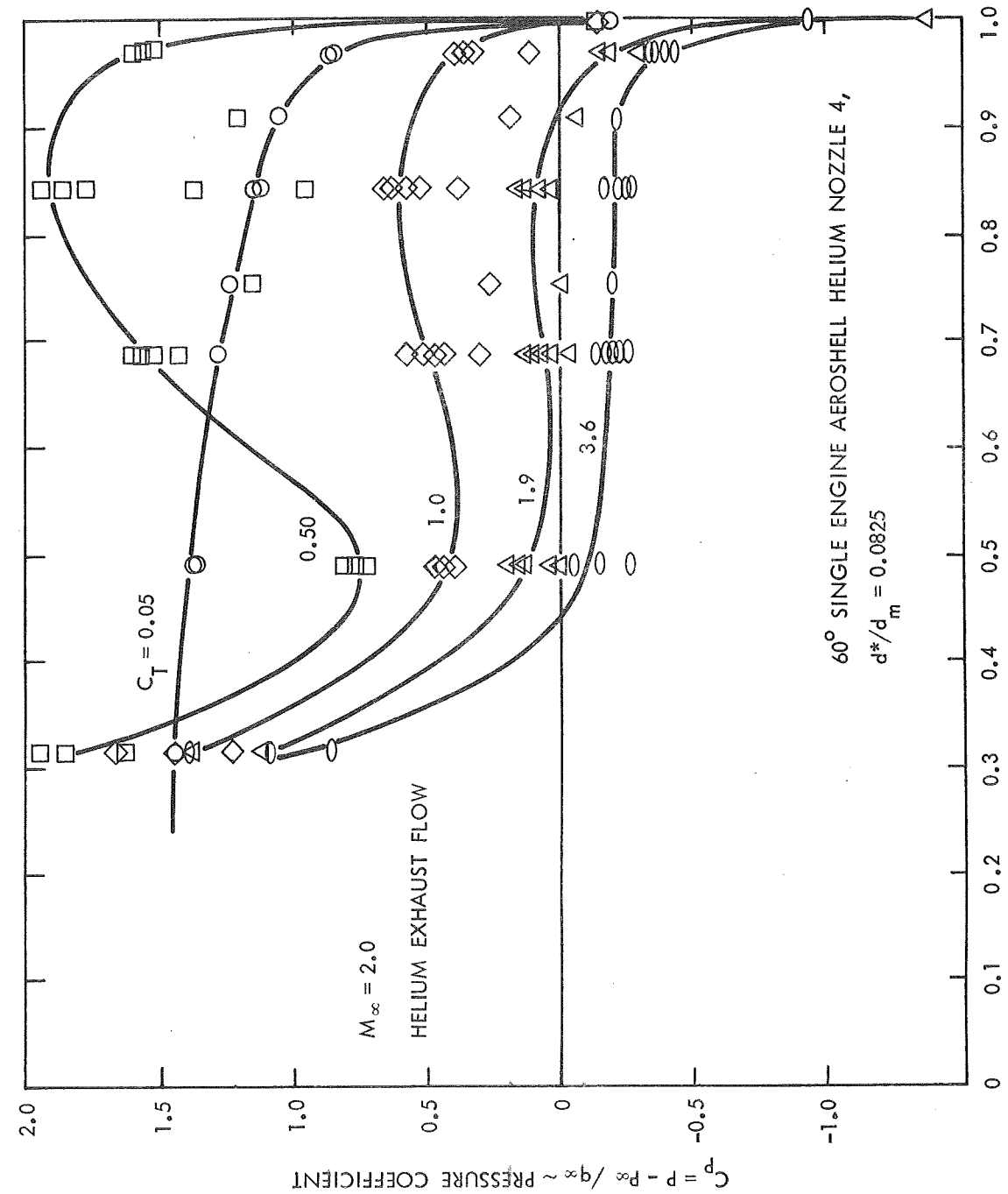

Figure 45 Pressure Distribution with Retrothrust - Helium Nozzle - 60° Single Engine Aeroshell - M_∞ = 2.0.

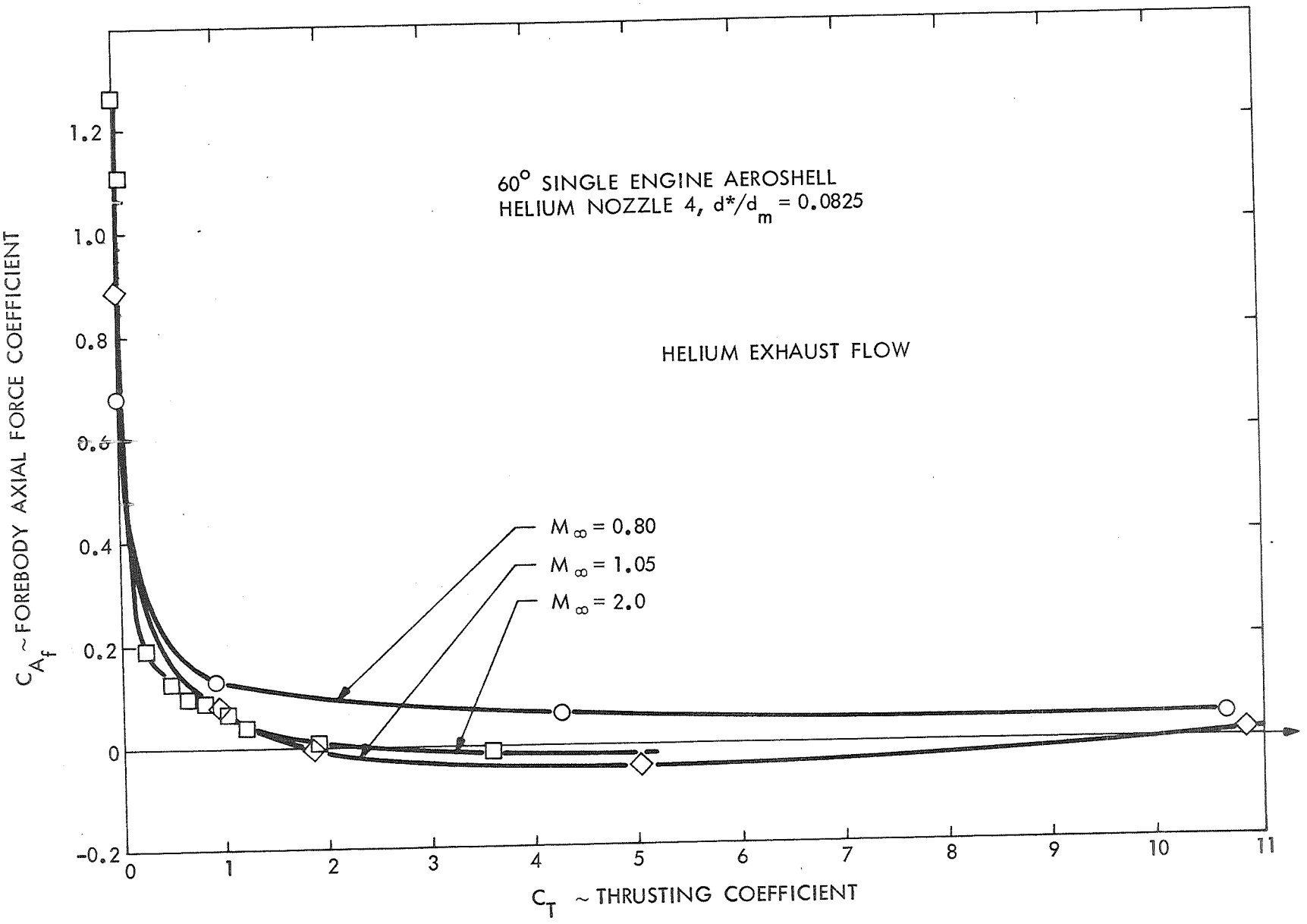

Figure 46 Effect of Retrothrust on Forebody Axial Force Coefficient - Helium Exhaust Flow - 60° Single Engine Aeroshell - M_∞ = 0.80, 1.05 and 2.0.

3.1.13 Flow Field at Angle of Attack

A shadowgraph of the flow field about a 60^{o} single engine aeroshell at minus 16.7 degrees angle of attack and $M_{\infty} = 2.0$ is shown in Figure 47.

3.2 Three Engine Aeroshell Data

3.2.1 Shadowgraphs of Retrorocket - Free Streams Interactions

A shadowgraph of the flow field about the three engine 60^{o} aeroshell at $M_{\infty} = 0.60$ and a thrusting coefficient of 3.9 is shown in Figure 48. The model has been rolled on the sting ($\phi = 30^{o}$) so that the flow from each engine is visible. At all subsonic Mach numbers, the jet flow penetrates far upstream from the model and the total head of a jet decays through mixing. A shadowgraph of the flow field at $M_{\infty} = 2.0$ and a thrusting coefficient of 1.02 is shown in Figure 49. In this case, each of the engine exhausts is bent outward by the oncoming free stream flow and the total head of the jet still decays through mixing. The pressure distribution on the face of the three engine 60^{o} aeroshell, for these conditions, shows that the aeroshell surface, inboard of the engines, is covered with a region of nearly uniform high pressure air with the pressure at the center of the aeroshell being equal to the free stream pitot pressure. The shock wave which is visible in Figure 49 near the nose of the aeroshell, sustains the high pressure levels. The pressure distribution data is discussed more fully in Section 3.2.5

A shadowgraph of the flow field about the three engine 60^{o} aeroshell vehicle at $M_{\infty} = 2.0$ and $C_{T} = 4.05$ is shown in Figure 50. The character of the flow field is changed when the thrusting coefficient is increased to $C_{T} = 4.05$ (Figure 50). Now the total head of the retrorocket exhaust flow decays by passing through a terminal shock wave instead of through a mixing process. Features such as the terminal shock wave and jet boundaries are readily visible. The individual jets interact directly with each other. The exhaust-free stream interaction appears to have local instabilities which affect the bow shock wave slope.

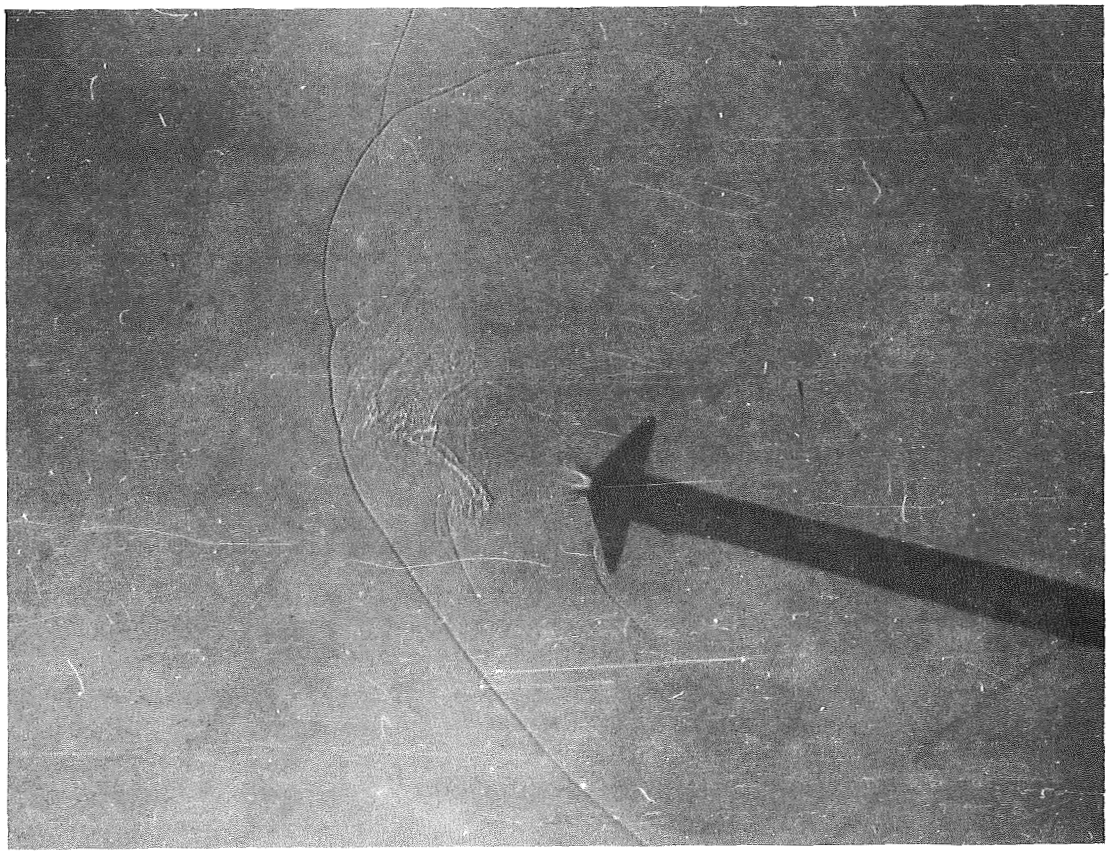

Figure 47 Shadowgraph of Flow Field at Angle of Attack -60° Single Engine Aeroshell $\alpha = -16.7^{\circ}$, $M_{\infty} = 2.0$, $C_T = 2.03$.

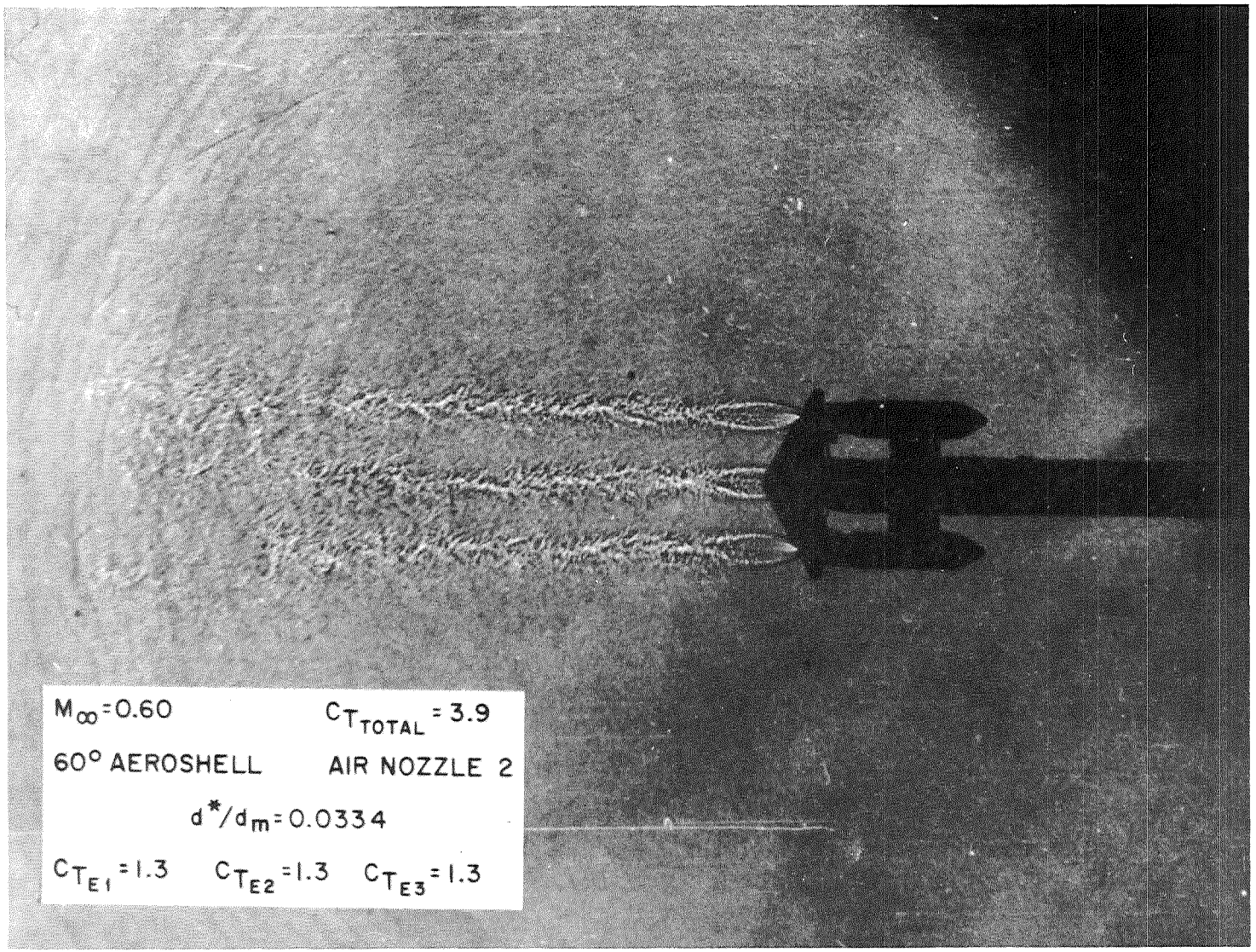

Figure 48 Three Engine 60° Aeroshell Flow Field $M_\infty = 0.60$, $C_{T_{TOTAL}} = 3.9$, $\phi = 30^\circ$.

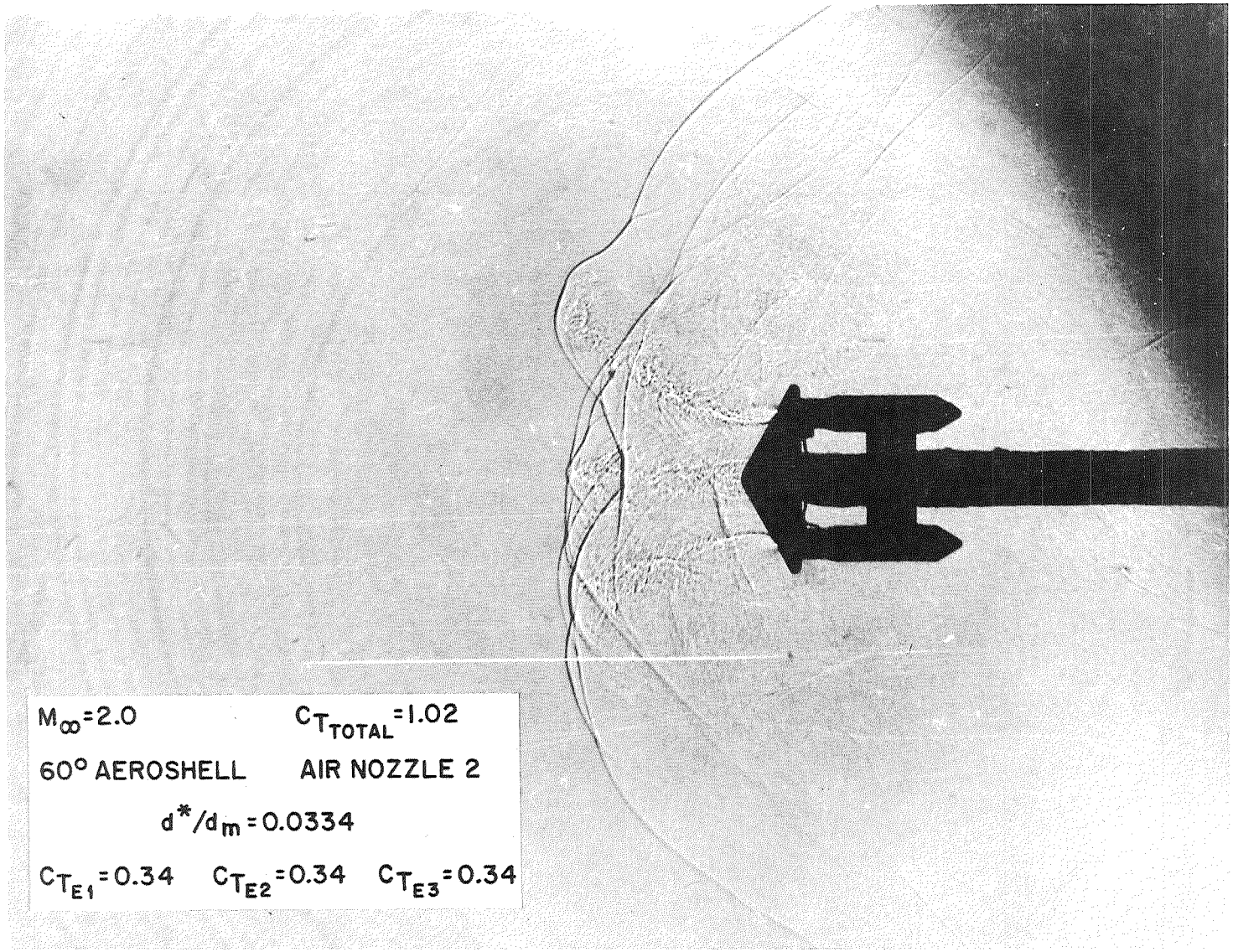

Figure 49 Three Engine 60° Aeroshell Flow Field M_∞ = 2.0, $C_{T_{TOTAL}}$ = 1.02, ϕ = 30°.

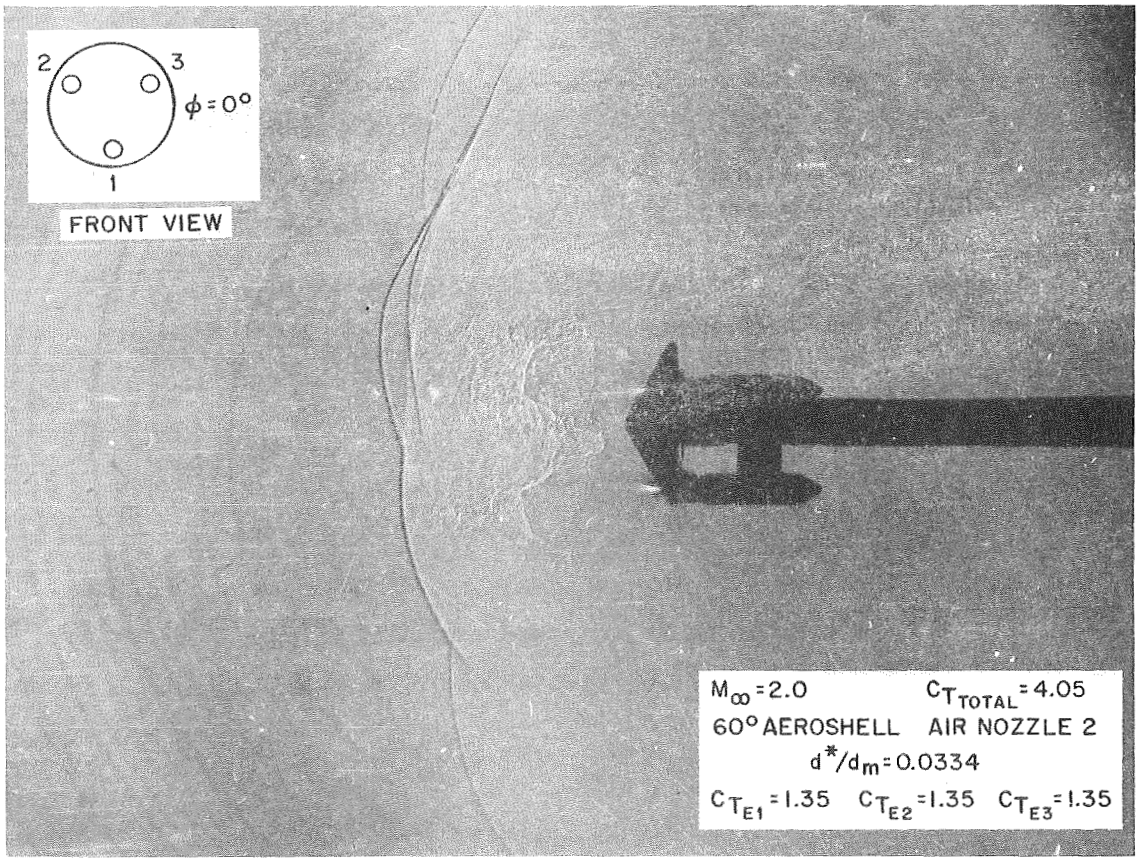

Figure 50 Flow Field of Three Engine, 60° Aeroshell - Equal Engine Thrusts $M_\infty = 2.0$; $C_{T_{TOTAL}} = 4.05$; $\phi = 0^\circ$.

3.2.2 Bow and Terminal Shock Locations

Shadowgraphs such as that shown in Figure 49 were scaled to determine the average location of the bow shock wave along the centerline of the flow and the location of the terminal shock waves with respect to the model base. The flow field geometry for the three engine 60^{o} aeroshell with air exhaust flow at $M_{\infty} = 1.5$ and $M_{\infty} = 2.0$ are noted in Figures 51 and 52 respectively.

3.2.3 Three Engine Aeroshell Forebody Axial Force Coefficients

The variations of the forebody axial force coefficient with thrusting coefficient for the three engine 60^{o} aeroshell is shown in Figures 53 through 55. The forebody axial force coefficient decreases substantially with the application of retrothrust at subsonic Mach numbers (Figures 53 and 54). A different behavior occurs at supersonic speeds (Figure 55). In this case, the forebody axial force coefficient remains at its no retrothrust ($C_T = 0$) value for low retrothrust coefficients and then decreases sharply with further increases in retrothrust.

The forebody axial force coefficient for the single engine 60^{o} aeroshell at $M_{\infty} = 0.6$ is shown for comparison in Figure 54. The data is plotted under the assumption that the single and three engine configurations operate at the same total thrusting coefficient. Subsonically, the three jet forebody axial force coefficient decreases more rapidly with retrothrust than the single engine case.

The forebody axial force coefficient for the three engine 60^{o} aeroshell at supersonic free stream conditions, $M_{\infty} = 2.0$, is shown in Figure 55 along with that for the single engine aeroshell. At supersonic speeds, the forebody axial force coefficient of the three engine aeroshell configuration remains substantially higher than the single engine aeroshell up to thrusting coefficients of $C_T = 2.0$.

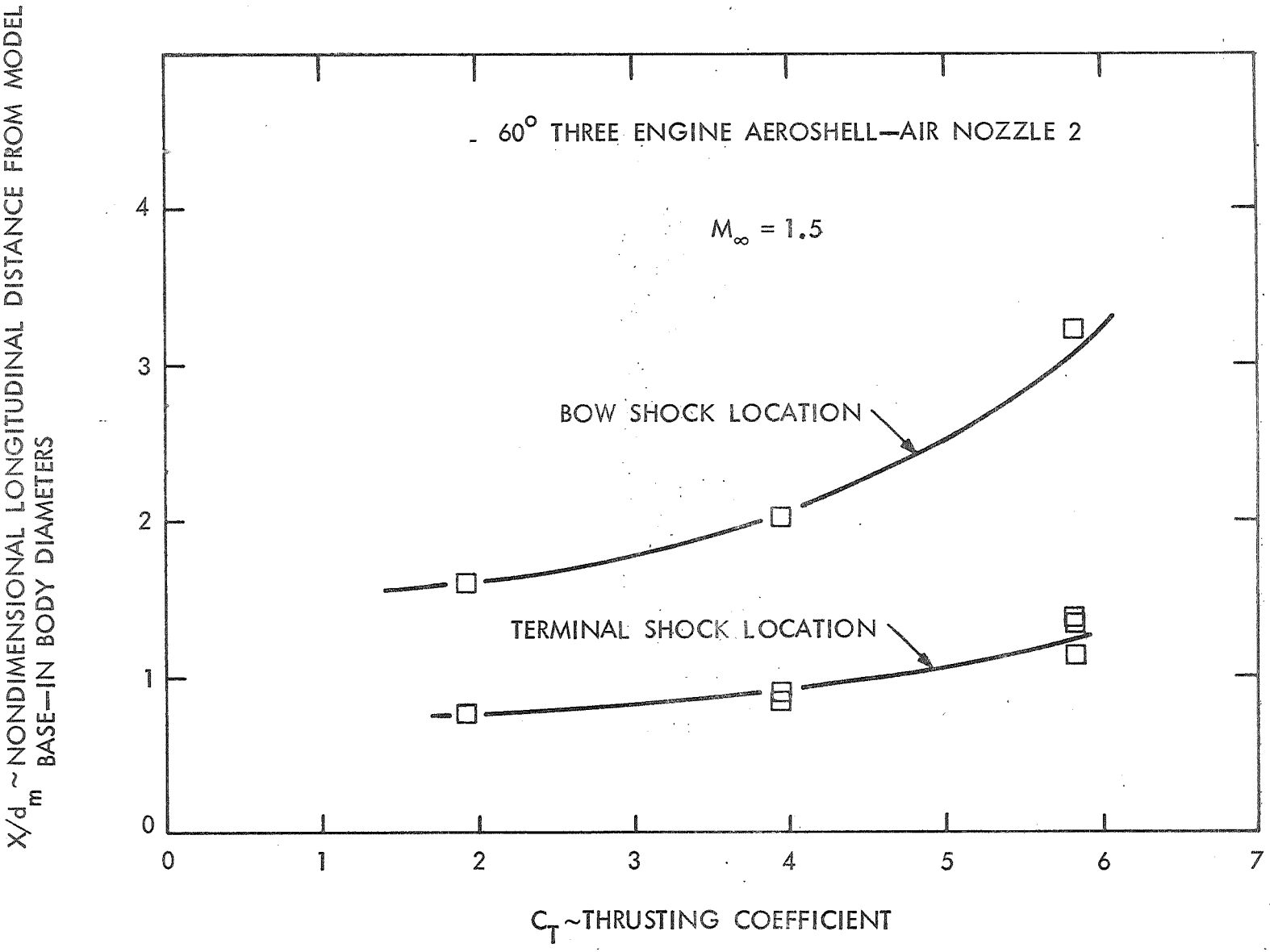

Figure 51 Flow Field Geometry - Three Engine 60° Aeroshell, $M_\infty = 1.5$, Air Nozzle 2.

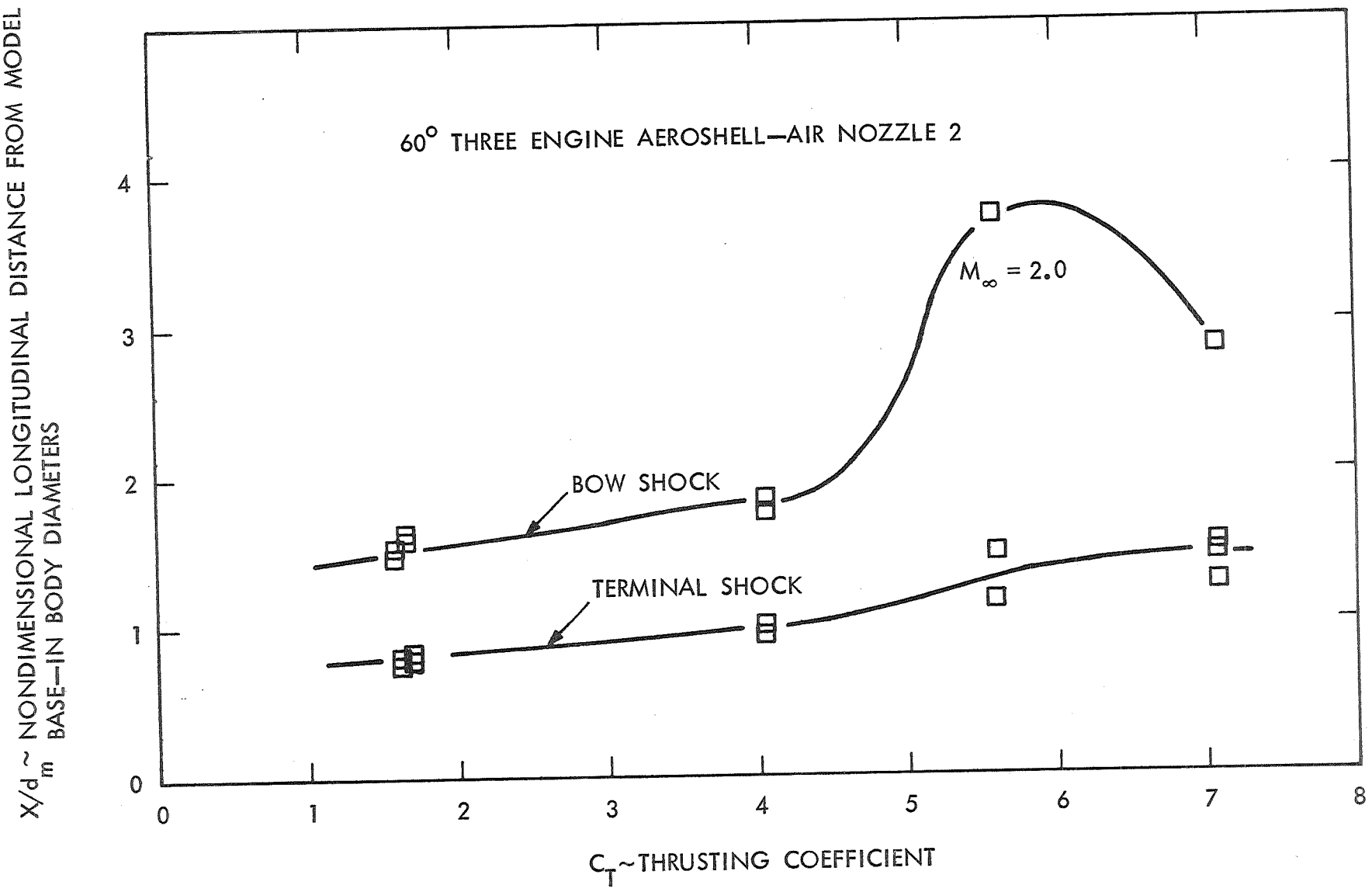

Figure 52 Flow Field Geometry - Three Engine 60° Aeroshell, M_∞ = 2.0, Air Nozzle 2.

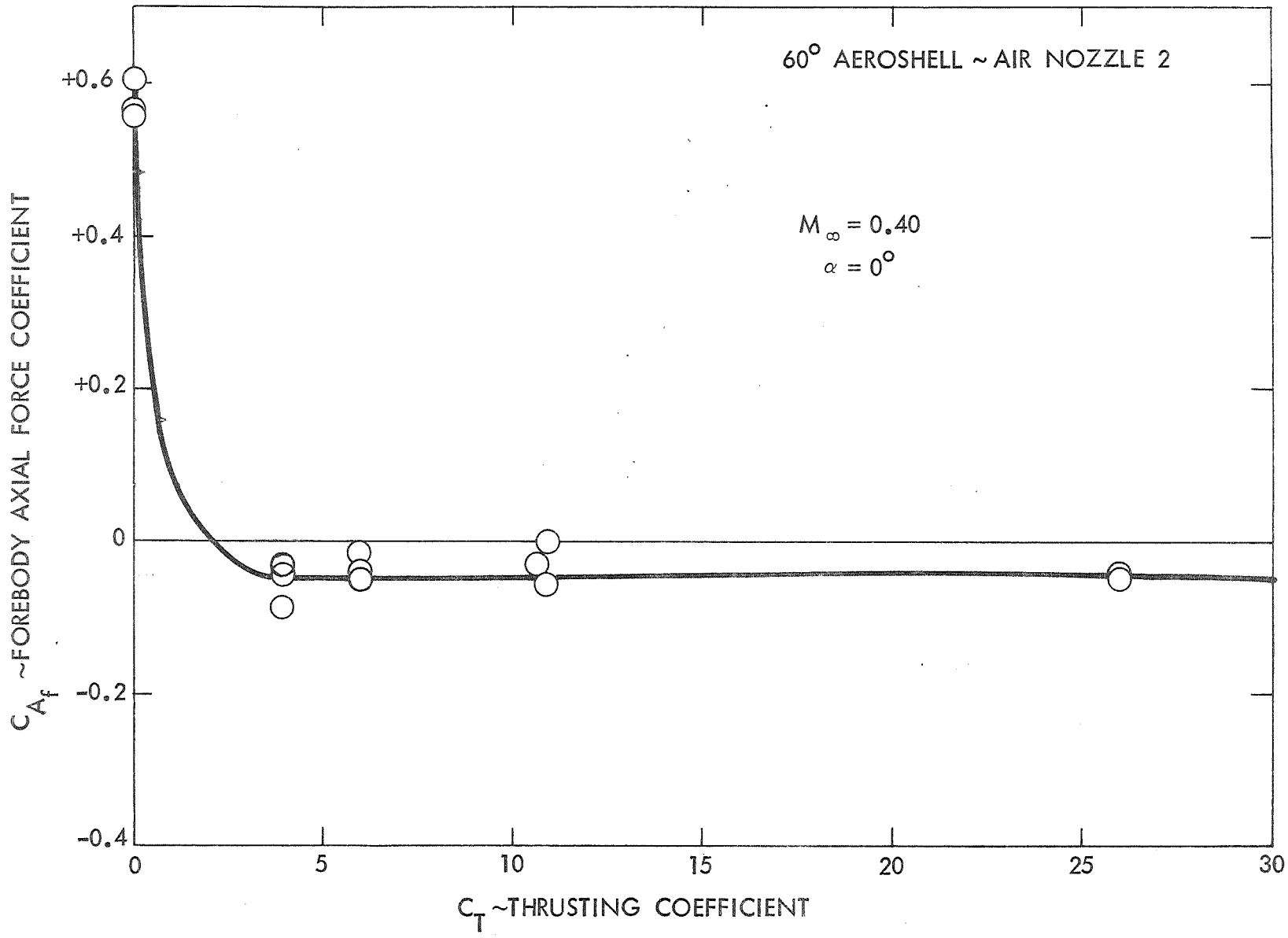

Figure 53 Three Engine 60° Aeroshell, Forebody Axial Force Coefficient, $M_\infty = 0.40$, Air Nozzle 2.

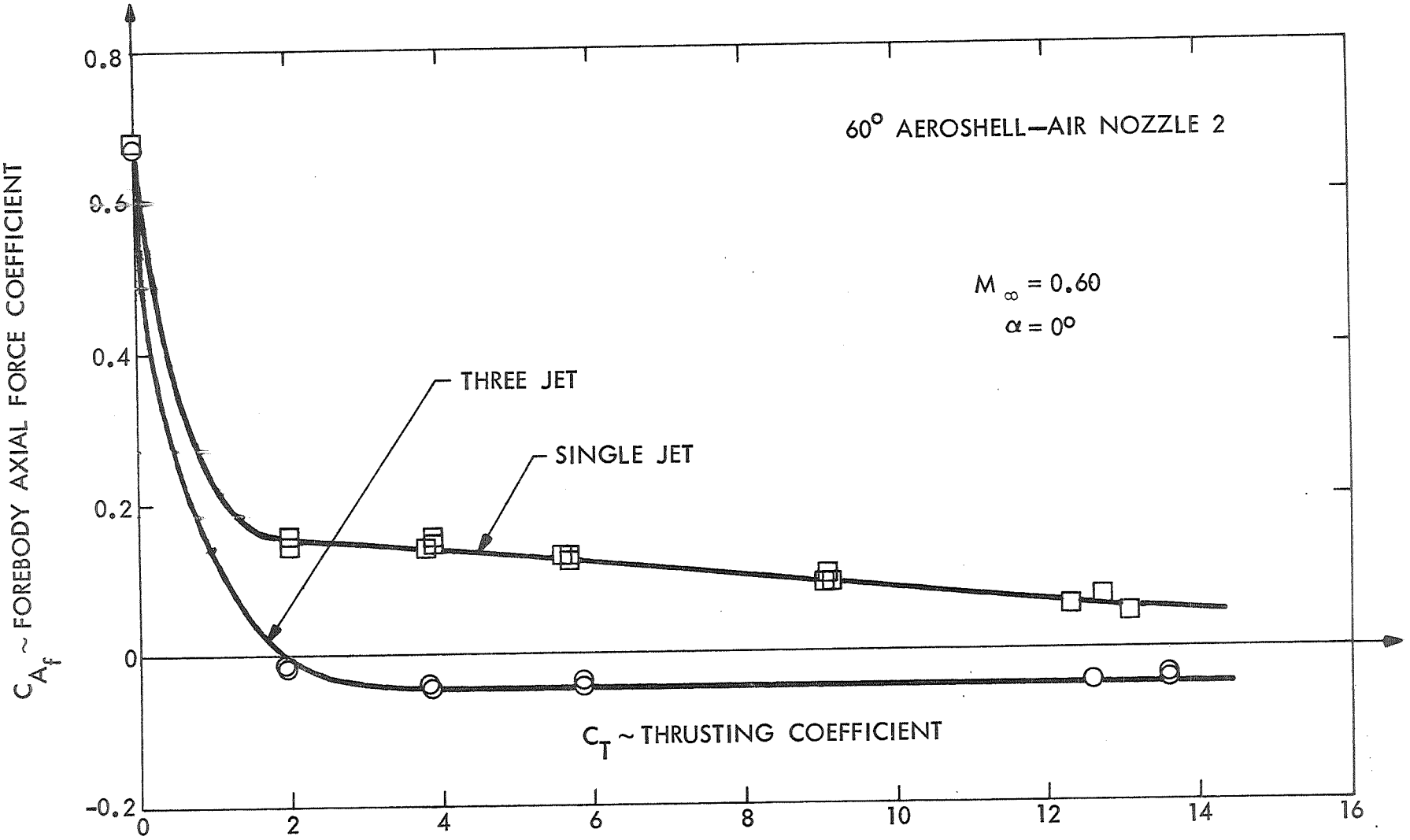

Figure 54 Three Engine, 60° Aeroshell, Forebody Axial Force Coefficient, $M_\infty = 0.60$, Air Nozzle 2.

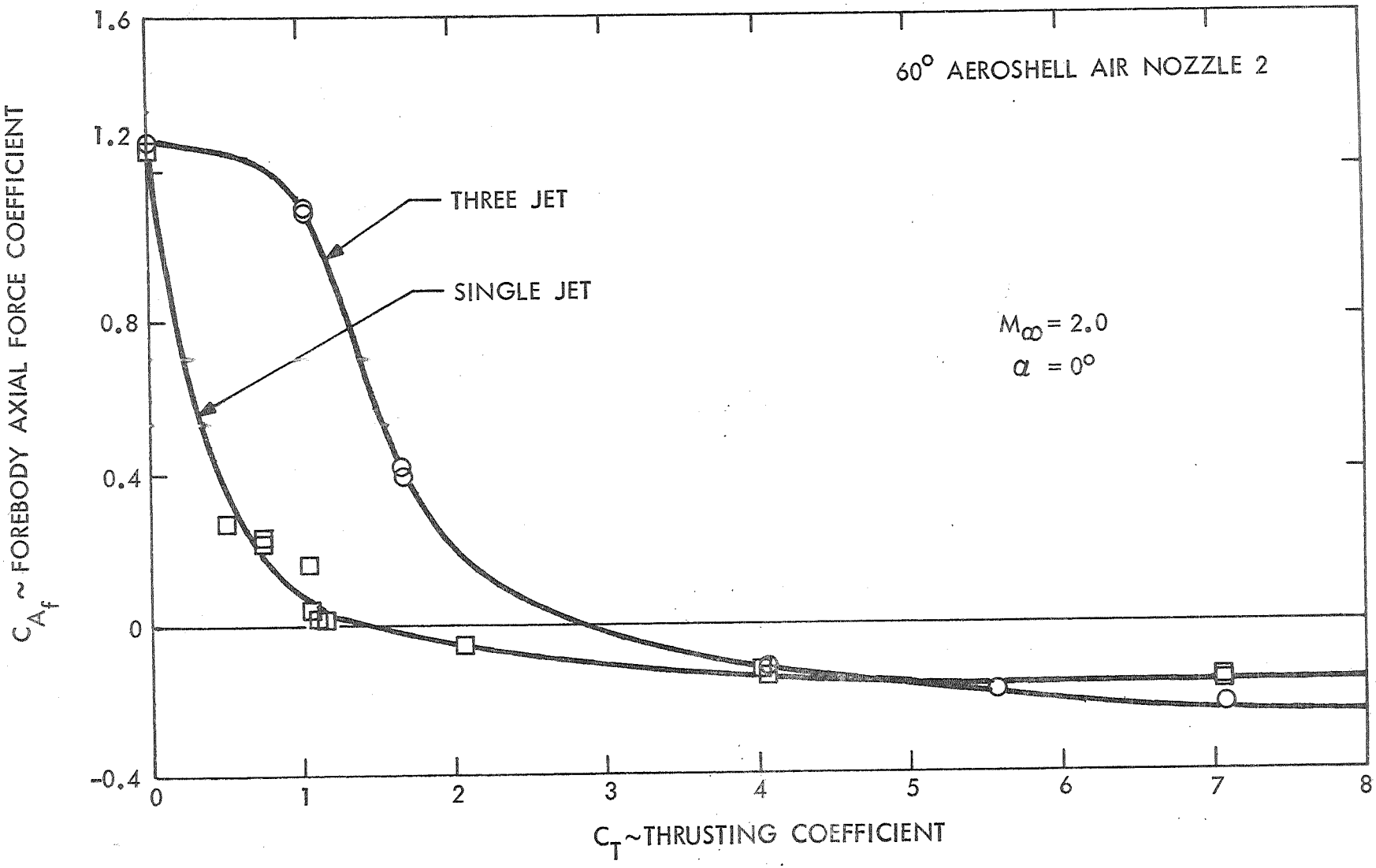

Figure 55 Three Engine, 60° Aeroshell, Forebody Axial Force Coefficient, $M_\infty = 2.0$.

The effect of retrothrust on the aerodynamic characteristics of three engine-aeroshell configurations is more evident when the total axial force coefficient is considered. The total axial force coefficient is defined as the sum of the forebody axial force coefficient and the total thrusting coefficient. (See data reduction-Section 2.6).

The variation of total axial force coefficient with thrusting coefficient is illustrated in Figure 56 for the three engine, sixty degree aeroshell at $M_\infty = 2.0$. The total axial force coefficient acting on a single engine sixty degree aeroshell is shown for comparison. The total axial force coefficient for the three engine aeroshell is substantially above the no retrothrust axial force coefficient ($C_T = 0$) and above the single engine values for thrusting coefficients up to two (2). At higher thrusting coefficients, the total axial force coefficients for both configurations are nearly equal to the thrusting coefficients alone.

All previous experimental investigations, with the exception of Keyes and Hefner[2], observed results characterized by the single engine data (i.e. a substantial decrease in axial force coefficient with application of low thrusting coefficients, followed by an increase in total force coefficient whose magnitude remained nearly equal to the thrusting coefficient alone).

Keyes and Hefner found in their tests, which were conducted at $M_\infty = 6.0$ with thrusting coefficients up to $C_T = 1.2$, that the aerodynamic drag of blunt configurations can be increased by using forward facing jets located near the periphery of the body.

The present investigation shows that there is a range of thrusting coefficients over which the three engine configuration with retrorockets mounted near the periphery of the aeroshell provides substantially more deceleration than a single centrally mounted engine operating at the same total thrusting coefficient. The behavior of the three engine aeroshell with retrothrust at different free stream Mach numbers is shown in Figure 57.

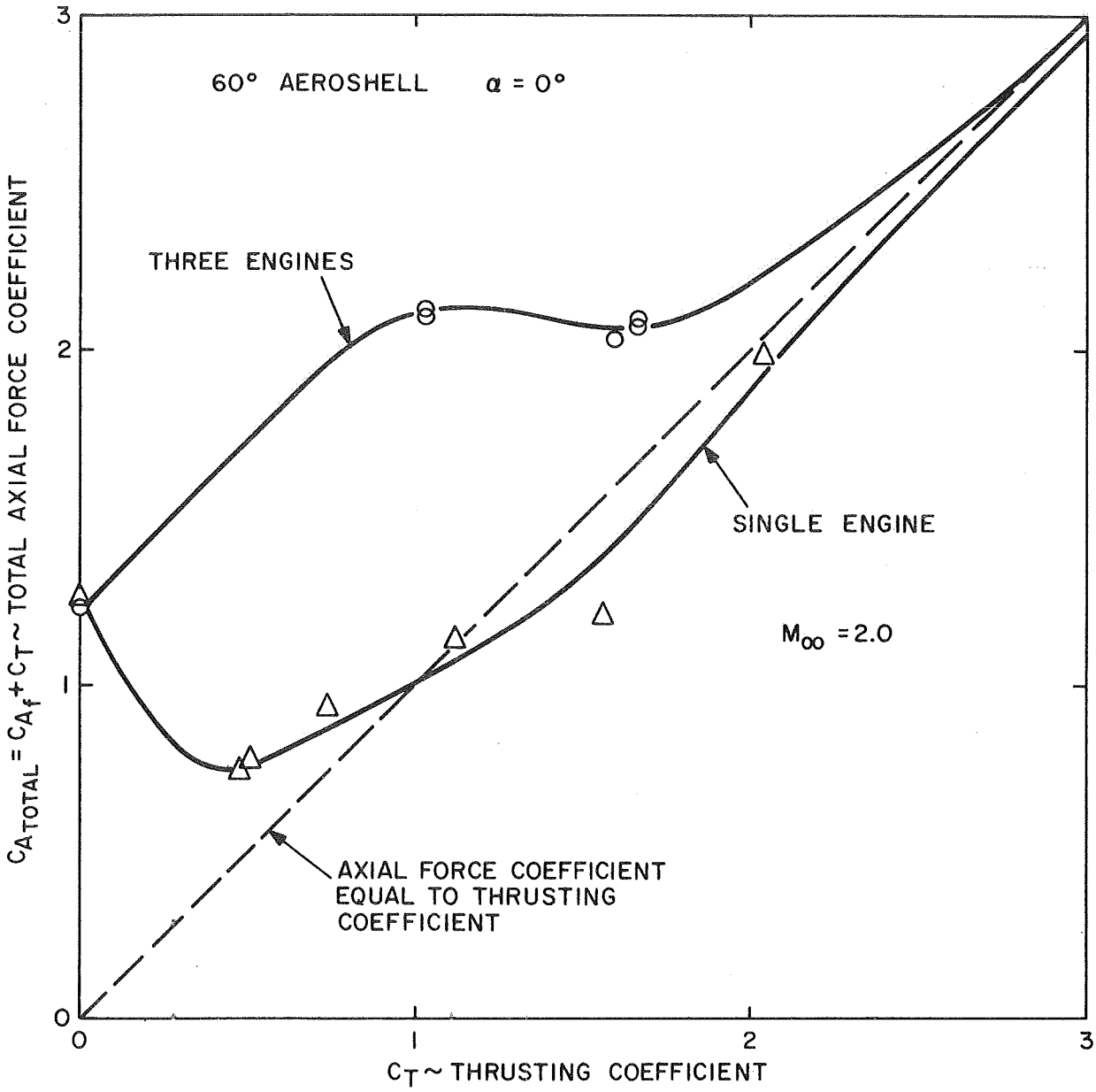

Figure 56 Comparison of Total Axial Force Coefficients of Single and Three Engine 60° Aeroshells; $M_\infty = 2.0$.

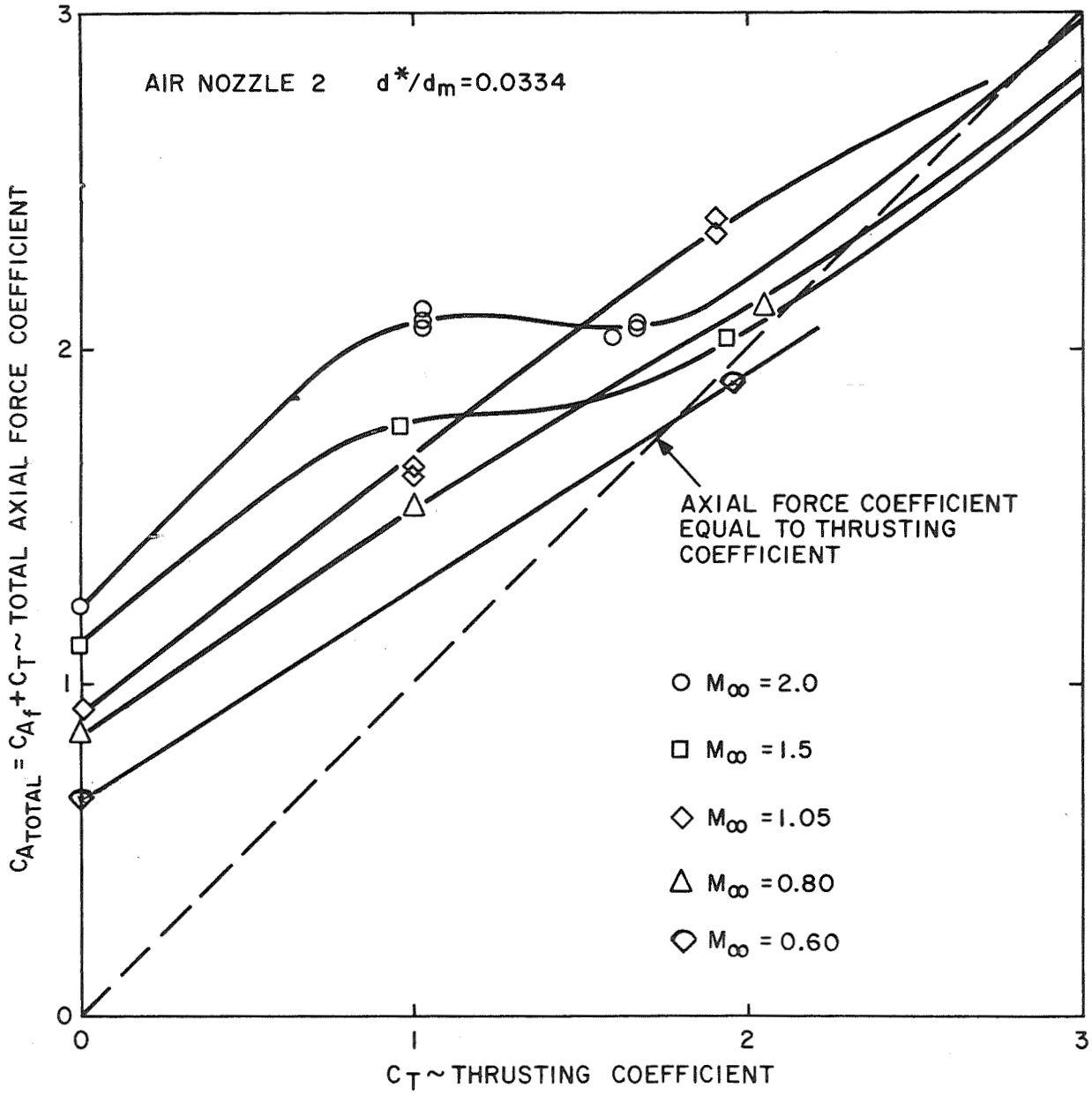

Figure 57 Effect of Retrothrust on Total Axial Force Coefficient - Three Engine 60° Aeroshell.

Data for free stream Mach numbers of M_∞ = 0.6, 0.8, 1.05, 1.5 and 2.0 are displayed. Total force amplification is present for free stream Mach numbers from M_∞ = 2.0 to M_∞ = 0.60, though the amount of amplification decreases with decreasing free stream Mach number.

3.2.4 Effect of Angle-of-Attack on Forebody Axial Force Coefficients with Retrothrust

The variation of the forebody axial force coefficient with angle-of-attack is shown for M_∞ = 0.6, 1.05 and 2.0 in Figures 58, 59, and 60 respectively. Angle-of-attack has little effect on the forebody axial force coefficient at all Mach numbers and thrusting coefficients tested, for angles between minus six and plus six degrees, $-6^\circ \leq \alpha \leq +6^\circ$. The data indicates that angle-of-attack effects may become significant outside of this range.

3.2.5 Surface Pressure Distributions

The variation and distribution of pressure over the surface of the three engine 60° aeroshell will now be considered. Surface pressure profiles along radial directions will be considered first. Circumferential pressure distributions at constant radial distance will be considered next.

Surface pressure profiles at $\phi = 0$, 90° and 180° (ϕ defined in Figure 6) are displayed in Figures 61 through 69. The radial pressure cut at $\phi = 0^\circ$ intersects engine 1 while radical cuts at $\phi = 90^\circ$ and 180° pass between engines 1 and 2 and engines 2 and 3 respectively. Pressure data at M_∞ = 0.60 is presented in Figures 61 through 65 for thrusting coefficients of C_T = 0.0, 1.9, 3.8, 5.8, and 13.6. The base pressure coefficient C_{P_B}, for each thrusting coefficient is noted on the ordinate, though the data was actually measured at a given radius ratio. The pressure forces acting on the aeroshell surface, when retrothurst is applied at subsonic speeds, increase with distance from the aeroshell centerline (Figures 62 through 65). The base pressure with retroth rust is higher than without. The pressure acting at the center of the forward surface of the aeroshell and the base pressure level

are about equal for thrusting coefficients equal to or greater than $C_T = 3.8$ (Figures 63 through 65). The change in forebody surface pressure with radial distance increases with increasing thrusting coefficient.

Surface pressure profiles at $M_\infty = 2.0$ and thrusting coefficients of $C_T = 1.0$, 1.7, 4.1 and 7.1 are shown in Figures 66 through 69 respectively. The pressure increases along the $\phi = 0^o$ cut in the vicinity of engine 1 for thrusting coefficients from 1.0 to 4.1. The pressure decreases with radial distance along cuts ($\phi = 90^o$ and 180^o) that pass between the engines for thrusting coefficients from 1.0 to 4.1.

The surface pressure profiles, in each of the radial directions ($\phi = 0^o$, 90^o and 180^o), have the same shape for $C_T = 7.1$ (Figure 69) and the surface pressure coefficients at non-dimensional radial distances greater than $r/r_m = .35$ are equal to the base pressure coefficients. This indicates that the aeroshell body is immersed in a constant pressure region. The region of increased pressure near the center of the aeroshell forebody surface is due to the recirculation region formed between the interacting exhaust plumes.

The circumferential pressure distributions with retrothrust, at $M_\infty = 0.6$ and $M_\infty = 2.0$ are shown in Figures 70 through 73. At $M_\infty = 0.6$, the circumferential pressure distributions at various radial distances ($r/r_m = 0.154$, 0.378, 0.625 and 0.875) are about the same (Figures 70 and 71). The influence of the engines on the local pressure distribution is quite evident in Figure 71.

The pressure distributions at $M_\infty = 2.0$ and thrusting coefficients of $C_T = 1.0$ and 1.66 are plotted in Figures 72 and 73 respectively. For $C_T = 1.0$, the aeroshell surface, inboard of the engines is covered with a region of nearly uniform, high pressure. The pressure level is independent of azimuth angle for $r/r_m = 0.154$ and 0.378. At $r/r_m = 0.625$, the pressure increases in front of each engine. Further outboard at $r/r_m = 0.875$, the pressure is nearly constant over a substantial portion of the region between engines but decreases sharply close to the engines. At $C_T = 1.66$, the circumferential pressure distribution is similar in many ways to what was observed at $C_T = 1.0$ but the pressure level has been reduced (Figure 73).

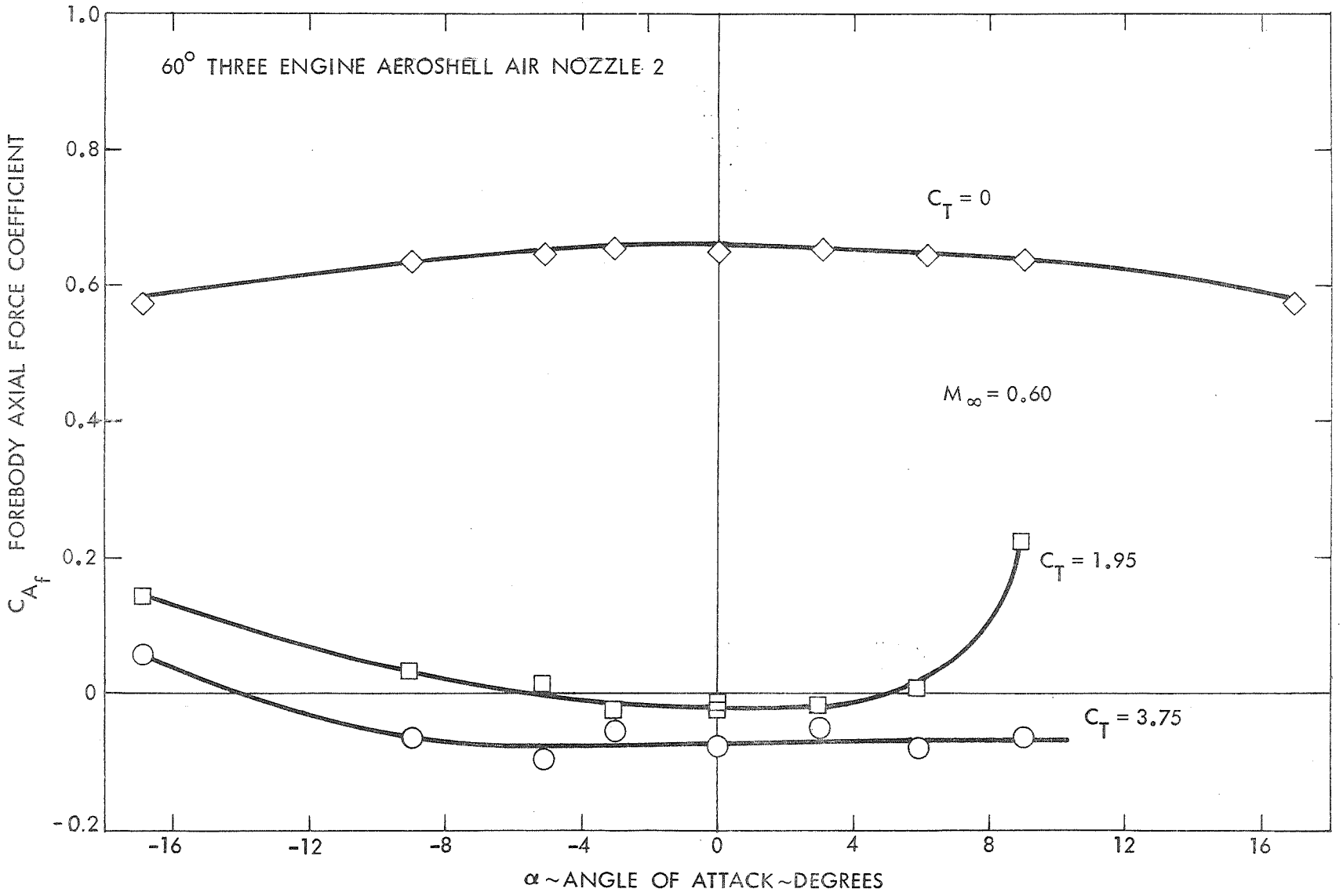

Figure 58 Effect of Angle of Attack on Forebody Axial Force Coefficient - Three Engine 60° Aeroshell - $M_\infty = 0.60$.

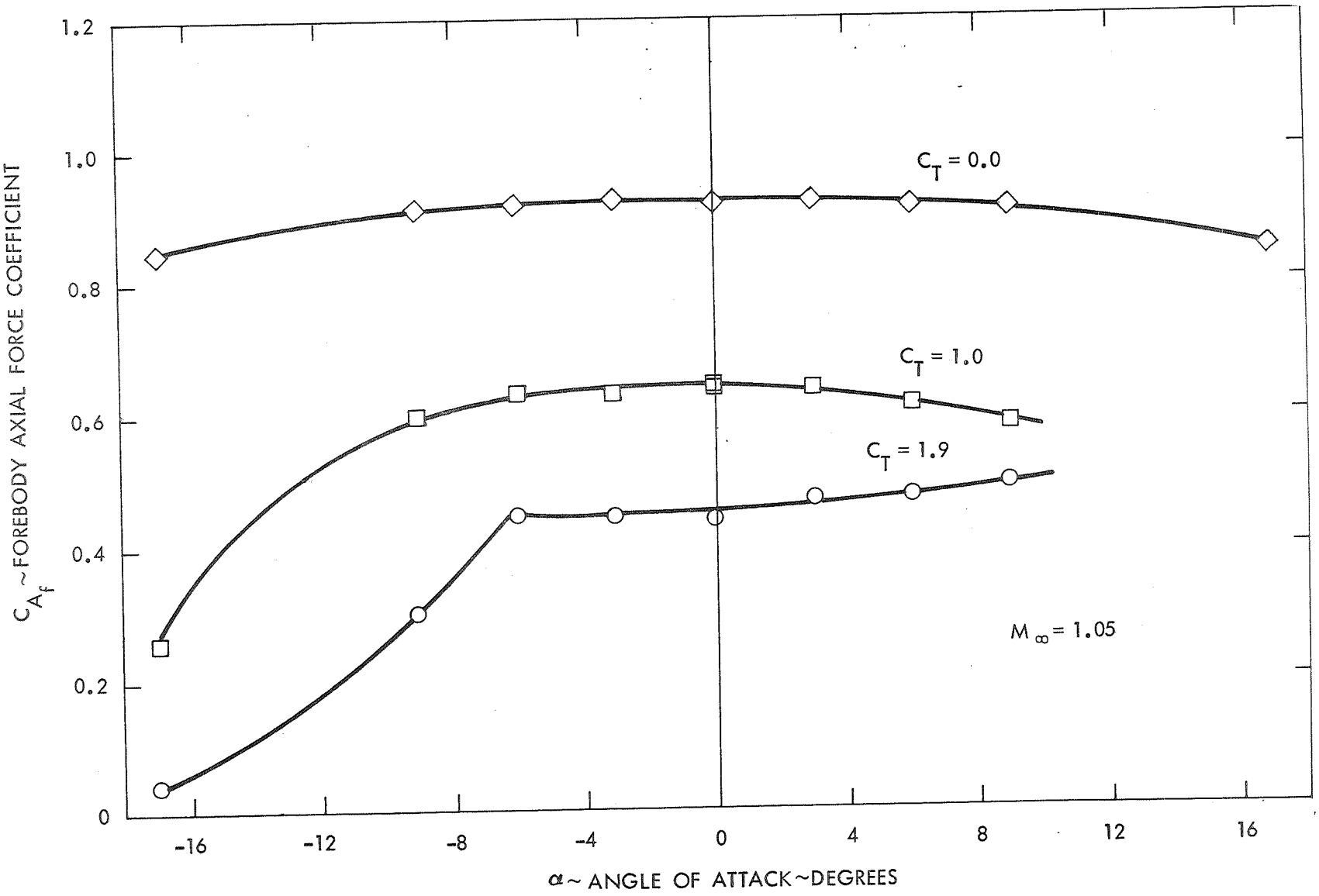

Figure 59 Effect of Angle of Attack on Forebody Axial Force Coefficient - Three Engine 60° Aeroshell - M_∞ = 1.05.

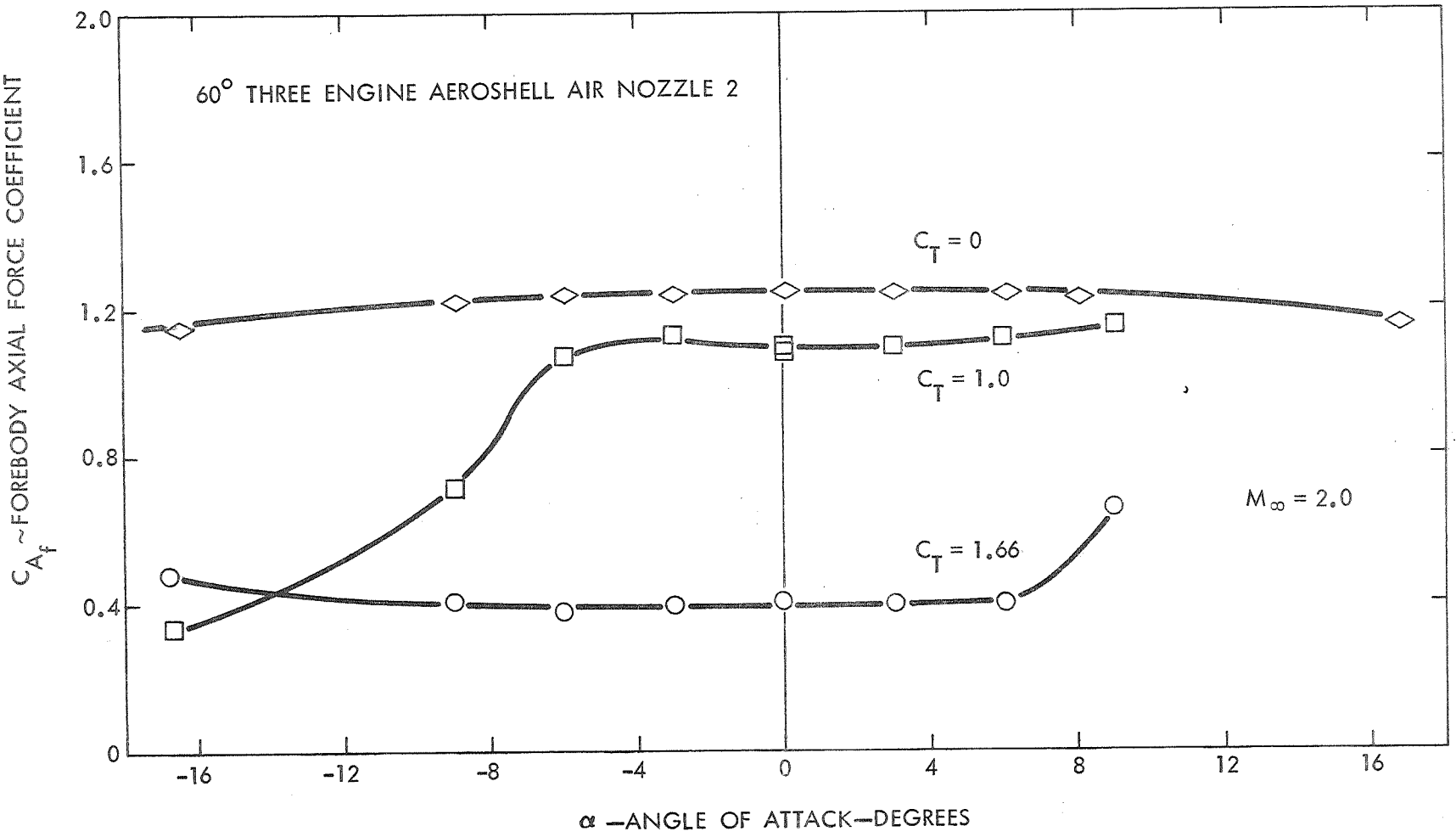

Figure 60 Effect of Angle of Attack on Forebody Axial Force Coefficient - Three Engine 60° Aeroshell - $M_\infty = 2.0$.

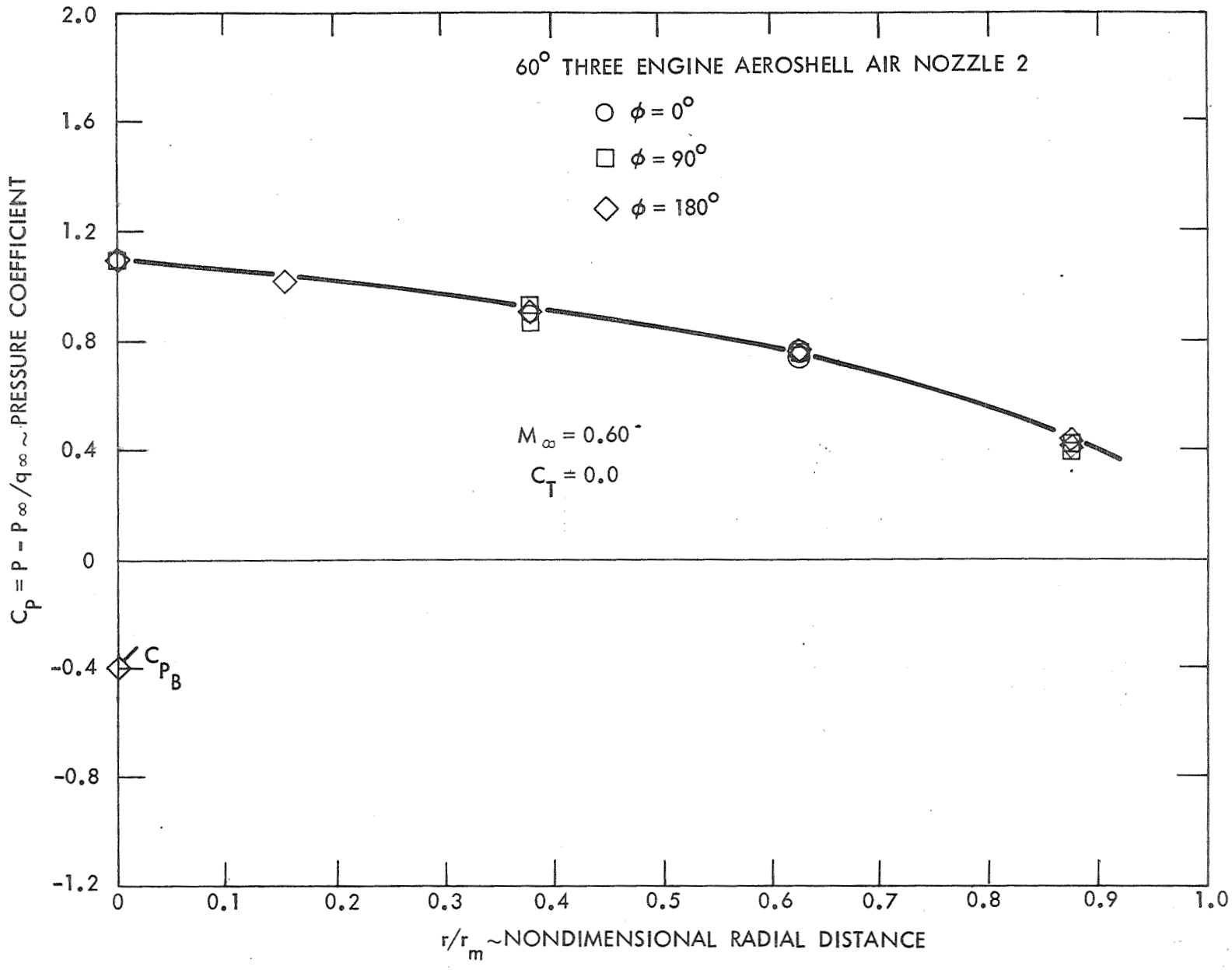

Figure 61 Surface Pressure Profiles - Three Engine 60° Aeroshell - $M_\infty = 0.60$, $C_T = 0.0$.

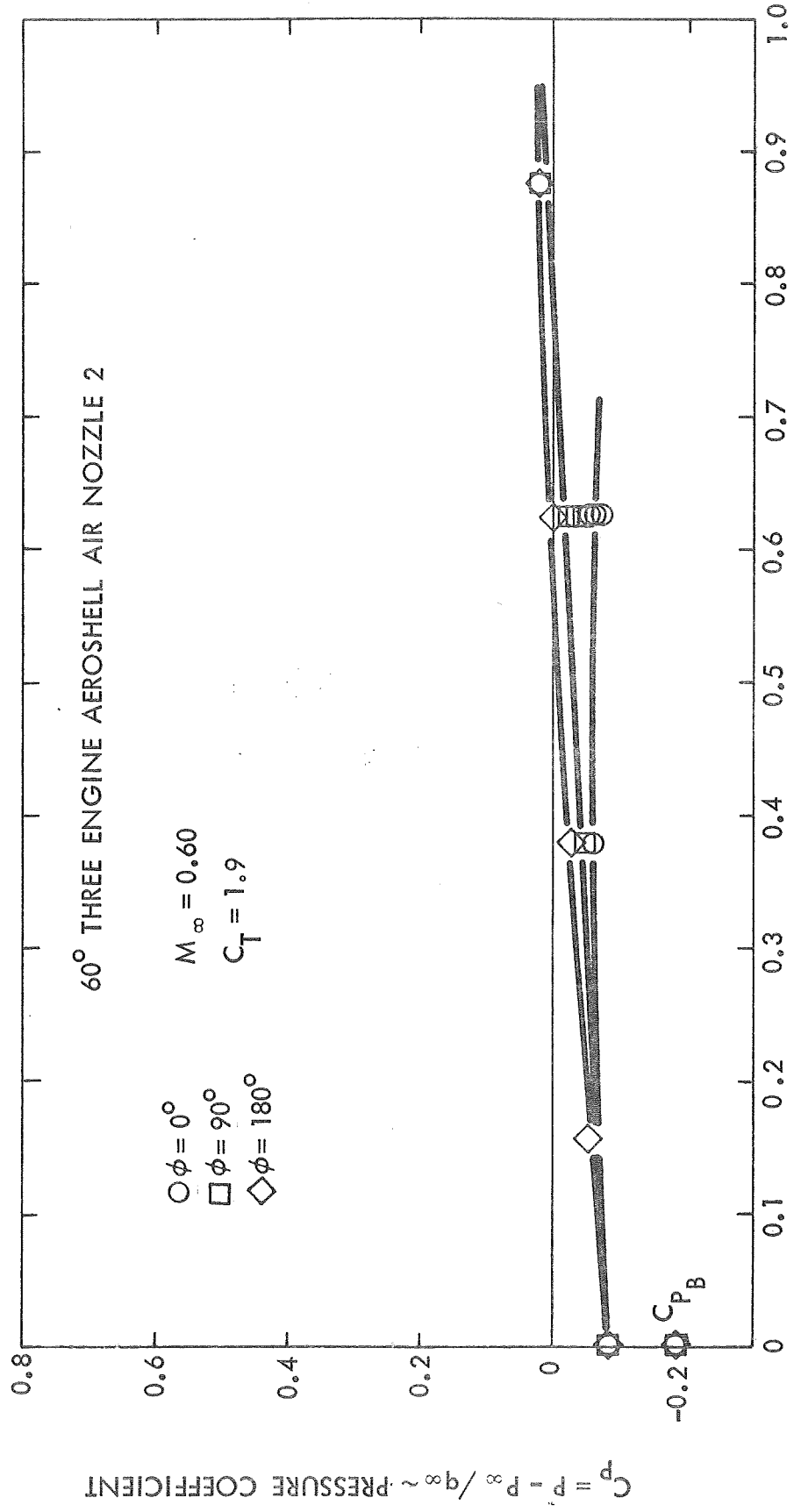

Figure 62 Surface Pressure Profiles - Three Engine 60° Aeroshell - $M_\infty = 0.60$, $C_T = 1.9$.

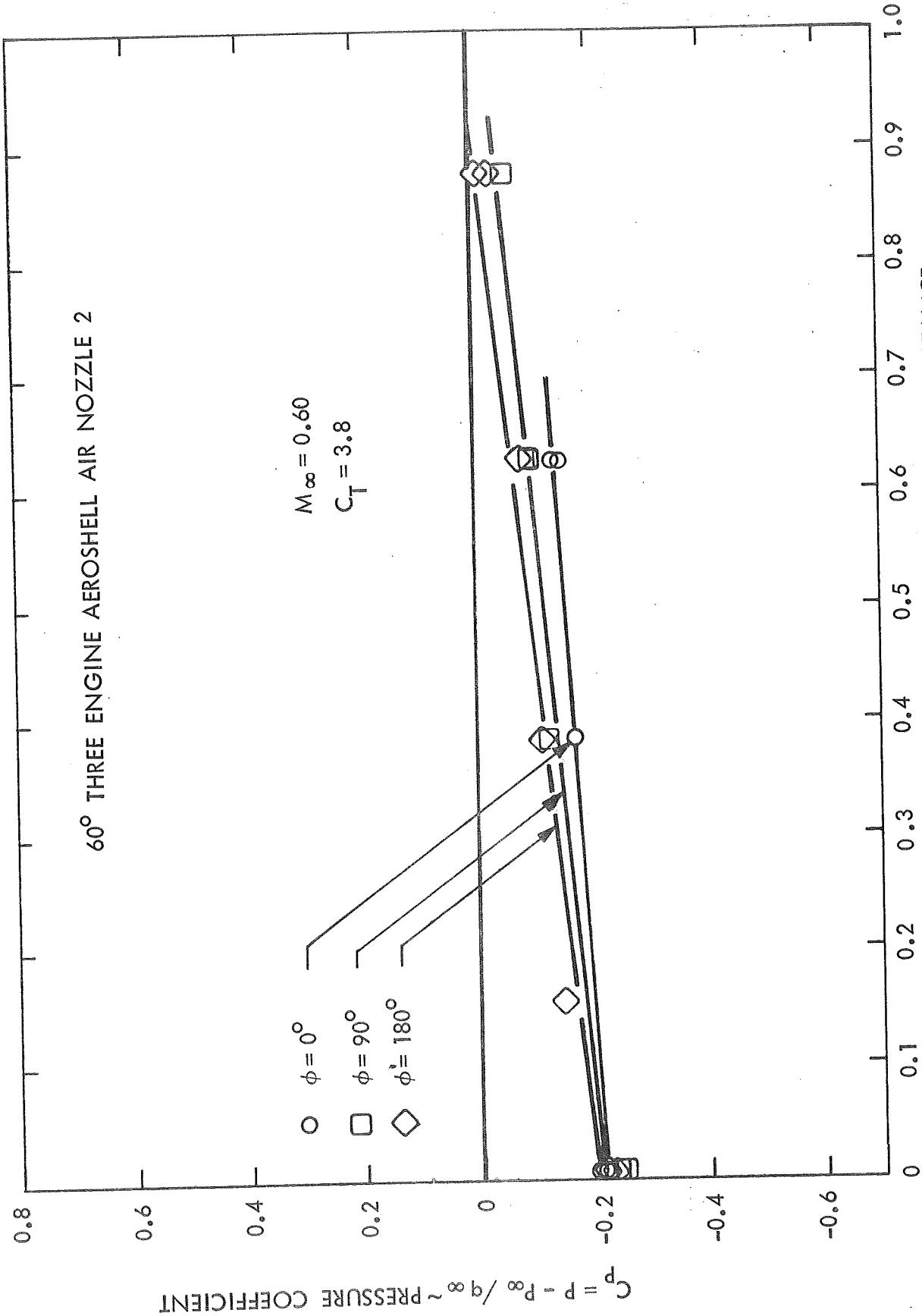

Figure 63 Surface Pressure Profiles - Three Engine 60° Aeroshell - $M_\infty = 0.60$, $C_T = 3.8$.

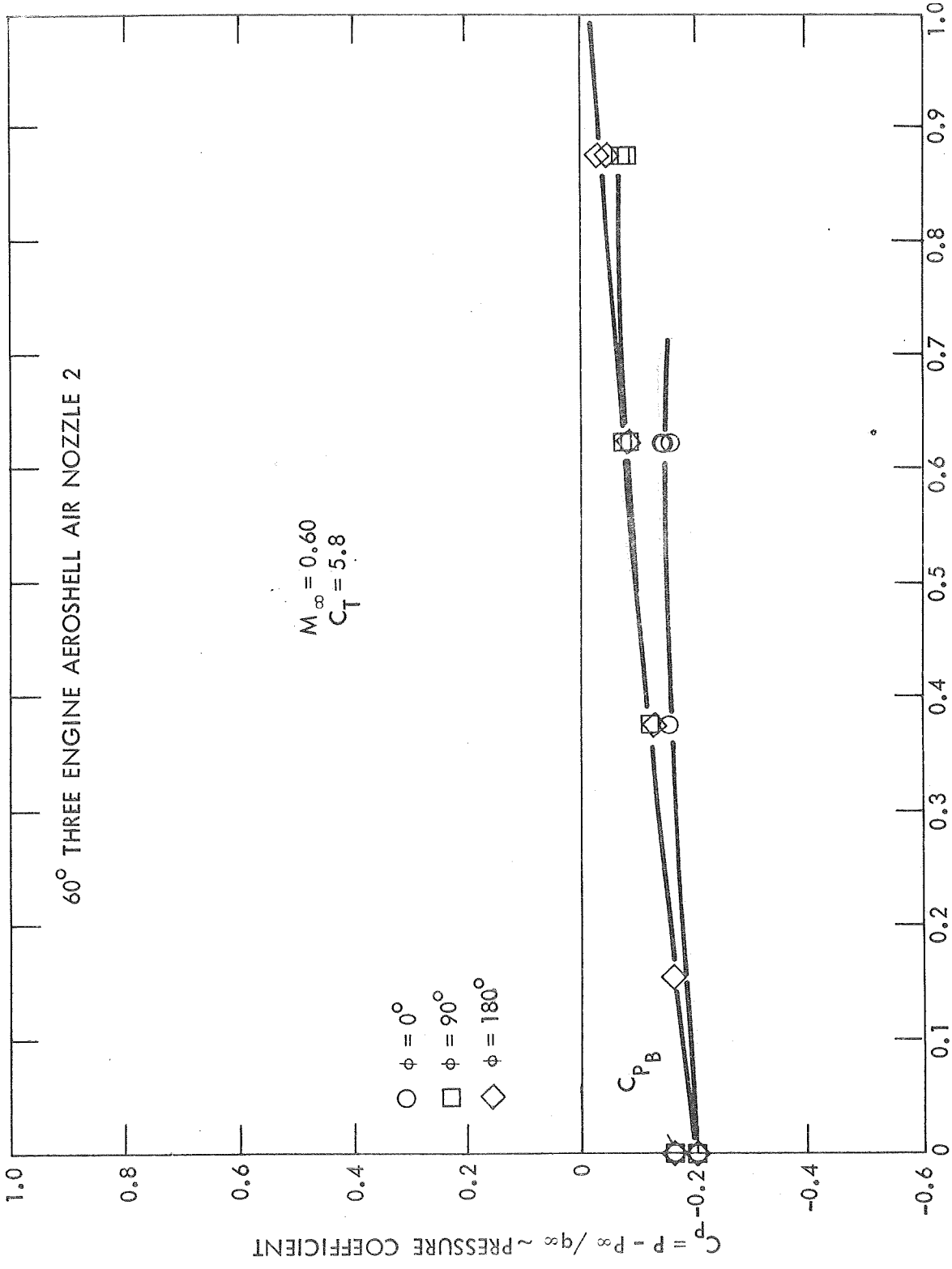

Figure 64 Surface Pressure Profiles - Three Engine 60° Aeroshell - $M_\infty = 0.60$, $C_T = 5.8$.

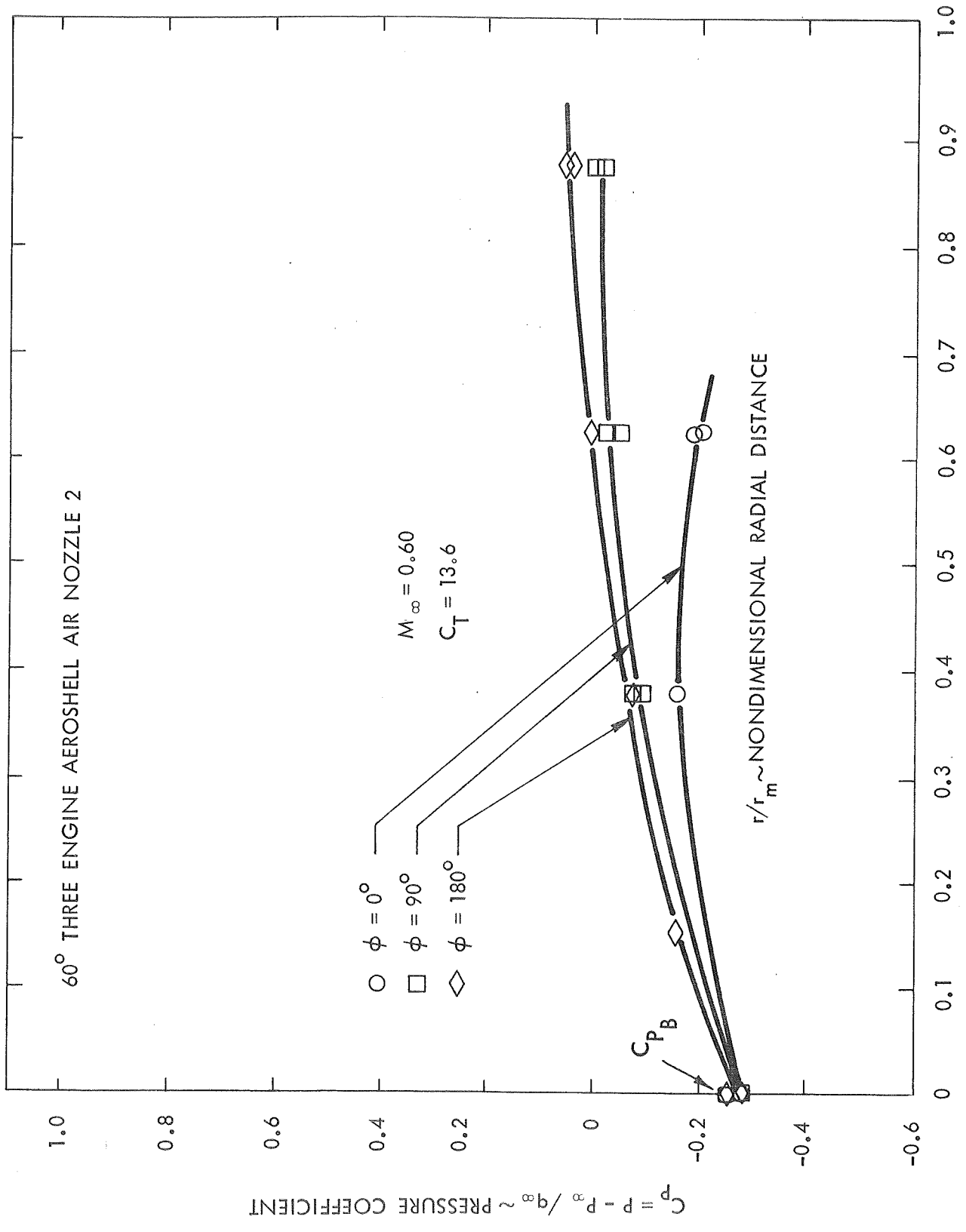

Figure 65 Surface Pressure Profiles - Three Engine 60° Aeroshell - $M_\infty = 0.60$, $C_T = 13.6$.

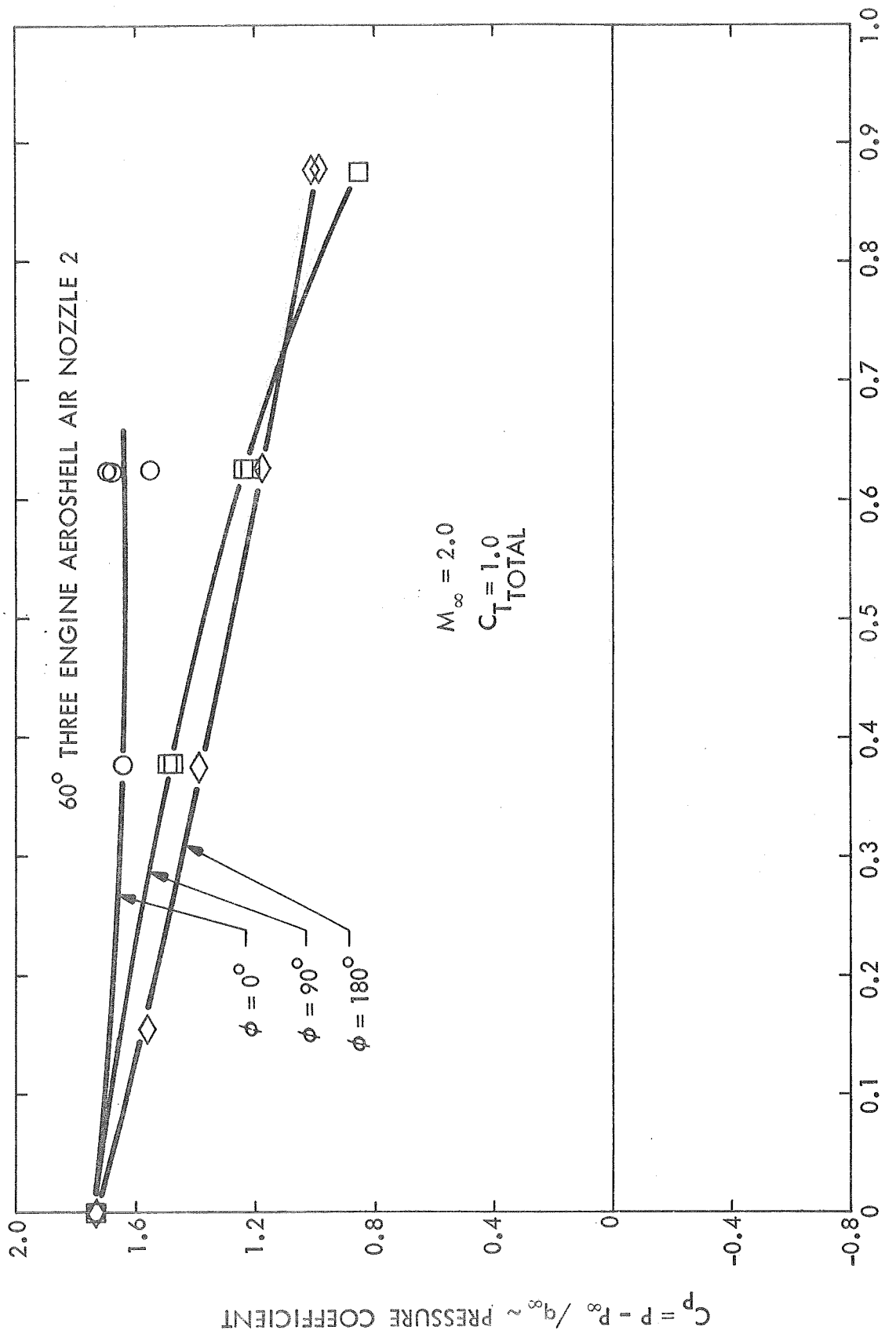

Figure 66 Surface Pressure Profiles - Three Engine 60° Aeroshell - $M_\infty = 2.0$, $C_T = 1.0$.

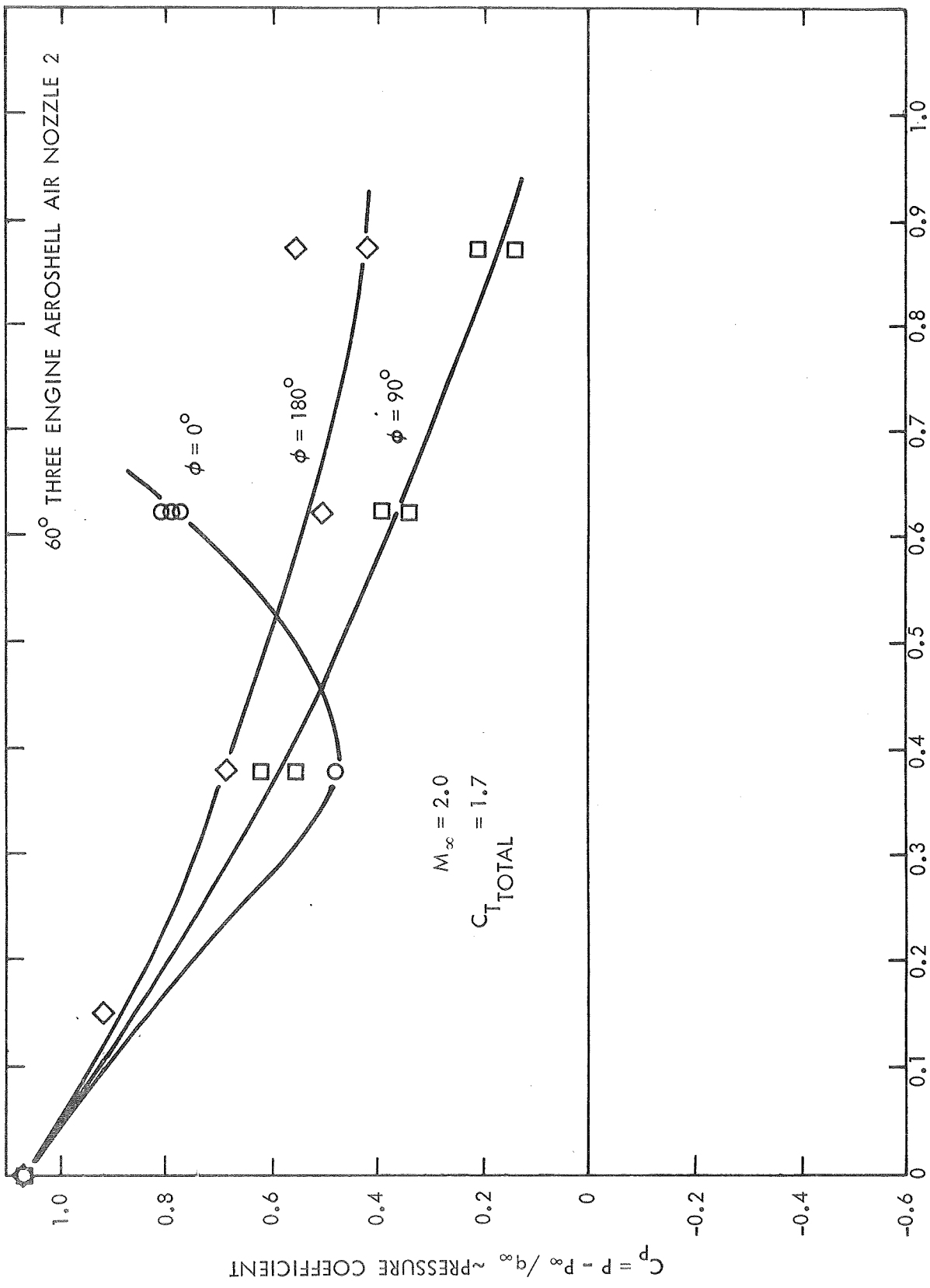

Figure 67 Surface Pressure Profiles - Three Engine 60° Aeroshell - $M_\infty = 2.0$, $C_T = 1.7$.

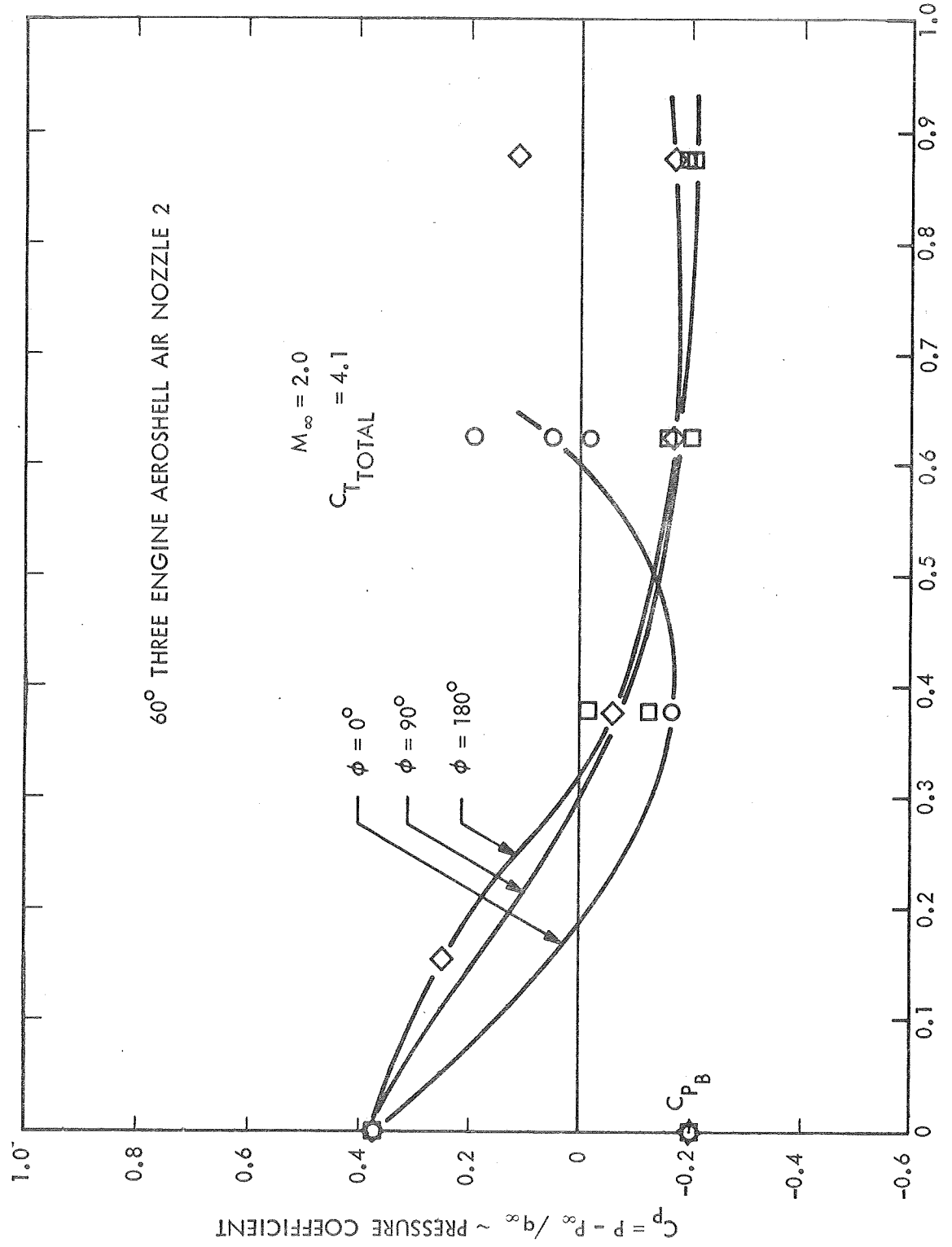

Figure 68 Surface Pressure Profiles - Three Engine 60° Aeroshell - $M_\infty = 2.0$ $C_T = 4.1$.

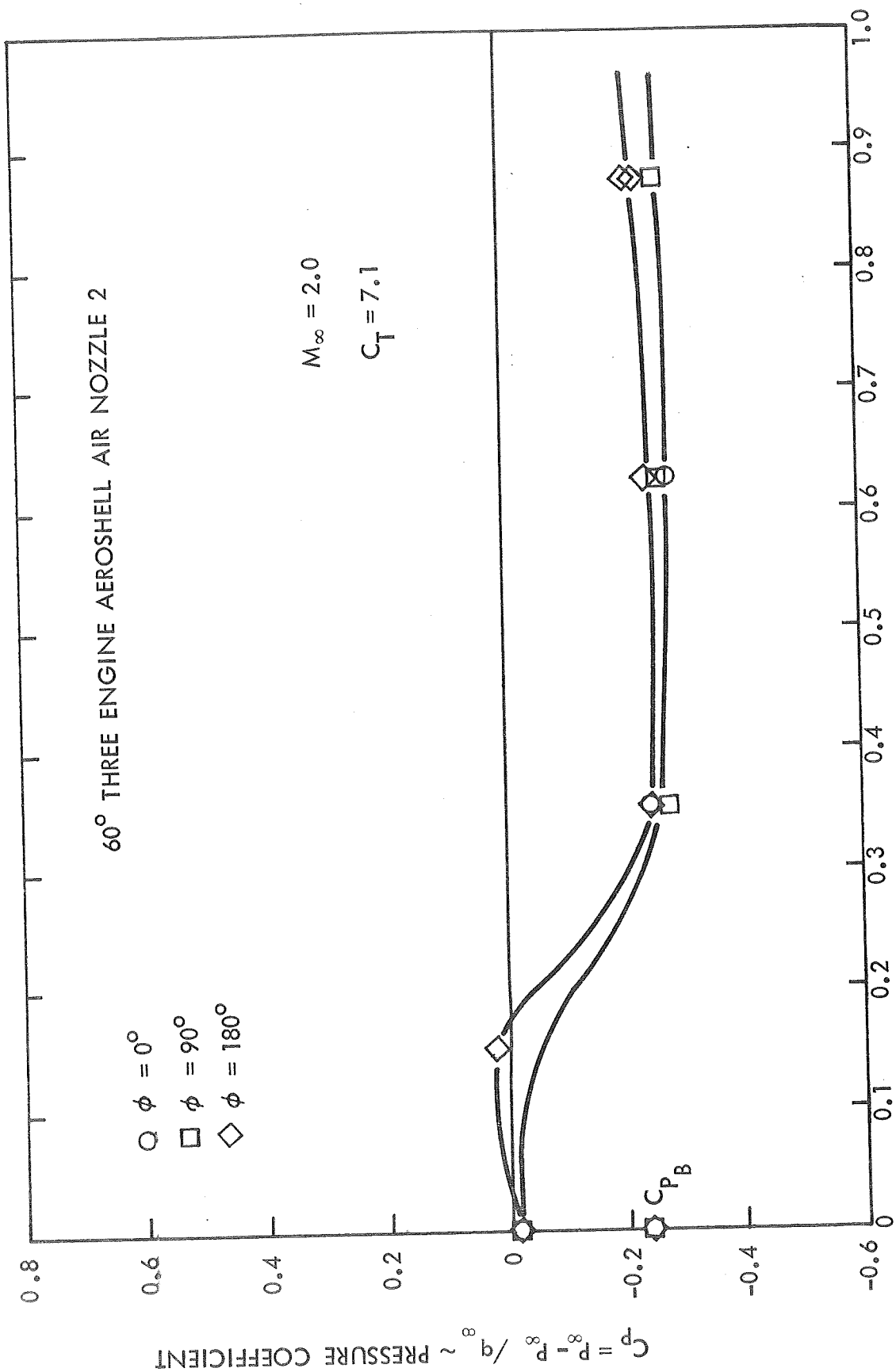

Figure 69 Surface Pressure Profiles - Three Engine 60° Aeroshell - $M_\infty = 2.0$, $C_T = 7.1$.

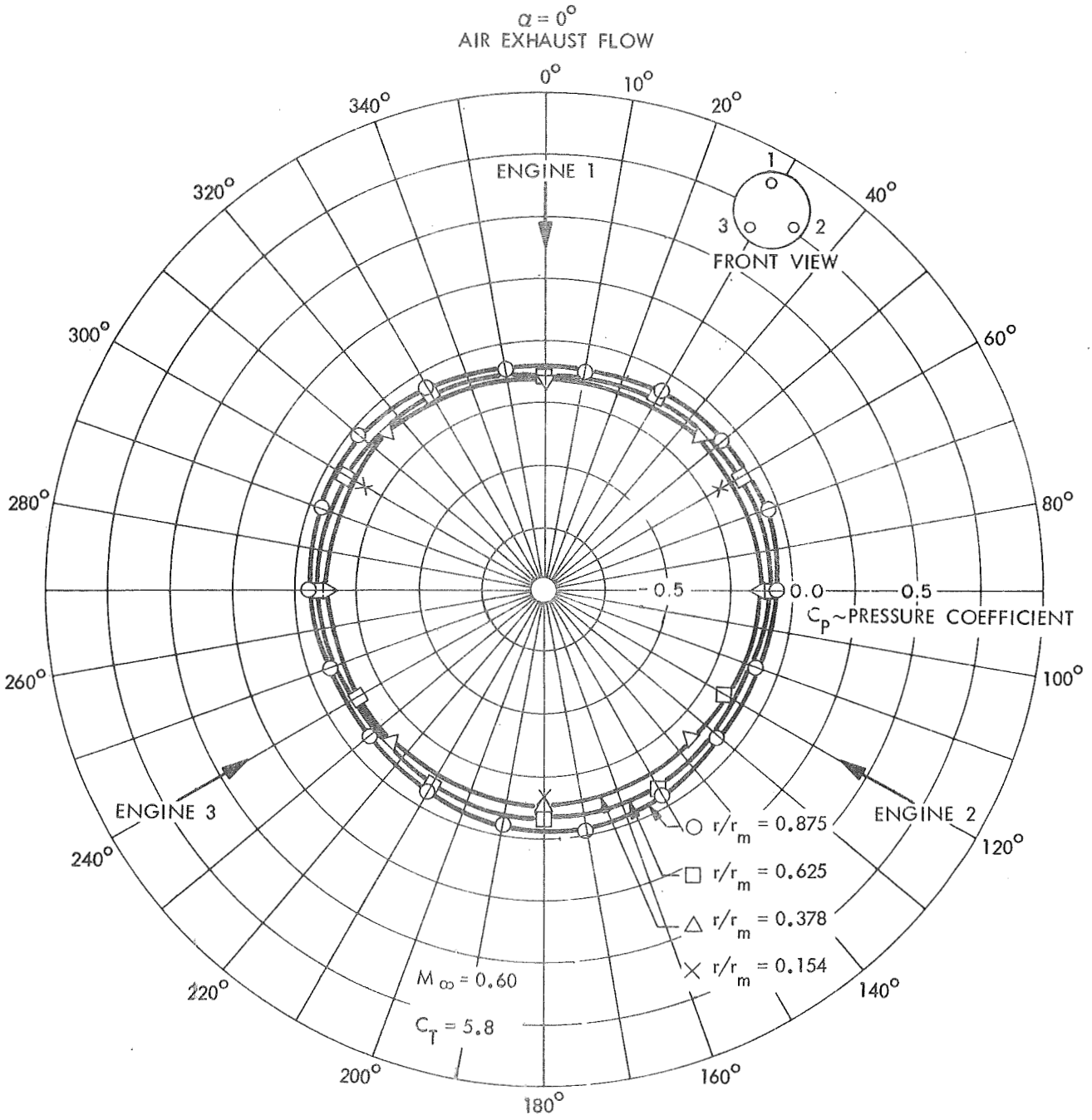

Figure 70 Circumferential Pressure Distribution - Three Engine 60° Aeroshell - $M_\infty = 0.60$, $C_T = 13.6$.

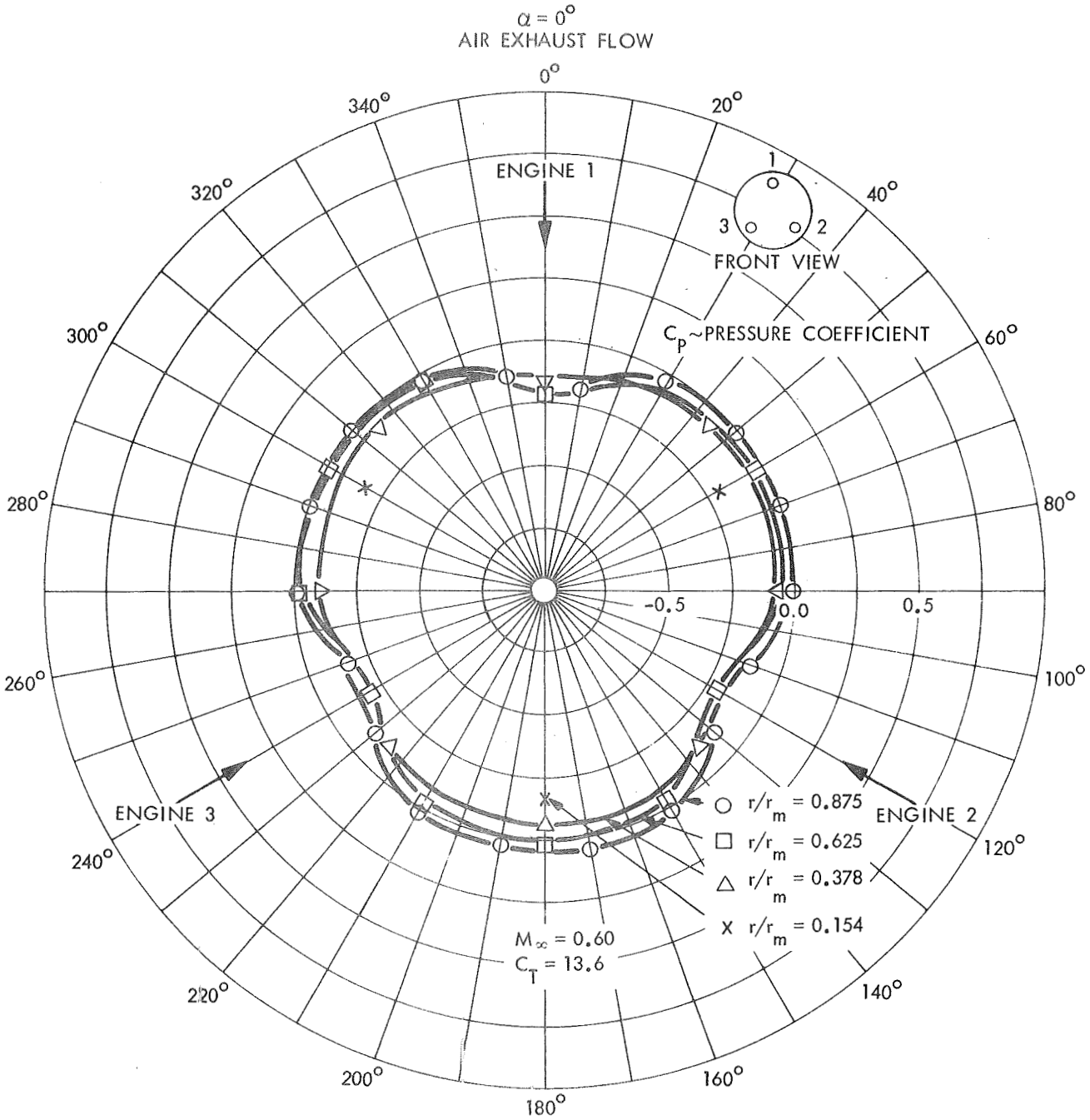

Figure 71 Circumferential Pressure Distribution - Three Engine 60° Aeroshell - $M_\infty = 0.60$, $C_T = 13.6$.

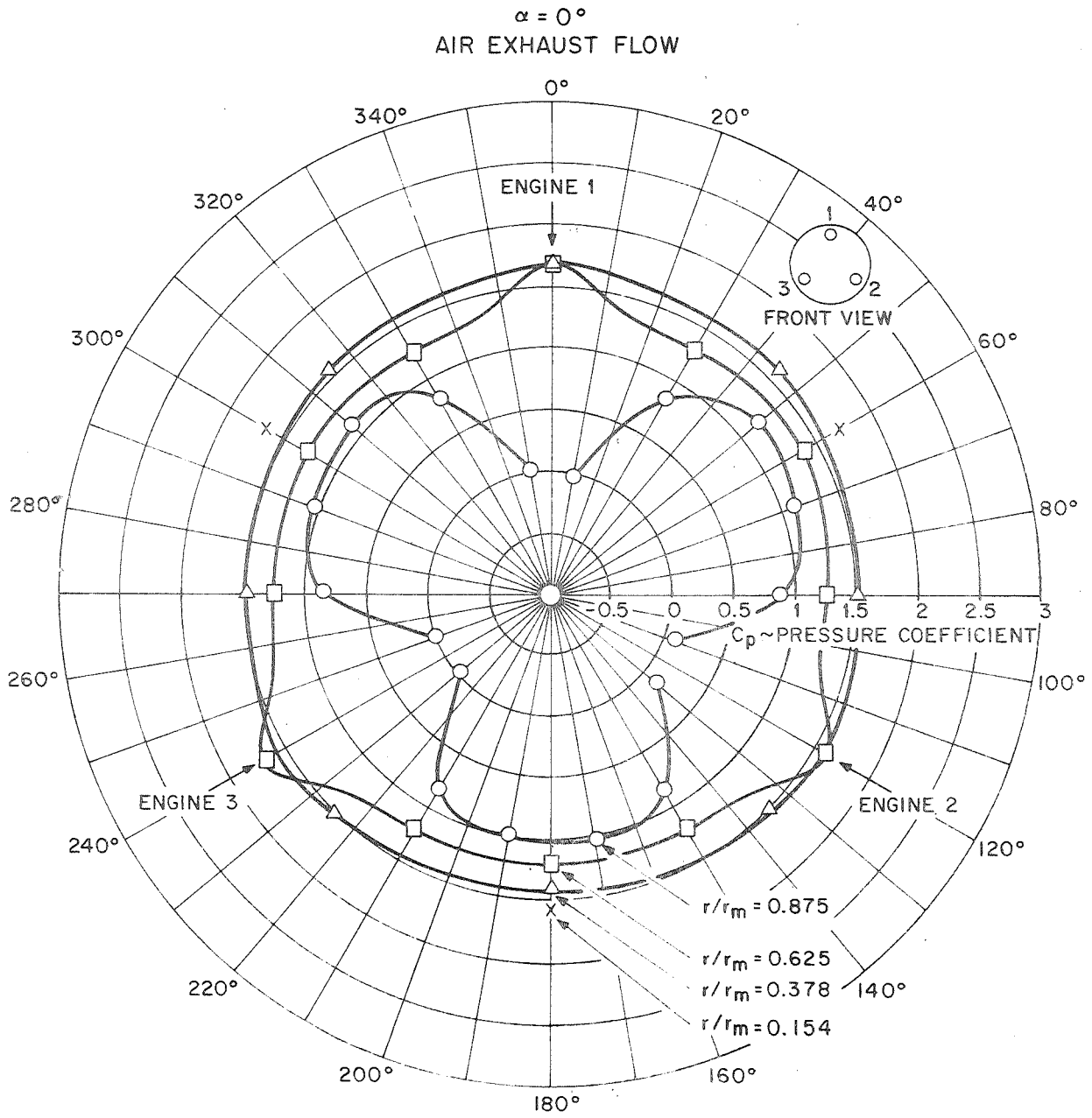

Figure 72 Circumferential Pressure Distribution - Three Engine 60° Aeroshell - M_∞ = 2.0, C_T = 1.0.

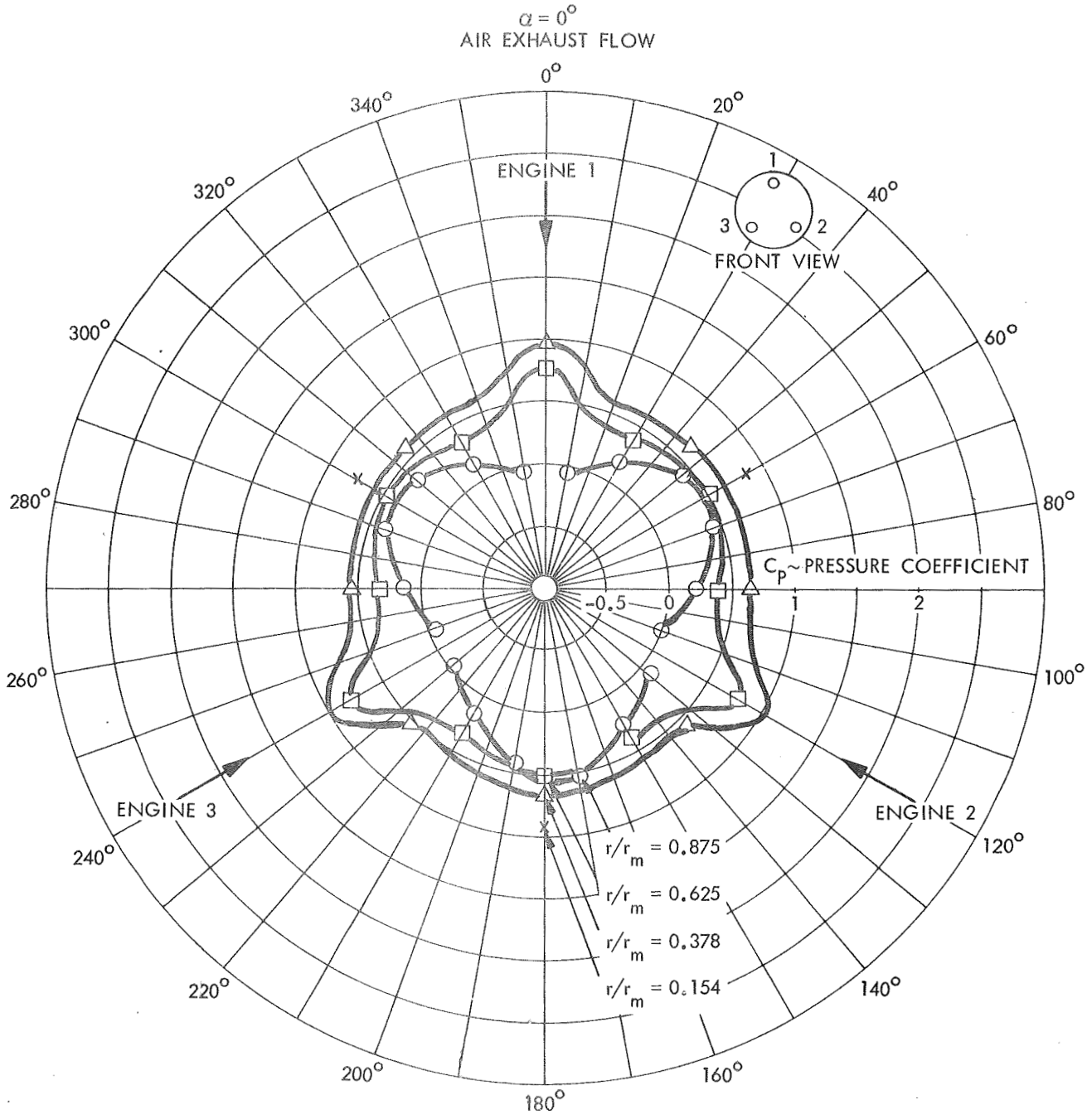

Figure 73 Circumferential Pressure Distribution - Three Engine 60° Aeroshell - $M_\infty = 2.0$, $C_T = 1.66$.

3.2.6 Aerodynamic Stability of Three Engine Aeroshell Models

The pitch stability of the three engine 60^{o} aeroshell at M_{∞} = 0.60, 1.05, and 2.0 is shown in Figures 74 through 79. Pitching moment and normal force coefficients at M_{∞} = 0.6 and C_T = 0.0, 1.95 and 3.75 are shown in Figures 74 and 75 respectively. Figures 76 and 77 depict the behavior at M_{∞} = 1.05 and C_T = 0.0, 1.0 and 1.9. The pitching moment and normal force at M_{∞} = 2.0 and C_T = 0.0, 1.04 and 1.66 are plotted in Figures 78 and 79. The overientation of the three engine configuration as viewed from head on is noted in the upper right hand corner of Figure 74. The pitch plane was in a vertical plane passing through the uppermost engine. The angle-of- attack is positive, nose up.

The pitching moment and normal force coefficient variation with angle-of-attack for the three engine aeroshell with retrothrust is not linear with angle-of-attack as was observed on the single engine aeroshell and the nonlinearity increases with increasing Mach numbers. The thrust coefficients noted in the figures are the sum of the individual and equal nozzle thrust coefficients. At M_{∞} = 0.60, the variation of pitching moment and normal force coefficient with angle-of-attack is different for plus and minus angles-of-attack (Figures 79 and 74). In addition, the variation of pitching moment and normal force coefficient with angle-of-attack is different for different magnitudes of thrusting coefficient.

At transonic free stream conditions, M_{∞} = 1.05, substantial nonlinearities appear, in the pitching moment and normal force coefficients variation with angle-of-attack, at negative angles-of-attack (Figures 76 and 77). At supersonic velocities, the nonlinearities at negative angles-of-attack become quite sever (Figures 78 and 79). At negative angles-of-attack, the pitching moment decreases nearly to zero for C_T = 1.04 and 1.06 at M_{∞} = 2.0 (Figure 78). The normal force coefficient shows the same nonlinear behavior (Figure 79). A region of pitch instability exists at negative angles-of-attack.

The yawing moment and side force coefficients measured during pitch angle-of-attack runs are displayed in Figures 80 and 81. The yawing moment and side force coefficients were small and varied little during an angle-of-attack sweep.

A comparison of the pitching moment acting on the three engine and single engine aeroshells at $M_\infty = 2.0$ and $C_T = 1.0$ is made in Figure 82. The pitching moments are substantially different at negative angles-of-attack. It should be noted that the shape of the pitching moment curve depends on the roll-orientation of the pitch plane with respect to the engines.

3.2.7 Shadowgraphs of the Flow Field about Multiple Engine Aeroshells at Angle-of-Attack

Shadowgraphs of the flow field about the three engine 60° aeroshell at angle-of-attack, at $M_\infty = 0.6$ and 2.0, are presented in Figures 83 and 84. The shadowgraph in Figure 83 was taken at an angle-of-attack of minus 16.8 degrees, $M_\infty = 0.60$ and $C_T = 3.92$. The shadowgraph (Figure 84) was made at minus 9 degrees angle-of-attack, $C_T = 1.03$ and $M_\infty = 2.0$.

3.2.8 Shadowgraphs of the Flow Field about Aeorshells with Throttled Engines - $\alpha = 0^\circ$

The aerodynamic characteristics of the three engine 60° aeroshell, with some of its engines throttled to partial thrust, was investigated at $M_\infty = 0.60$, 1.05 and 2.0. Measurements were made for engine 1 throttled to 1/2 and 1/4 thrust and for engines 2 and 3 simultaneously throttled to 1/2 and 1/4 thrust (Table IV). The effects of engine throttling were investigated because engine throttling affords an active means by which the aeroshell attitude may be controlled. Engine throttling was accomplished by placing orifices in the individual engine supply tubes on the supply side of the flow straightener.

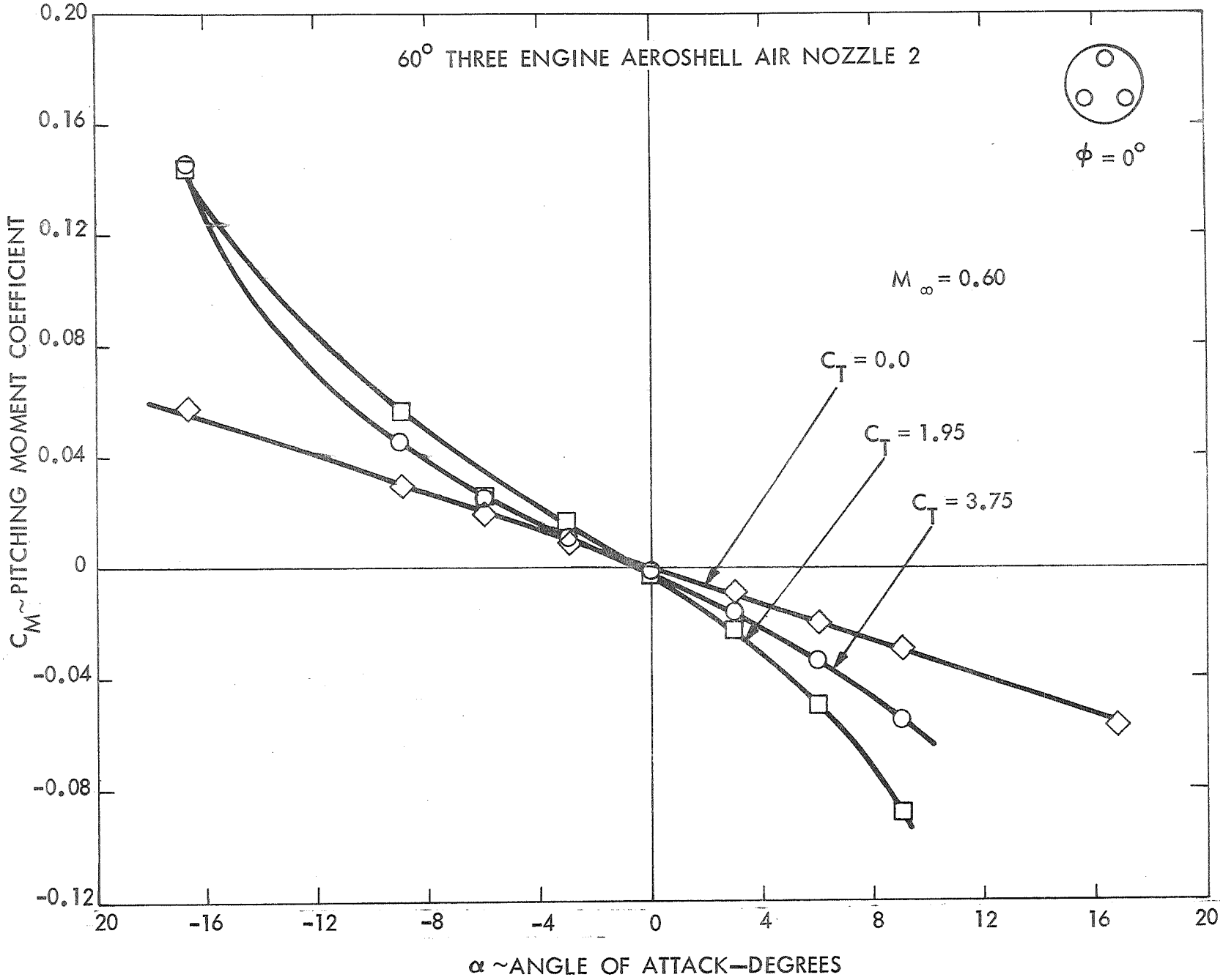

Figure 74 Pitching Moment Coefficients - Three Engine 60° Aeroshell - M_∞ = 0.60.

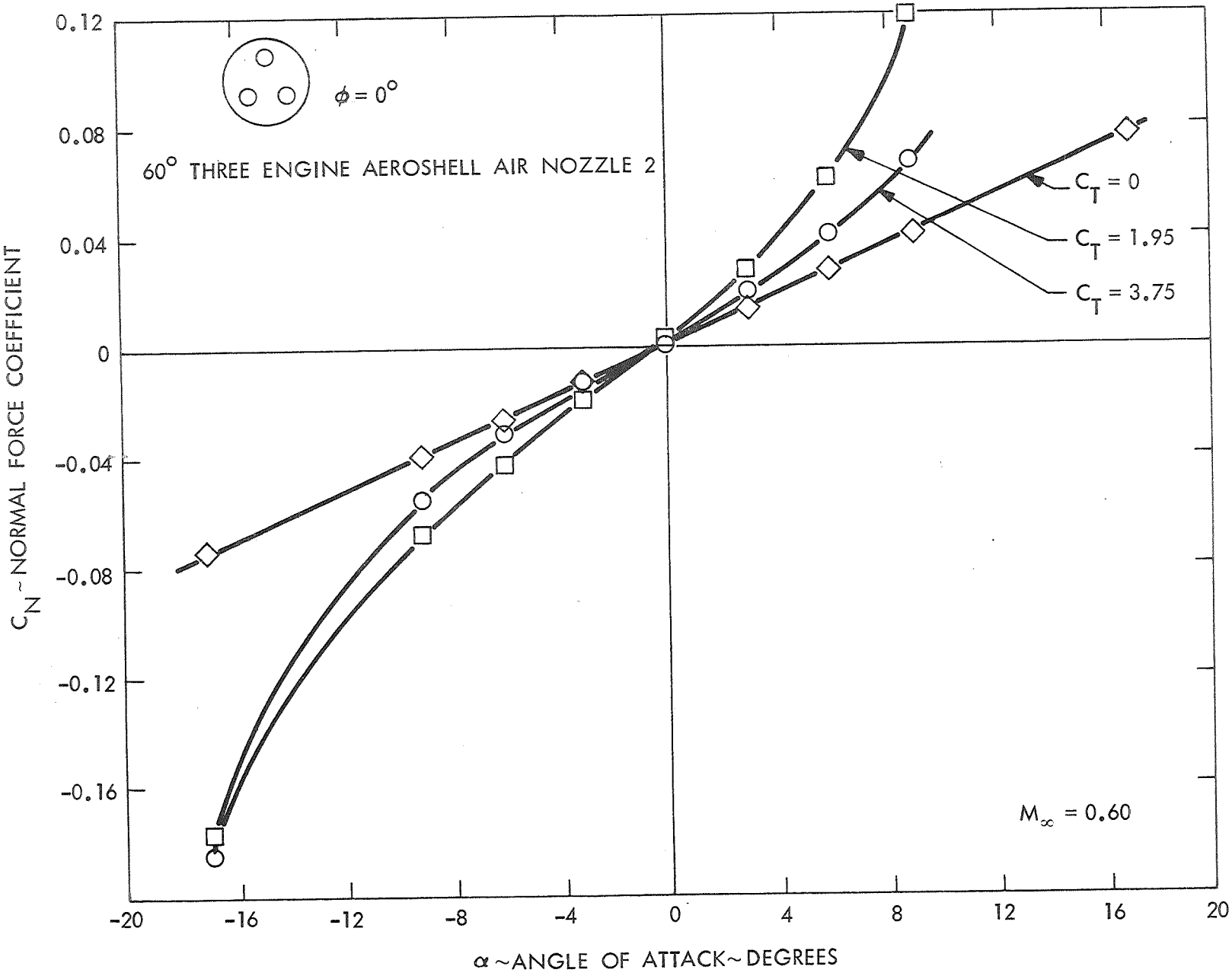

Figure 75 Normal Force Coefficients - Three Engine 60° Aeroshell - $M_\infty = 0.60$.

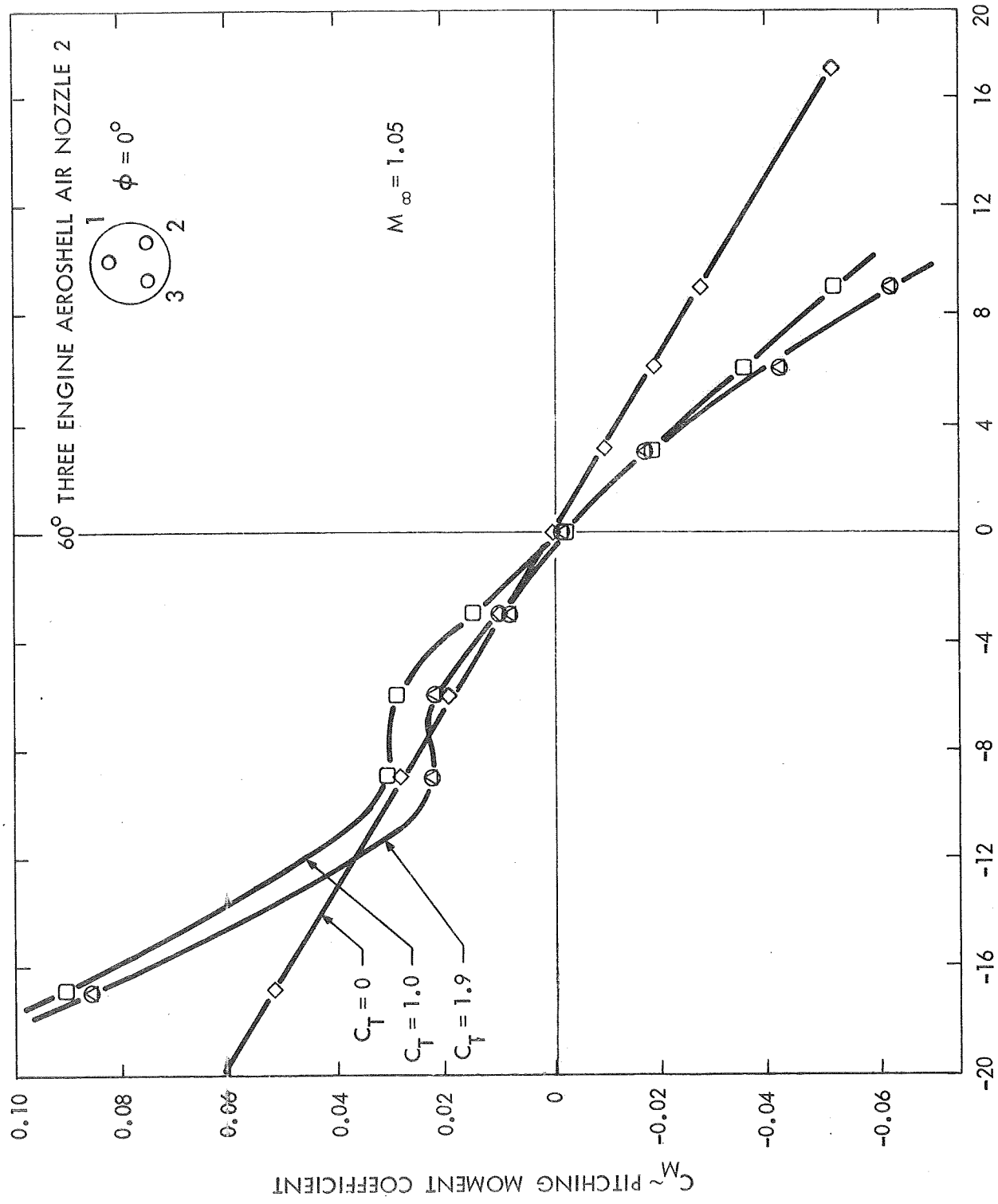

Figure 76 Pitching Moment Coefficients - Three Engine 60° Aeroshell - M_∞ = 1.05.

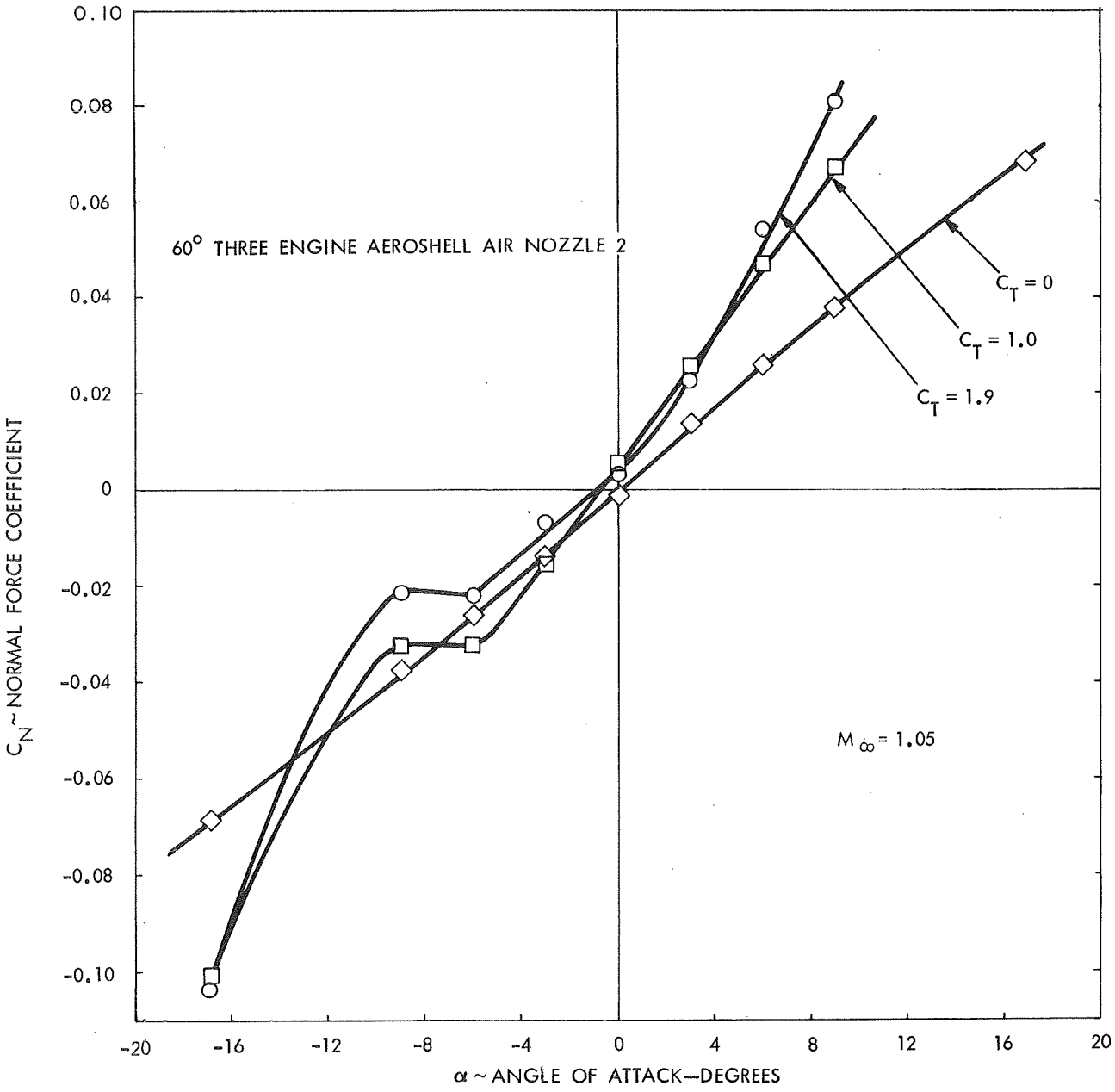

Figure 77 Normal Force Coefficients - Three Engine 60° Aeroshell - $M_\infty = 1.05$.

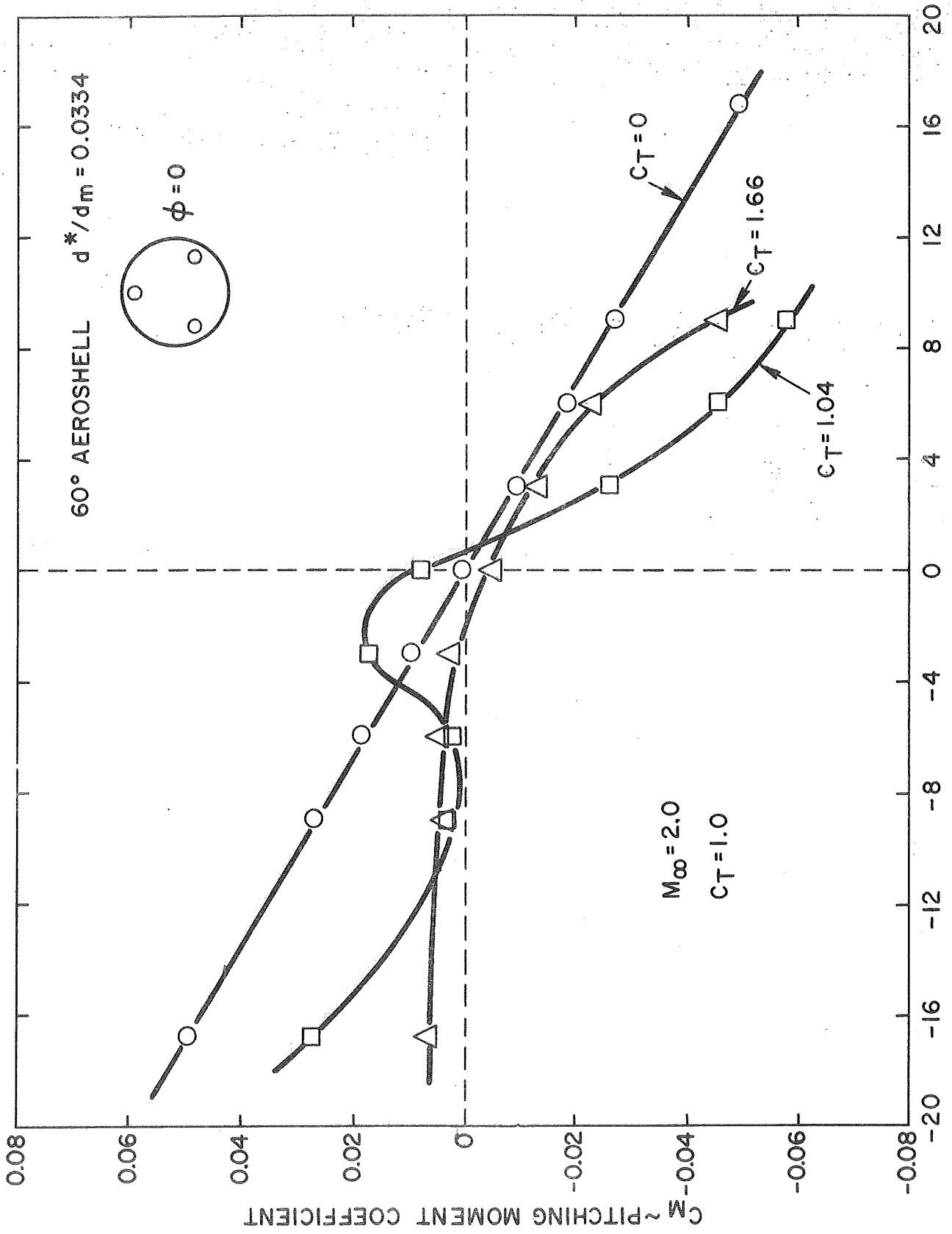

Figure 78 Pitching Moment Coefficient 3 Engine 60° Aeroshell; $M_\infty = 2.0$.

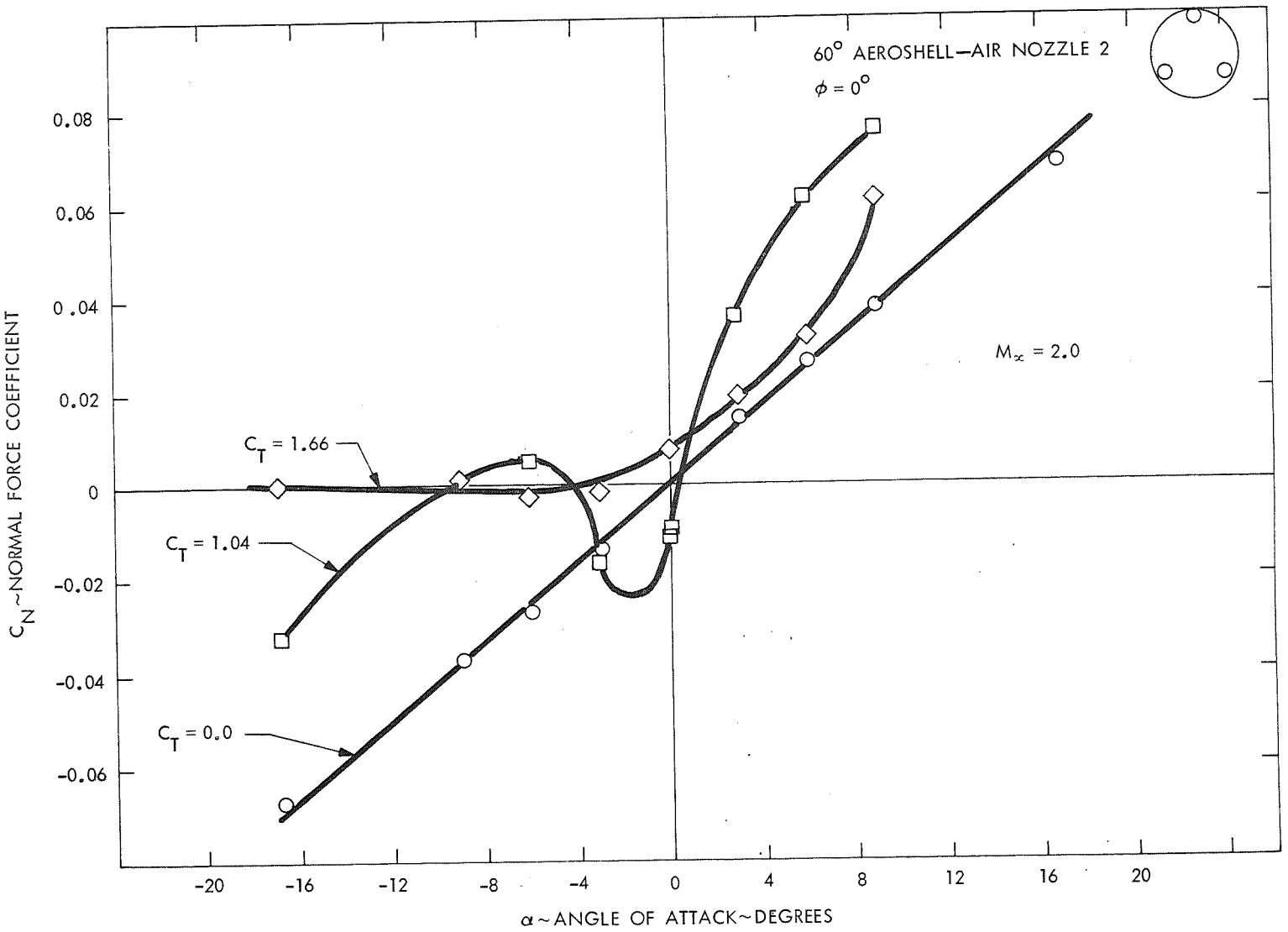

Figure 79 Normal Force Coefficient - 3 Engine 60° Aeroshell, $M_\infty = 2.0$.

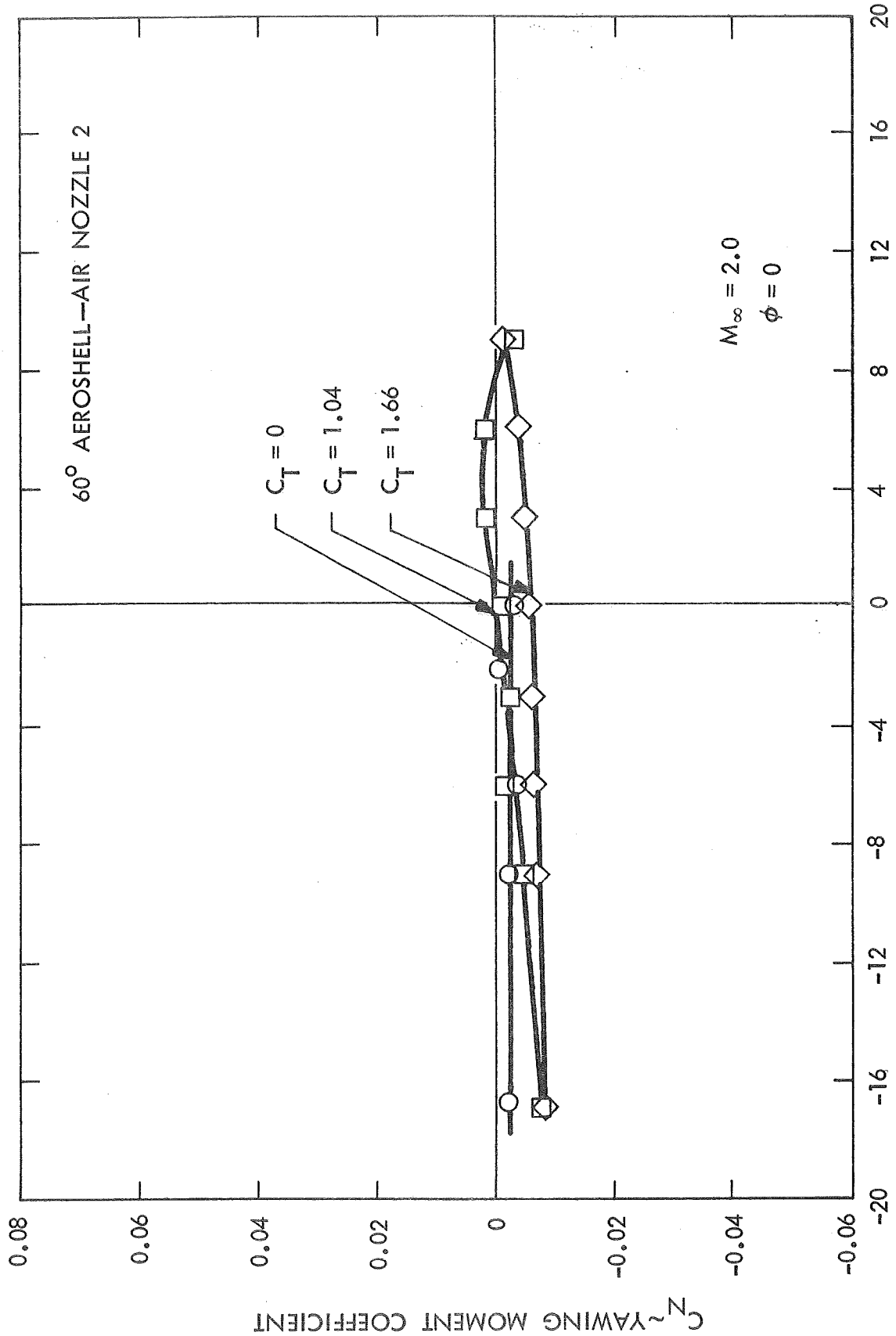

Figure 80 Yawing Moment Coefficient - 3 Engine 60° Aeroshell, $M_\infty = 2.0$.

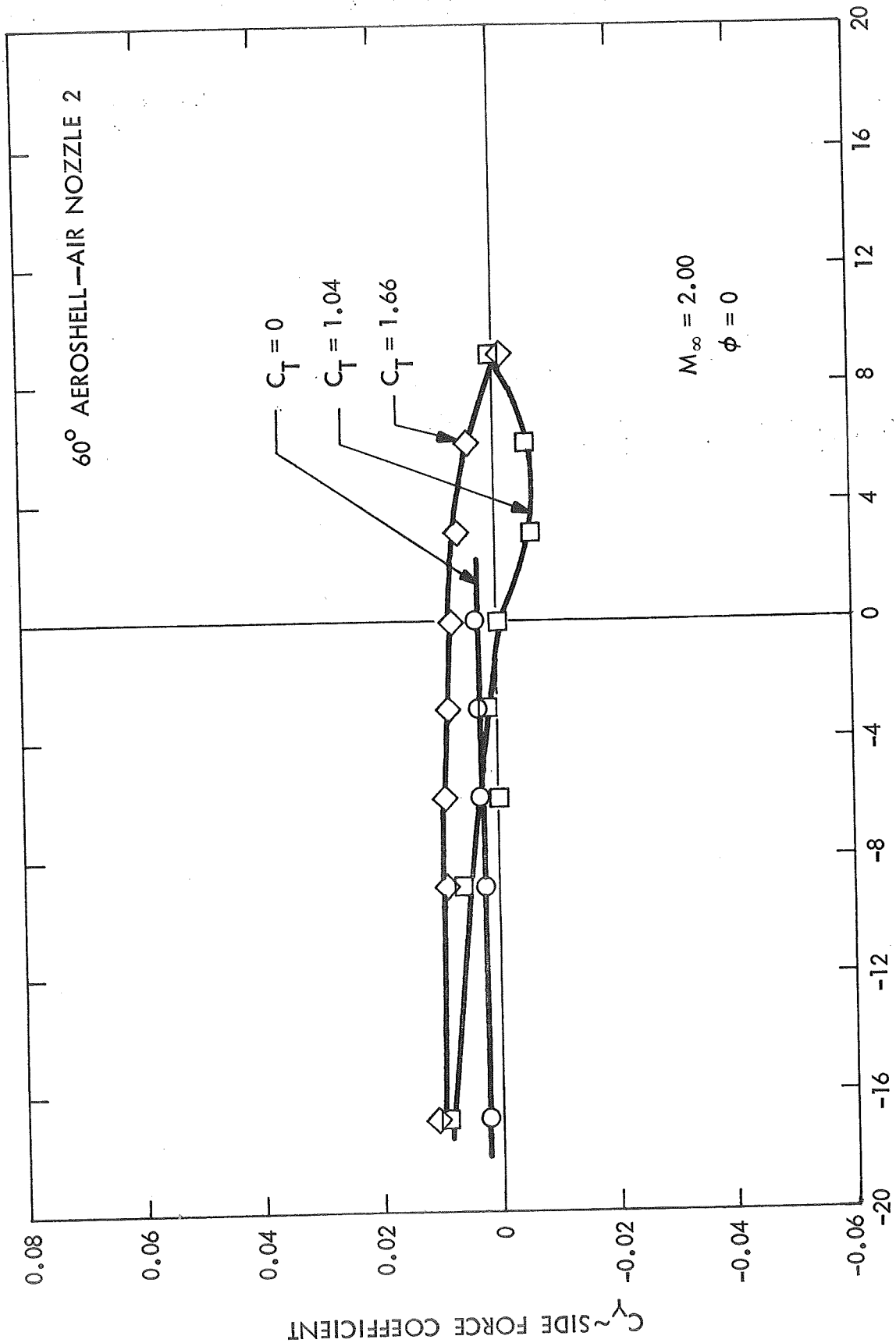

Figure 81 Side Force Coefficient - 3 Engine 60° Aeroshell, $M_\infty = 2.0$.

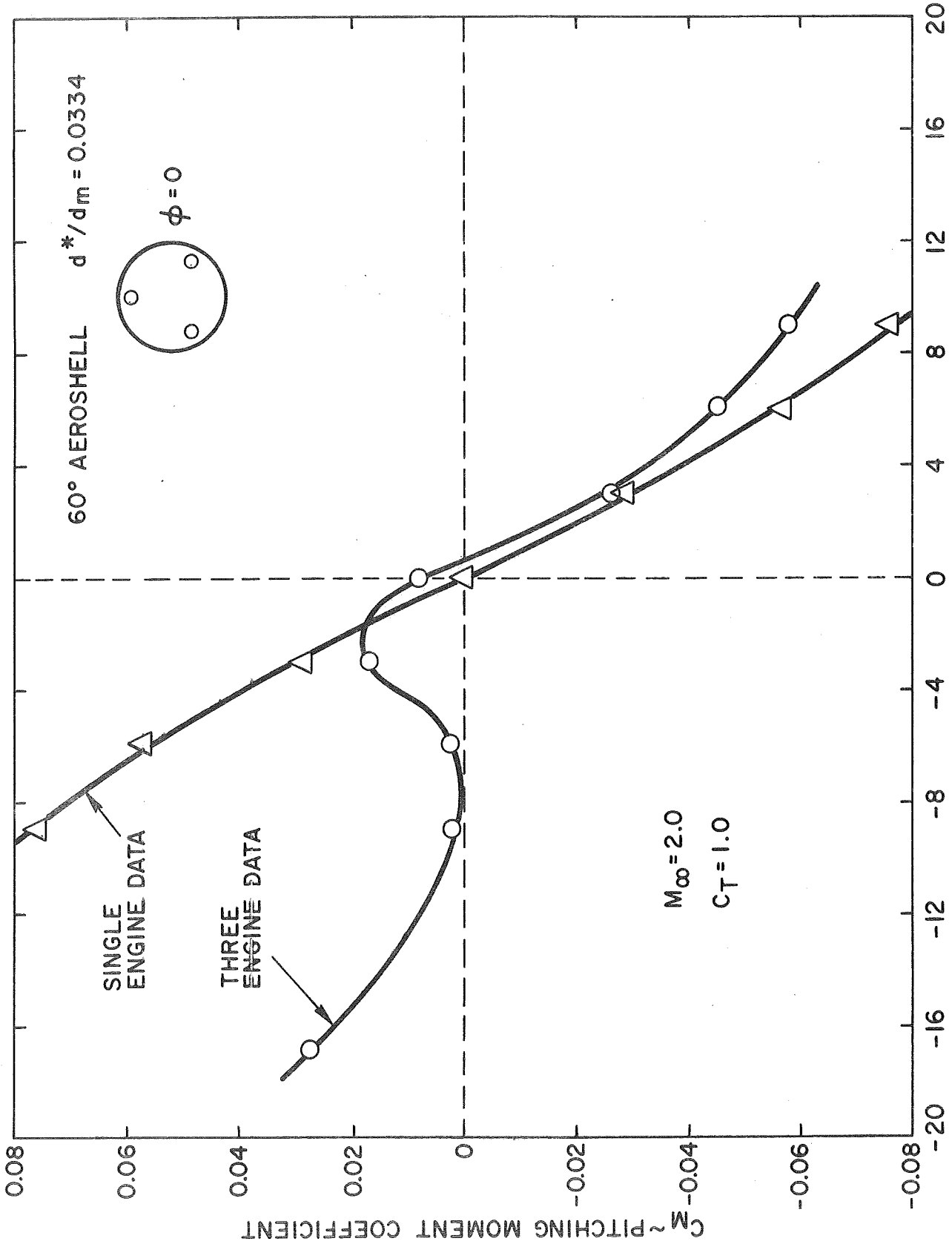

Figure 82 Comparison of Pitching Moment Coefficients of Single and Three Nozzle Aeroshell Models $C_T = 1.0$; $M_\infty = 2.0$.

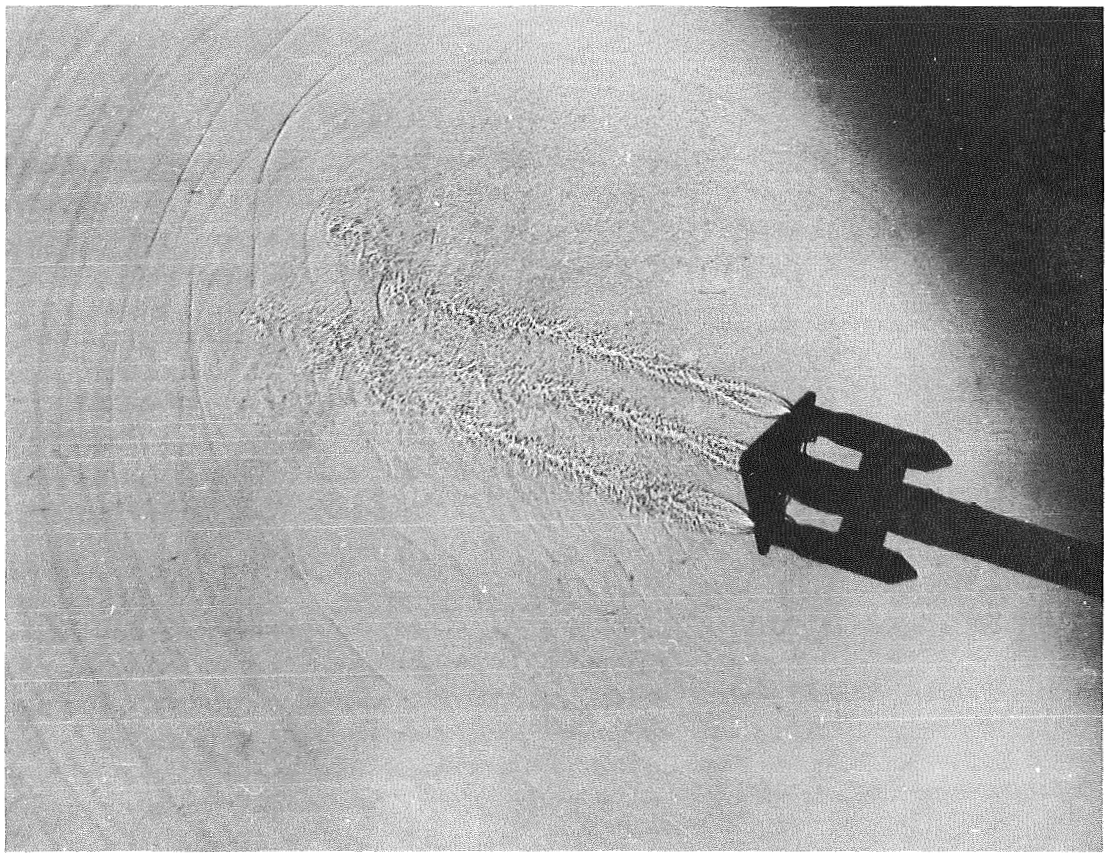

Figure 83 Shadowgraph of Flow Field About Three Engine 60^{o} Aeroshell at Angle of Attack $M_{\infty} = 0.60$, $\alpha = -16.8^{o}$, $C_T = 3.92$.

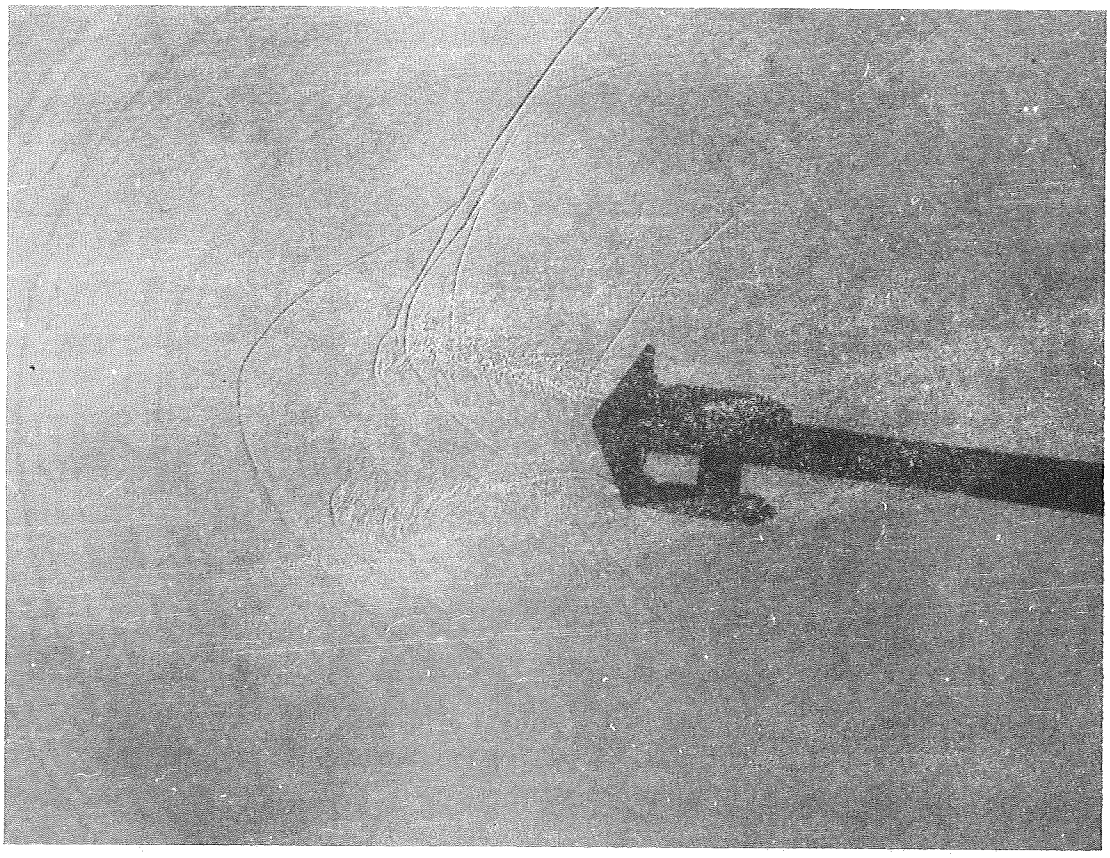

Figure 84 Shadowgraph of Flow Field About Three Engine 60° Aeroshell at Angle of Attack $M_{\infty} = 2.0$, $\alpha = -9.0^{\circ}$, $C_T = 1.03$.

Shadowgraphs of the flow field about the multiple engine aeroshell at zero angle-of-attack are offered in Figures 85 and 86. Figure 85 considers the flow field at $M_\infty = 2.0$ when engine 1 is throttled to 1/4 thrust. The total thrusting coefficient was 4.0 with the individual engine thrusting coefficients of $C_{T_{E1}} = 0.4$, $C_{T_{E2}} = 1.8$ and $C_{T_{E3}} = 1.8$. A front view of the aeroshell, noting the engine orientation for the shadowgraph (Figure 85), is displayed in the upper left hand corner. Figure 86 presents a shadowgraph of the flow field at $M_\infty = 2.0$ with engine 2 and engine 3 simultaneously throttled to 1/4 thrust. The total thrusting coefficient is 2.8 with the following distribution: $C_{T_{E1}} = 1.7$, $C_{T_{E2}} = 0.5$ and $C_{T_{E3}} = 0.6$.

3.2.9 Effect of Engine Throttling on the Forebody Axial Force Coefficient

The forebody axial force coefficients for various engine throttling configurations are plotted in Figures 87 through 92. The variation of forebody drag coefficient with thrusting coefficient for engine 1 throttled to 1/2 and 1/4 thrust and $M_\infty = 0.60$, 1.05 and 2.0 are noted in Figures 87, 89 and 91. The variation of forebody axial force coefficient, for aeroshell vehicles which are not throttled but operate at the same total thrusting coefficient, is noted on these figures for comparison. The variations of forebody drag coefficient with thrusting coefficient, for engine 2 and engine 3 simultaneously throttled to 1/2 and 1/4 thrust and $M_\infty = 0.60$, 1.05 and 2.0, are noted in Figures 88, 90 and 92. Data for the three engine 60^o aeroshell, without throttling, is shown for comparison. At subsonic speeds ($M_\infty = 0.60$) and low thrusting coefficients ($C_T < 6$), the axial force coefficient increases as the engines are throttled (Figures 87 and 88). At transonic speeds, the axial force coefficient are the same, with and without throttling if the thrusting coefficient is less than about three, i.e. $C_T \leq 3.0$ (Figures 89 and 90). While at supersonic free stream conditions, the variation of axial force with and without throttling are appreciably different (Figures 91 and 92).

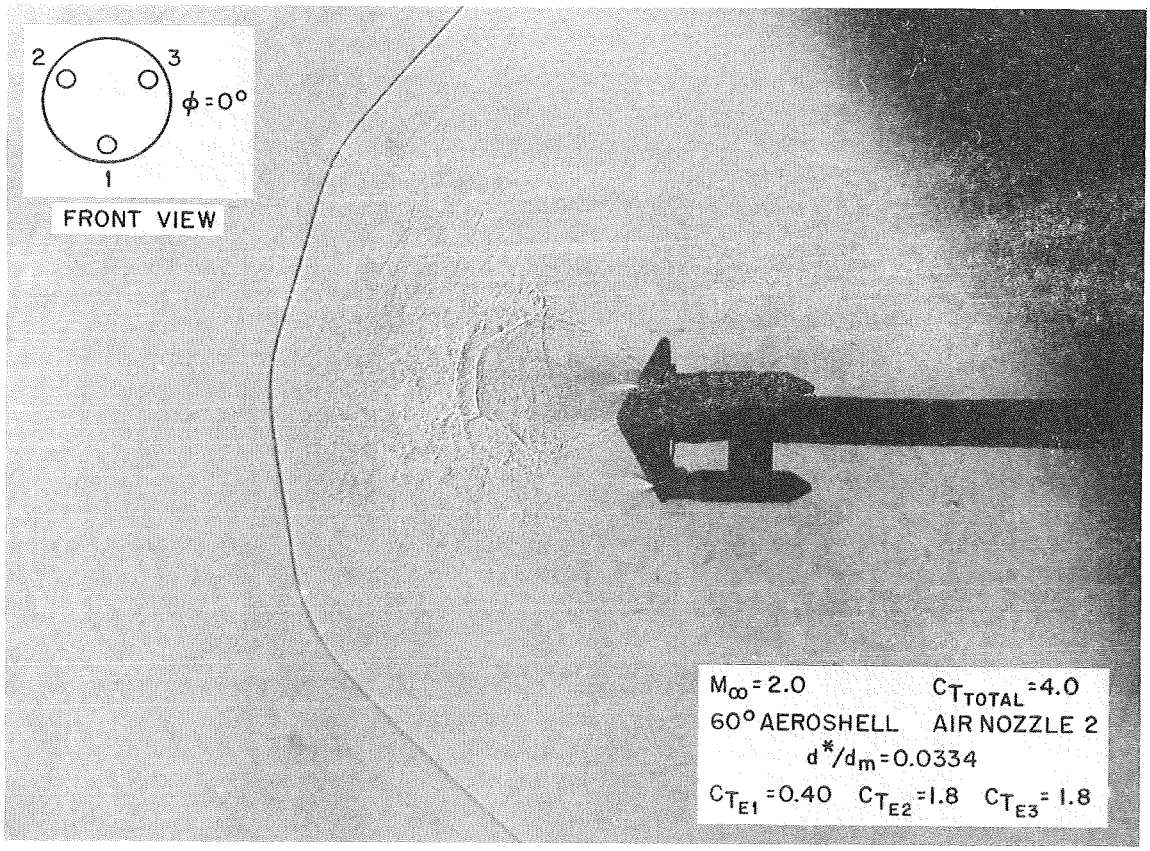

Figure 85 Flow Field of Three Engine, 60° Aeroshell - Engine 1 Throttled to 1/4 Thrust $M_\infty = 2.0$; $C_{T_{TOTAL}} = 4.0$; $\phi = 0^\circ$.

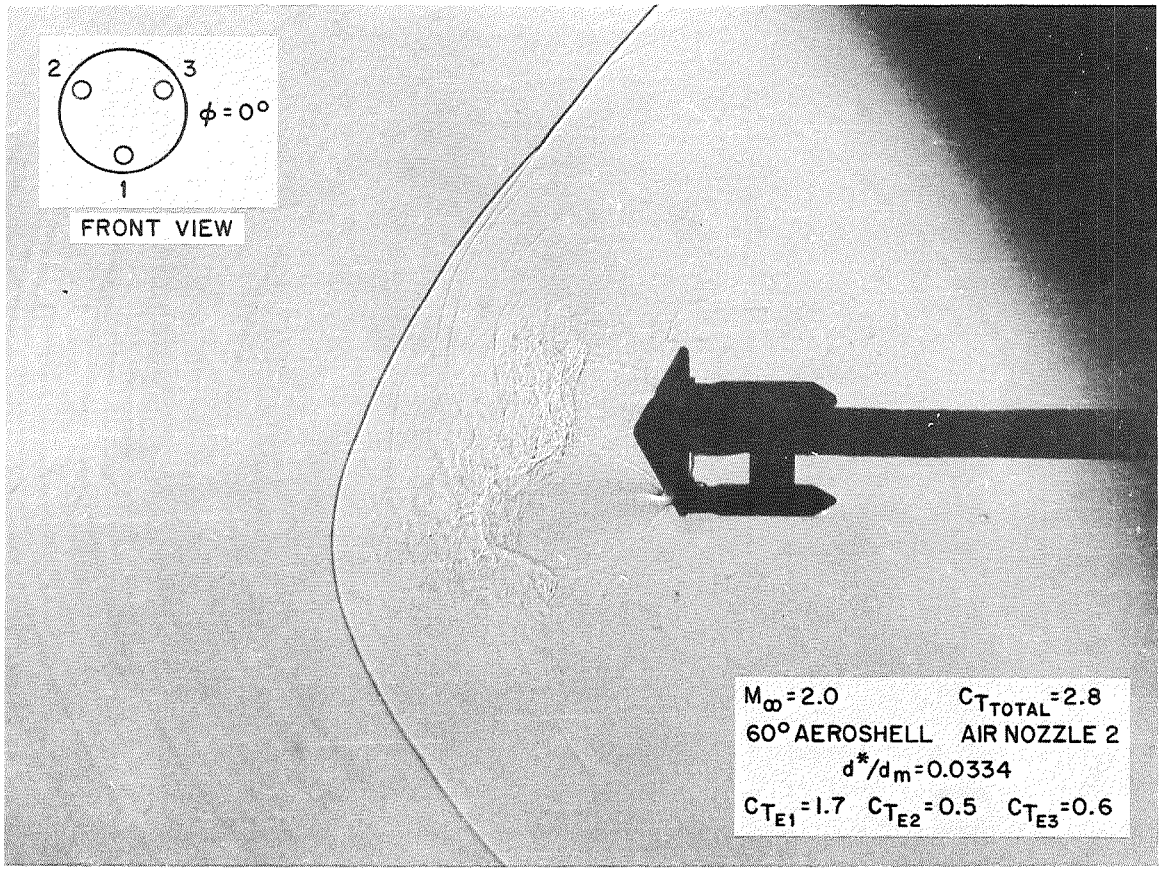

Figure 86 Flow Field of Three Engine, 60° Aeroshell - Engine 2 and Engine 3 Throttled to 1/4 Thrust $M_\infty = 2.0$; $C_{T_{TOTAL}} = 2.8$; $\phi = 0°$.

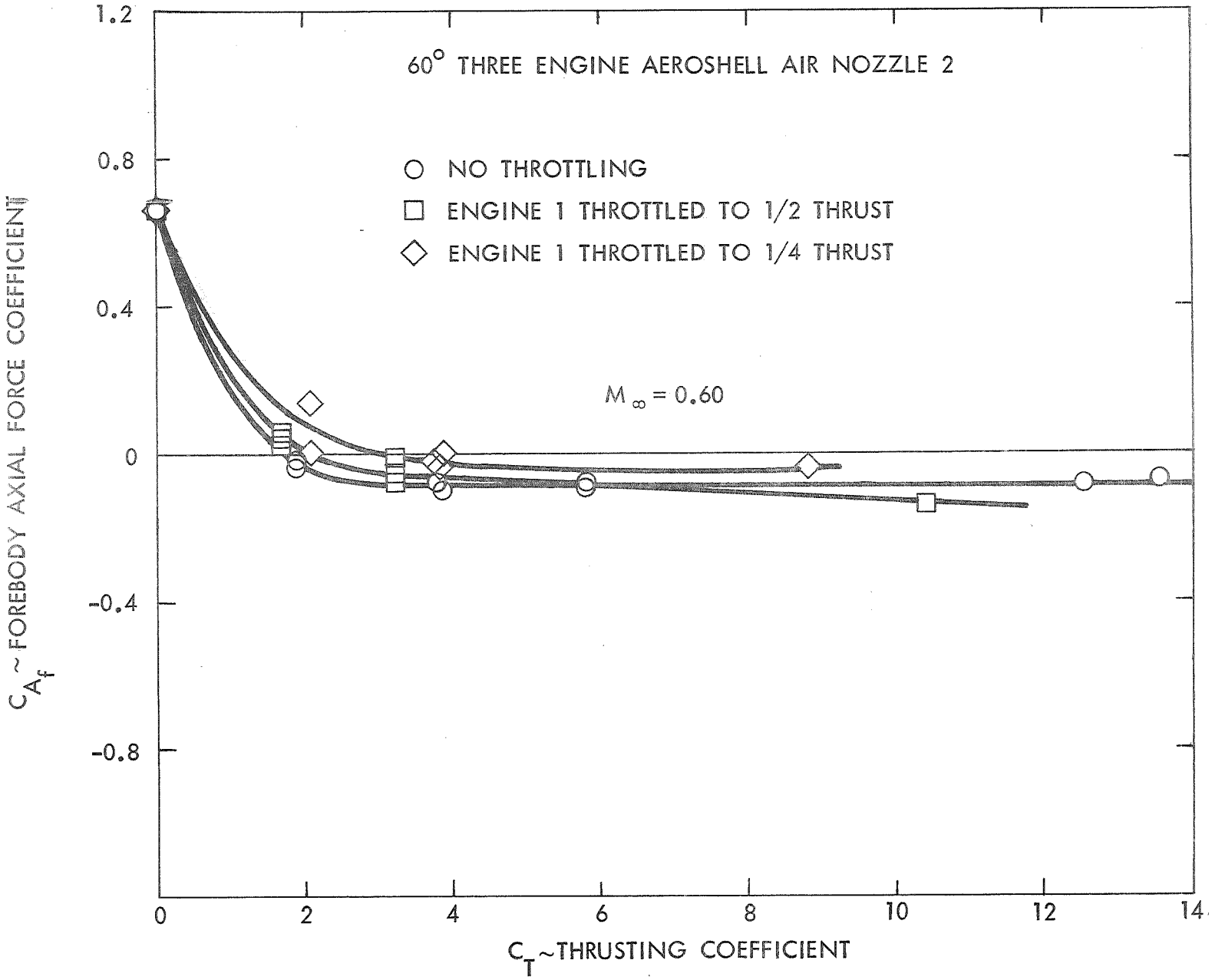

Figure 87 Forebody Axial Force Coefficient with Engine 1 Throttled - Three Engine 60° Aeroshell - $M_\infty = 0.60$.

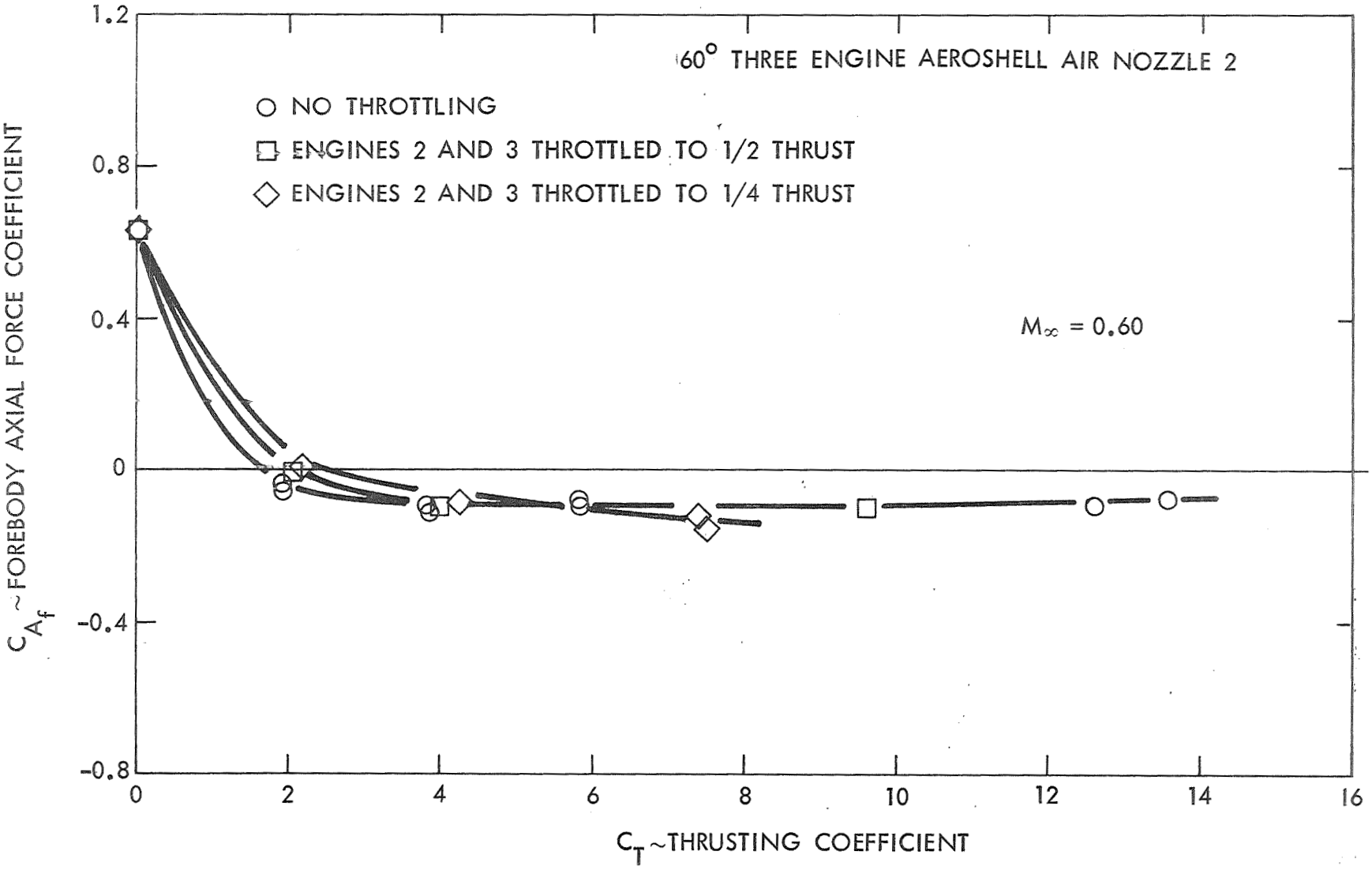

Figure 88 Forebody Axial Force Coefficient with Engine 2 and Engine 3 Throttled - Three Engine 60° Aeroshell - $M_\infty = 0.60$.

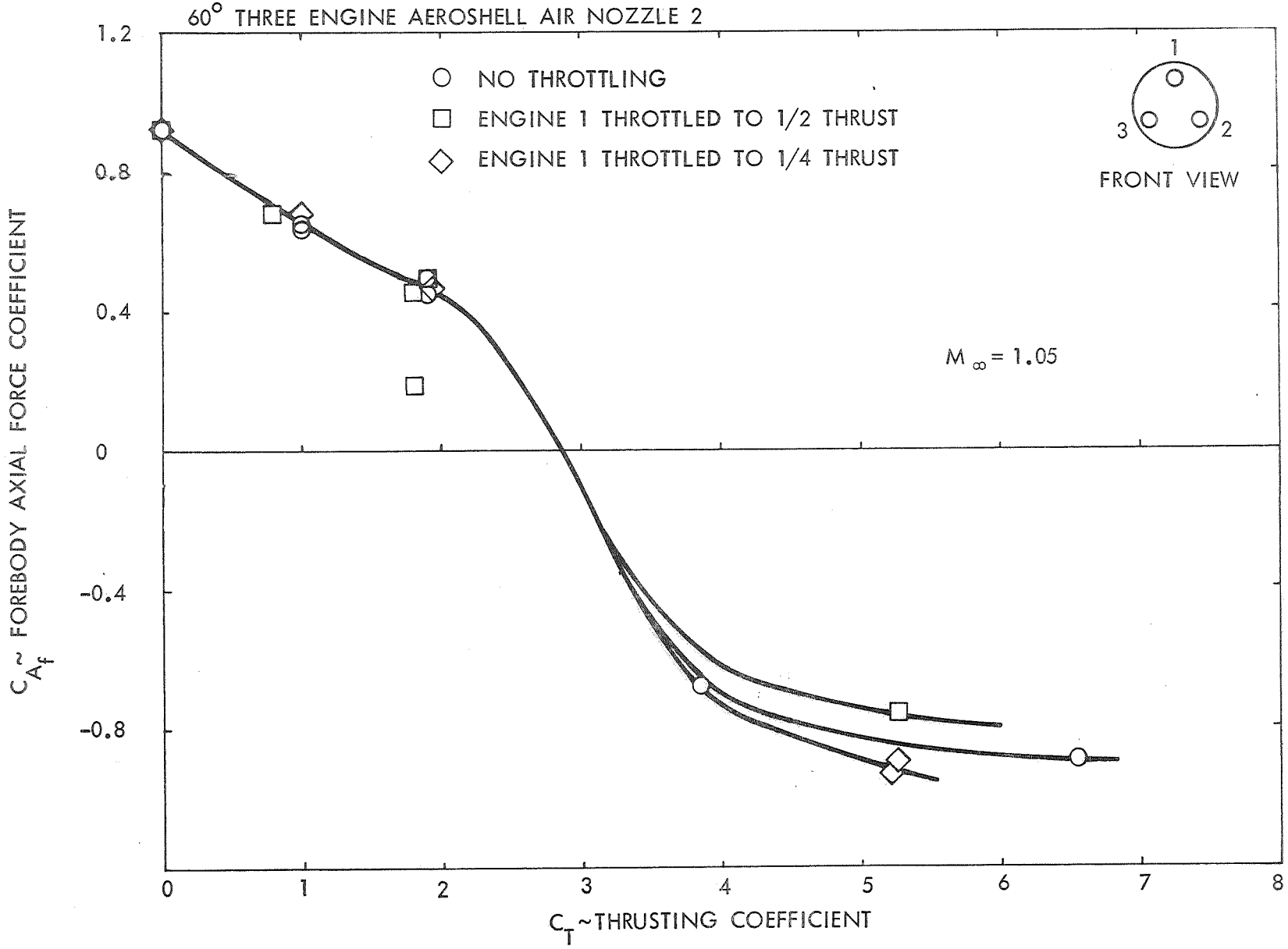

Figure 89 Forebody Axial Force Coefficient with Engine 1 Throttled - Three Engine 60° Aeroshell - $M_\infty = 1.05$.

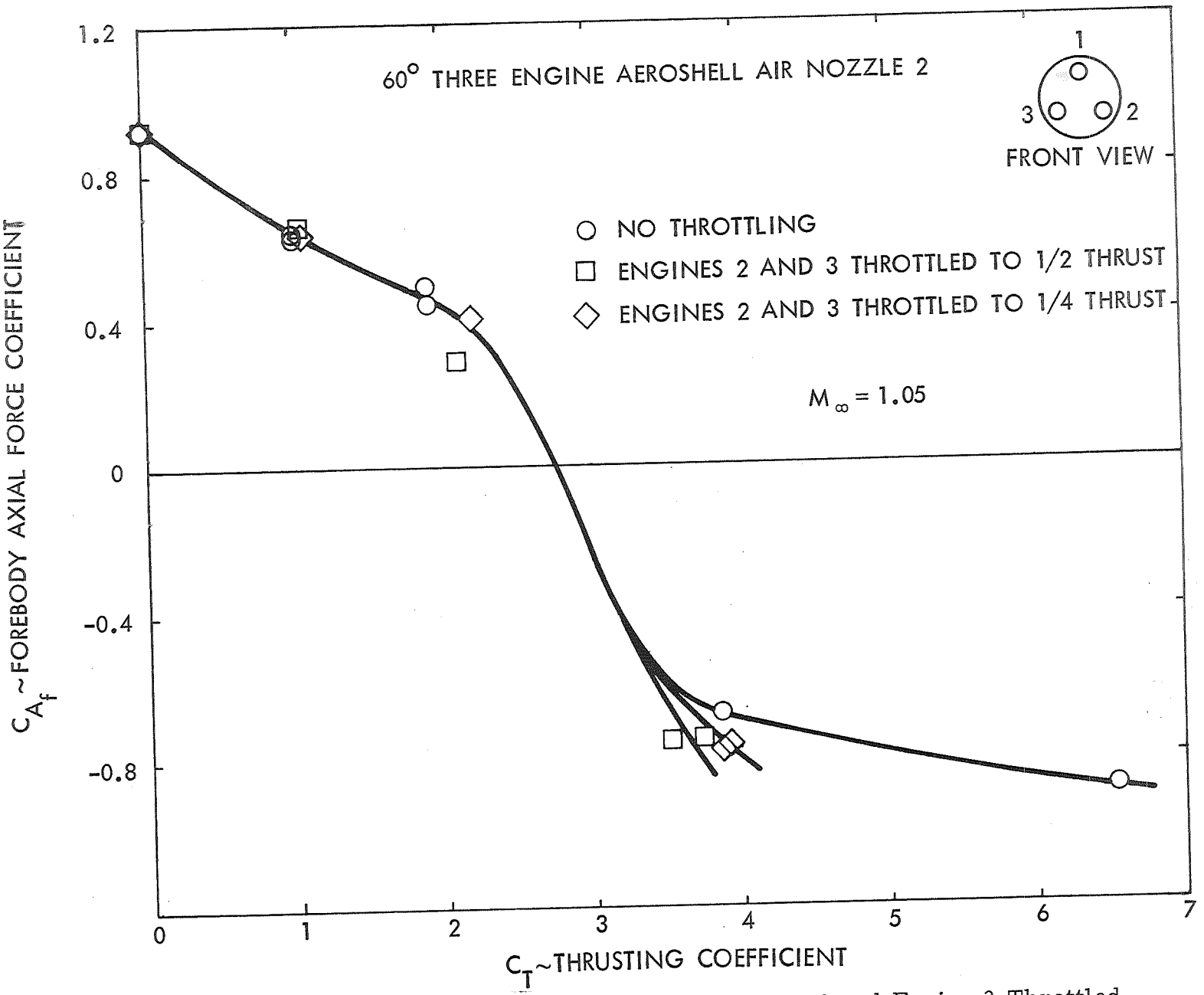

Figure 90 Forebody Axial Force Coefficient with Engine 2 and Engine 3 Throttled - Three Engine 60° - $M_\infty = 1.05$.

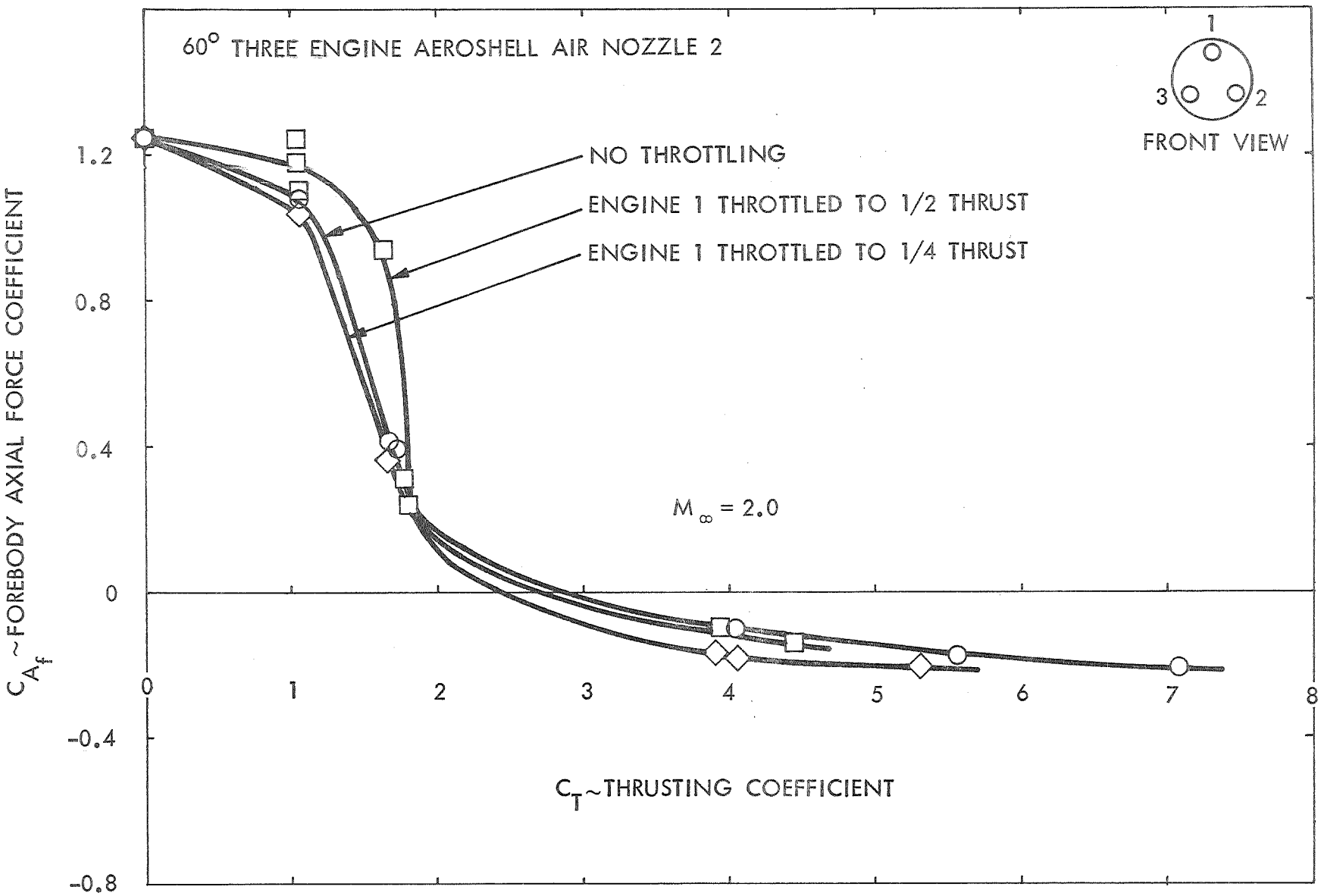

Figure 91 Forebody Axial Force Coefficient with Engine 1 Throttled - Three Engine 60° Aeroshell - $M_\infty = 2.0$.

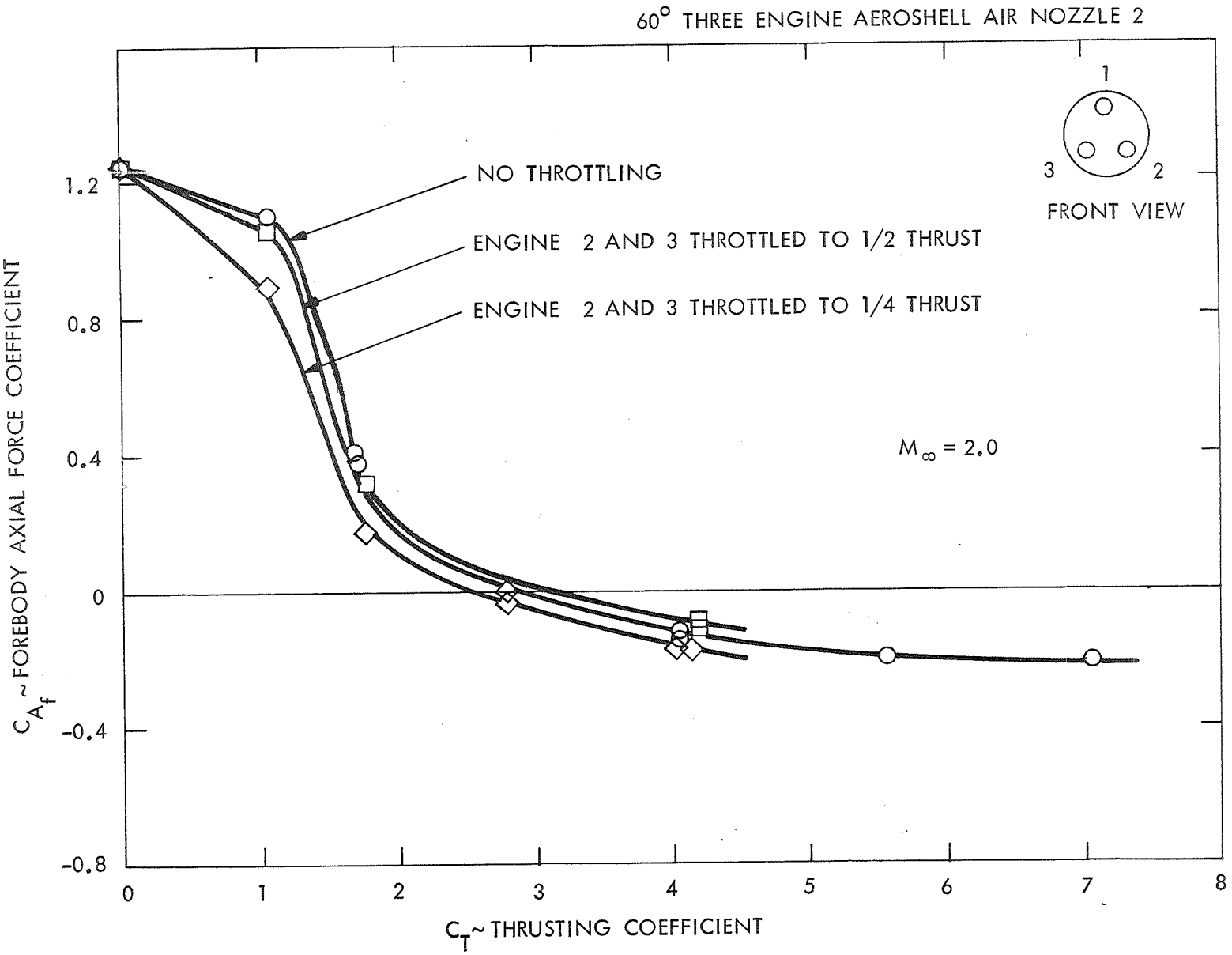

Figure 92 Forebody Axial Force Coefficient with Engine 2 and Engine 3 Throttled - Three Engine 60° Aeroshell - $M_\infty = 2.0$.

3.2.10 Effectiveness of Engine Throttling for Pitch Control

The total pitching moment acting on the aeroshell is the sum of the pitching moment due to pressure forces acting on the aeroshell surface, C_{M_f}, and the pitching moment due to imbalances in the engine thrusts, C_{M_E} (i.e. $C_M = C_{M_f} + C_{M_E}$). Pitching moment coefficients were presented in Section 3.2.6 for the three engine 60^o aeroshell operating with equal engine thrusts (no throttling). In that case, the pitching moment was due entirely to imbalances in the pressure forces acting on the surface of the aeroshell (i.e. $C_M = C_{M_f}$). The pitching moment due to imbalances in thrust was zero. ($C_{M_E} = 0$). In the present case which considers engine throttling, contributions from pressure forces and unbalanced thrust must be considered to obtain the total pitching moment acting on the aeroshell.

The total pitching moment acting on the three engine 60^o aeroshell, as engine one is throttled to 1/2 and then to 1/4 thrust, is shown in Figure 93 for $M_\infty = 2.0$. A nose down pitching moment is applied to the vehicle when engine 1 is throttled. The theoretical change in pitching moment due to throttling engine 1 alone is given by the formula:

$$\Delta C_{M_{E1}} = -.4|\Delta C_T|$$

The corresponding theoretical change in pitching moment due to throttling engine 2 and engine 3 simultaneously is:

$$\Delta C_{M_{E2-E3}} = +.4|\Delta C_T|$$

where ΔC_T is the change in thrust of one of the engines. A nose up pitcing moment is applied to the aeroshell when engine 2 and engine 3 are throttled simultaneously.

The theoretical change in pitching moment due to throttling engine 1 (Figure 93) to 1/2 thrust for $C_T = 1.71$ is $\Delta C_{M_{E1}} = -.137$ while that for 1/4 thrust and $C_T = 1.62$ is $\Delta C_{M_{E2-E3}} = -.216$. The data indicates that the theoretical change in pitching moment expected from imbalances in thrust was not realized (Figure 93). A change in pitching moment in the nose down direction did occur but not of the expected magnitude. This is due to the fact that the pressures acting on the aeroshell increased as the engine was throttled thus reducing the expected change of pitching moment. Tests were not performed at negative angles-of-attack with engine 1 throttled in order to minimize the tunnel test time and because throttling engine 1 at negative angles would force the aeroshell to increasingly negative angles.

The pitching moment coefficient, with engine 2 and engine 3 throttled to 1/2 and then 1/4 thrust, is shown in Figure 94 for $M_\infty = 2.0$.

The effectiveness of engine throttling for pitch control is shown in Figures 95 and 96 for $M_\infty = 2.0$ and Figures 97 and 98 for $M_\infty = 1.05$. Throttling effectiveness is defined as the ratio of change in pitching moment measured experimentally to the theoretical change in pitching moment due to unbalanced engine thrust, $\Delta C_{M_{EXP}} / \Delta C_{M_{THEOR}}$. The effectiveness varies markedly with thrusting coefficient level and at transonic and supersonic flight speeds, a twenty percent reduction in the effectiveness may be experienced. At subsonic speeds the expected change in pitching moment was almost achieved.

3.2.11 Aeroshell Characteristics with Helium Exhaust Flow

The three engine 60° aeroshell was tested in conjunction with helium exhaust flow. The variation in forebody axial force coefficient with helium exhaust flow is plotted in Figure 99 for $M_\infty = 0.60$. The results with multiple air nozzles are shown for comparison. Single engine air and helium nozzle data is also plotted in Figure 99. The forebody drag coefficient for the aeroshell with helium exhaust flow decreases more rapidly with thrusting coefficient than for air exhaust flow.

The variations of the total axial force coefficient with helium exhaust flow at M_∞ = 1.5 and 2.0 are shown in Figures 100 and 101 respectively. Data for three engine air nozzle 2 - aeroshell configuration is shown for comparison, as well as single engine air and helium exhaust flow data. The total axial force with three engine helium exhaust flow lies below the three engine air nozzle data at both Mach numbers. Total axial force amplification still occurs, but at a reduced level. However, the difference between the single and three engine helium data is about equal to the difference between the single and three engine air data. The thrusting coefficient for which the helium total axial force becomes nearly equal to the thrusting coefficient alone occurs at lower thrusting coefficients for the helium exhaust flow data than for the air exhaust flow data. This data indicates that substantial differences occur when different exhaust gas compositions are used.

The circumferential pressure distribution for the three engine 60° aeroshell with helium exhaust flow is noted in Figures 102 through 105. Conditions at M_∞ = 1.5 and C_T = 0.3 are shown in Figure 102 while those at M_∞ = 1.5 and C_T = 0.7, M_∞ = 2.0 and C_T = 0.3, and M_∞ = 2.0 and C_T = 0.6 are shown in Figures 103, 104 and 105 respectively.

3.3 Comparisons of Theory and Experiment

The elements used in the solution[1] of the flow field about a single jet aeroshell in the blunt flow regime are shown in Figure 106. The atmospheric and retrorocket gases are treated as chemically frozen perfect gases in the analyses. The analytical analysis of Hill and Draper[11] is used to describe the flow from the nozzle. The jet boundary is located by the simple approximate method of Charwat[12]. The terminal shock is located so that it will increase the jet pressure to that of the decelerated free stream at the free stagnation point.

For a specified free stream stagnation point pressure, the terminal shock location is determined using the jet flow model of Hill and Draper for the centerline density and Mach number decay and equations for conditions across a normal shock. The final location of the terminal shock wave is found by iterating on the difference between the desired pressure and the pressure behind the normal shock until this difference is zero.

The interface between the shocked free stream gases and the retrojet gases is determined using a momentum balance analysis which is similar to that used by Finley[13]. The control surface used for the momentum balance is taken to be a spherically blunted cone with cone semi-apex angle α_c and the diameter of the blunting sphere d_f. For supersonic free stream Mach numbers greater than $M_\infty \geq 1.5$, the pressure acting on the spherical portion of the control volume is assumed to be that given by modified Newtonian theory.

In Reference 1, it was shown that the distance to the terminal shock and the diameter of the blunting sphere, d_f, vary as the square root of the thrusting coefficient i.e. $\sqrt{C_T}$. The location of the center of the blunting sphere is found by determining the interface standoff distance, δ (i.e. the distance between the jet terminal shock wave and the interface) from a conservation of mass balance. The bow shock location is determined by considering the interface as an equivalent solid spherical body with a given nose radius and using the method of Reference 14.

A comparison of theory and experiment is made in Figures 107 through 109 for a single centrally mounted retrorocket using air exhaust flow. The shadowgraph (Figure 107) was taken at $M_\infty = 2.0$ and $C_T = 4.0$. Surface pressure measurement at these conditions indicate that reattachment of the mixing layer to the aeroshell surface is occurring creating a separated region bounded by the aeroshell surface, jet boundary and mixing layer.

A comparison of theory and experiment is made in Figure 108 for $M_\infty = 1.5$ and $C_T = 4.0$. At this thrusting coefficient, the aeroshell is immersed in a constant pressure separated flow region whose pressure is equal to 55 percent of the free stream static pressure and wake type flow exists.

Another comparison of theory and experiment is made in Figure 109 for $M_\infty = 2.0$ and $C_T = 6.0$. A comparison in graphical form is presented in Figure 110. In all the preceding comparisons, the shadowgraph flow field geometry is within 10% of that predicted analytically.

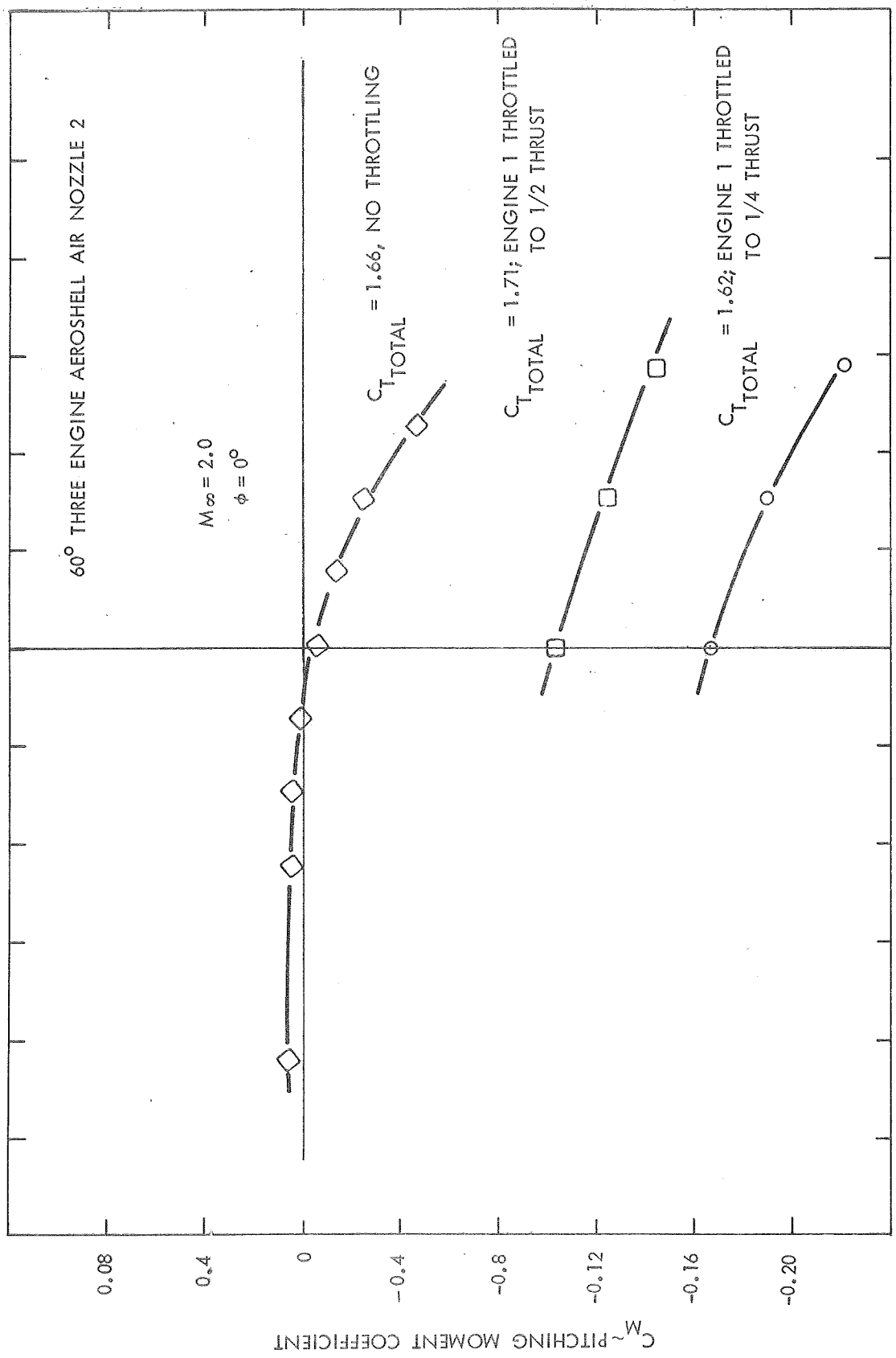

Figure 93 Pitching Moment Coefficient with Engine 1 Throttled - Three Engine Aeroshell - $M_\infty = 2.0$.

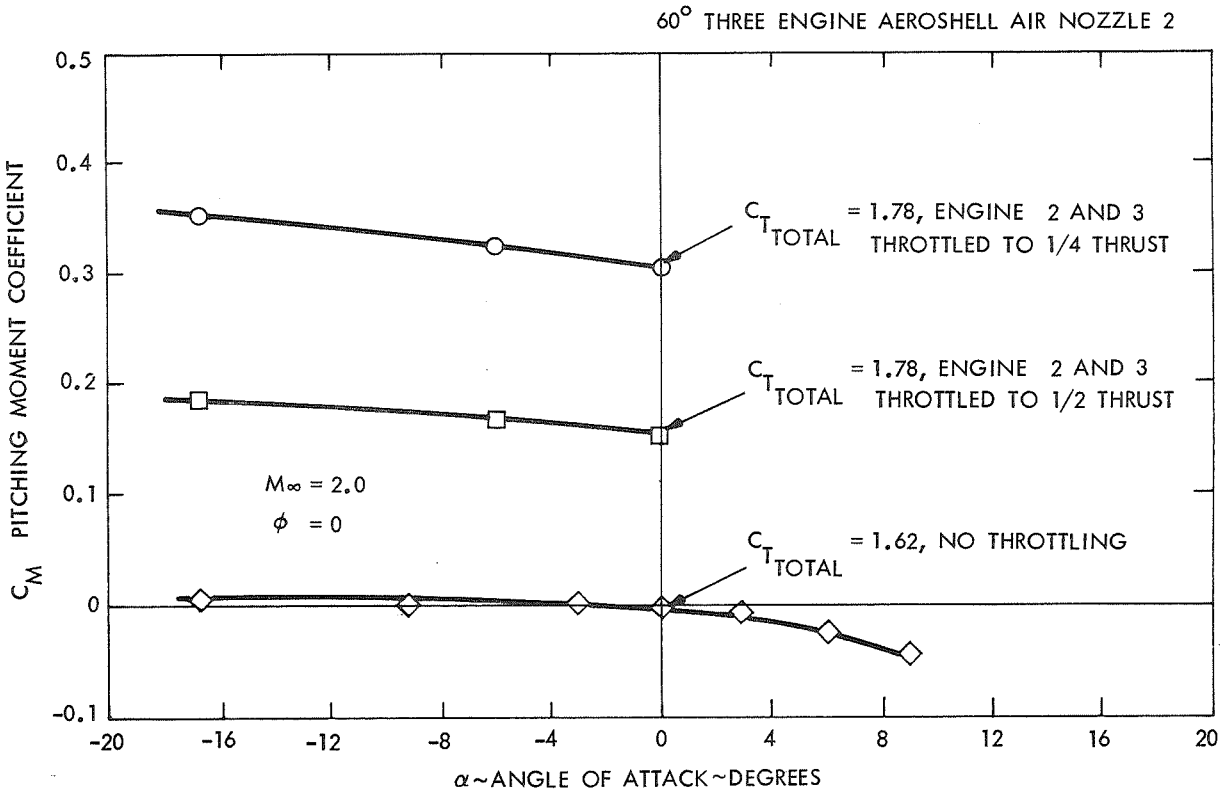

Figure 94. Pitching Moment Coefficient with Engine 2 and Engine 3 Throttled - Three Engine 60° Aeroshell - M_∞ = 2.0

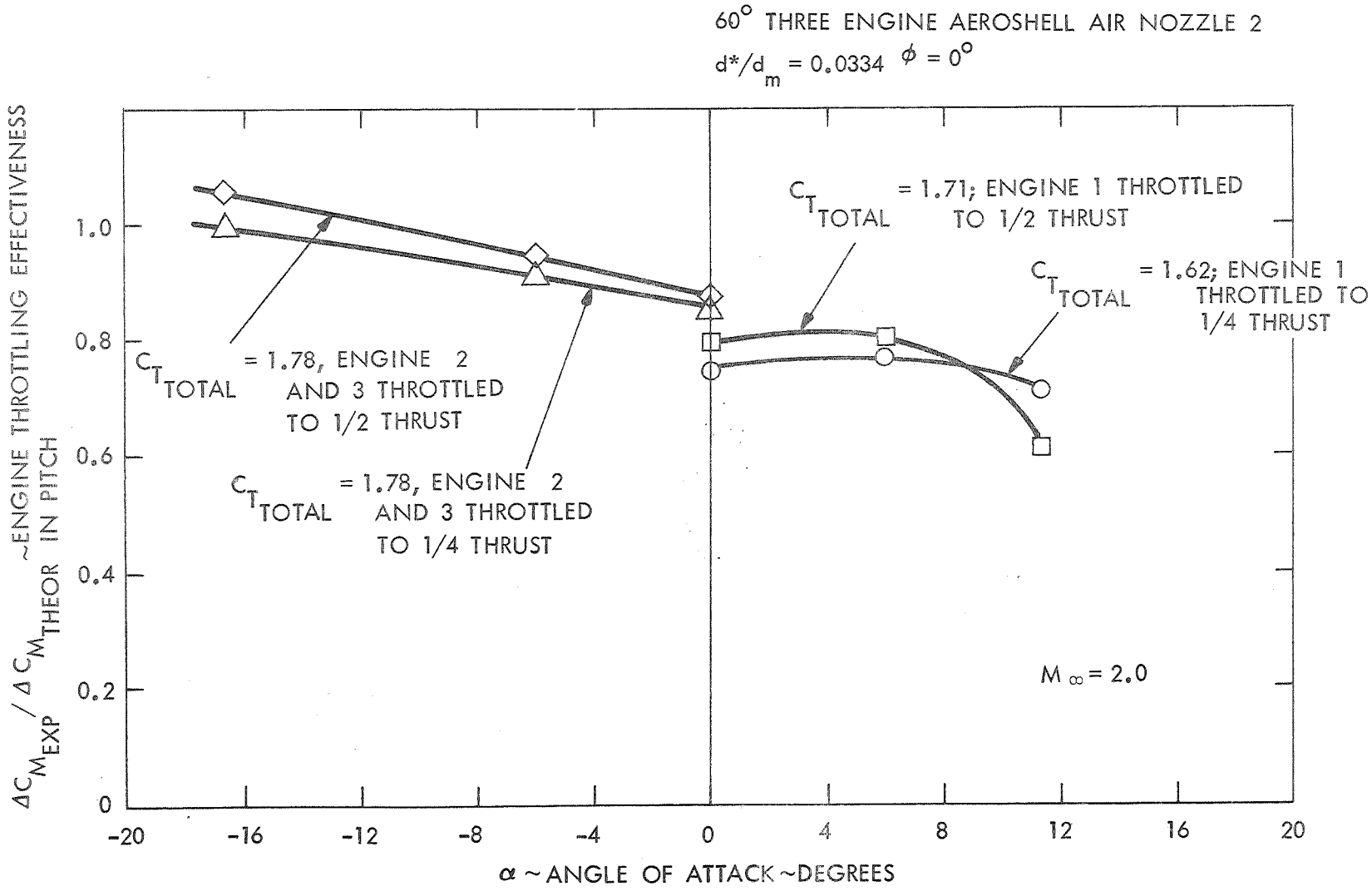

Figure 95 Throttling Effectiveness in Pitch, $M_\infty = 2.0$.

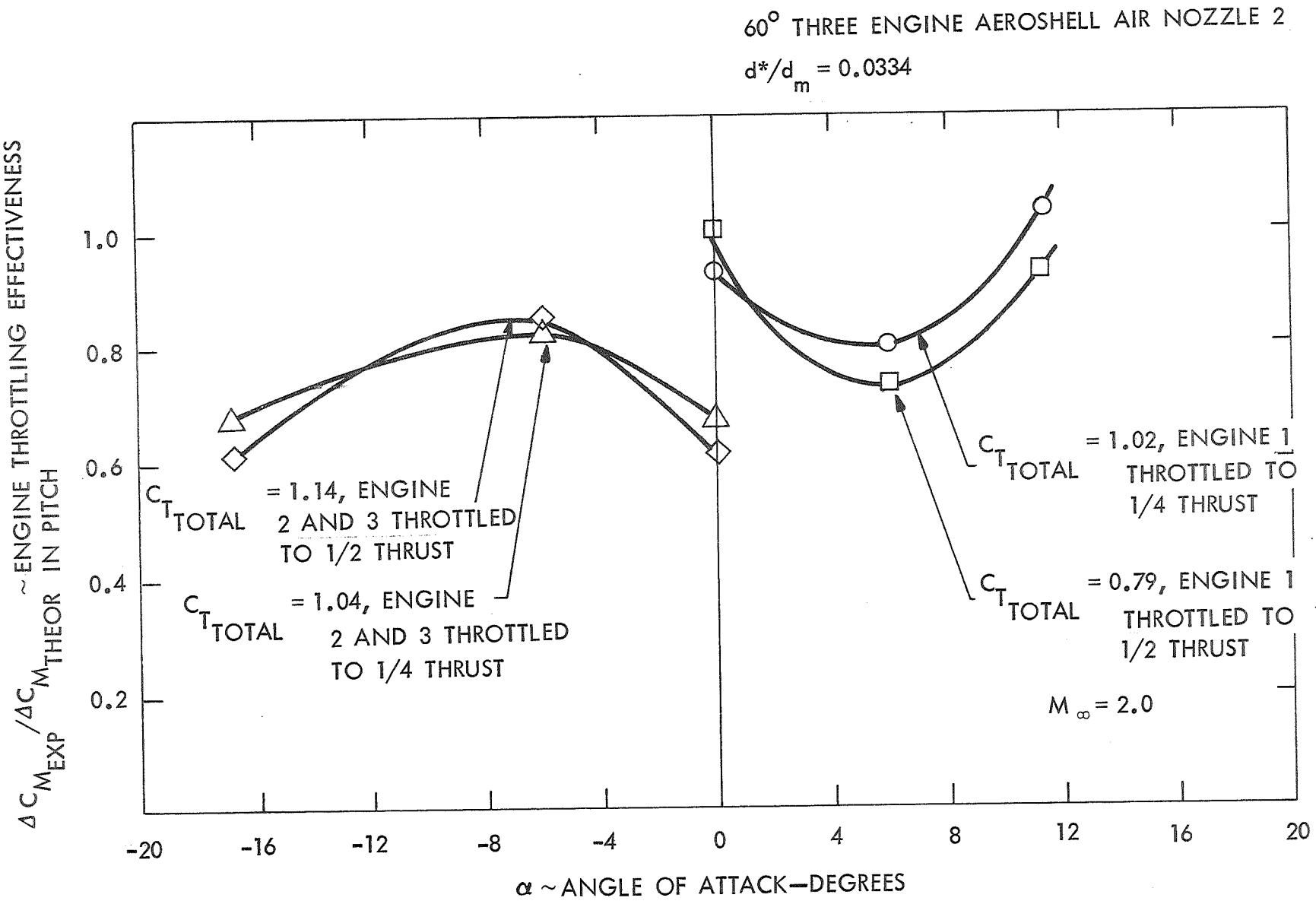

Figure 96 Throttling Effectiveness in Pitch, $M_\infty = 2.0$.

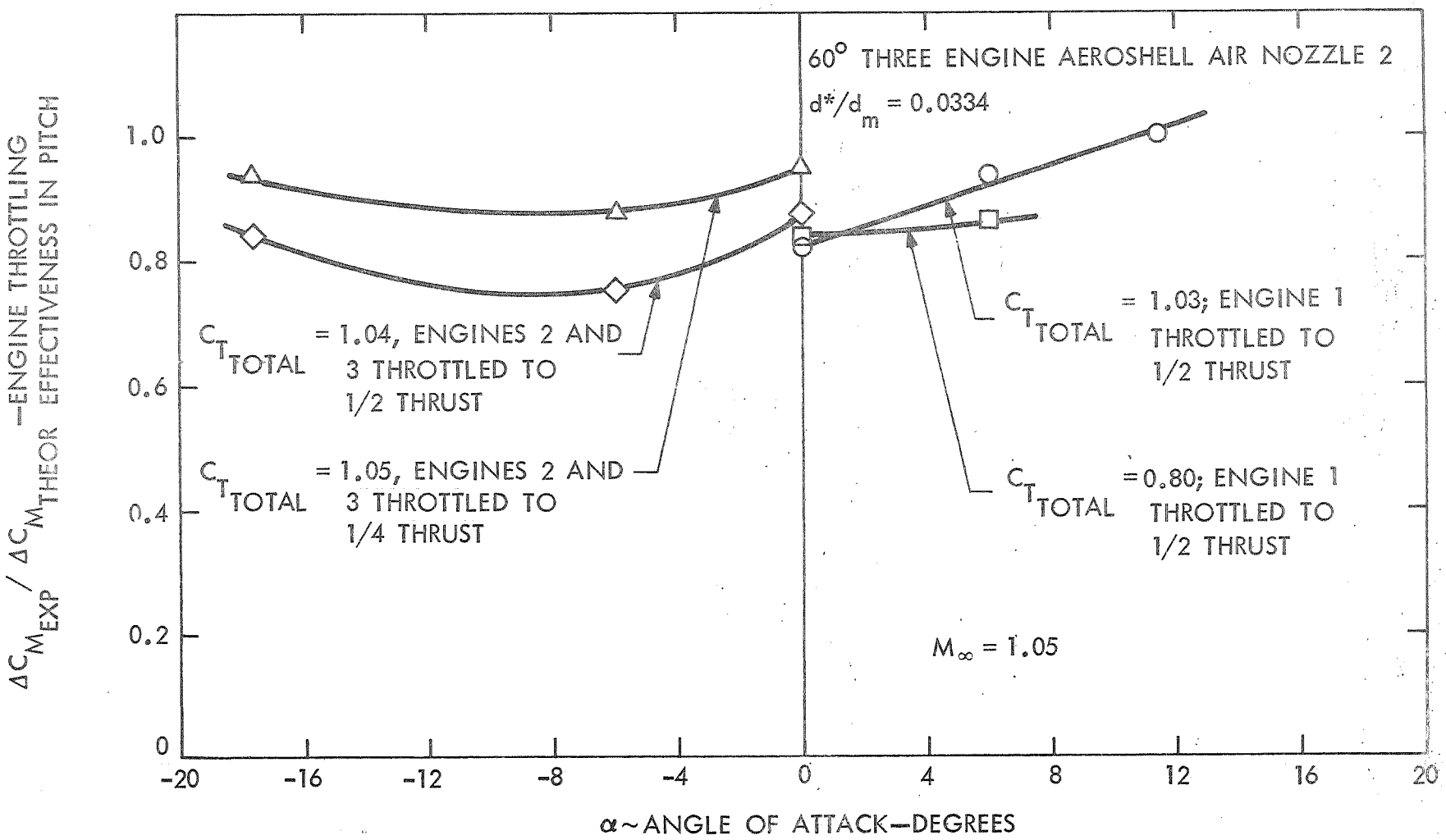

Figure 97 Throttling Effectiveness in Pitch, $M_\infty = 1.05$.

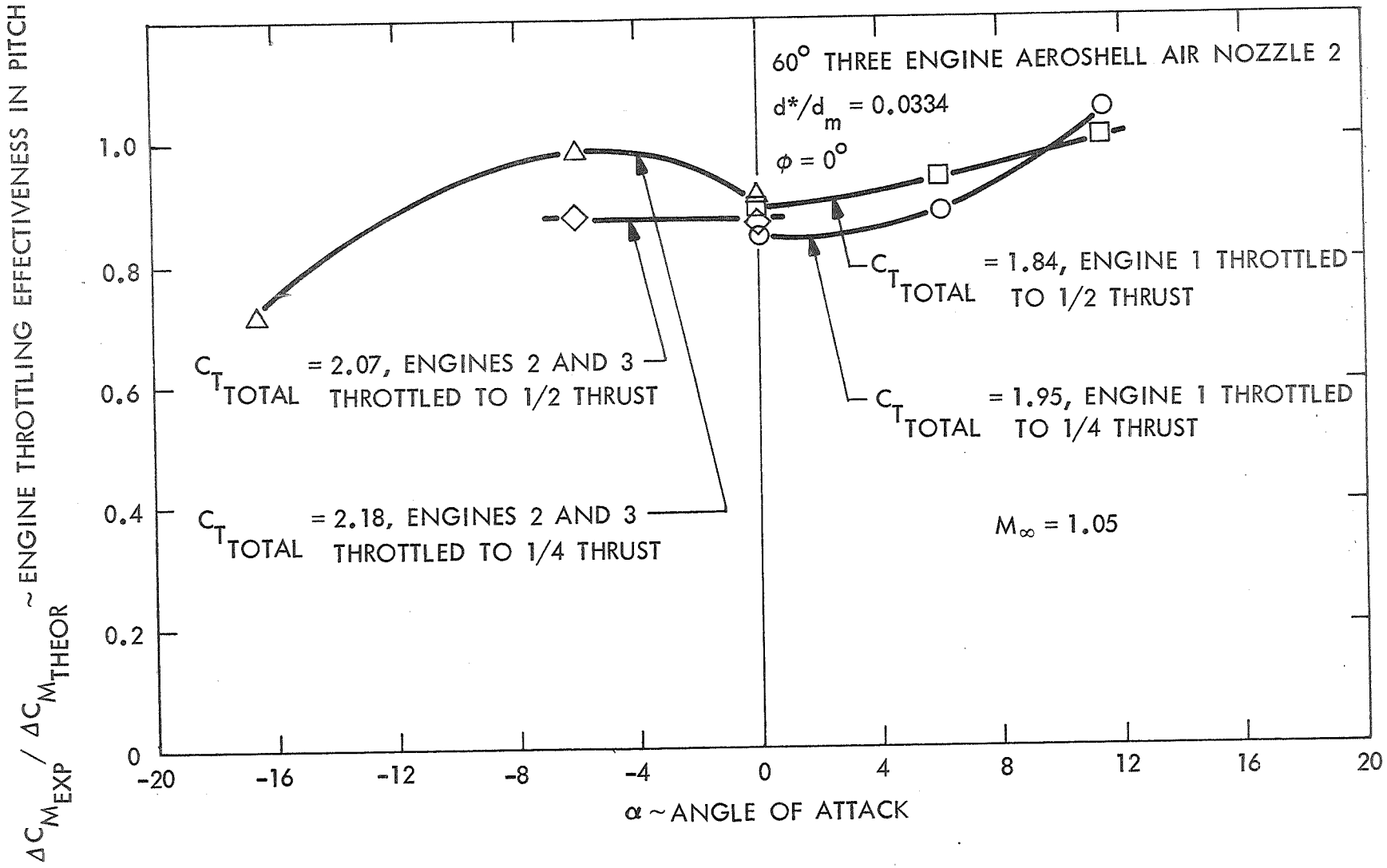

Figure 98 Throttling Effectiveness in Pitch, $M_\infty = 1.05$.

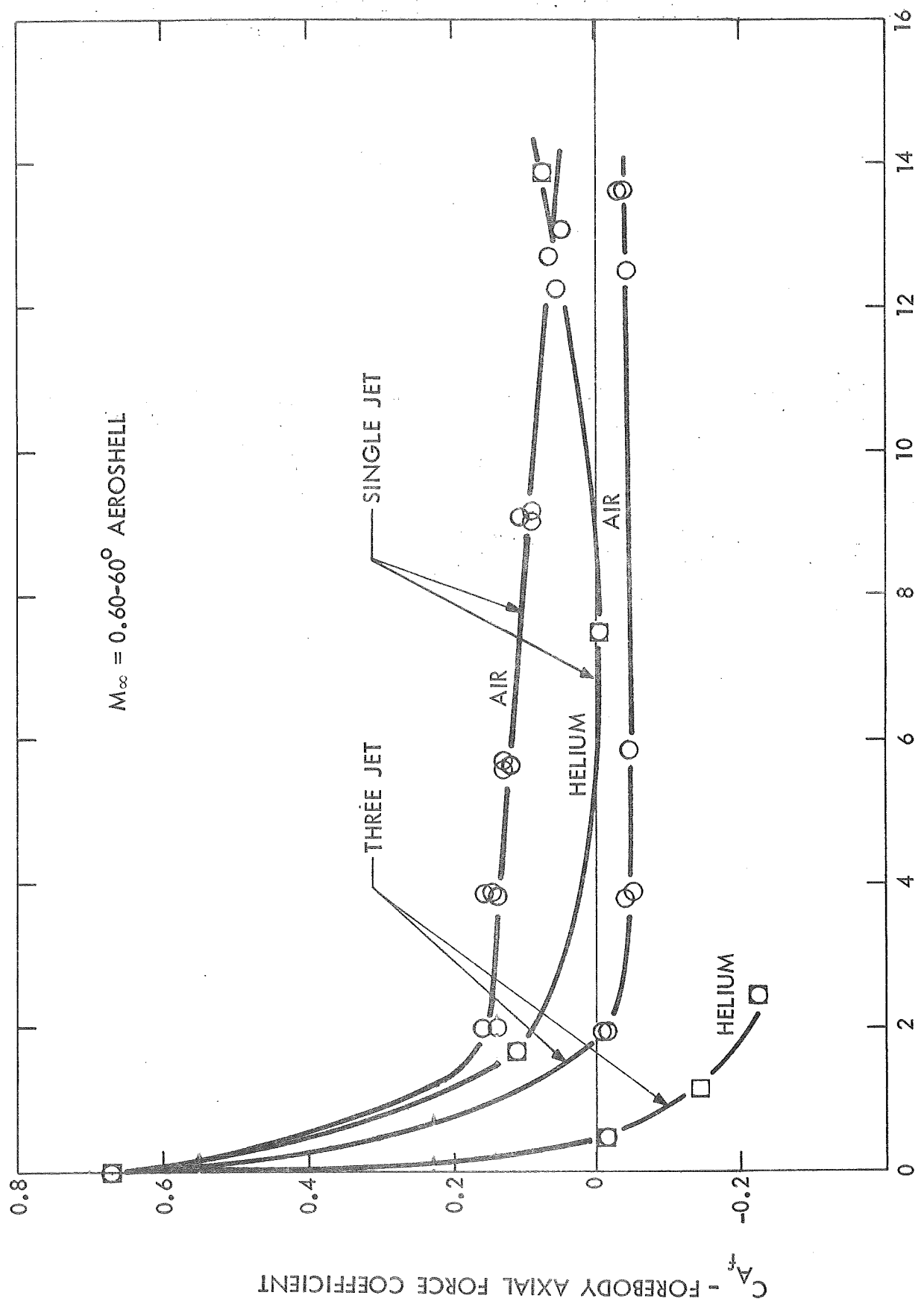

Figure 99 Forebody Axial Force Coefficients with Helium Exhaust Flow, M_∞ = 0.60.

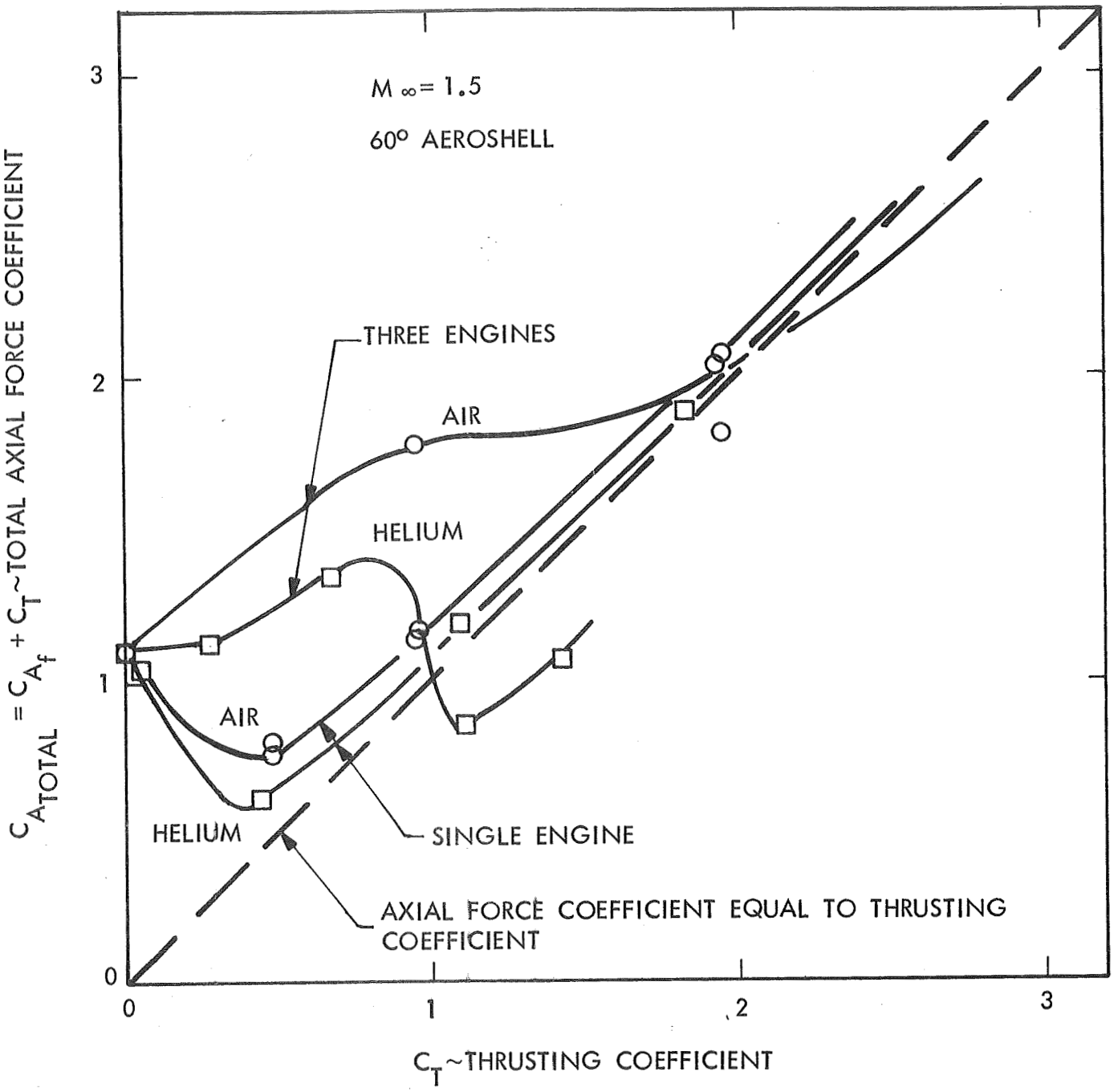

Figure 100 Total Axial Force Coefficient with Helium Exhaust Flow, $M_\infty = 1.5$.

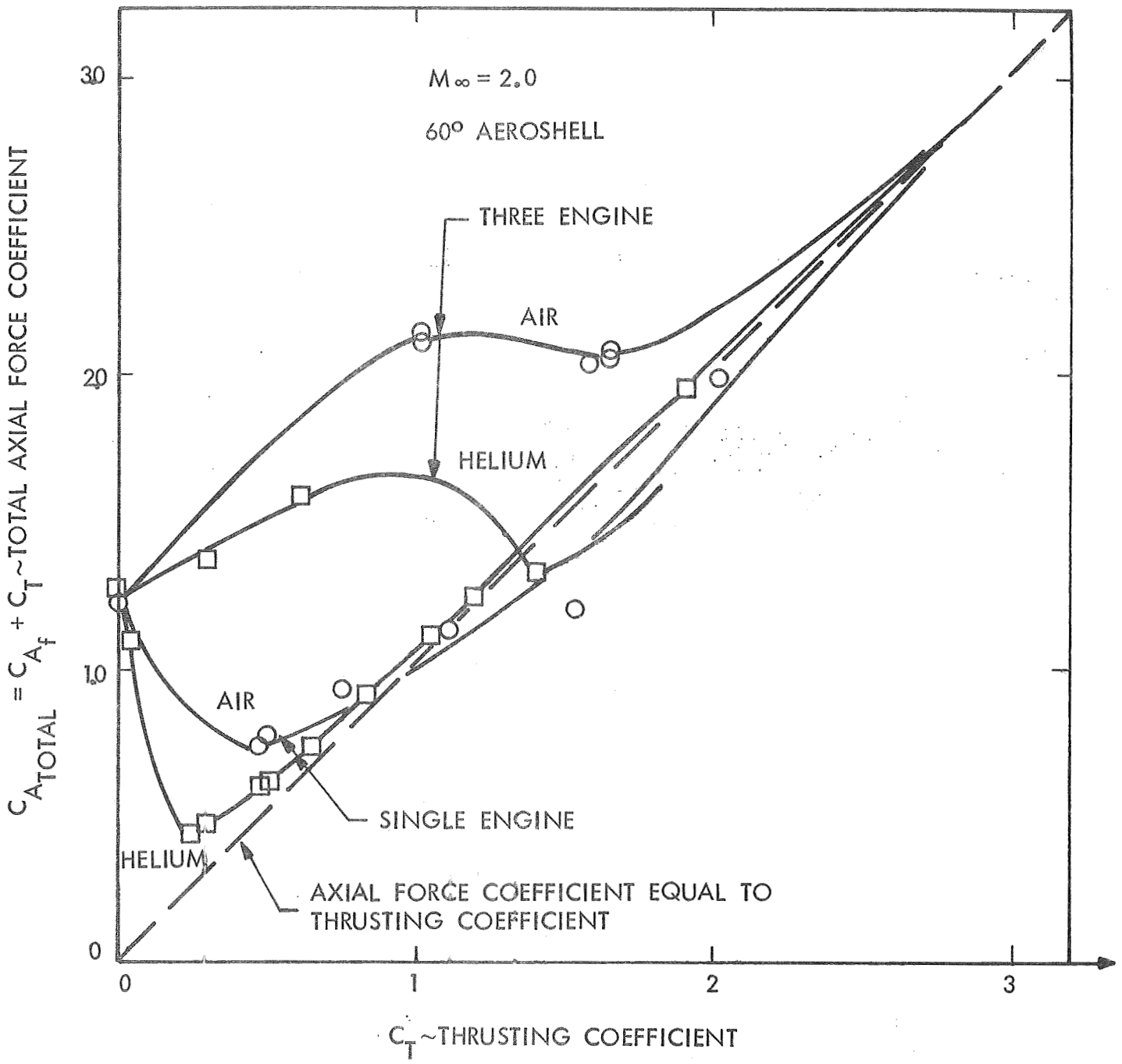

Figure 101 Total Axial Force Coefficient with Helium Exhaust Flow, $M_\infty = 2.0$.

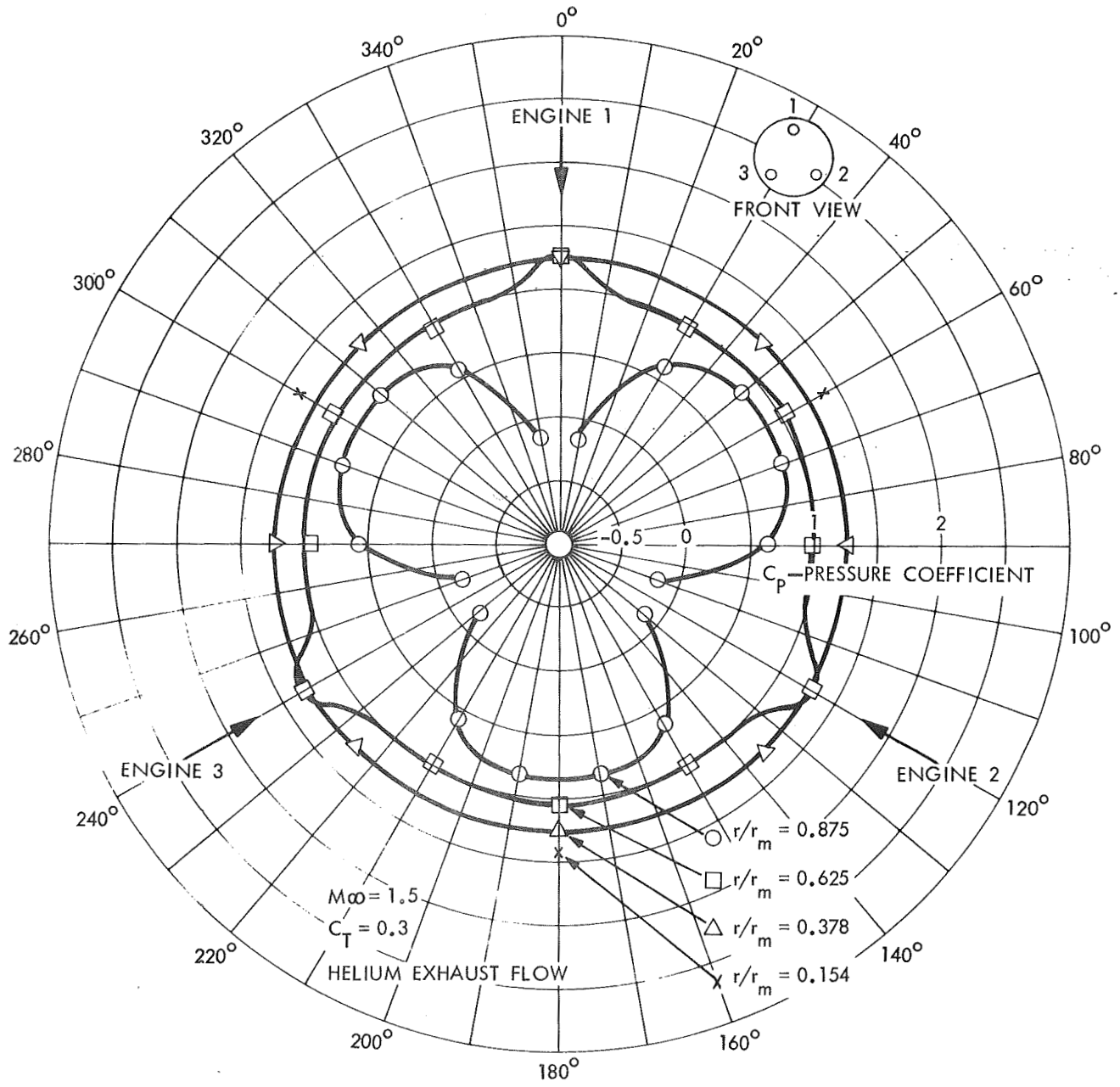

Figure 102 Circumferential Pressure Distribution - Three Engine 60° Aeroshell With Helium Exhaust Flow, $M_\infty = 1.5$, $C_T = 0.3$.

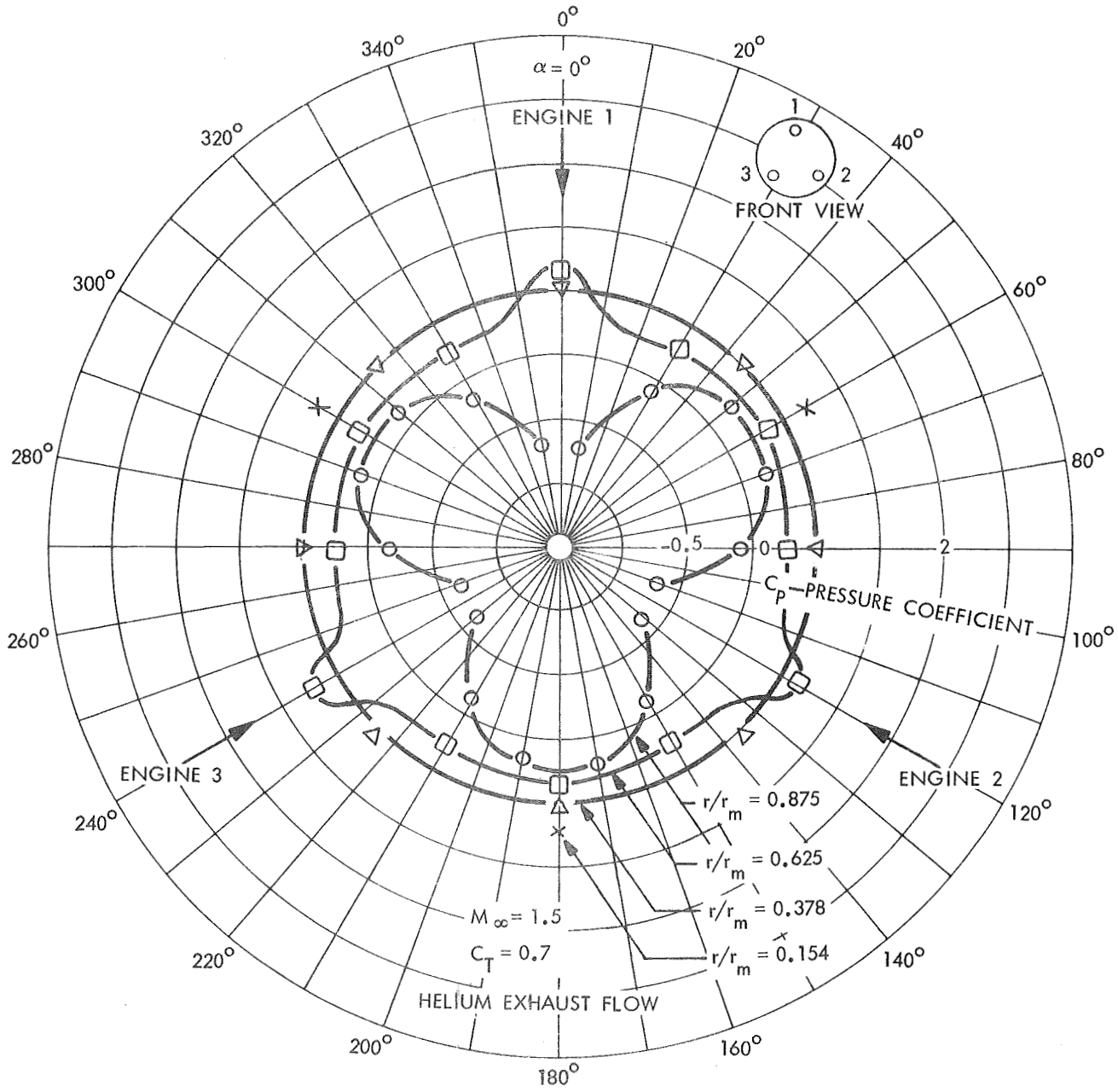

Figure 103 Circumferential Pressure Distribution - Three Engine 60° Aeroshell With Helium Exhaust Flow, $M_\infty = 1.5$, $C_T = 0.7$.

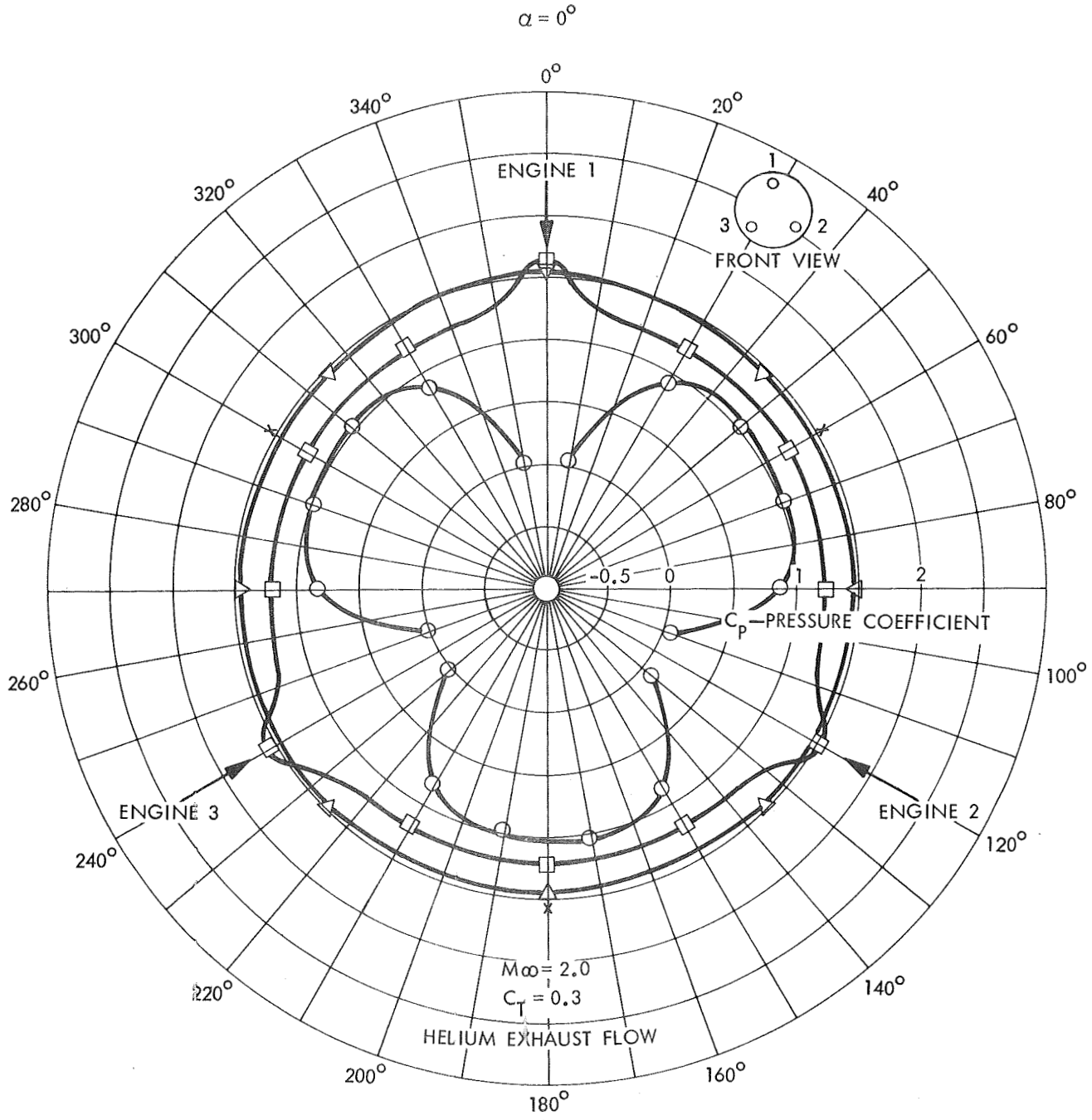

Figure 104 Circumferential Pressure Distribution - Three Engine 60° Aeroshell With Helium Exhaust Flow, $M_\infty = 2.0$, $C_T = 0.3$.

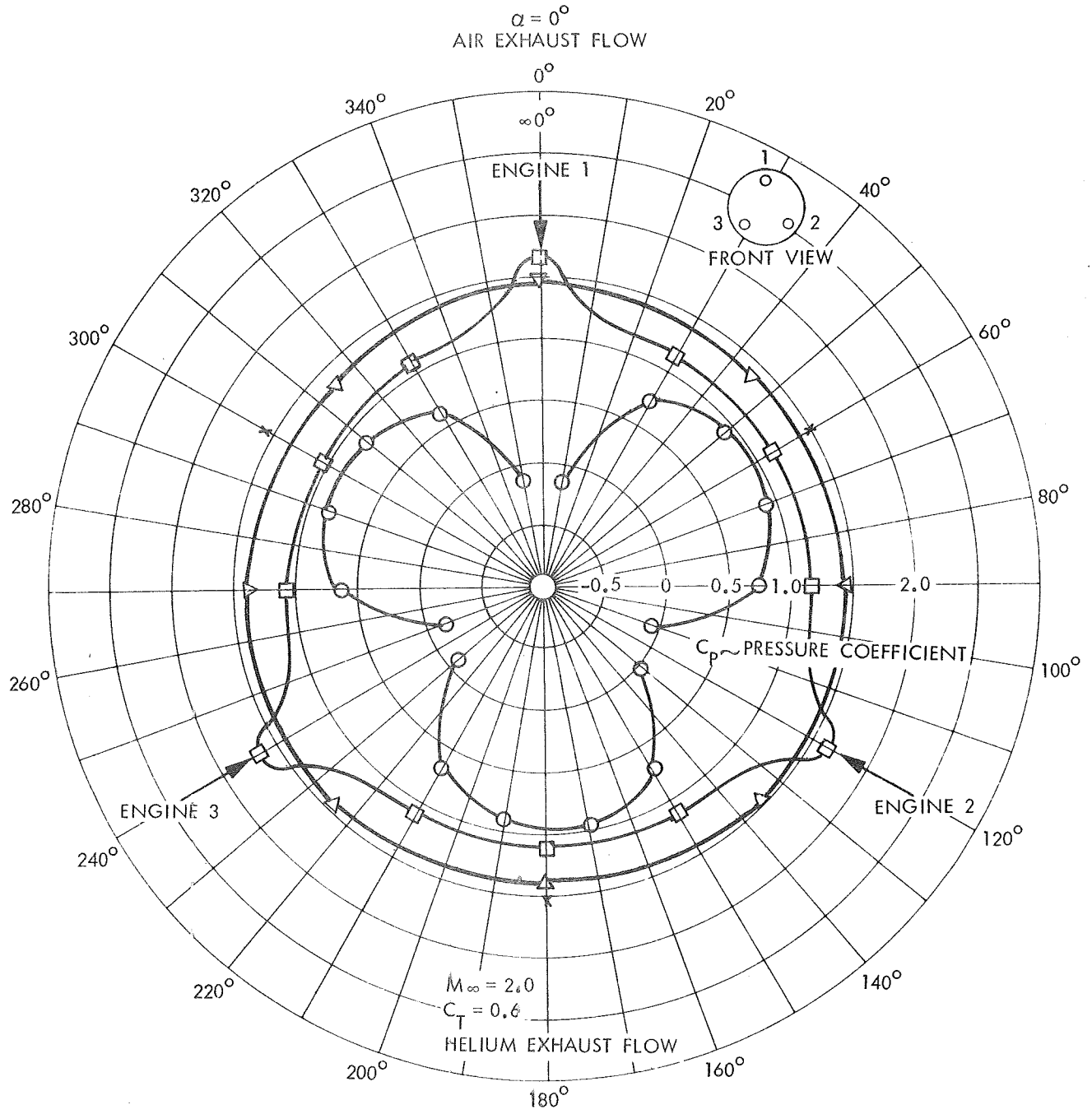

Figure 105 Circumferential Pressure Distribution - Three Engine 60° Aeroshell with Helium Exhaust Flow, $M_\infty = 2.0$, $C_T = 0.6$.

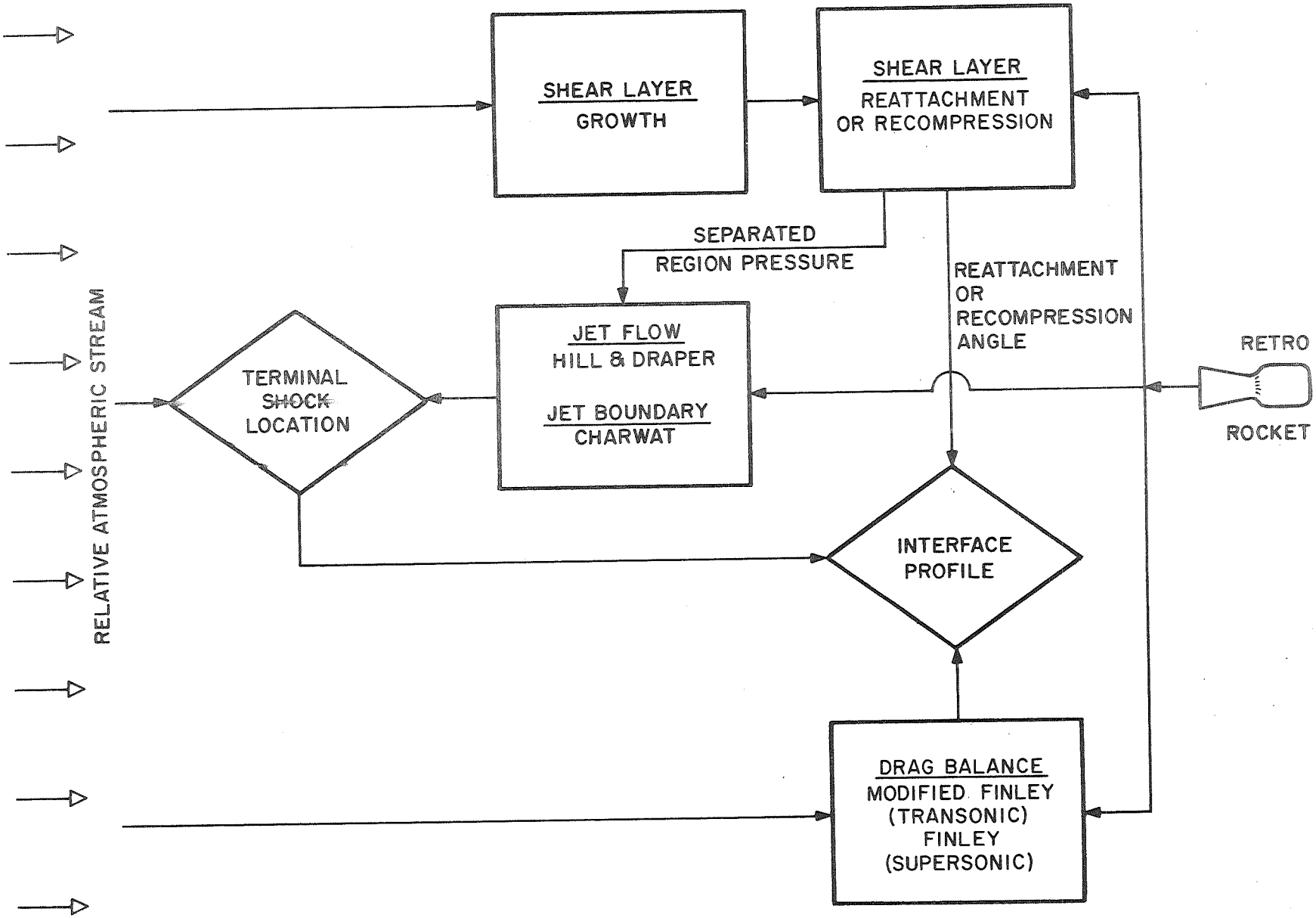

Figure 106 Schematic of Analysis.

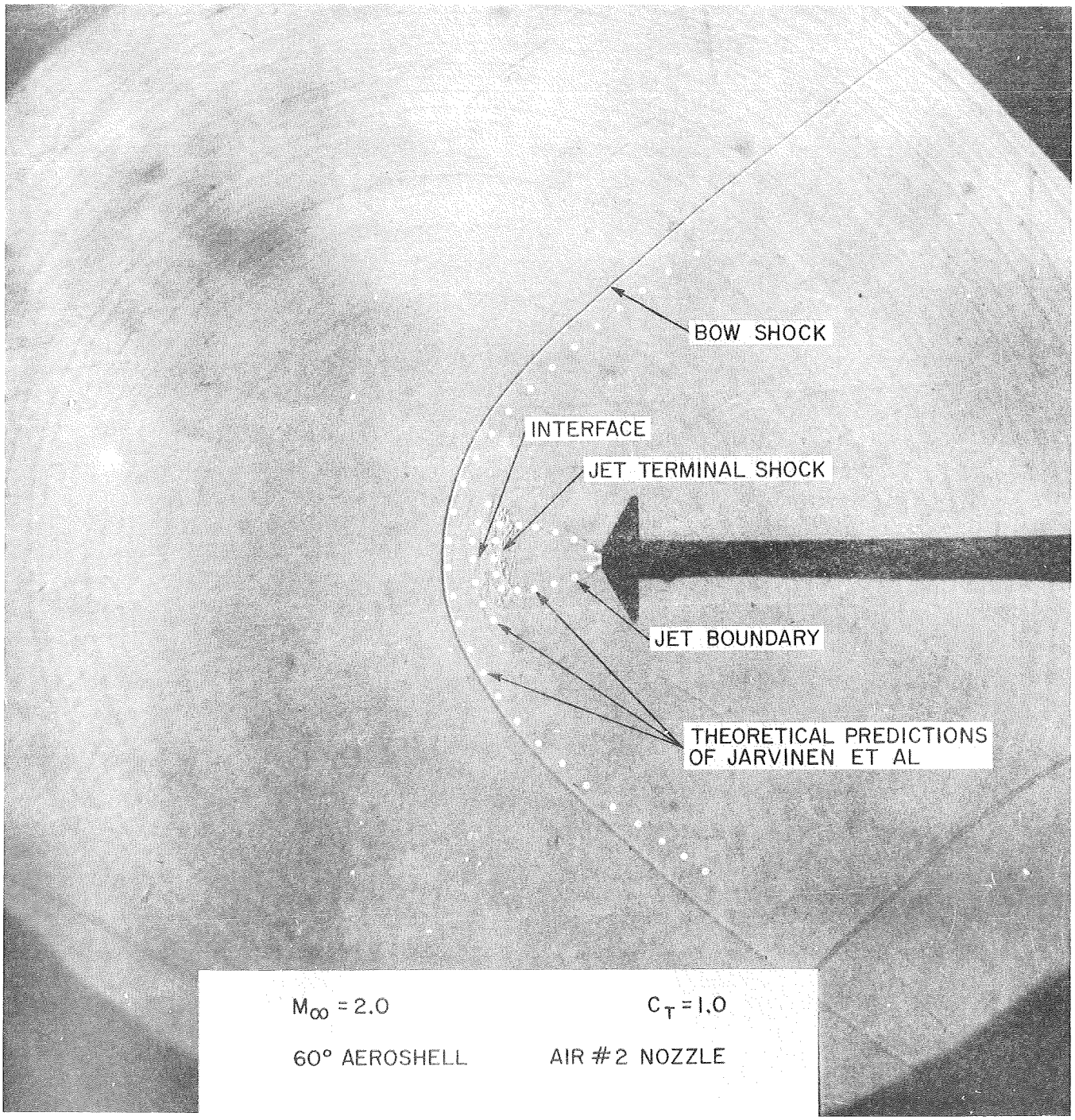

Figure 107 Comparison of Theory and Experiment on Single Nozzle 60° Aeroshell.

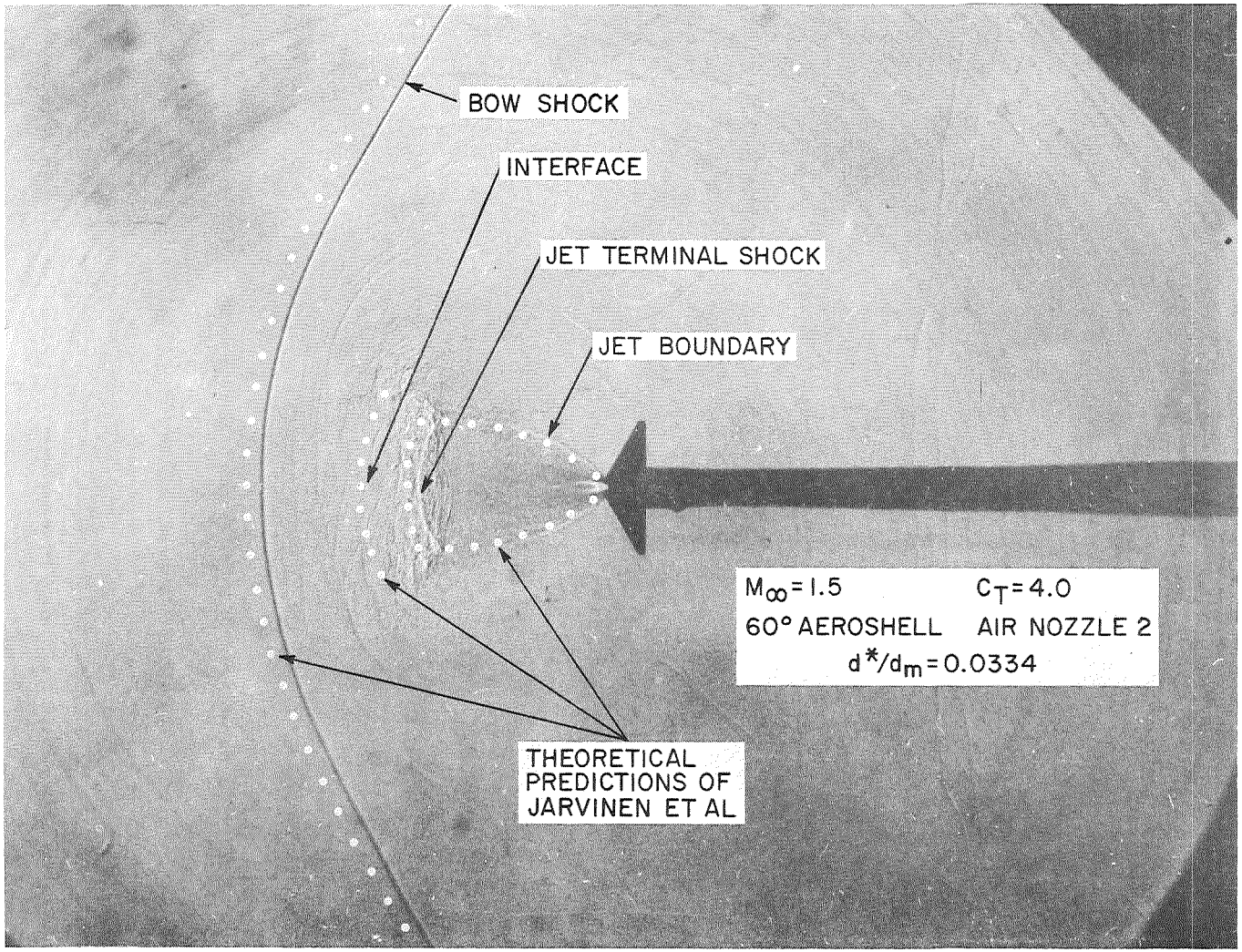

Figure 108 Comparison of Theory and Experiment on Single Nozzle 60° Aeroshell.

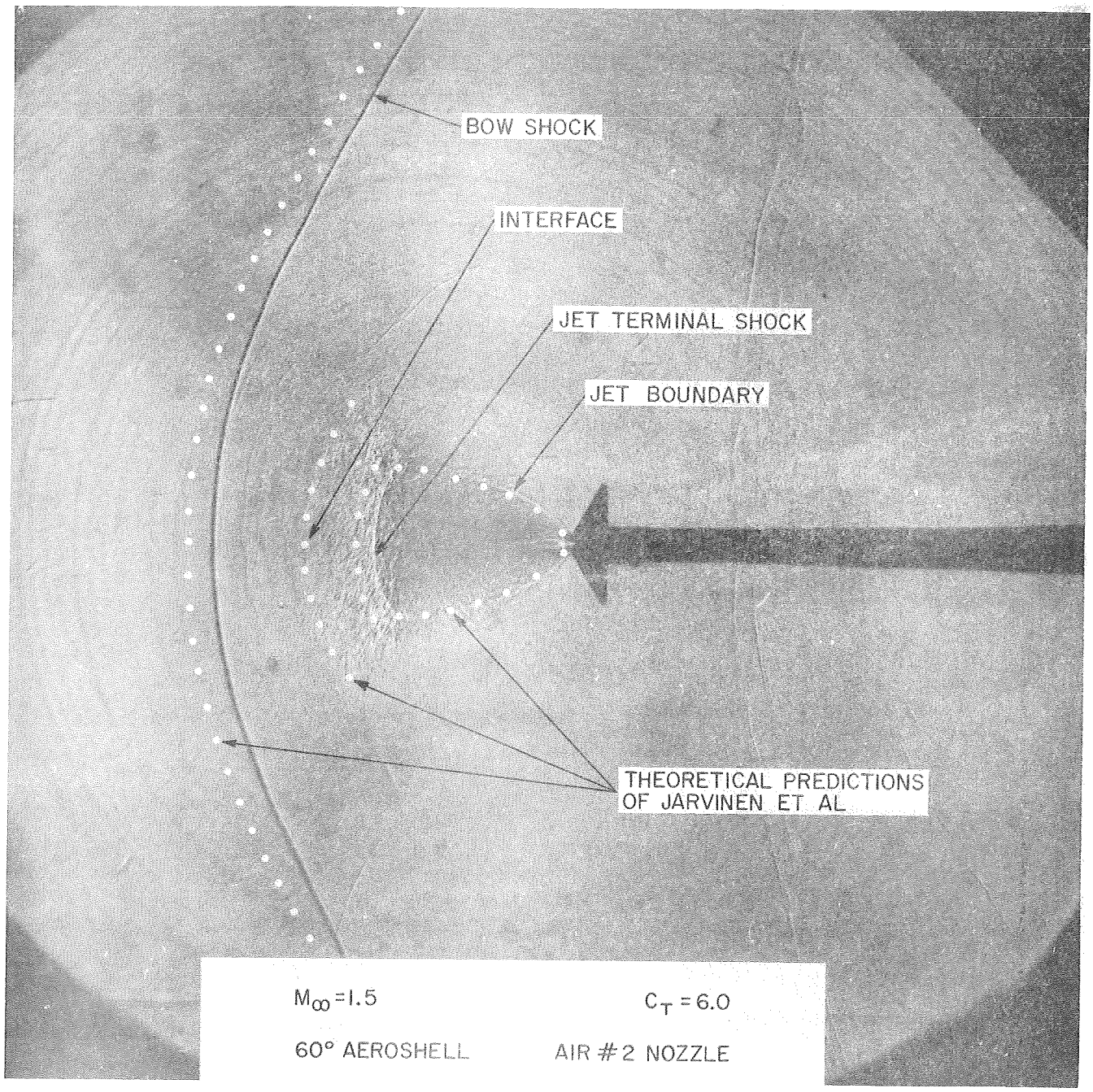

Figure 109 Comparison of Theory and Experiment on Single Nozzle 60° Aeroshell.

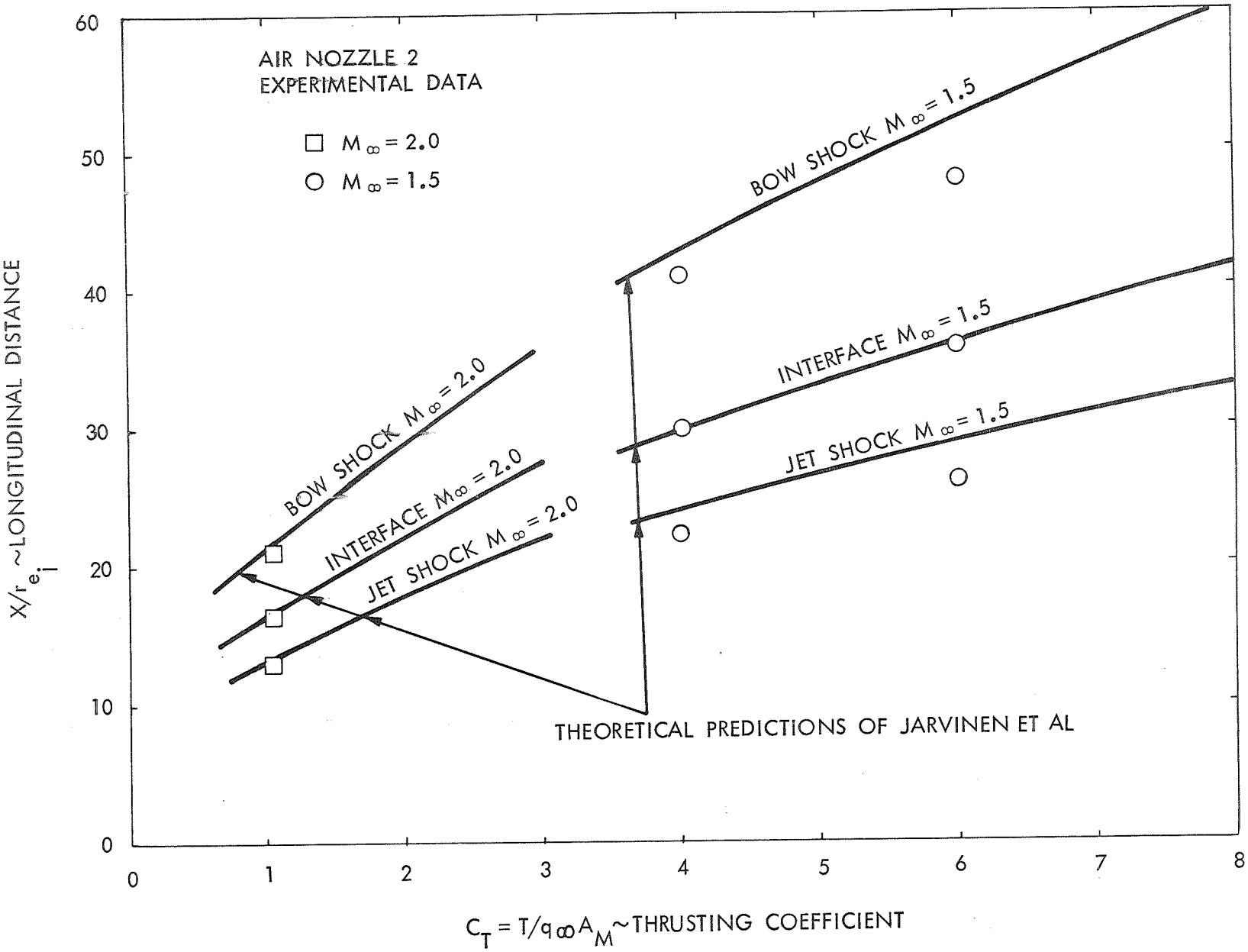

Figure 110 Comparison of Experimental Data and Theoretical Predictions for Bow Shock, Interface and Jet Shock.

4. CONCLUSIONS

The following conclusions may be drawn from the above summarized investigations.

1. Mars lander conditions can be simulated in a wind tunnel. Simulation of both the variation of thrusting coefficient, C_T, with Mach number, M_∞ and nozzle parameters with different free stream and engine specific heat ratios was achieved.

2. The single nozzle flow field exhibits two regimes of jet penetration. At low thrusting coefficients, long jet penetration occurs and the jet total head decays by mixing. At larger thrusting coefficients, a short, blunt jet-flow interaction occurs and jet total head decays then by a terminal shock wave.

3. Transition between long jet penetration and blunt jet-flow interaction occurs at a fixed ratio of the jet exit to free stream pressure, P_{e_j} / P_∞, for all supersonic free stream Mach numbers and engine sizes tested. Corresponding thrusting coefficients (C_T's) are in the range $0.5 < C_T < 3.0$.

4. In the blunt jet-flow interaction regime, a theoretical analysis is presented which predicts the main features of the flow pattern quite well. The theory locates the terminal shock, jet boundary, interface and bow shock wave.

5. For the single engine configurations, the total retroforce is first reduced by applying retrothrust. Then as the thrusting coefficient increases ($C_T \geq 1$), the total retroforce becomes approximately equal to the retrothrust.

6. For the three engine 60^{o} aeroshell configuration, the total retroforce is increased by applying retrothrust. The magnitude of the enlargement increases as the free stream Mach number increases and at $M_{\infty} = 2.0$ leads to a total retroforce of twice the retrothrust at $C_T = 1.0$. At larger values of thrusting coefficient, the total retroforce levels off and eventually ($C_T > 3$) it becomes approximately equal to the retrothrust. The total axial force of the three engine configuration is substantially greater at $M_{\infty} = 2.0$ than that of a single engine aeroshell when both operate at the same total retrothrust and $C_T \leq 2.0$.

7. For the single engine configuration, the pitching moment curve is linear up to angles-of-attack of at least six degrees at all free stream Mach numbers and thrusting coefficients tested. Application of retrothrust is stabilizing at all Mach numbers for $C_T \leq 2.5$.

8. Application of retrothrust to the three engine 60^{o} aeroshell configuration produces non-linear pitching moment and normal force curves at subsonic ($M_{\infty} = 0.6$), transonic ($M_{\infty} = 1.05$) and supersonic ($M_{\infty} = 2.0$) Mach numbers. The amount of nonlinearity increases with increasing Mach number. The shape of the pitching moment curve depends on the roll-orientation of the pitch plane with respect to the engines.

9. At transonic and supersonic free stream Mach numbers, a twenty percent reduction in the effectiveness of engine throttling for pitch controls was found.

10. The engine exhaust gas composition (air or helium) influences the aerodynamic characteristics of the aeroshell-retrorocket system.

11. The number and location of the engines in a retrorocket-aeroshell combination has a strong influence on the stability and drag when retrothrust is applied.

REFERENCES

1. Jarvinen, P. O., Luce, R. W., and Wachsler, E., "Propulsive Re-Entry Aerodynamics", Interim Report, "MITHRAS Report No. MC68-3001-R1 (BNY), MITHRAS, a division of Sanders Associates, Inc., Cambridge, Mass., June 1968.

2. Keyes, J. W. and Hefner, J. N., "Effect of Forward-Facing Jets on the Aerodynamic Characteristics of Blunt Configurations at Mach 6", Journal of Spacecraft and Rockets, Vol. 4, No. 4, pp 533-534, April 1967.

3. Peterson, V. L. and McKenzie, R. L., "Effects of Simulated Retrorockets on the Aerodynamic Characteristics of a Body of Revolutions at Mach Numbers from 0.25 to 1.90", NASA TND-1300, National Aeronautics and Space Administration, May 1962.

4. Goethert, B. H., "Base Flow Characteristics of Missiles with Cluster-Rocket Exhausts", Aerospace Engineering, 20, pp. 28-29, March 1961.

5. Adams, R. H., "Wind Tunnel Simulation of Rocket Vehicles in Flight with Two Phase-Flow Rocket Plumes", Journal of Spacecraft and Rockets, 4, No. 4, pp 518-524, April 1967.

6. Owens, R. V., "Aerodynamic Characteristics of Spherically Blunted Cones at Mach Numbers from 0.5 to 5.0", NASA TND-3088, National Aeronautics and Space Administration, December 1965.

7. Campbell, J. F., "Longitudinal Aerodynamic Characteristics of Several High-Drag Bodies at Mach Numbers from 1.50 to 4.63", NASA TND-3915, National Aeronautics and Space Administration, April 1967.

8. Campbell, J. F. and Howell, D. T., "Supersonic Aerodynamics of Large-Angle Cones", NASA TND-4719, National Aeronautics and Space Administration August 1968.

9. Nichols, J. O. and Nierengarten, E. A., "Aerodynamic Characteristics of Blunt Bodies", Jet Propulsion Laboratory, TR No. 32-677, November 1964.

10. Devechis, W. D. and Sawyer, J. W., "Effects of Cone Angle, Base Flare Angle, and Corner Radius on Mach 3.0 Aerodynamic Characteristics of Large Angle Cones", NASA TND-5048, National Aeronautics and Space Administration, March 1969.

11. Hill, J.A.F., and Draper, J. S., "Analytical Approximation for the Flow from a Nozzle into a Vacuum", Journal of Spacecraft and Rockets, Vol. 3, No. 10, pp 1552-1554, October 1966.

12. Charwat, A. F., "Boundary of Underexpanded Axisymmetric Jets Issuing into Still Air", AIAA Journal, Vol. 2, No. 1, pp 161-163, January 1964.

13. Finley, P. J., "The Flow of a Jet from a Body Opposing a Supersonic Freestream", Journal of Fluid Mechanics, Vol. 26, Part 2, pp 337-368, 1966.

14. Van Dyke, M. D. and Gordon, H. D., "Supersonic Flow Past a Family of Blunt Axisymmetric Bodies", NASA TR R-1, National Aeronautics and Space Administration, 1959.

15. Jarvinen, P. O. and Adams, R. H., "The Effects of Retrorockets on the Aerodynamic Characteristics of Conical Aeroshell Planetary Entry Vehicles," AIAA Paper 70-219, AIAA 8th Aerospace Sciences Meeting, New York, N. Y., January 21, 1970.

16. Hill, J. A. F. and Jarvinen, P. O., "Retrorocket Plumes in Subsonic Counterflows," Paper presented at JANNAF 6 th Plume Technology Meeting, Monterey, California, March 9-11, 1971.

APPENDIX A

COMPUTER PROGRAM
E. Wachsler

A.1 THE MACHINE - PDP-10

The program was written on the Sanders Associates Time Sharing Computer, the Digital Equipment Corporation PDP-10. The required core storage is approximately 20K.

A.2 THE LANGUAGE - FORTRAN IV

The program was written in the PDP-10 version of FORTRAN IV[1]. USA Standard Fortran[2] is a subset of PDP-10 FORTRAN. For example, mixed mode expressions are allowed, but were not used in order to make the program compatible with IBM 7094 FORTRAN IV, VERSION 13[3], or UNIVAC 1108 FORTRAN V[4]. Just about the only things not allowed in PDP-10 FOR IV are ENTRY, non-standard RETURNS, and T field descriptors.

A.3 MODIFICATIONS FOR BATCH PROCESSING ON OTHER THAN PDP-10 COMPILERS

In order to follow the progress of the iteration schemes, the current version of the program does not have a formal output subroutine, but has a number of TYPE statements throughout the program. The following items in the program would probably have to be changed for other FORTRAN compilers.

a) Replace TYPE 105, list by WRITE (IOUT, 105), list in a formal output subroutine.

b) Delete the leading 5X or 6X in input (READ) formats.

c) Alphameric variables (either integer or real) are modulo A5.

d) ' (apostrophe) is used as delimiter for Hollerith fields.

e) $ (dollar sign) at the end of a format is used to hold the print line.

f) The free field formats (such as I, 5F) would have to be changed.

g) INPUT/OUTPUT logical unit assignment as well as the file handling calls (IFILE, RELEAS). are probably incompatible.

h) The DATE, TIME calls are usually different for each installation.

i) The FUNCTIONS COTAN, TAN and ERF are included because they were not in the PDP-10 library. They should be deleted if they exist in the local library.

A.4 PROGRAM ELEMENTS

The program consists of a MAIN program and a long number of FUNCTION and SUBROUTINE subprograms.

The following program elements are used:

a) Arithmetic operations

b) Logical and arithmetic IF's

c) Library functions, sepcifically

ABS, AMAX1, FLOAT, MIN0, SQRT, SIN, COS, ATAN,

ASIN (called ARSIN in some systems) and EXP (in ERF only)

d) BLOCK DATA subprogram, labeled COMMON, CALL EXIT, and the DATA, DIMENSION, EXTERNAL, STOP, RETURN and END statements.

e) READing is from cards and WRITEing is on the printer.

A.5 PROGRAM STRUCTURE AND DESCRIPTION

A.5.1 Naming Conventions

In order to facilitate reading, modification and debugging of the program, variable names and subscripts were made as mnemonic as possible. Furthermore, double subscripts were used to denote a function of two variables or their ratio. The following examples will clarify the notation.

WMOL (JET) is the jet molecular weight

EMACH (INF) is the free stream Mach Number

A (JET, ITOTAL) is the jet total sound speed

T (INF, ISTAT) is the free stream static temperature

RHO (INF, IRATIO) is the ratio of the free stream total to the free stream static density.

P (INF, IPITOT) is the free stream pitot pressure

ENTHAL (INF, 1) is the free stream total enthalpy

ENTHAL (JET, 1) is the jet total enthalpy

ENTHAL (INF, JET) is the ratio H_∞/H_{jet}

AR (JEXIT, JSTAR) is the area ratio, jet exit area to jet throat area

A.5.2 Input Data

Input data is read from cards (6 cards required per case) in subroutine READIN. The data structure is set up for convenient input for the free flight case (rather than for the wind tunnel case).

Card 1: NCAS, UNITIN, UNITOUT (I1, 1X, 2A5)
NCAS = 0 terminates the run
UNITIN, UNITOUT are the names of system of units of the input and output data (i.e. CGS, MKS, ENGLISH)

Card 2: IEND (I2)
IEND is the maximum number of complete iteration loops

Card 3: GAMMA(INF), WMOL(INF), P(INF, ISTAT), T(INF, ISTAT), V(INF) (5F10.4)
Free stream properties - names are self-explanatory

Card 4: GAMMA(JET), WMOL(JET), P(JET, ITOTAL), T(JET, ITOTAL) (4F10.4)
Jet properties - self-explanatory

Card 5: AR(JSTAR, 1), AR(JEXIT, 1), THETA(JEXIT) (3F10.4)
Jet throat area, exit area and nozzle exit (half) angle

Card 6: AR(JBASE, 1), AR(JFACE, 1), THETA(MOD) (3F10.4)
Base area of the aeroshell, face area of the aeroshell if other than nozzle exit area, aeroshell (half) angle

For the wind tunnel case, input should be modified to read in the free stream total pressure, total temperature and Mach Number and the calculation of free stream properties in subroutine PRELIM rearranged.

A.5.3 Generalized Program Flow-Chart

After the input data has been read and the preliminary calculations have been finished, the blunting sphere diameter is calculated with the assumption that the dead air pressure is equal to the free stream static pressure.

If the blunting sphere diameter is less than the aeroshell base diameter, the flow geometry is the shoulder attachment case (referred to in the program comments as the Two-Dimensional Case). Conversely, the flow geometry will be of the wake type (referred to in the program comments as the Three-Dimensional Case).

A.5.3.1 Shoulder Attachment Case

The dead air pressure is found by iteration: the scheme is regula falsi with updating anchors. The dead air pressure is assumed to be the geometric mean of the free stream static and pitot pressures. The blunting sphere diameter and the location of its center are calculated. The geometry of the problem defines the angle α of the conical portion of the flow and hence the dead air pressure.

The dead air enthalpy and concentration are found by iteration: the scheme is Newton-Raphson and the derivatives are obtained numerically. Hence it is necessary to go through the loop 3 times to update the variables.

The dead air enthalpy and concentration are assumed to be the geometric and arithmetic mean, respectively, of the jet and free stream properties. In subroutine MIXING, the location of the 2nd interface (between the blunting sphere-cone and body) is calculated as well as the mass flows entrained along one side of jet boundary and the two interfaces. The merging point is reached where the sum of the entrained mass flows equals the jet mass flow.

The merged layer properties are calculated in subroutine MERGEO. The integration is carried out by a standard Adams-Moulton routine, with Ringe-Kutta starting and variable step size (subroutine HPCG). The integration is terminated at the shoulder (the attachment point) and the three profile parameters λ, μ, and ν associated with the velocity, enthalpy and concentration profiles at the attachment point respectively are calculated. The method is regula falsi iteration with updating anchor (subroutine PGEW) and 8 point Gaussian quadrature of the profiles (subroutine QG8).

The separation streamline location is found simularly and from it, the recompression pressure.

A.5.3.2 Wake Flow Case

The general scheme is very similar to the shoulder attachment case. Only the differences will be pointed out below. In order to obtain wake type flow, the dead air region pressure must be less than the free stream static pressure and the sphere-cone tangency point, THETA(NS), must occur at $\phi \geq 90^{o}$. Thus the Prandtl-Mayer equation is used to relate local pressure and anlge for $\phi > 90^{o}$. Clearly this is not possible if the Mach Number at 90^{o} is less than 1.0 and computation is terminated.

The dead air pressure is assumed to be equal to half the free stream static pressure. Since there is no geometric constraint as in the shoulder attachment case, the iteration scheme must solve simultaneously for dead air pressure, enthalpy and concentration, hence it is necessary to go through the loop 4 times to update the variables. Furthermore, it is not known a priori when to terminate the merged layer integration. This is done by a mass balance which involves calculating the profiles as the integration proceeds along the conical portion of the flow. Integration is terminated when the height required to pass the mass flow exceeds the geometrical height (in subroutine OUTP).

The separation streamline location is calculated and the recompression pressure. This is compared with the static pressure behind the oblique shock wave at the wake neck.

REFERENCES

A-1 PDP-10 FORTRAN IV Programming Manual, DEC-10-AFCO-D, and Science Library and FORTRAN Utility Subprograms, DEC-10-SFLC-D Digital Equipment Corporation, 1968.

A-2 USA Standard FORTRAN, USA Standards Institute X3.9-1966, 7 March 1966.

A-3 IBM System Reference Library, IBM 7090/7094 IBSYS Operating System Version 13, FORTRAN IV Language, Form C28-6390-3, 1966.

A-4 Univac 1108 FORTRAN V Reference Manual, UP-4060, 1966.

```
*****************************************************
*****************************************************
***                                               ***
***  NAME: E. WACHSLER  PHONE: 16136820039        ***
***  PROJECT: 61000       PROGRAMMER:  60089      ***
***  ADDRESS:  CAM  1-1/61000                     ***
***  CHARGE: 06525/E,WACHSLER                     ***
***                                               ***
***                                               ***
***  FILE NAME: TOTAL .F4                         ***
***  TIME: 23:23          DATE:  11 MAR 1970      ***
***                                               ***
***        PDP-10 TIME SHARING SYSTEM             ***
***         SANDERS ASSOCIATES, INC.              ***
***              NASHUA, N. H.                    ***
***                                               ***
*****************************************************
*****************************************************
```

```
00010     C
00020     C.....................................................................
00030     C
00040     C        MAIN PROGRAM,
00050     C CALCULATES THE FLOW FIELD ABOUT A BLUNT CONE, FROM WHICH IS ISSUI
00060     C A COUNTER-CURRENT ROCKET EXHAUST,
00070     C
00080     C SET UP IN JUNE-OCTOBER 1969 BY E,WACHSLER (WITH HELP FROM
00090     C SA,ROBERGE) FOR THE SANDERS PDP-10, BUT TO BE COMPATIBLE
00100     C WITH OTHER, MORE LIMITED, FORTRAN IV COMPILERS,
00110     C
00120     C THE MAIN PROGRAM CONSISTS OF AN ITERATION LOOP,THE SPECIFIC
00130     C PROCEDURE DEPENDS ON WHETHER THE BLUNTING SPHERE DIAMETER IS
00140     C GREATER THAN (OR LESS THAN) THE BASE DIAMETER,
00150     C THE ITERATION METHOD IS BASED ON THE NEWTON-RAPHSON METHOD
00160     C WITH THE DERIVATIVES CALCULATED NUMERICALLY, FOR THAT
00170     C REASON IT IS NECESSARY TO HAVE TWO INITIAL GUESSES AND TO
00180     C GO THROUGH THE LOOP N+1 TIMES FOR N EQUATIONS BEFORE UPDATING,
00190     C
00200           COMMON/CONSTS/PI,RUNIV
00210           COMMON/CONFAC/CONV(10,4),UN(4),IUNIN,IUNOUT
00220           COMMON/IDENT/IDEAD,INF,JET,JTERM,LAYER,MIX,MJBDY,M1INT,M2INT,
00230          1  IEXIT,IPITOT,IRATIO,ISTAT,ITOTAL,INFRAT,IPIRAT,JRETRN
00240           COMMON/JDENT/JBASE,JCENTR,JEXIT,JFACE,JSPHER,JSTAR,
00250          1  JTERSH,MAX,MERGE,MOD,NO,NPI,NS
00260           COMMON/PAGE/DAT(4)
00270           COMMON/AERO/A(12,7),CD,CONC(10),CP(10),CT,EMACH(10),
00280          1  ENTHAL(10,7),GAMMA(10),P(10,7),Q(10),
00290          2  RHO(10,7),T(10,7),V(10),WDOT(10,7),WMOL(10)
00300           COMMON/GEOM/ALPHA,AR(14,14),R(14,14),
00310          1  THETA(14),X(14,14),Y(14,14),XNU(14)
00320           COMMON/ROOT/NSSWCH,CAPPA,RHOES,UES,XBARI,XK,XLAM,YØ,YSSL
00330           COMMON/ZZINT/ZNT1,ZNT2,ZNT3,ZNT4,XMU,XNU1,YK1,YK2,YK3,YSS(5)
00340           DIMENSION XJ(200),YJ(200),X1IN(100),Y1IN(100),
00350          1  X2IN(100),Y2IN(100)
00360           EXTERNAL VEL2D1,VEL2D2,ENT2D,CON2D,VEL3D1,VEL3D2,ENT3D,CON3D
00370     C
00380       228   FORMAT(29H0THE BLUNTING SPHERE RADIUS =,1PE12,4,
00390          1  32H IS TOO NEAR TO THE BASE RADIUS, ,E12,4,/)
00400       308   FORMAT(17H0P(IDEAD,ISTAT) =,1PE12.4,6H AFTER,I4,
00410          1  12H ITERATIONS,,/)
00420       /38   FORMAT(48H0THE JACOBIAN IS TOO SMALL IN THE ITERATION, I =,I
00430       600   FORMAT(15H2ENTHAL(IDEAD,1) =,1PE12,4,/,14H CONC(IDEAD) =,
00440          1  E12,4,6H AFTER,I4,12H ITERATIONS,,/)
00450      1003   FORMAT(17H0P(IDEAD,ISTAT) =,1PE12,4,13H ENTHAL(IDEAD,1) =,
00460          1  E12,4,/,14H CONC(IDEAD) =,E12,4,6H AFTER,I4,12H ITERATIONS,,/
00470     C
00480           IIN=26
00490           IOUT=6
00500           XA=0,520
00510           YA=2,23
00520           DELTA=0,210
00530           DAT1=4HDAT1
00540           CALL IFILE(IIN,DAT1)
00550           CALL DATE(DAT(1),DAT(2))
00560           CALL TIME(DAT(3))
00570           DAT(4)=1,2
00580     C
00590       102   ISWCH=0
```

```
00610           CALL READIN(IEND)
00620           CALL PRELIM(IERROR)
00630           TYPE 13,CI,P(INF,ISTAT),P(INF,IPITOT),P(JET,ITOTAL),
00640          1  P(JET,IEXIT)
00650        13   FORMAT('0CT=',F12.5,/' PINF,P0F,P0J,PEJ=',1P4E12.4)
00660           TYPE 17,T(INF,ISTAT),T(INF,ITOTAL),T(JET,IEXIT),T(JET,ITOTAL)
00670        17   FORMAT(' T,T0,TEJ,T0J=',4F12.2)
00680           P1=PFIT(PI/2.0,P(INF,IPTRAT))
00690           PTS=P(INF,IPITOT)/P1
00700           EMS=PMACH(GAMMA(INF),PTS)
00710           IF(EMS.GT. 1.0) GO TO 140
00720     C
00730     C NSWCH=1 IMPLIES THAT THE BLUNTING SPHERE DIAMTER IS GREATER THAN THE
00740     C BASE DIAMETER AND THAT THE FLOW IS NOT SUPERSONIC AT THE
00750     C SPHERE SHOULDER.
00760           NSWCH=1
00770           GO TO 150
00780      140  XNU(NPI)=PMNU(GAMMA(INF),EMS,IERROR)
00790           IF(IERROR.EQ. 1) GO TO 100
00800           XNUXX=XNU(NPI)*CONV(1,IUNIN)
00810           TYPE 21,EMS,XNUXX
00820        21   FORMAT(' EMS,NU(PI/2)=',2F10.4,/)
00830     C NOTE THAT THE ORIGIN IS AT X(JFACE,1), HENCE X(JBASE,1) IS NEGATIVE.
00840      150  X(JFACE,1)=0.0
00850           X(JBASE,1)=(R(JFACE,1)-R(JBASE,1))/TAN(THETA(MOD))
00860     C
00870     C INITIAL GUESSES FOR THE PARAMETERS, SPECIFICALLY THE DEAD AIR
00880     C REGION PRESSURE, ARE BASED ON WHETHER THE BLUNTING SPHERE DIAMETER
00890     C IS GREATER OR LESS THAN THE BASE DIAMETER.
00900     C IN THE FORMER CASE, P(IDEAD,ISTAT) MUST BE LESS THAN P(INF,ISTAT)
00910     C AND VICEVERSA, RESPECTIVELY.
00920     C
00930           P(IDEAD,ISTAT)=P(INF,ISTAT)
00940           CALL SPHERE(IERROR)
00950           IF(IERROR.EQ. 1) GO TO 100
00960     C
00970           IF(R(JSPHER,JBASE).LT. 1.0) GO TO 180
00980           IF(NSWCH.EQ. 0) GO TO 170
00990           P(IDEAD,ISTAT)=CPCOE
01000           GO TO 300
01010      170  P(IDEAD,ISTAT)=P(INF,ISTAT)/2.0
01020           GO TO 190
01030      180  P(IDEAD,ISTAT)=SQRT(P(INF,ISTAT)*P(INF,IPITOT))
01040      190  Z11=P(IDEAD,ISTAT)
01050           Z12=1.2*Z11
01060           ENTHAL(IDEAD,1)=SQRT(ENTHAL(INF,1)*ENTHAL(JET,1))
01070           Z21=ENTHAL(IDEAD,1)
01080           Z22=Z21*(1.0+DELTA)
01090           CONC(IDEAD)=2.50
01100           Z31=CONC(IDEAD)
01110           Z32=Z31*(1.0+DELTA)
01120     C
01130     C IF THE BLUNTING SPHERE DIAMETER IS LESS THAN THE BASE DIAMETER,
01140     C THE ITERATION SCHEME CONSISTS OF TWO LOOPS.
01150     C THE FIRST LOOP IS FOR PRESSURE ONLY,BASED ON THE GEOMETRIC
01160     C CONSTRAINT THAT THE BLUNTING CONE IS TANGENT TO THE BODY
01170     C AT THE SHOULDER.
01180     C
01190     C BEGIN THE DEAD AIR PRESSURE ITERATION LOOP.
01200     C
```

```
01210           DO 300 I=1,IEND
01220           CALL JETSCA(XJ,YJ,IERROR)
01230           IF(IERROR.EQ. 1) GO TO 100
01240           CALL SPHERE(IERROR)
01250           IF(IERROR.EQ. 1) GO TO 100
01260           IF(R(JSPHER,JBASE).GT. 1.050) GO TO 1000
01270           IF(R(JSPHER,JBASE).LT. 0.950) GO TO 230
01280           WRITE (IOUT,228) R(JSPHER,1),R(JBASE,1)
01290           GO TO 100
01300     C
01310     C CALCULATION OF ALPHA FOR R(JSPHER,JBASE) LESS THAN 0.950 ,
01320     C THETA(NS) IS NECESSARILY LESS THAN PI/2 ,
01330       230   XBAR=(X(JCENTR,1)-X(JBASE,1))/R(JBASE,1)
01340             YBAR=R(JSPHER,JBASE)
01350             SINALF=( SQRT(1.0+XBAR*XBAR-YBAR*YBAR) -XBAR*YBAR )
01360          1  /(1.0+XBAR*XBAR)
01370             ALPHA=ASIN(SINALF)
01380             THETA(NS)=PI/2.0-ALPHA
01390             X(NS,JEXIT)=R(JSPHER,JEXIT)*COS(THETA(NS))+X(JCENTR,JEXIT)
01400             Y(NS,JEXIT)=R(JSPHER,JEXIT)*SIN(THETA(NS))
01410             THMAX=ATAN(R(JBASE,1)/(X(JCENTR,1)-X(JBASE,1)))
01420             THETA(MAX)=PI-THMAX
01430             PTRY=PFIT(THETA(NS),P(INF,IPTRAT))
01440             P(IDEAD,ISTAT)=PTRY
01450             IF(I.GT. 1) GO TO 250
01460             F11=P(IDEAD,ISTAT)-Z11
01470     C P(IDEAD,ISTAT) IS NOW RESET TO THE SECOND GUESS VALUE,
01480             P(IDEAD,ISTAT)=Z12
01490             GO TO 300
01500       250   F12=P(IDEAD,ISTAT)-Z12
01510             G12=F12-F11
01520             Z13=Z12-(Z12-Z11)*F12/G12
01530             P(IDEAD,ISTAT)=Z13
01540             IF(ABS(Z13/Z12-1.0),LT. 5.0E-4) GO TO 520
01550     C
01560     C UPDATING OF THE ANCHOR POINTS,
01570             Z11=Z12
01580             Z12=Z13
01590             F11=F12
01600       300   CONTINUE
01610     C
01620     C THE SCHEME DID NOT CONVERGE AFTER THE MAXIMUM NUMBER OF ITERATIONS,
01630             WRITE (IOUT,320) P(IDEAD,ISTAT),IEND
01640     C GO BACK TO THE BEGINNING FOR ANOTHER CASE,
01650             GO TO 100
01660     C
01670     C THE PRESSURE ITERATION WAS SUCCESSFUL,NOW WE SOLVE ITERATIVELY
01680     C FOR THE ENTHALPY AND CONCENTRATION IN THE DEAD AIR REGION,
01690     C
01700       520   IND=3*IEND
01710             TYPE 23,X(JTERSH,JEXIT),X(JCENTR,JEXIT)
01720        23   FORMAT(' XJTERM/REJ,XC/REJ=',2F11.5)
01730             TYPE 31,R(JSPHER,1),R(JSPHER,JEXIT),R(JSPHER,JBASE)
01740        31   FORMAT(' RF,RF/REJ,RF/RM =',3E13.5)
01750             ALFX=ALPHA*CONV(1,IUNIN)
01760             TYPE 35,P(IDEAD,ISTAT)
01770        35   FORMAT(' PD=',1PE12.4)
01780             ALFX=ALPHA*CONV(1,IUNIN)
01790             Z1X=THETA(ND)*CONV(1,IUNIN)
01800             Z1Y=THETA(NS)*CONV(1,IUNIN)
```

```
01810           TYPE 41,ZTHX,ZTHY
01820        41 FORMAT(' THETA ND,NS=',2F10.4)
01830      C
01840      C NOW CALCULATE THE THREE CONSTANTS NECESSARY FOR THE PROPER
01850      C LIMITING BEHAVIOR OF U/UE, H* AND C*,
01860      C
01870           XLAM=0.0
01880           XMU=0.0
01890           XNU1=0.0
01900      C
01910           CALL QG8(-Y0,Y0,VEL2D1,ZNT1)
01920           CALL QG8(-Y0,Y0,VEL2D2,ZNT2)
01930           YK1=0.50-ZNT2/ZNT1
01940      C
01950      C ENTHAL(IDEAD,INF)=0.0 FOR CONVENIENCE ONLY,
01960           ENTHAL(IDEAD,INF)=0.0
01970           CALL QG8(-Y0,Y0,ENT2D,ZNT3)
01980           YK2=(1.0+ENTHAL(IDEAD,INF))/2.0-ZNT3/ZNT1
01990      C
02000      C CONC(IDEAD)=1.0 FOR CONVENIENCE ONLY,
02010           CONC(IDEAD)=1.0
02020           CALL QG8(-Y0,Y0,CON2D,ZNT4)
02030           YK3=0.50-ZNT4/ZNT1
02040      C
02050           TYPE 42,ZNT1,ZNT2,ZNT3,ZNT4,ENTHAL(IDEAD,INF),CONC(IDEAD)
02060        42 FORMAT(' Z1,2,3,4=',1P4E12.4,/' H*,C*=',2E12.4)
02070           TYPE 43,YK1,YK2,YK3
02080        43 FORMAT(' K1,2,3=',1P3E14.6)
02090      C
02100      C RESET CONC(IDEAD) TO THE PROPER INITIAL VALUE,
02110           CONC(IDEAD)=Z31
02120      C
02130      C BEGIN THE ENTHALPY AND CONCENTRATION ITERATION LOOP,
02140      C
02150           DO 800 I=1,IND
02160           ENTHAL(IDEAD,INF)=ENTHAL(IDEAD,1)/ENTHAL(INF,1)
02170      C
02180           CALL MIXING(XJ,YJ,X1IN,Y1IN,X2IN,Y2IN,IERROR)
02190           IF(IERROR.EQ. 1) GO TO 100
02200           CALL MERGE0(IERROR)
02210           IF(IERROR.EQ. 1) GO TO 100
02220      C
02230           IF(I+2 .EQ. 3*((I+2)/3)) GO TO 600
02240           IF(I+1 .EQ. 3*((I+1)/3)) GO TO 650
02250           GO TO 700
02260      C
02270        600 F21=ENTHAL(IDEAD,1)-Z21
02280           F31=CONC(IDEAD)-Z31
02290           ENTHAL(IDEAD,1)=Z22
02300      C RESET CONC(IDEAD) TO THE INITIAL VALUE,
02310           CONC(IDEAD)=Z31
02320           GO TO 800
02330      C
02340        650 F22=ENTHAL(IDEAD,1)-Z22
02350           F32=CONC(IDEAD)-Z31
02360           G22=F22-F21
02370           G32=F32-F31
02380      C NOW WE HAVE THE DERIVATIVES WITH RESPECT TO A CHANGE IN ENTHAL(IDEAD,
02390      C THE ENTHALPY IS RESET TO THE FORMER VALUE FOR THE NEXT ITERATION STEP
02400           ENTHAL(IDEAD,1)=Z21
```

```
02410           CONC(IDEAD)=Z32
02420           GO TO 800
02430     C
02440       700 F23=ENTHAL(IDEAD,1)-Z21
02450           F33=CONC(IDEAD)-Z32
02460           G23=F23-F21
02470           G33=F33-F31
02480     C NOW WE HAVE THE DERIVATIVES WITH RESPECT TO A CHANGE IN CONC(IDEAD).
02490           XJACOB=G22*G33-G23*G32
02500           IF(ABS(XJACOB).GT. 1.0E-30) GO TO 710
02510           WRITE (IOUT,708) I
02520           GO TO 100
02530     C NO SOLUTION IS POSSIBLE IF THE JACOBIAN OF THE DERIVATIVES VANISHES.
02540       710 Z23=Z22-(Z22-Z21)*(F22*G33-F32*G23)/XJACOB
02550           Z33=Z32-(Z32-Z31)*(F33*G22-F23*G32)/XJACOB
02560     C
02570           TYPE 73,F21,F31
02580        73 FORMAT('0H,C RESID,=',1P2E12.4)
02590           TYPE 75,Z23,Z33
02600        75 FORMAT(' THE NEW VAL OF H,C=',1P2E12.4,/)
02610           ENTHAL(IDEAD,1)=Z23
02620           CONC(IDEAD)=Z33
02630           IF(ABS(Z23/Z21-1.0).GT. 5.0E-4) GO TO 720
02640           IF(ABS(Z33/Z31-1.0).LT. 5.0E-4) GO TO 820
02650     C
02660     C SAVING AND RESETTING OF VALUES FOR THE NEXT ITERATION.
02670       720 Z21=Z23
02680           Z22=Z21*(1.0+DELTA)
02690           Z31=Z33
02700           Z32=Z31*(1.0+DELTA)
02710       800 CONTINUE
02720     C
02730     C THE SCHEME DID NOT CONVERGE AFTER THE MAXIMUM NUMBER OF ITERATIONS.
02740           WRITE (IOUT,808) ENTHAL(IDEAD,1),CONC(IDEAD),IEND
02750     C GO BACK TO THE BEGINNING FOR ANOTHER CASE.
02760           GO TO 100
02770     C
02780     C THE ENTHALPY AND CONCENTRATION ITERATION WAS SUCCESSFUL, NOW WE
02790     C CALCULATE THE MERGING STREAMLINE VELOCITY,ENTHALPY AND MACH NUMBER.
02800     C
02810       820 UUE=VEL2D1(YSSL)
02820           USSL=UUE*UES*V(INF)
02830           HSSL=ENTHAL(INF,1)*ENT2D(YSSL)/UUE
02840           CONSSL=CON2D(YSSL)/UUE
02850           CPSSL=CONSSL*CP(JET)+(1.0-CONSSL)*CP(INF)
02860           CVSSL=CONSSL*(CP(JET)-RUNIV/WMOL(JET))+(1.0-CONSSL)
02870          1*(CP(INF)-RUNIV/WMOL(INF))
02880           GMSSL=CPSSL/CVSSL
02890           WMSSL=1.0/(CONSSL/WMOL(JET)+(1.0-CONSSL)/WMOL(INF))
02900           EMSSL=USSL*SQRT( WMSSL*CPSSL/( GMSSL*RUNIV*(HSSL
02910          1-0.50*USSL*USSL) ) )
02920           PR=P(IDEAD,ISTAT)*PRATIO(GMSSL,EMSSL)
02930     C
02940           TYPE 81,USSL,HSSL,EMSSL,GMSSL,PR
02950        81 FORMAT(' USSL,HSSL,MSSL,GMSSL,PR=',/1H ,1P5E12.4,/)
02960           CALL OUTPUT
02970     C GO BACK TO THE BEGINNING FOR ANOTHER CASE.
02980           GO TO 100
02990     C
03000     C.....
```

```
C
C CALCULATION FOR BLUNTING SPHERE DIAMETER GREATER THAN THE
C BASE DIAMETER.
C
C THE ITERATION SCHEME CONSISTS OF THE SIMULTANEOUS SOLUTION
C OF ALL THREE VARIABLES, NAMELY PRESSURE, ENTHALPY AND CONCENTRATION
C IN THE DEAD AIR REGION.
C
 1000   Z12=Z11*(1.0+DELTA)
        IND=4*IEND
C
C NOW CALCULATE THE THREE CONSTANTS NECESSARY FOR THE PROPER
C LIMITING BEHAVIOR OF U/UE, H* AND C*.
C
        XLAM=0.0
        XMU=0.0
        XNU1=0.0
C
        CALL QG8(0.0,2.0*Y0,VEL3D1,ZNT1)
        CALL QG8(0.0,2.0*Y0,VEL3D2,ZNT2)
        YK1=0.50-ZNT2/ZNT1
C
C ENTHAL(IDEAD,INF)=0.0 FOR CONVENIENCE ONLY.
        ENTHAL(IDEAD,INF)=0.0
        CALL QG8(0.0,2.0*Y0,ENT3D,ZNT3)
        YK2=(1.0*ENTHAL(IDEAD,INF))/2.0-ZNT3/ZNT1
C
C CONC(IDEAD)=1.0 FOR CONVENIENCE ONLY.
        CONC(IDEAD)=1.0
        CALL QG8(0.0,2.0*Y0,CON3D,ZNT4)
        YK3=0.50-ZNT4/ZNT1
C
        TYPE 42,ZNT1,ZNT2,ZNT3,ZNT4,ENTHAL(IDEAD,INF),CONC(IDEAD)
        TYPE 43,YK1,YK2,YK3
C BEGIN THE ITERATION LOOP FOR THE PRESSURE,ENTHALPY AND CONCENTRATION
C IN THE DEAD AIR REGION.
C
C RESET CONC(IDEAD) TO THE PROPER INITIAL VALUE.
        CONC(IDEAD)=731
C
        DO 1800 I=1,IND
        ENTHAL(IDEAD,INF)=ENTHAL(IDEAD,1)/ENTHAL(INF,1)
        IF(I.EQ. 1) GO TO 1100
        CALL JETSCK(XJ,YJ,IERROR)
        IF(IERROR.EQ. 1) GO TO 100
        CALL SPHERE(IERROR)
        IF(IERROR.EQ. 1) GO TO 100
C
        IF(R(JSPHER,JBASE).GT. 1.050) GO TO 1100
        WRITE (IOUT,228) R(JSPHER,1),R(JBASE,1)
        GO TO 100
C
C CALCULATION OF ALPHA FOR R(JSPHER,JBASE) GREATER THAN 1.050 .
C THETA(NS) IS NECESSARILY GREATER THAN PI/2 .
 1100   IF(NSWCH.EQ. 1) GO TO 1200
        ENTHS=PMACH(GAMMA(INF),P(INF,IPITOT)/P(IDEAD,ISTAT))
        XNUTHS=PMNU(GAMMA(INF),EMTHS,IERROR)
        IF(IERROR.EQ. 1) GO TO 100
        ALPHA=XNUTHS-XNU(NPI)
        GO TO 1220
```

```
03610     1200    ALPHA=0.0
03620     1220    THETA(NS)=PI/2.0+ALPHA
03630             ALFX=ALPHA*CONV(1,IUNIN)
03640             ZTHX=THETA(NO)*CONV(1,IUNIN)
03650             ZTHY=THETA(NS)*CONV(1,IUNIN)
03660             XNUXX=XNUTHS*CONV(1,IUNIN)
03670             TYPE 113,EMTHS,XNUXX,ALFX,ZTHX,ZTHY
03680      113    FORMAT('0EMTHS,NU,ALPH,TH(O),TH(S)=',5F9.4)
03690             TYPE 23,X(JTERSH,JEXIT),X(JCENTR,JEXIT)
03700             TYPE 61,R(JSPHER,1),R(JSPHER,JEXIT),R(JSPHER,JBASE)
03710             TYPE 99,P(IDEAD,ISTAT)
03720             X(NS,JEXIT)=R(JSPHER,JEXIT)*COS(THETA(NS))+X(JCENTR,JEXIT)
03730             Y(NS,JEXIT)=R(JSPHER,JEXIT)*SIN(THETA(NS))
03740             IF(NSWCH.EQ. 1) GO TO 1820
03750     C NO FURTHER ITERATIONS ARE POSSIBLE IF NSWCH=1 ,
03760     C
03770     C CALCULATE THE WAVE, ANGLE FOR A PLANE OBLIQUE SHOCK WAVE,
03780             BETA=WAVE(GAMMA(INF),EMTHS,ALPHA,IERROR)
03790             IF(IERROR.EQ. 1) GO TO 100
03800             EMCS=EMTHS*SIN(BETA)
03810             EMCS=EMCS*EMCS-1.0
03820     C CALCULATE THE RECOMPRESSION STATIC PRESSURE,
03830             PT=P(IDEAD,ISTAT)*( 1.0+2.0*GAMMA(INF)*EMCS/(GAMMA(INF)+1.0) )
03840             BETT=BETA*CONV(1,IUNIN)
03850             TYPE 127,BETT,PT
03860      127    FORMAT(' BETA,PT=',F10.4,1PE12.4)
03870     C
03880             CALL MIXING(XJ,YJ,X1IN,Y1IN,X2IN,Y2IN,IERROR)
03890             IF(IERROR.EQ. 1) GO TO 100
03900             CALL MERGE2(IERROR)
03910             IF(IERROR.EQ. 1) GO TO 100
03920     C
03930             UUE=VEL2D1(YSSL-Y0)
03940             USSL=UUE*UES*V(INF)
03950             HSSL=ENTHAL(INF,1)*ENT2D(YSSL-Y0)/UUE
03960             CONSSL=CON2D(YSSL-Y0)/UUE
03970             CPSSL=CONSSL*CP(JET)+(1.0-CONSSL)*CP(INF)
03980             CVSSL=CONSSL*(CP(JET)-RUNIV/WMOL(JET))+(1.0-CONSSL)
03990          1  *(CP(INF)-RUNIV/WMOL(INF))
04000             GMSSL=CPSSL/CVSSL
04010             WMSSL=1.0/(CONSSL/WMOL(JET)+(1.0-CONSSL)/WMOL(INF))
04020             EMSSL=USSL*SQRT( WMSSL*CPSSL/( GMSSL*RUNIV*(HSSL
04030          1  -0.5*USSL*USSL) ) )
04040             PR=P(IDEAD,ISTAT)*PRATIO(GMSSL,EMSSL)
04050     C
04060             TYPE 81,USSL,HSSL,EMSSL,GMSSL,PR
04070             IF(I+3 .EQ. 4*((I+3)/4)) GO TO 1500
04080             IF(I+2 .EQ. 4*((I+2)/4)) GO TO 1550
04090             IF(I+1 .EQ. 4*((I+1)/4)) GO TO 1600
04100             GO TO 1650
04110     C
04120      1500   F11=PI=PR
04130             F21=ENTHAL(IDEAD,1)-Z21
04140             F31=CONC(IDEAD)-Z31
04150     C RESET ENTHAL(IDEAD,1) AND CONC(IDEAD) TO THE INITIAL VALUES,
04160             P(IDEAD,ISTAT)=Z12
04170             ENTHAL(IDEAD,1)=Z21
04180             CONC(IDEAD)=Z31
04190             GO TO 1800
          C
```

```
04210     1550    F12=PT-PR
04220             F22=ENTHAL(IDEAD,1)-Z21
04230             F32=CONC(IDEAD)-Z31
04240             G12=F12-F11
04250             G22=F22-F21
04260             G32=F32-F31
04270     C NOW WE HAVE THE DERIVATIVES WITH RESPECT TO A CHANGE IN P(IDEAD,ISTAT
04280     C THE PRESSURE AND CONCENTRATION ARE RESET TO THE FORMER VALUES
04290     C FOR THE NEXT ITERATION STEP,
04300             P(IDEAD,ISTAT)=Z11
04310             ENTHAL(IDEAD,1)=Z22
04320             CONC(IDEAD)=Z31
04330             GO TO 1600
04340     C
04350     1600    F13=PT-PR
04360             F23=ENTHAL(IDEAD,1)-Z22
04370             F33=CONC(IDEAD)-Z31
04380             G13=F13-F11
04390             G23=F23-F21
04400             G33=F33-F31
04410     C NOW WE HAVE THE DERIVATIVES WITH RESPECT TO A CHANGE IN ENTHAL(IDEAD,
04420     C THE PRESSURE AND ENTHALPY ARE RESET TO THE FORMER VALUES
04430     C FOR THE NEXT ITERATION STEP,
04440             P(IDEAD,ISTAT)=Z11
04450             ENTHAL(IDEAD,1)=Z21
04460             CONC(IDEAD)=Z32
04470             GO TO 1800
04480     C
04490     1650    F14=PT-PR
04500             F24=ENTHAL(IDEAD,1)-Z21
04510             F34=CONC(IDEAD)-Z32
04520             G14=F14-F11
04530             G24=F24-F21
04540             G34=F34-F31
04550     C NOW WE HAVE THE DERIVATIVES WITH RESPECT TO A CHANGE IN CONC(IDEAD),
04560             XJACOB=G12*(G23*G34-G24*G33) -G22*(G13*G34-G14*G33)
04570          1  +G32*(G13*G24-G14*G23)
04580     C NO SOLUTION IS POSSIBLE IF THE JACOBIAN OF THE DERIVATIVES VANISHES,
04590             IF(ABS(XJACOB).GT. 1.0E-35) GO TO 1710
04600             WRITE (IOUT,708) I
04610             GO TO 100
04620     1710    Z13=Z12-(Z12-Z11)*( F12*(G23*G34-G24*G33)
04630          1  -F23*(G13*G34-G14*G33) +F34*(G13*G24-G14*G23) )/XJACOB
04640             Z23=Z22-(Z22-Z21)*( -F12*(G22*G34-G24*G32)
04650          1  +F23*(G12*G34-G14*G32) -F34*(G12*G24-G14*G22) )/XJACOB
04660             Z33=Z32-(Z32-Z31)*( F12*(G22*G33-G23*G32)
04670          1  -F23*(G12*G33-G13*G32) +F34*(G12*G23-G13*G22) )/XJACOB
04680     C
04690             P(IDEAD,ISTAT)=Z13
04700             ENTHAL(IDEAD,1)=Z23
04710             CONC(IDEAD)=Z33
04720             TYPE 173,F11,F21,F31
04730       173   FORMAT('0PC,H,C RESID=',1P3E12.4)
04740             TYPE 175,Z13,Z23,Z33
04750       175   FORMAT(' THE NEW VAL OF PO,H,C=',1P3E12.4,/)
04760             IF(ABS(Z13/Z11-1.0),GT. 5.0E-4) GO TO 1750
04770             IF(ABS(Z23/Z21-1.0),GT. 5.0E-4) GO TO 1750
04780             IF(ABS(Z33/Z31-1.0),LT. 5.0E-4) GO TO 1820
04790     C
04800     C SAVING AND RESETTING OF VALUES FOR THE NEXT ITERATION.
```

```
 1750    Z11=Z13
         Z12=Z11*(1.0+DELTA)
         Z21=Z23
         Z22=Z21*(1.0+DELTA)
         Z31=Z33
         Z32=Z31*(1.0+DELTA)
 1800    CONTINUE
C
C THE SCHEME DID NOT CONVERGE AFTER THE MAXIMUM NUMBER OF ITERATIONS,
         WRITE (IOUT,1808) P(IDEAD,ISTAT),ENTHAL(IDEAD,1),
     1   CONC(IDEAD),IEND
C GO BACK TO THE BEGINNING FOR ANOTHER CASE.
         GO TO 100
C
 1820    CALL OUTPUT
C
C GO BACK TO THE BEGINNING FOR ANOTHER CASE.
         GO TO 100
C
         STOP
         END
C
C.....
C
         BLOCK DATA
C SETS UP THE COMMON BLOCKS AND INITIALIZES SOME OF ITS VALUES,
C IN PARTICULAR, IT SPECIFIES THE I/O CONVERSION FACTORS AND SETS
C UP THE CORRESPONDENCE BETWEEN SUBSCRIPT NAMES AND SUBSCRIPT VALUES,
C
         COMMON/CONSTS/PI,RUNIV
         COMMON/CONFAC/CONV(10,4),UN(4),IUNIN,IUNOUT
         COMMON/IDENT/IDEAD,INF,JEI,JTERM,LAYER,MIX,MJBDY,M1INI,M2INI,
     1   IEXIT,IPITOT,IRATIO,ISTAT,ITOTAL,INFRAT,IPTRAI,JRETRN
         COMMON/JDENT/JBASE,JCENTR,JEXIT,JFACE,JSPHER,JSTAR,
     1   JTERSH,MAX,MERGE,MOD,ND,NPI,NS
         COMMON/PAGE/DAT(4)
         COMMON/AERO/A(10,7),CD,CONC(10),CP(10),CT,EMACH(10),
     1   ENTHAL(10,7),GAMMA(10),P(10,7),Q(10),
     2   RHO(10,7),T(10,7),V(10),WDOT(10,7),WMOL(10)
         COMMON/GEOM/ALPHA,AR(14,14),R(14,14),
     1   THETA(14),X(14,14),Y(14,14),XNU(14)
         COMMON/ROOT/ESSNCH,CAPPA,RHOES,UES,XBAR1,XK,XLAM,Y0,YSSL
         COMMON/ZZINT/ZNT1,ZNT2,ZNT3,ZNT4,XMU,XNU1,YK1,YK2,YK3,YSS(5)
C
         DATA PI,RUNIV /3.141592653,8314.30/
C THE NEXT DATA STATEMENT SPECIFIES 3 SETS OF CONVERSION FACTORS,
C THE SEQUENCE 1,2,3,4,5,6,7  CORRESPONDS TO THE VARIABLES
C ANGLE,AREA,DENSITY,PRESSURE,TEMPERATURE,VELOCITY AND MOLECULAR
C WEIGHT, RESPECTIVELY,
C THE ENGLISH UNITS ARE FEET,SLUGS/FT**3,PSI,DEG.R., AND LBS/LBS-MOLE.
         DATA (CONV(1,J),J=1,4)/4*57.295779513/,
     1   (CONV(I,1),I=2,10) /9*1.0/,
     2   (CONV(I,2),I=2,10) /1.0E-4,1.0E+3,0.10,1.0,0.010,4*1.0/,
     3   (CONV(I,3),I=2,10) /0.092903E-4,515.3790,6894.7572,
     4   0.555555555,0.3048,4*1.0/
         DATA (UN(I),I=1,4) /5HMKS, ,5HCGS, ,5HENGL.,5HOTHER/
C NOTE THAT THE SUBSCRIPT IEXIT HAS THE SAME VALUE AS ISTAT, AND THAT
C THE SUBSCRIPT 1 (ONE) IS SAVED FOR DIMENSIONED VALUES.
C ALSO NOTE THAT THE SUBSCRIPTS JTERM AND JTERSH REFER TO THE SAME
C LOCATION, BUT HAVE DIFFERENT VALUES.
```

```
      DATA IDEAD,INF,JET,JTERM,LAYER,MIX,MJBDY,M1INT,M2INT,
     1 IEXIT,IPITOT,IRATIO,ISTAT,ITOTAL,INFRAT,IPTRAT,JRETRN
     2 /2,3,4,5,6,7,8,9,10, 4,2,3,4,5,6,7,7/
      DATA JBASE,JCENTR,JEXIT,JFACE,JSPHER,JSTAR,
     1 JTERSH,MAX,MERGE,MOD,ND,NPI,NS
     2 /2,3,4,5,6,7,8,9,10,11,12,13,14/
C
      END
C
C.....
C
      SUBROUTINE READIN(IEND)
C READS IN THE INPUT DATA AND CONVERTS IT,
C ANGLES ARE INPUT AND OUTPUT IN DEGREES,CARRIED IN RADIANS WITHIN THE
C PROGRAM.
C
C INPUT AND OUTPUT MAY BE IN ENGLISH, CGS, MKS, OR OTHER UNITS,
C BUT MKS UNITS ARE USED WITHIN THE PROGRAM.
C
      COMMON/CONFAC/CONV(10,4),UN(4),IUNIN,IUNOUT
      COMMON/IDENT/IDEAD,INF,JET,JTERM,LAYER,MIX,MJBDY,M1INT,M2INT,
     1 IEXIT,IPITOT,IRATIO,ISTAT,ITOTAL,INFRAT,IPTRAT,JRETRN
      COMMON/JDENT/JBASE,JCENTR,JEXIT,JFACE,JSPHER,JSTAR,
     1 JTERSH,MAX,MERGE,MOD,ND,NPI,NS
      COMMON/PAGE/DAT(4)
      COMMON/AERO/A(10,7),CD,CONC(10),CP(10),CT,EMACH(10),
     1 ENTHAL(10,7),GAMMA(10),P(10,7),Q(10),
     2 RHO(10,7),T(10,7),V(10),WDOT(10,7),WMOL(10)
      COMMON/GEOM/ALPHA,AR(14,14),R(14,14),
     1 THETA(14),X(14,14),Y(14,14),XNU(14)
C
  110 FORMAT(1H1,6X,12HRETRO-ROCKET,10X,2A5,4X,A5,14X,4HPAGE,F3.0,/)
  120 FORMAT(6X,I1,1X,2A5)
  125 FORMAT(29H0END OF INPUT DATA AND OF RUN,/)
  138 FORMAT(33H0THE NAME OF THE SYSTEM OF UNITS ,A5,
     1 27H IS NOT PROPERLY SPECIFIED.,/)
  155 FORMAT(13H INPUT IS IN ,A5,17H SYSTEM OF UNITS,)
  175 FORMAT(14H OUTPUT IS IN ,A5,17H SYSTEM OF UNITS,)
  190 FORMAT(6X,I)
  191 FORMAT(29H THE MAX, ND, OF ITERATIONS =,I4,/
     1 1HC,10X,21HIMAGE OF INPUT CARDS.,/)
  220 FORMAT(6X,5F)
  221 FORMAT(1H ,5F12.4)
  270 FORMAT(6X,4F)
  271 FORMAT(1H ,4F12.4)
  310 FORMAT(6X,3F)
  311 FORMAT(1H ,3F12.4)
C
      IIN=26
      IOUT=6
  100 WRITE (IOUT,110) (DAT(I),I=1,4)
      DAT(4)=DAT(4)+1.0
C
C READ IN INPUT AND OUTPUT SYSTEM OF UNITS, NCAS=0 IS USED TO
C TERMINATE THE RUN.
C
      READ (IIN,120) NCAS,UNITIN,UNIOUT
      IF(NCAS.EQ.0) GO TO 130
      WRITE (IOUT,110) (DAT(I),I=1,4)
      WRITE (IOUT,125)
```

```
      CALL RELEAS(IIN)
      CALL EXIT
C
  130 DO 140 I=1,4
      IF(UNITIN.EQ.UN(I)) GO TO 150
  140 CONTINUE
      WRITE (IOUT,138) UNITIN
      GO TO 100
  150 IUNIN=I
      WRITE (IOUT,155) UN(IUNIN)
C
      DO 160 I=1,4
      IF(UNIOUT.EQ.UN(I)) GO TO 170
  160 CONTINUE
      WRITE (IOUT,138) UNIOUT
      GO TO 100
  170 IUNOUT=I
      WRITE (IOUT,175) UN(IUNOUT)
C
C IEND IS THE MAXIMUM NUMBER OF ITERATIONS, BUT NO MORE THAN 30 .
      READ (IIN,190) IEND
      IEND=MIN0(IEND,30)
      WRITE (IOUT,191) IEND
C
C READ IN THE FREE STREAM PROPERTIES.
      READ (IIN,220) GAMMA(INF),WMOL(INF),P(INF,ISTAT),T(INF,ISTAT),
     1 V(INF)
      WRITE (IOUT,221) GAMMA(INF),WMOL(INF),P(INF,ISTAT),
     1 T(INF,ISTAT),V(INF)
      WMOL(INF)=WMOL(INF)*CONV(7,IUNIN)
      P(INF,ISTAT)=P(INF,ISTAT)*CONV(4,IUNIN)
      T(INF,ISTAT)=T(INF,ISTAT)*CONV(5,IUNIN)
      V(INF)=V(INF)*CONV(6,IUNIN)
C
C READ IN THE JET PROPERTIES.
      READ (IIN,270) GAMMA(JET),WMOL(JET),P(JET,ITOTAL),T(JET,ITOTAL
      WRITE (IOUT,271) GAMMA(JET),WMOL(JET),P(JET,ITOTAL),T(JET,
     1 ITOTAL)
      WMOL(JET)=WMOL(JET)*CONV(7,IUNIN)
      P(JET,ITOTAL)=P(JET,ITOTAL)*CONV(4,IUNIN)
      T(JET,ITOTAL)=T(JET,ITOTAL)*CONV(5,IUNIN)
C
C READ IN THE JET GEOMETRY.
      READ (IIN,312) AR(JSTAR,1),AR(JEXIT,1),THETA(JEXIT)
      WRITE (IOUT,311) AR(JSTAR,1),AR(JEXIT,1),THETA(JEXIT)
      AR(JSTAR,1)=AR(JSTAR,1)*CONV(2,IUNIN)
      AR(JEXIT,1)=AR(JEXIT,1)*CONV(2,IUNIN)
      THETA(JEXIT)=THETA(JEXIT)/CONV(1,IUNIN)
C
C READ IN THE MODEL GEOMETRY.
      READ (IIN,312) AR(JBASE,1),AR(JFACE,1),THETA(MOD)
      WRITE (IOUT,311) AR(JBASE,1),AR(JFACE,1),THETA(MOD)
      AR(JBASE,1)=AR(JBASE,1)*CONV(2,IUNIN)
      AR(JFACE,1)=AR(JFACE,1)*CONV(2,IUNIN)
      AR(JFACE,1)=AMAX1(AR(JFACE,1),AR(JEXIT,1))
C THE ABOVE CORRECTS FOR POSSIBLE INPUT ERROR, THE MODEL FACE RADIUS
C MUST BE AT LEAST EQUAL TO THE JET NOZZLE EXIT RADIUS.
      THETA(MOD)=THETA(MOD)/CONV(1,IUNIN)
      RETURN
      END
```

```
      C
      C.....
      C
            SUBROUTINE PRELIM(IERROR)
      C THIS SUBROUTINE CALCULATES FREE STREAM, JET AND OTHER PROPERTIES
      C WHICH ARE BASED ON THE INPUT DATA AND WHICH REMAIN UNCHANGED
      C THROUGHOUT THE PROGRAM FOR EACH SET OF INPUT DATA.
      C
            COMMON/CONSTS/PI,RUNIV
            COMMON/IDENT/IDEAD,INF,JET,JTERM,LAYER,MIX,MJBOY,M1INT,M2INT,
           1  IEXIT,IPITOT,IRATIO,ISTAT,ITOTAL,INFRAT,IPTRAT,JRETRN
            COMMON/JDENT/JBASE,JCENTR,JEXIT,JFACE,JSPHER,JSTAR,
           1  JTERSH,MAX,MERGE,MOD,ND,NPI,NS
            COMMON/AERO/A(10,7),CD,CONC(10),CP(10),CT,EMACH(10),
           1  ENTHAL(10,7),GAMMA(10),P(10,7),Q(10),
           2  RHO(10,7),T(10,7),V(10),WDOT(10,7),WMOL(10)
            COMMON/GEOM/ALPHA,AR(14,14),R(14,14),
           1  THETA(14),X(14,14),Y(14,14),XNU(14)
      C
            TYPE 12
        12  FORMAT('0ENTERING PRELIM ')
      C CALCULATION OF THE FREE STREAM PARAMETERS.
            RHO(INF,ISTAT)=GASRHO(P(INF,ISTAT),WMOL(INF),T(INF,ISTAT))
            A(INF,ISTAT)=SOUND(GAMMA(INF),WMOL(INF),T(INF,ISTAT))
            EMACH(INF)=V(INF)/A(INF,ISTAT)
            Q(INF)=GAMMA(INF)*P(INF,ISTAT)*EMACH(INF)*EMACH(INF)/2.0
            P(INF,IRATIO)=PRATIO(GAMMA(INF),EMACH(INF))
            RHO(INF,IRATIO)=RHORAT(GAMMA(INF),EMACH(INF))
            T(INF,IRATIO)=TRATIO(GAMMA(INF),EMACH(INF))
            P(INF,ITOTAL)=P(INF,ISTAT)*P(INF,IRATIO)
            RHO(INF,ITOTAL)=RHO(INF,ISTAT)*RHO(INF,IRATIO)
            T(INF,ITOTAL)=T(INF,ISTAT)*T(INF,IRATIO)
            A(INF,ITOTAL)=A(INF,ISTAT)*SQRT(T(INF,IRATIO))
            P(INF,IPITOT)=P(INF,ISTAT)*PPITOT(GAMMA(INF),EMACH(INF))
            P(INF,IPTRAT)=P(INF,ISTAT)/P(INF,IPITOT)
            CP(INF)=GAMMA(INF)*RUNIV/(WMOL(INF)*(GAMMA(INF)-1.0))
            ENTHAL(INF,1)=CP(INF)*T(INF,ITOTAL)
            CONC(INF)=2.0
      C
      C CALCULATION OF THE JET EXIT PARAMETERS.
            AR(JEXIT,JBASE)=AR(JEXIT,1)/AR(JBASE,1)
            AR(JEXIT,JSTAR)=AR(JEXIT,1)/AR(JSTAR,1)
            RHO(JET,ITOTAL)=GASRHO(P(JET,ITOTAL),WMOL(JET),T(JET,ITOTAL))
            EMACH(JET)=AMACH(GAMMA(JET),AR(JEXIT,JSTAR),1,IERROR)
            IF(IERROR.EQ.1) RETURN
            P(JET,IRATIO)=PRATIO(GAMMA(JET),EMACH(JET))
            RHO(JET,IRATIO)=RHORAT(GAMMA(JET),EMACH(JET))
            T(JET,IRATIO)=TRATIO(GAMMA(JET),EMACH(JET))
            P(JET,IEXIT)=P(JET,ITOTAL)/P(JET,IRATIO)
            RHO(JET,IEXIT)=RHO(JET,ITOTAL)/RHO(JET,IRATIO)
            T(JET,IEXIT)=T(JET,ITOTAL)/T(JET,IRATIO)
            A(JET,IEXIT)=SOUND(GAMMA(JET),WMOL(JET),T(JET,IEXIT))
            A(JET,ITOTAL)=A(JET,IEXIT)*SQRT(T(JET,IRATIO))
            P(JET,IPITOT)=P(JET,IEXIT)*PPITOT(GAMMA(JET),EMACH(JET))
            V(JET)=EMACH(JET)*A(JET,IEXIT)
            CP(JET)=GAMMA(JET)*RUNIV/(WMOL(JET)*(GAMMA(JET)-1.0))
            WDOT(JET,1)=RHO(JET,IEXIT)*V(JET)*AR(JEXIT,1)
            ENTHAL(JET,1)=CP(JET)*T(JET,ITOTAL)
            ENTHAL(JET,INF)=ENTHAL(JET,1)/ENTHAL(INF,1)
            CONC(JET)=1.0
```

```
C
C CALCULATION OF JET AND MODEL RADII,
      R(JSTAR,1)=SQRT(AR(JSTAR,1)/PI)
      R(JEXIT,1)=SQRT(AR(JEXIT,1)/PI)
      R(JEXIT,JSTAR)=R(JEXIT,1)/R(JSTAR,1)
      R(JBASE,1)=SQRT(AR(JBASE,1)/PI)
      R(JFACE,1)=SQRT(AR(JFACE,1)/PI)
C
C CALCULATION OF THE THRUSTING COEFFICIENT ,
      TEMP=RHO(JET,IEXIT)*AR(JEXIT,JBASE)*V(JET)*V(JET)/Q(INF)
      CT=TEMP*(1.0+1.0/(GAMMA(JET)*EMACH(JET)*EMACH(JET)))
      RETURN
      END
C
C.....
C
      SUBROUTINE SPHERE(IERROR)
C CALCULATES THE RADIUS OF THE BLUNTING SPHERE AND THE LOCATION OF
C ITS CENTER WITH RESPECT TO THE NOZZLE EXIT PLANE,
C
      COMMON/CONSTS/PI,RUNIV
      COMMON/CONFAC/CONV(10,4),UN(4),IUNIN,IUNOUT
      COMMON/IDENT/IDEAD,INF,JET,JTERM,LAYER,MIX,MJBOY,M1INT,M2INT,
     1  IEXIT,IPITOT,IRATIO,ISTAT,ITOTAL,INFRAT,IPTRAT,JRETRN
      COMMON/JDENT/JBASE,JCENTR,JEXIT,JFACE,JSPHER,JSTAR,
     1  JTERSH,MAX,MERGE,MOD,ND,NPI,NS
      COMMON/AERO/A(10,7),CD,CONC(10),CP(10),CT,EMACH(10),
     1  EMINAL(10,7),GAMMA(10),P(10,7),Q(10),
     2  RHO(10,7),T(10,7),V(10),WDOT(10,7),WMOL(10)
      COMMON/GEOM/ALPHA,AR(14,14),R(14,14),
     1  THETA(14),X(14,14),Y(14,14),XNU(14)
      EXTERNAL FCTCN
C
  998 FORMAT('0CONVERGENCE FAILURE, DUMMY=',1PE13.5,'  FCTCN=',
     1  E13.5,'  IER=',I4,/)
C
      TYPE 12
   12 FORMAT('  SPHERE ')
      IOUT=6
C CALCULATION OF THE BLUNTING SPHERE DIAMETER,
      PDEAD=P(IDEAD,ISTAT)
      IF(P(INF,ISTAT).GT.P(IDEAD,ISTAT)) PDEAD=P(INF,ISTAT)
C THIS FORMULATION IS NECESSARY TO CALCULATE PROPERLY THE BLUNTING
C SPHERE DIAMETER WHEN IT IS LARGER THAN THE BASE DIAMETER,
      EMACH(LAYER)=PMACH(GAMMA(JET),P(INF,IPITOT)/PDEAD)
      VJET=VASTAR(GAMMA(JET),EMACH(JET))
      IF(EMACH(INF).GT. 1.50) GO TO 500
C
C CALCULATION FOR FREE STREAM MACH NO. LESS THAN OR = 1.50 .
C NOTE THAT SINALF=SIN(ALF), COSALF=COS(ALF) AND THAT
C ALF=PI/2.0-IPETA(NS) = ALPHA IF THE BLUNTING SPHERE DIAMETER
C IS LESS THAN THE BASE DIAMETER,
      VLAYER=VASTAR(GAMMA(JET),EMACH(LAYER))
      EM=PI*EMACH(INF)/2.0
      TEMP=(COS(EM)**2)+0.380*(SIN(EM)**2)
      DUMMY=(PDEAD/P(INF,IPITOT)-TEMP)/(1.0-TEMP)
      SINALF=SQRT(DUMMY)
      CD=P(INF,IPITOT)/Q(INF)*TEMP/2.0-P(IDEAD,ISTAT)/Q(INF)
      GM=1.0+1.0/(GAMMA(JET)*EMACH(JET)*EMACH(JET))
      CT=CT/CD*(1.0+(VLAYER/VJET)/GM)**2.0*AS(JEXIT)/AS(JBASE)/CD
```

```
     1   *GAMMA(INF)*EMACH(INF)*EMACH(INF))
         R(JSPHER,1)=SQRT(AR(JBASE,1)*TEMP/PI)
         GO TO 600
C
C CALCULATION FOR FREE STREAM MACH NO. GREATER THAN 1.50 .
 500     TEMP=(PDEAD-P(INF,ISTAT))/(P(INF,IPITOT)-P(INF,ISTAT))
         SINALF=SQRT(TEMP)
         COSALF=SQRT(1.0- SINALF*SINALF)
         DF1=2.0*AR(JEXIT,1)*P(JET,ITOTAL)/(PI*(COSALF**4)
     1   *(P(INF,IPITOT)-P(INF,ISTAT)))
         DF2=(P(JET,IEXIT)-P(IDEAD,ISTAT))/P(JET,ITOTAL)+2.0*GAMMA(JET)
     1   /(GAMMA(JET)+1.0)*VJET*VJET/RHO(JET,IRATIO)
         DF2=DF2*SQRT(2.0*GAMMA(JET)/(GAMMA(JET)+1.0))*VJET
     1   /RHO(JET,IRATIO)*EMACH(LAYER)*COSALF*SQRT(GAMMA(JET)
     2   /IRATIO(GAMMA(JET),EMACH(LAYER)))
         R(JSPHER,1)=SQRT(DF1*DF2)
C
 600     AR(JSPHER,1)=PI*R(JSPHER,1)*R(JSPHER,1)
         WDOT(INF,1)=AR(JSPHER,1)*RHO(INF,ISTAT)*V(INF)
C THE ABOVE IS USED TO NON-DIMENSIONALISE SOME MASS FLOWS.
         R(JSPHER,JEXIT)=R(JSPHER,1)/R(JEXIT,1)
         AR(JEXIT,JSPHER)=AR(JEXIT,1)/AR(JSPHER,1)
         R(JSPHER,JBASE)=R(JSPHER,1)/R(JBASE,1)
C
C LOCATION OF THE CENTER OF THE BLUNTING SPHERE,
C THE COORDINATES ARE NON-DIMENSIONALIZED WITH THE JET NOZZLE EXIT
C RADIUS AND ARE MEASURED FROM THE CENTER OF THAT PLANE.
         EM1=EMACH(LAYER)/2.0
         EM2=EMACH(LAYER)/3.0
         CALL PGEN(DUMMY,VAL,FCTCN,EM1,EM2,1.0E-6,100,IER)
         IF(IER.EQ. 0) GO TO 700
         WRITE (IOUT,698) DUMMY,VAL,IER
         IERROR=1
         RETURN
C
 700     X(JCENTR,JEXIT)=X(ND,JEXIT)-Y(ND,JEXIT)*COTAN(THETA(ND))
         X(JCENTR,1)=X(JCENTR,JEXIT)*R(JEXIT,1)
         X(JCENTR,JTERSH)=X(JCENTR,JEXIT)/X(JTERSH,JEXIT)
         RETURN
         END
C
C.....
C
         SUBROUTINE JETSCK(XJ,YJ,IERROR)
C CALCULATES THE LOCATION OF THE JET TERMINAL SHOCK, THEN BY A RUNGE-
C KUTTA INTEGRATION, IT CALCULATES THE LOCATION OF THE JET BOUNDARY
C AND ITS INTERSECTION WITH THE TERMINAL SHOCK.
C
         COMMON/CONSTS/PI,RUNIV
         COMMON/IDENT/IDEAD,INF,JET,JTERM,LAYER,MIX,MJBOY,M1INT,M2INT,
     1   IEXIT,IPITOT,IRATIO,ISTAT,ITOTAL,INFRAT,IPIRAT,JRETRN
         COMMON/JDENT/JBASE,JCENTR,JEXIT,JFACE,JSPHER,JSTAR,
     1   JTERSH,MAX,MERGE,MOD,NO,NPI,NS
         COMMON/AERO/A(10,7),CD,CONC(10),CP(10),CT,EMACH(10),
     1   ENTHAL(10,7),GAMMA(10),P(10,7),Q(10),
     2   RHO(10,7),T(10,7),V(10),WDOT(10,7),WMOL(10)
         COMMON/GEOM/ALPHA,AR(14,14),R(14,14),
     1   THETA(14),X(14,14),Y(14,14),XND(14)
         COMMON/FCTA1/PHI,XX,YY
         DIMENSION XJ(200),XOUT(12),YJ(200),YOUT(10)
```

```
      EXTERNAL FCTRK,FCTPJ
C
  110 FORMAT(31H0THE JET NOZZLE EXIT PRESSURE =,1PE12.4,
     1 30H IS LESS THAN THE DEAD AIR PRESSSURE =,E12.4,/)
  140 FORMAT(32H0THE JET NOZZLE PITOT PRESSURE =,1PE12.4,
     1 25H IS LESS THAN THE FREE ,/,
     2 24H STREAM PITOT PRESSURE =,E12.4,/)
  190 FORMAT('0CONVERGENCE FAILURE, DUMMY=',1PE13.5,' FCTPJ=',
     1 E13.5,' IER=',I4,/)
  300 FORMAT(30H0THE VALUE OF H,THE STEP SIZE,,
     1 14H IS LESS THAN ,1PE12.4,/)
C
      TYPE 12
   12 FORMAT(' ENTERING JETSCK  ',$)
      IOUT=8
C THE JET NOZZLE EXIT PRESSURE MUST BE GREATER THAN THE DEAD AIR
C PRESSURE.
      IF(P(JET,IEXIT).GT.P(IDEAD,ISTAT)) GO TO 120
      WRITE (IOUT,110) P(JET,IEXIT),P(IDEAD,ISTAT)
      GO TO 900
C
C THE JET NOZZLE EXIT PITOT PRESSURE MUST BE GREATER THAN THE FREE
C STREAM PITOT PRESSURE.
  120 IF(P(JET,IPITOT).GT.P(INF,IPITOT)) GO TO 150
      WRITE (IOUT,140) P(JET,IPITOT),P(INF,IPITOT)
      GO TO 900
  150 P(IDEAD,IPTRAT)=P(IDEAD,ISTAT)/P(INF,IPITOT)
C
C A CALL IS MADE TO -PGEW- SUBROUTINE TO FIND ITERATIVELY THE JET
C TERMINAL SHOCK MACH NUMBER, BY MATCHING THE FREE STREAM AND JET
C PITOT PRESSURES.
      VSQLIM=2.0*ENTHAL(JET,1)
      RHO1=P(INF,IPITOT)/VSQLIM
      RHO2=1.5*RHO1
      CALL PGEW(DUMMY,VAL,FCTPJ,RHO1,RHO2,1.0E-6,100,IER)
C DUMMY=P(JTERM,IPITOT)/P(INF,IPITOT)-1.0 .
      IF(IER.EQ. 0) GO TO 200
      WRITE (IOUT,190) DUMMY,VAL,IER
      GO TO 900
C
C THE JET AND FREE STREAM PITOT PRESSURE ARE NOW EQUAL.
C
C CALCULATION OF THE AXIAL DISTANCE OF THE JET TERMINAL SHOCK FROM
C THE JET NOZZLE EXIT PLANE.
  200 CJ=SQRT(1.0-1.0/TRATIO(GAMMA(JET),EMACH(JTERM)))
      CJST=SQRT((GAMMA(JET)-1.0)/(GAMMA(JET)+1.0))
      DUMMY=CFVAC(GAMMA(JET),AR(JEXIT,JSTAR),PRAT,IERROR)
      IF(IERROR.EQ. 1) GO TO 960
      TEMP=SQRT(PI)*(1.0-DUMMY/(CJ*CFMAX(GAMMA(JET))))
      XLMD=1.0/TEMP
      TEMP=(2.0/(GAMMA(JET)+1.0))**(1.0/(GAMMA(JET)-1.0))
      X(JTERSH,JSTAR)=SQRT(TEMP*XLMD/SQRT(PI)*CJST/CJ
     1 *RHO(JTERM,IRATIO))
      X(JTERSH,JEXIT)=X(JTERSH,JSTAR)/R(JEXIT,JSTAR)
C
C CALCULATION OF THE JET BOUNDARY LOCATION.
      EMACH(IDEAD)=PMACH(GAMMA(JET),P(JET,ITOTAL)/P(IDEAD,ISTAT))
      SQM=EMACH(IDEAD)*EMACH(IDEAD)
      PSI=2.0/(GAMMA(JET)+1.0)*SQRT(SQM-1.0)/SQM*AR(JEXIT,JSTAR)
     1 /ARATIO(GAMMA(JET),EMACH(IDEAD))
```

```
09010            XNU(JEXIT)=PRNU(GAMMA(JET),EMACH(JET),IERROR)
09020            IF(IERROR.EQ. 1) GO TO 960
09030            XNUDED=PRNU(GAMMA(JET),EMACH(IDEAD),IERROR)
09040            IF(IERROR.EQ. 1) GO TO 960
09050            THET=XNUDED-XNU(JEXIT)+THETA(JEXIT)
09060            RROA=SQRT(1.0+THET/PSI)
09070            XR=1.0/RROA
09080            PHI=PSI+THET
09090            XBARMX=X(JTERSH,JEXIT)*XR
09100            RSS=XBARMX*XBARMX
09110            H=XR/10.0
09120    C
09130    C THIS LOOP FINDS THE UPPER LIMIT OF THE INTEGRAL, I.E, THE
09140    C ASYMPTOTIC PLUME RADIUS.
09150      290   XI=XR
09160            YI=0.
09170    C NOTE THAT IN THE TRANSFORMED COORDINATES IN WHICH THE INTEGRATION IS
09180    C BEING CARRIED OUT,XBAR CORRESPONDS TO YJ AND CAPITAL R TO XJ,
09190            DO 300 I=1,181
09200            CALL RUNGK(FCTRK,H,XI,YI,1,1,XJ,YJ)
09210            IF(YJ(1).GT.XBARMX) GO TO 310
09220            XI=XJ(1)
09230            YI=YJ(1)
09240      300   CONTINUE
09250    C THE ASYMPTOTIC PLUME RADIUS HAS NOT BEEN REACED BECAUSE THE STEP
09260    C SIZE WAS TOO SMALL, INCREASE THE STEP SIZE.
09270            H=2.0*H
09280            GO TO 290
09290    C
09300    C STEP SIZE IS ADJUSTED SO THAT THE ASYMPTOTIC PLUME RADIUS IS
09310    C REACHED JUST BEFORE THE END OF THE INTEGRATION.
09320      310   H=(XI+H-XR)/181.0
09330            CALL RUNGK(FCTRK,H,XR,0.0,1,181,XJ,YJ)
09340    C
09350    C THIS AND THE FOLLOWING LOOP FIND THE LOCATION OF THE INTERSECTION OF
09360    C THE JET TERMINAL SHOCK WITH THE JET BOUNDARY.
09370            DO 320 I=2,181
09380            IF(XJ(I)*XJ(I)+YJ(I)*YJ(I).GT.RSS) GO TO 330
09390      320   CONTINUE
09400    C
09410      330   XI=XJ(I-1)
09420            YI=YJ(I-1)
09430    C
09440      340   H=H/10.0
09450            CALL RUNGK(FCTRK,H,XI,YI,1,10,XOUT,YOUT)
09460            DO 350 I=1,10
09470            IF(XOUT(I)*XOUT(I)+YOUT(I)*YOUT(I).GT.RSS) GO TO 360
09480      350   CONTINUE
09490      360   IF(I.EQ. 1) GO TO 340
09500            XI=XOUT(I-1)
09510            YI=YOUT(I-1)
09520            IF(H.GT. 1.0E-20) GO TO 390
09530            WRITE (IOUT,388) H
09540            GO TO 900
09550      390   IF(ABS((XI*XI+YI*YI)/RSS -1.0).GT. 5.0E-4) GO TO 340
09560    C
09570    C THE STEP SIZE IS NOW SET SO THAT THE INTERSECTION POINT IS REACHED
09580    C EXACTLY IN AN EVEN NUMBER OF STEPS.
09590            H=(XI-XR)/181.0
09600            CALL RUNGK(FCTRK,H,XR,0.0,1,181,XJ,YJ)
```

```
C TRANSFORMING BACK TO REAL COORDINATES,
      DO 500 I=1,181
      TEMP=XJ(I)
      XJ(I)=RHOA*YJ(I)
  500 YJ(I)=RHOA*TEMP
      X(ND,JEXIT)=XJ(181)
      Y(ND,JEXIT)=YJ(181)
      GO TO 960
C
  900 IERROR=1
  960 RETURN
      END
C
C.....
C
      SUBROUTINE MIXING(XJ,YJ,X1IN,Y1IN,X2IN,Y2IN,IERROR)
C THIS SUBROUTINE CALCULATES THE LOCATION OF THE TWO INTERFACES AND
C THE MASS ENTRAINMENT ALONG THE JET BOUNDARY, THE BLUNTING
C SPHERE AND THE INNER INTERFACE,
C
      COMMON/CONSTS/PI,RUNIV
      COMMON/CONFAC/CONV(10,4),UN(4),IUNIN,IUNOUT
      COMMON/IDENT/IDEAD,INF,JET,JTERM,LAYER,MIX,MJBDY,M1INT,M2INT,
     1 IEXIT,IPITOT,IRATIO,ISTAT,ITOTAL,INFRAT,IPTRAT,JRETRN
      COMMON/JDENT/JBASE,JCENTR,JEXIT,JFACE,JSPHER,JSTAR,
     1 JTERSH,MAX,MERGE,MOD,ND,NPI,NS
      COMMON/AERO/A(10,7),CD,CONC(10),CP(10),CT,EMACH(10),
     1 ENTHAL(10,7),GAMMA(10),P(10,7),Q(10),
     2 RHO(10,7),T(10,7),V(10),WDOT(10,7),WMOL(10)
      COMMON/GEOM/ALPHA,AR(14,14),R(14,14),
     1 THETA(14),X(14,14),Y(14,14),XNU(14)
      DIMENSION COSW(6),DETA(8),DYJ(200),ETA(8),F1(8),F2(8),
     1 VEL(8),XJ(200),X1IN(100),X2IN(100),YJ(200),Y1IN(100),Y2IN(100)
C
  150 FORMAT('0LAYERS DID NOT MERGE WITH THETA=',F12.6,/)
C
      TYPE 12
   12 FORMAT('0ENTERING MIXING')
      IOUT=6
      SINTHS=SIN(THETA(NS))
      COSTHS=COS(THETA(NS))
C
C CALCULATE THE PROPERTIES OF THE MIXTURE IN THE DEAD AIR REGION,
      CP(IDEAD)=CONC(IDEAD)*CP(JET)+(1.0-CONC(IDEAD))*CP(INF)
      WMOL(IDEAD)=1.0/( CONC(IDEAD)/WMOL(JET)+(1.0-CONC(IDEAD))
     1 /WMOL(INF) )
      CVDEAD=CONC(IDEAD)*(CP(JET)-RUNIV/WMOL(JET))
     1 +(1.0-CONC(IDEAD))*(CP(INF)-RUNIV/WMOL(INF))
      GAMMA(IDEAD)=CP(IDEAD)/CVDEAD
      T(IDEAD,ITOTAL)=ENTHAL(IDEAD,1)/CP(IDEAD)
      RHO(IDEAD,ISTAT)=GASRHO(P(IDEAD,ISTAT),WMOL(IDEAD),
     1 T(IDEAD,ITOTAL))
      RHO(IDEAD,INFRAT)=RHO(IDEAD,ISTAT)/RHO(INF,ISTAT)
C
      RHO02=GASRHO(P(INF,IPITOT),WMOL(JET),T(JET,ITOTAL))
      RHO01=GASRHO(P(INF,IPITOT),WMOL(INF),T(INF,ITOTAL))
      ACON=0.10*AR(JSPHER,1)*A(JET,ITOTAL)*SQRT(RHO02*RHO01)
     1 /WDOT(JET,1)
C
      EMD=PMACH(GAMMA(JET),1.0/P(IDEAD,IPTRAT))
```

```
10210           TO=T(JET,ITOTAL)/TRATIO(GAMMA(JET),EMO)
10220           PEROTO=P(IDEAD,ISTAT)*EMO/SQRT(TO)
10230           BCON=0.1E*AR(JSPHER,1)*A(JET,ITOTAL)*SQRT(RHO02
10240         1 *RHO(IDEAD,ISTAT))/WDOT(JET,1)
10250           C2A=AR(JEXIT,JSPHER)*EMACH(JET)*P(JET,IEXIT)
10260         1 /SQRT(T(JET,IEXIT))
10270     C
10280     C MASS ENTRAINMENT ALONG THE JET BOUNDARY.
10290           CO=0.050*SQRT(RHO(IDEAD,ISTAT)/(RHO(JTERM,ISTAT)*TRATIO(
10300         1 GAMMA(JET),EMACH(JTERM))))
10310           V(JTERM)=A(JET,ITOTAL)*EMACH(JTERM)/SQRT(TRATIO(GAMMA(JET),
10320         1 EMACH(JTERM)))
10330           H=YJ(2)-YJ(1)
10340           CALL DERIV(1,101,H,YJ,DYJ)
10350     C DYJ(I) NOW BECOMES THE INTEGRAND.
10360           DO 120 I=1,101
10370       120 DYJ(I)=YJ(I)*SQRT(1.0+DYJ(I)*DYJ(I))/DYJ(I)
10380     C PERFORM THE INTEGRATION FOR THE JET BOUNDARY.
10390           CALL SIMPS(1,101,H,DYJ,0,0,SUM2)
10400           WDOT(MJBDY,1)=2.0*PI*RHO(JTERM,ISTAT)*V(JTERM)*CO*SUM2
10410           WDOT(MJBDY,JET)=WDOT(MJBDY,1)/WDOT(JET,1)
10420     C
10430           I=0
10440           J=0
10450           M=0
10460           MNSW=0
10470     C MNSW BECOMES 1 WHEN M REACHES 5 FOR THE FIRST TIME.
10480         + NSSW=0
10490     C NSSW BECOMES 1 WHEN THET IS GREATER THAN THETA(NS) .
10500           S1IN=0.0
10510           S2IN=0.0
10520           THINC=0.250/CONV(1,IUNIN)
10530     C STEP SIZE = 0.250 DEGREES.
10540           DUMMY=THETA(MAX)
10550           IF(THETA(NS).GT. PI/2.0) DUMMY=PI-2.0*THINC
10560           NMO=THETA(NO)/THINC
10570           NMO=2*((NMO+1)/2)
10580           THINC=THETA(NO)/FLOAT(NMO)
10590     C THIS INSURES THAT THE SUMMATIONS OVER SUBSCRIPTS I AND M TRACK.
10600           H1STP=ACON*THINC
10610           H2STP=BCON*THINC
10620           THET=-THINC
10630     C
10640       150 THET=THET+THINC
10650           IF(THET.LT.DUMMY) GO TO 160
10660     C THE JET MASS FLOW HAS NOT BEEN ENTRAINED EVEN WITH THET=THETA(MAX)
10670     C FURTHER CALCULATIONS ARE NOT POSSIBLE.
10680           ZTHET=THET*CONV(1,IUNIN)
10690           WRITE (IOUT,158) ZTHET
10700           GO TO 900
10710     C
10720       160 I=I+1
10730           J=J+1
10740     C MASS ENTRAINMENT ALONG THE FIRST INTERFACE ONLY.
10750           IF(NSSW.EQ. 1) GO TO 300
10760           IF(THET.GT. PI/2.0) GO TO 200
10770           P1=PFIT(THET,P(INF,IPTRAT))
10780           GO TO 250
10790       200 XNU1=ANU(NPI)+THET-PI/2.0
10800           EM1=XNMACH(GAMMA(INF),XNU1,IERROR)
```

```
10810           IF(IERROR.EQ. 1) GO TO 960
10820           P1=P(INF,IPITOT)/PRATIO(GAMMA(INF),EM1)
10830     230   PTS=P(INF,IPITOT)/P1
10840           P2=P1
10850           EM2=PMACH(GAMMA(JET),PTS)
10860 C MASS ENTRAINMENT ALONG THE BLUNTING SPHERE,
10870           F1(I)=EM2*SIN(THET)/PTS
10880 C
10890           IF(THET.LT.THETA(ND)) GO TO 500
10900           M=M+1
10910           MSW=1
10920           COSW(M)=1.0
10930           T2=T(JET,ITOTAL)/TRATIO(GAMMA(JET),EM2)
10940           VEL(M)=EM2*SQRT(T2)
10950 C CALCULATION OF ETA(M),
10960     250   C2=C2A/((REMOTD*COSW(M)+EM2*P2/SQRT(T2))*SIN(THET))
10970           IF(C2 .GT. 0.50) GO TO 700
10980 C ETA(M) IS THE DISTANCE,NON-DIMENSIONALISED BY THE BLUNTING
10990 C SPHERE RADIUS, BETWEEN THE TWO INTERFACES AND IT IS ALWAYS
11000 C NEGATIVE,
11010           ETA(M)=-1.0+SQRT(1.0-2.0*C2)
11020 C MASS ENTRAINMENT ALONG THE SECOND INTERFACE,
11030           RBAR=(1.0+ETA(M))*SIN(THET)
11040           F2(M)=EM2*RBAR/SQRT(PTS*T(JET,ITOTAL)/T2)
11050           GO TO 350
11060 C
11070     300   M=M+1
11080 C P1,P2 ARE NOW CONSTANT,THEREFORE EM1,EM2,T2 AND C2 ARE ALSO CONSTANT
11090 C AND HAVE THE VALUES WHICH WERE EVALUATED AT THETA(NS),
11100 C
11110           THX=THET-THETA(NS)
11120           ZBAR=TAN(THX)
11130 C MASS ENTRAINMENT ALONG CONICAL PORTION OF THE FIRST INTERFACE,
11140           F1(I)=(SINTHS+ZBAR*COSTHS)/(COS(THX)**2)
11150 C CALCULATION OF ETA(M)
11160           B2=1.0+ZBAR*COSTHS/SINTHS
11170           IF(2.0*C2 .GT. B2*B2) GO TO 700
11180           ETA(M)=-B2+SQRT(B2*B2-2.0*C2)
11190 C MASS ENTRAINMENT ALONG THE SECOND INTERFACE,
11200           RBAR=(1.0+ETA(M))*SINTHS+ZBAR*COSTHS
11210           F2(M)=RBAR
11220 C
11230     350   IF(MNSW.EQ. 1) GO TO 370
11240           IF(M.LT. 5) GO TO 150
11250 C NOW M=5 FOR THE FIRST TIME,
11260           MNSW=1
11270           CALL DERIV(1,5,THINC,ETA,DETA)
11280 C NOW THAT WE HAVE DETA/DTHETA, WE CAN MAKE THE CORRECTION FOR
11290 C COSW(M) NOT EQUAL TO 1.0 . RESET TO THET=THETA(ND) .
11300           I=I-5
11310           M=M-5
11320           THET=THET-5.*THINC
11330           GO TO 150
11340 C
11350     370   GO TO (401,402,402,405,405),M
11360     401   DETA(1)=(-1.50*ETA(1)+2.0*ETA(2)-0.50*ETA(3))/THINC
11370           GO TO 410
11380     402   DETA(M)=0.50*(ETA(M+1)-ETA(M-1))/THINC
11390           GO TO 410
11400     405   DETA(M)=(0.50*ETA(M-2)-2.0*ETA(M-1)+1.50*ETA(M))/THINC
```

```
11410      410   CONTINUE
11420            IF(NSSW.EQ. 1) GO TO 460
11430            IF(MSW.EQ. 1) GO TO 420
11440            TEMP=DETA(M)/(1.0+ETA(M))
11450            COSN(M)=1.0/SQRT(1.0+TEMP*TEMP)
11460            IF(COSN(M).LT. 0.50) COSN(M)=0.50
11470            MSW=1
11480            GO TO 250
11490      C CALCULATE THE INTEGRAND OF THE INNER INTERFACE FOR THET LESS
11500      C THAN THETA(NS) .
11510        420   F2(M)=F2(M)*SQRT((1.0+ETA(M))*(1.0+ETA(M))+DETA(M)*DETA(M))
11520            GO TO 500
11530      C SAME AS ABOVE, BUT FOR THET GREATER THAN THETA(NS) .
11540        460   F2(M)=F2(M)*SQRT( ( ((1.0+ETA(M))/(COS(THX)**2))**2 )
11550           1  +DETA(M)*DETA(M) )
11560      C
11570        500   IF(I.LT. 3) GO TO 150
11580      C PERFORM THE INTEGRATION FOR THE BLUNTING SPHERE.
11590            CALL SIMPS(1,3,H1STP,F1,S1IN,S1OUT)
11600            IF(THET.LT.THETA(ND)) GO TO 580
11610      C
11620            IF(M.EQ. 5) GO TO 520
11630            IF(M.EQ. 3) CALL SIMPS(1,3,H2STP,F2,S2IN,S2OUT)
11640            GO TO 150
11650      C
11660      C PERFORM THE INTEGRATION FOR THE INNER INTERFACE.
11670        520   CALL SIMPS(3,5,H2STP,F2,S2IN,S2OUT)
11680            IF(THET.LT.THETA(NS)) GO TO 540
11690            NSSW=1
11700      C CHANGE OF -STEP SIZE- WHEN THET IS GRETER THAN THETA(NS) .
11710            H1STP=H1STP*EM2/PTS
11720            H2STP=H2STP*EM2/SQRT(PTS*T(JET,ITOTAL)/T2)
11730      C
11740        540   IF(WDOT(MJBDY,JET)+S1OUT+S2OUT.GE. 1.0) GO TO 720
11750      C RESET FOR CONTINUATION OF THE INTEGRATION.
11760            S2IN=S2OUT
11770            DO 560 MJ=1,3
11780            F2(MJ)=F2(MJ+2)
11790            VEL(MJ)=VEL(MJ+2)
11800        560   ETA(MJ)=ETA(MJ+2)
11810            M=3
11820        580   S1IN=S1OUT
11830            F1(1)=F1(3)
11840            I=1
11850      C
11860            IF(J-1 .EQ. 20*((J-1)/20)) GO TO 600
11870            GO TO 150
11880      C
11890      C CALCULATION OF THE INTERFACES LOCATION.
11900        600   K=1+(J-1)/20
11910            IF(THET.GT.THETA(NS)) GO TO 650
11920      C LOCATION OF THE BLUNTING SPHERE.
11930            X1IN(K)=R(JSPHER,JEXIT)*COS(THET)+X(JCENTR,JEXIT)
11940            Y1IN(K)=R(JSPHER,JEXIT)*SIN(THET)
11950      C
11960            IF(THET.LT.THETA(ND)) GO TO 660
11970            GO TO 664
11980      C
11990      C LOCATION OF THE JET TERMINAL SHOCK.
12000        650   PHI=THET-ASIN(X(JCENTR,JTERSH)*SIN(THET))
```

```
      X2IN(K)=X(JTERSH,JEXIT)*COS(PHI)
      Y2IN(K)=X(JTERSH,JEXIT)*SIN(PHI)
      GO TO 150
C
C LOCATION OF THE CONICAL PORTION OF THE FIRST INTERFACE.
  650 X1IN(K)=X(NS,JEXIT)-ZBAR*R(JSPHER,JEXIT)*SINTHS
      Y1IN(K)=Y(NS,JEXIT)+ZBAR*R(JSPHER,JEXIT)*COSTHS
C LOCATION OF THE SECOND INTERFACE.
  660 X2IN(K)=X1IN(K)+ETA(M)*R(JSPHER,JEXIT)*COS(THET)
      Y2IN(K)=Y1IN(K)+ETA(M)*R(JSPHER,JEXIT)*SIN(THET)
      GO TO 150
C
  700 FRAC=0.0
C THE SEPARATION BETWEEN THE TWO INTERFACES HAS VANISHED.
C MASS FLOW ENTRAINMENT IS FORCIBLY STOPPED, BUT PROGRAM CONTINUES.
      GO TO 750
C THE JET MASS FLOW HAS BEEN SUCCESSFULLY ENTRAINED.
  720 FRAC=(1.0-WDOT(MJBDY,JET)-S1IN-S2IN)/(S1OUT+S2OUT-(S1IN+S2IN))
  750 WDOT(M1INT,JET)=S1IN+FRAC*(S1OUT-S1IN)
      WDOT(M1INT,1)=WDOT(M1INT,JET)*WDOT(JET,1)
      WDOT(M2INT,JET)=S2IN+FRAC*(S2OUT-S2IN)
      WDOT(M2INT,1)=WDOT(M2INT,JET)*WDOT(JET,1)
      DVEL=VEL(M)-VEL(M-2)
      V(MIX)=A(JET,ITOTAL)*(VEL(M-2)+FRAC*DVEL)/SQRT(T(JET,ITOTAL))
      THETA(MERGE)=THET-2.0*THIRC*(1.0-FRAC)
C
      ZHX=THETA(MERGE)*CONV(1,IUNIN)
      THY=THETA(MAX)*CONV(1,IUNIN)
      TYPE 67,ZHX,THY
   67 FORMAT(' THETA MERGE,MAX=',2F10.4)
      TYPE 91,WDOT(JET,1),WDOT(MJBDY,JET),WDOT(M1INT,JET),
     1 WDOT(M2INT,JET)
   91 FORMAT(' WDOT JET,JETBDY,1,2=',1P4E13.5,/)
      GO TO 960
  900 IERROR=1
  960 RETURN
      END
C
C.................................................................
C
      SUBROUTINE MERGE0(IERROR)
C THIS SUBROUTINE IS FOR BLUNTING SPHERE DIAMETER LESS THAN
C THE BASE DIAMETER.
C
C THIS SUBROUTINE ,BY CALLING SUBROUTINES -HPCG- AND -FCTSS-,
C PERFORMS THE INTEGRATION OF THE FIVE DIFFERENTIAL EQUATIONS.
C THE STARTING VALUE IS THAT ANGLE AT WHICH THE LAYERS HAVE MERGED,
C AND THE FINAL VALUE IS THAT WHICH JUST GRAZES THE BODY SHOULDER.
C
      COMMON/CONSTS/PI,RUNIV
      COMMON/CONFAC/CONV(10,4),UN(4),IUNIN,IUNOUT
      COMMON/IDENT/IDEAD,INF,JET,JTERM,LAYER,MIX,MJBDY,M1INT,M2INT,
     1 IEXIT,IPITOT,IRATIO,ISTAT,ITOTAL,INFRAT,IPTRAT,JRETRN
      COMMON/JIDENT/JBASE,JCENTR,JEXIT,JFACE,JSPHER,JSTAR,
     1 JTERSH,MAX,MERGE,MOD,NO,NPI,NS
      COMMON/AERO/A(10,7),CD,CONC(10),CP(10),CT,EMACH(10),
     1 ENTHAL(10,7),GAMMA(10),P(10,7),Q(10),
     2 RHO(10,7),T(10,7),V(10),WDOT(10,7),WHOL(10)
      COMMON/GEOM/ALPHA,AR(14,14),R(14,14),
     1 THETA(14),X(14,14),Y(14,14),XSJ(14)
```

```
12010           COMMON/KOUT/NSSWCH,CAPPA,RHOES,UES,XBARI,XK,XLAM,Y0,YSSL
12020           COMMON/ZZINT/ZNT1,ZNT2,ZNT3,ZNT4,XNU,XNU1,YK1,YK2,YK3,YSS(5)
12030           DIMENSION PRMT(6),YSSTAR(5),DERY(5),AUX(16,5)
12040           EXTERNAL FCTSS,OUTP,ENT2D,CON2D,FCTLAM,FCTMU,FCTNU,FCTYSS
12050     C
12060       418 FORMAT('0CONVERGENCE FAILURE, LAMDA=',1PE13.5,'  FCTLAM=',
12070          1 E13.5,'  IER=',I4,/)
12080       438 FORMAT('0CONVERGENCE FAILURE, MU=',1PE13.5,'  FCTMU=',
12090          1 E13.5,'  IER=',I4,/)
12100       458 FORMAT('0CONVERGENCE FAILURE, NU=',1PE13.5,'  FCTNU=',
12110          1 E13.5,'  IER=',I4,/)
12120       478 FORMAT('0CONVERGENCE FAILURE, YSSL=',1PE13.5,'  FCTYSS=',
12130          1 E13.5,'  IER=',I4,/)
12140       898 FORMAT('0ERROR IN INTEGRATION SUBROUTINE, SSTAR=',1PE13.5,
12150          1 '  IHLF=',I4,/)
12160     C
12170           TYPE 12
12180        12 FORMAT(' ENTERING MERGE0')
12190           IOUT=8
12200           NDIM=5
12210           TEMP=1.0/FLOAT(NDIM)
12220     C
12230     C THE FOLLOWING CALL IS NECESSARY BECAUSE THE INITIAL VALUES
12240     C OF YSSTAR ARE CALCULATED IN SUBROUTINE -FCTSS- ,
12250     C NSSWCH IS USED TO STEER -FCTSS- TO CALCULATE INITIAL
12260     C VALUES AND TO SKIP CALCULATIONS FOR THET GREATER THAN THETA(NS),
12270     C
12280     C XBARI IS THE INITIAL VALUE OF THET AT THETA(MERGE), SSTAR IS 0.0
12290           XBARI=THETA(MERGE)
12300           IF(XBARI.GT.THETA(NS)) XBARI=THETA(NS)
12310     C
12320           NSSWCH=1
12330           SSTAR=0.0
12340           CALL FCTSS(SSTAR,YSSTAR,DERY,IERROR)
12350           IF(IERROR.EQ. 1) GO TO 960
12360     C
12370           NSSWCH=2
12380           TYPE 17,(YSSTAR(KK),KK=1,5)
12390           PRMT(1)=0.0
12400           PRMT(2)=THETA(NS)-THETA(MERGE)
12410     C THE STEP SIZE IS SET INITIALLY TO 1.0 DEGREES, HOWEVER,THE
12420     C INTEGRATION SUBROUTINE MAY CHANGE THE STEP SIZE.
12430           PRMT(3)=1.0/CONV(1,IUNIN)
12440           PRMT(4)=1.0E-4
12450     C
12460           IF(THETA(MERGE).LT.THETA(NS)) GO TO 120
12470           XBARI=THETA(NS)+TAN(THETA(MERGE)-THETA(NS))
12480           GO TO 220
12490     C
12500     C YSSTAR(1)=MDOT*=MDOT/(AR(JSPNER,1)*RHO(INF,ISTAT)*V(INF))
12510     C THAT IS =MDOT/MDOT(INF,1)
12520     C YSSTAR(2)=UBAR*=UBAR/V(INF)
12530     C YSSTAR(3)=HBAR*=HBAR/ENTHAL(INF,1)
12540     C YSSTAR(4)=CBAR=CONC
12550     C YSSTAR(5)=MDOTR*=MASS FLOW ENTRAINED FROM THE DEAD AIR REGION
12560     C FROM THE MERGING POINT TO THE END OF THE INTEGRATION NORMALIZED
12570     C BY MDOT(INF,1) .
12580     C
12590       121 DO 130 I=1,NDIM
12600       130 DERY(I)=TEMP
```

```
C INTEGRATION FROM THETA(MERGE) TO THETA(NS),WITH SSTAR AS THE
C RUNNING VARIABLE,
      CALL HPCG(PRMT,YSSTAR,DERY,NDIM,IHLF,FCTSS,OUTP,AUX,IERROR)
      IF(IHLF.GT. 10) GO TO 900
C
C INTEGRATION FROM THETA(NS) TO THETA(MAX), IF THETA(MERGE) IS
C GREATER THAN THETA(NS), THE INTEGRATION IS FROM THETA(MERGE)
C TO THETA(NS) ONLY AND THE INITIAL VALUES ARE CALCULATED AT
C THETA(NS),
C
C RESET LOWER LIMIT OF INTEGRATION TO THETA(NS),
      PRMT(1)=PRMT(2)
  220 ASSIGN=3
      DO 230 I=1,NDIM
  230 DERY(I)=TEMP
      PRMT(2)=THETA(NS)+TAN(THETA(MAX)-THETA(NS))-XBAR)
      CALL HPCG(PRMT,YSSTAR,DERY,NDIM,IHLF,FCTSS,OUTP,AUX,IERROR)
      IF(IHLF.GT. 10) GO TO 900
C
C THE INTEGRATION IS NOW FINISHED, PROCEED TO CALCULATE THE
C THREE PROFILE PARAMETERS, LAMDA(XLAM), MU(XMU) AND NU(XNU1),
C
      DO 400 I=1,NDIM
  400 YSS(I)=YSSTAR(I)
C
C FIND LAMDA BY AN ITERATIVE PROCEDURE,
      CALL PGEN(XLAM,VAL,FCTLAM,0.50,1.0,1.0E-6,100,IER)
      IF(IER.EQ. 0) GO TO 420
      WRITE (IOUT,418) XLAM,VAL,IER
      GO TO 930
C
C FIND MU BY AN ITERATIVE PROCEDURE,
  420 CALL PGEN(XMU,VAL,FCTMU,0.0,0.50,1.0E-6,100,IER)
      IF(IER.EQ. 0) GO TO 440
      WRITE (IOUT,438) XMU,VAL,IER
      GO TO 930
C
C FIND NU BY AN ITERATIVE PROCEDURE,
  440 CALL PGEN(XNU1,VAL,FCTNU,0.0,0.50,1.0E-6,100,IER)
      IF(IER.EQ. 0) GO TO 460
      WRITE (IOUT,458) XNU1,VAL,IER
      GO TO 930
C
  460 CONTINUE
      TYPE 16,XLAM,XMU,XNU1
   16 FORMAT(' LAMDA,MU,NU=',1P3E13.5)
      TYPE 17,(YSSTAR(KK),KK=1,5)
   17 FORMAT(' Y*=',1P5E13.5)
C THE TOTAL ENTRAINED AND THE RECIRCULATED MASS FLOW IS NOW MADE
C DIMENSIONAL ONCE AGAIN,
      YSSTAR(1)=YSSTAR(1)*WDOT(INF,1)
      YSS(1)=YSSTAR(1)
      YSSTAR(5)=YSSTAR(5)*WDOT(INF,1)
      YSS(5)=YSSTAR(5)
C
C CALCULATE THE MASS RETURNED TO THE DEAD AIR REGION,
      WDOT(JRETRN,1)=WDOT(MJBODY,1)+WDOT(M2INF,1)+YSSTAR(5)
C
C FIND THE SEPARATION STREAMLINE BY AN ITERATIVE PROCEDURE,
      CALL PGEN(YSSL,VAL,FCTYSS,0.0,0.0,1.0E-6,100,IER)
```

```
13810            IF(IER.EQ. 0) GO TO 500
13820            WRITE (IOUT,498) YSSL,VAL,IER
13830            GO TO 930
13840    C
13850    C CALCULATE THE MERGED ENTHALPY,
13860      500   CALL WGB(-Y0,YSSL,ENT20,ZNT3)
13870            ENTHAL(IDEAD,INF)=ZNT3/ZNT2
13880            ENTHAL(IDEAD,1)=ENTHAL(IDEAD,INF)*ENTHAL(INF,1)
13890    C
13900            TYPE 81,YSSL
13910       81   FORMAT(' YSSL=',1PE13.5)
13920    C
13930    C CALCULATE THE MERGED CONCENTRATION,
13940            CALL WGB(-Y0,YSSL,CON20,ZNT4)
13950            CONC(IDEAD)=ZNT4/ZNT2
13960            TYPE 15,ENTHAL(IDEAD,1),CONC(IDEAD)
13970       15   FORMAT(' H,CONC ',1P2E13.4)
13980    C
13990            GO TO 960
14000      900   WRITE (IOUT,898) PRMT(6),IHLF
14010      930   IERROR=1
14020      960   RETURN
14030            END
14040    C
14050    C.....
14060    C
14070            SUBROUTINE MERGE2(IERROR)
14080    C THIS SUBROUTINE IS FOR BLUNTING SPHERE DIAMETER GREATER THAN
14090    C THE BASE DIAMETER,
14100    C
14110    C THIS SUBROUTINE ,BY CALLING SUBROUTINES -HPCG- AND -FCTSS-,
14120    C PERFORMS THE INTEGRATION OF THE FIVE DIFFERENTIAL EQUATIONS,
14130    C THE STARTING VALUE IS THAT ANGLE AT WHICH THE LAYERS HAVE MERGED,
14140    C AND THE FINAL VALUE, WHICH PRESUMABLY OCCURRS FOR THETA LESS THAN PI,
14150    C IS DETERMINED IN SUBROUTINE -OUTP- BY COMPARISON OF TWO DIFFERENTLY
14160    C CALCULATED VALUES OF PHYSICAL LENGTHS,
14170    C
14180            COMMON/CONSTS/PI,RUNIV
14190            COMMON/CONFAC/CONV(10,4),UN(4),IUNIN,IUNOUT
14200            COMMON/IDENT/IDEAD,INF,JET,JTERM,LAYER,MIX,MJBDY,M1INT,M2INT,
14210         1  IEXIT,IPITOT,IRATIO,ISTAT,ITOTAL,INFRAT,IPTRAT,JRETRN
14220            COMMON/JDENT/JBASE,JCENTR,JEXIT,JFACE,JSPHER,JSTAR,
14230         1  JTERSH,MAX,MERGE,MOD,ND,NMI,NS
14240            COMMON/AERO/A(10,7),CD,CONC(10),CP(10),CT,EMACH(10),
14250         1  ENTHAL(10,7),GAMMA(10),P(10,7),Q(10),
14260         2  RHO(10,7),T(10,7),V(10),WDOT(10,7),WMOL(10)
14270            COMMON/GEOM/ALPHA,AR(14,14),R(14,14),
14280         1  THETA(14),X(14,14),Y(14,14),XNU(14)
14290            COMMON/ROOT/ASSOCH,CAPPA,RHOES,UES,XBAR1,XK,XLAM,R0,RSSL
14300            COMMON/ZZINT/ZNT1,ZNT2,ZNT3,ZNT4,XNU,XNU1,YK1,YK2,YK3,YSS(5)
14310            DIMENSION PRMT(6),YSSTAR(5),DERY(5),AUX(16,5)
14320            EXTERNAL FCTSS,OUTP,ENT3D,CON3D
14330    C
14340      898   FORMAT('0ERROR IN INTEGRATION SUBROUTINE, SSTAR=',1PE13.5,
14350         1  ' IHLF=',I4,/)
14360    C
14370            TYPE 12
14380       12   FORMAT(' ENTERING MERGE2')
14390            IOUT=6
14400            NUM=5
```

```
14410            TEMP=1.0/FLOAT(NDIM)
14420    C
14430    C THE FOLLOWING CALL IS NECESSARY BECAUSE THE INITIAL VALUES
14440    C OF YSSTAR ARE CALCULATED IN SUBROUTINE -FCTSS- ,
14450    C NSSWCH IS USED TO STEER -FCTSS- TO CALCULATE INITIAL
14460    C VALUES AND TO SKIP CALCULATIONS FOR THET GREATER THAN THETA(NS).
14470    C
14480    C XBAR1 IS THE INITIAL VALUE OF THET AT THETA(MERGE), SSTAR IS 0.0
14490            XBAR1=THETA(MERGE)
14500            IF(XBAR1.GT.THETA(NS)) XBAR1=THETA(NS)
14510    C
14520            NSSWCH=1
14530            SSTAR=0.0
14540            CALL FCTSS(SSTAR,YSSTAR,DERY,IERROR)
14550            IF(IERROR.EQ. 1) GO TO 960
14560    C
14570            NSSWCH=2
14580            TYPE 47,(YSSTAR(KK),KK=1,5)
14590            PRMT(1)=0.0
14600            PRMT(2)=PI/2.0-THETA(MERGE)
14610    C THE STEP SIZE IS SET INITIALLY TO 1.0 DEGREES, HOWEVER,THE
14620    C INTEGRATION SUBROUTINE MAY CHANGE THE STEP SIZE.
14630            PRMT(3)=1.0/CONV(1,IUNIN)
14640            PRMT(4)=1.0E-4
14650    C
14660            IF(THETA(MERGE).LT. PI/2.0) GO TO 120
14670            IF(THETA(MERGE).LT.THETA(NS)) GO TO 220
14680            XBAR1=THETA(NS)*TAN(THETA(MERGE)-THETA(NS))
14690            GO TO 320
14700    C
14710    C YSSTAR(1)=MDOT*=MDOT/(AR(JSPHER,1)*RHO(INF,ISTAT)*V(INF))
14720    C THAT IS =MDOT/WDOT(INF,1)
14730    C YSSTAR(2)=UBAR*=UBAR/V(INF)
14740    C YSSTAR(3)=HBAR*=HBAR/ENTHAL(INF,1)
14750    C YSSTAR(4)=CBAR=CONC
14760    C YSSTAR(5)=MDOTR*=MASS FLOW ENTRAINED FROM THE DEAD AIR REGION
14770    C FROM THE MERGING POINT TO THE END OF THE INTEGRATION NORMALIZED
14780    C BY WDOT(INF,1) .
14790    C
14800      120   DO 130 I=1,NDIM
14810      130   DERY(I)=TEMP
14820    C INTEGRATION FROM THETA(MERGE) TO PI/2.0
14830            CALL HPCG(PRMT,YSSTAR,DERY,NDIM,IHLF,FCTSS,OUTP,AUX,IERROR)
14840            IF(IHLF.GT. 10) GO TO 900
14850    C
14860            PRMT(1)=PRMT(2)
14870      220   DO 230 I=1,NDIM
14880      230   DERY(I)=TEMP
14890            PRMT(2)=THETA(NS)-THETA(MERGE)
14900    C INTEGRATION FROM PI/2 TO THETA(NS)
14910            CALL HPCG(PRMT,YSSTAR,DERY,NDIM,IHLF,FCTSS,OUTP,AUX,IERROR)
14920            IF(IHLF.GT. 10) GO TO 900
14930    C
14940            PRMT(1)=PRMT(2)
14950      320   NSSWCH=0
14960            DO 330 I=1,NDIM
14970      330   DERY(I)=TEMP
14980            PRMT(2)=THETA(NS)+TAN(PI-2.0*PRMT(3)-THETA(NS))-XBAR1
14990    C INTEGRATION FROM THETA(NS) TO THE INTEGRATION LIMIT, WHICH IS
15000    C FOUND FROM THE MATCHING OF PHYSICAL LENGTHS, BUT CAN BE NEARLY
```

```
C AS LARGE AS PI,
      CALL HPCG(PRMT,YSSTAR,DERY,NDIM,IHLF,FCTSS,OUTP,AUX,IERROR)
      IF(IHLF.GT. 10) GO TO 900
C
C THE INTEGRATION IS NOW FINISHED, THE PROFILE PARAMETERS LAMDA(XLAM), ,
C MU(XMU), AND NU(XNU1)  AND KAPPA WERE EVALUATED IN SUBROUTINE
C -OUTP- IN ORDER TO TERMINATE THE INTEGRATION PROCESS,
C
      TYPE 16,RSSL,XLAM,XMU,XNU1
   16 FORMAT(' RSSL,LAMDA,MU,NU=',1P4E12.5)
      TYPE 17,(YSSTAR(KK),KK=1,5)
   17 FORMAT(' Y*=',1P5E13.5)
C
C CALCULATE THE MERGED ENTHALPY,
      CALL QG8(0,0,RSSL,ENTSD,ZNT3)
      ENTHAL(IDEAD,INF)=ZNT3/ZNT2
      ENTHAL(IDEAD,1)=ENTHAL(IDEAD,INF)*ENTHAL(INF,1)
C
C CALCULATE THE MERGED CONCENTRATION,
      CALL QG8(0,0,RSSL,CONSD,ZNT4)
      CONC(IDEAD)=ZNT4/ZNT2
C
      TYPE 15,ENTHAL(IDEAD,1),CONC(IDEAD)
   15 FORMAT(' H,CONC ',1P2E13.4)
      GO TO 960
  900 WRITE (IOUT,698) PRMT(6),IHLF
      IERROR=1
  960 RETURN
      END
C
C.....
C
      SUBROUTINE OUTPUT
C CONVERTS INTERNAL INFORMATION TO THE PROPER SYSTEM OF UNITS
C AND OUTPUTS IT,
C
      COMMON/CONSTS/PI,RUNIV
      COMMON/CONFAC/CONV(14,4),UN(4),IUNIN,IUNOUT
      COMMON/IDENT/IDEAD,INF,JET,JTERM,LAYER,MIX,MJBOY,M1INT,M2INT,
     1 IEXIT,IPITOT,IRATIO,ISTAT,ITOTAL,INFRAT,IPIRAT,JRETRN
      COMMON/JDENT/JBASE,JCENTR,JEXIT,JFACE,JSPHER,JSTAR,
     1 JTERSH,MAX,MERGE,MOD,ND,NPI,NS
      COMMON/PAGE/DAT(4)
      COMMON/AERO/A(12,7),CD,CONC(14),CP(10),CT,EMACH(10),
     1 ENTHAL(10,7),GAMMA(10),P(10,7),Q(10),
     2 RHO(10,7),T(10,7),V(10),WDOT(10,7),WMOL(10)
      COMMON/GEOM/ALPHA,AR(14,14),R(14,14),
     1 THETA(14),X(14,14),Y(14,14),XNU(14)
C
      IOUT=6
      WRITE (IOUT,12)
   12 FORMAT(' ENTERING OUTPUT,',/)
      RETURN
      END
C
C.....
C
      FUNCTION COTAN(Z)
C CALCULATES THE COTANGENT OF Z ( Z IN RADIANS),
C
```

```
15610           COTAN=COS(Z)/SIN(Z)
15620           RETURN
15630           END
15640   C
15650   C.....
15660   C
15670           FUNCTION TAN(Z)
15680   C CALCULATES THE TANGENT OF Z ( Z IN RADIANS).
15690   C
15700           TAN=SIN(Z)/COS(Z)
15710           RETURN
15720           END
15730   C
15740   C.....
15750   C
15760           FUNCTION ERF(Z)
15770   C CALCULATES THE ERROR FUNCTION OF Z .
15780   C
15790           X=ABS(Z)
15800           IF(X.LT.4.17) GO TO 100
15810           ERF=1.0
15820           GO TO 200
15830     100   T=1.0/(1.0+0.3275911*X)
15840           ERF=0.254829592+T*(-0.284496736+T*(1.421413741+T
15850        1  *(-1.453152027+1.061405429*T)))
15860           ERF=1.0-EXP(-X*X)*T*ERF
15870     200   ERF=SIGN(ERF,Z)
15880           RETURN
15890           END
15900   C
15910   C.....
15920   C
15930           FUNCTION TRATIO(GAM,EMACH)
15940   C CALCULATES THE ADIABATIC TOTAL TO STATIC TEMPERATURE RATIO.
15950   C
15960           TRATIO=1.0+(GAM-1.0)/2.0*EMACH*EMACH
15970           RETURN
15980           END
15990   C
16000   C.....
16010   C
16020           FUNCTION PRATIO(GAM,EMACH)
16030   C CALCULATES THE ISENTROPIC TOTAL TO STATIC PRESSURE RATIO.
16040   C
16050           PRATIO=TRATIO(GAM,EMACH)**(GAM/(GAM-1.0))
16060           RETURN
16070           END
16080   C
16090   C.....
16100   C
16110           FUNCTION RHORAT(GAM,EMACH)
16120   C CALCULATES THE ISENTROPIC TOTAL TO STATIC DENSITY RATIO.
16130   C
16140           RHORAT=TRATIO(GAM,EMACH)**(1.0/(GAM-1.0))
16150           RETURN
16160           END
16170   C
16180   C.....
16190   C
16200           FUNCTION PPITOT(GAM,EMACH)
```

```
C RALEIGH PITOT FORMULA, CALCULATES THE RATIO OF THE TOTAL PRESSURE
C BEHIND A NORMAL SHOCK TO THE UPSTREAM STATIC PRESSURE.
C
      IF(EMACH.GT. 1.0) GO TO 100
      PPITOT=PRATIO(GAM,EMACH)
      RETURN
  100 GMP=GAM+1.0
      GMN=GAM-1.0
      SQM=EMACH*EMACH
      PPITOT=((GMP*SQM/2.0)**(GAM/GMN))*((GMP/(2.0*GAM*SQM-GMN))
     1 **(1.0/GMN))
      RETURN
      END
C
C.....
C
      FUNCTION ARATIO(GAM,EMACH)
C CALCULATES THE ISENTROPIC STREAM TUBE AREA-RATIO A/A*.
C
      GMP=(GAM+1.0)/2.0
      GMN=GAM-1.0
      ARATIO=((1.0+GMN/2.0*EMACH*EMACH)/GMP)**(GMP/GMN)/EMACH
      RETURN
      END
C
C.....
C
      FUNCTION PRNU(GAM,EMACH,IERROR)
C CALCULATES THE PRANDTL-MEYER TURNING ANGLE (NU).
C
   98 FORMAT(34H0THE PRANDTL-MEYER FUNCTION IS NOT,
     1 21H SPECIFIED FOR MACH =,1PE12.4,/)
C
      IOUT=6
      IF(EMACH.LT. 1.0) GO TO 100
      GO TO 200
  100 WRITE (IOUT,98) EMACH
      IERROR=1
      RETURN
  200 GM=SQRT((GAM+1.0)/(GAM-1.0))
      PRNU=GM*ATAN(SQRT(EMACH*EMACH-1.0)/GM)-ACOS(1.0/EMACH)
      RETURN
      END
C
C.....
C
      FUNCTION VASTAR(GAM,EMACH)
C CALCULATES THE FUNCTION V/A*.
C
      VASTAR=EMACH*SQRT((GAM+1.0)/(2.0+(GAM-1.0)*EMACH*EMACH))
      RETURN
      END
C
C.....
C
      FUNCTION AMACH(GAM,AR,MSW,IERROR)
C CALCULATES BY ITERATION THE MACH NO. FOR A GIVEN A/A*.
C MSW=0 SUBSONIC, MSW=1 SUPERSONIC.
C
      COMMON/FCTA1/GAMMA,AREA,XX
```

```
      EXTERNAL FCTAM
C
  296 FORMAT('0CONVERGENCE FAILURE (MACH NO, FROM AREA RATIO),',
     1 ' MACH NO,=',1PE12.4,'  FCTAM=',E12.4,'  IER=',I4,/)
C
      IOUT=6
      EM1=1.0
      IF(MSW.EQ. 1) GO TO 120
      DELM=-0.20
      GO TO 160
  120 DELM=1.5
  160 EM2=EM1+DELM
      AR2=ARATIO(GAM,EM2)
      IF(AR2 .GT.AR) GO TO 200
      EM1=EM2
      IF(EM1 .LT. 0.21) DELM=DELM/2.0
      GO TO 160
  200 GAMMA=GAM
      AREA=AR
      CALL PGEW(EMACH,VAL,FCTAM,EM1,EM2,1.0E-6,100,IER)
      IF(IER.EQ. 0) GO TO 300
      WRITE (IOUT,298) EMACH,VAL,IER
      IERROR=1
      RETURN
  300 AMACH=EMACH
      RETURN
      END
C
C.....
C
      FUNCTION FCTAM(EMACH)
C THIS FUNCTION IS CALLED BY FUNCTION  -AMACH- ,VIA SUBROUTINE
C -PGEW- , TO ITERATIVELY FIND THE MACH NO. FROM THE GIVEN
C AREA RATIO (A/A*).
C
      COMMON/FCTA1/GAM,AR,XX
C
      FCTAM=ARATIO(GAM,EMACH)/AR-1.0
      RETURN
      END
C
C.....
C
      FUNCTION RMMACH(GAM,RHOTS)
C CALCULATES THE MACH NO, FROM THE ISENTROPIC TOTAL TO STATIC
C DENSITY RATIO.
C
      RMMACH=SQRT(2.0/(GAM-1.0)*((RHOTS**(GAM-1.0))-1.0))
      RETURN
      END
C
C.....
C
      FUNCTION PMACH(GAM,PTS)
C CALCULATES THE MACH NO, FROM THE ISENTROPIC TOTAL TO STATIC
C PRESSURE RATIO.
C
      PMACH=SQRT(2.0/(GAM-1.0)*((PTS**((GAM-1.0)/GAM))-1.0))
      RETURN
      END
```

```
C
C.....
C
      FUNCTION XNMACH(GAM,XNU,IERROR)
C CALCULATES BY ITERATION THE MACH NO. FROM THE PRANDTL-MAYER
C ISENTROPIC EXPANSION ANGLE NU.
C
      COMMON/CONSTS/PI,RUNIV
      COMMON/CONFAC/CONV(12,4),UN(4),IUNIN,IUNOUT
      COMMON/FCTA1/GAMMA,XNUX,XX
      EXTERNAL FCTXM
C
  118 FORMAT('0THE PRANDTL-MEYER TURNING ANGLE,NU=',1PE12.4,
     1 ' IS GREATER THAN 90.0 DEGREES.',/)
  148 FORMAT('0THE PRANDTL-MEYER TURNING ANGLE,NU=',1PE12.4,
     1 ' IS LESS THAN 0.0 DEGREES.',/)
  595 FORMAT('0CONVERGENCE FAILURE (MACH NO. FROM ANGLE NU).',
     1 ' MACH NO.=',1PE12.4,'  FCTXM=',E12.4,'  IER=',I4,/)
C
C     XNUMAX=(SQRT((GAM+1.0)/(GAM-1.0))-1.0)*PI/2.0
C
      IOUT=8
      IF(XNU.LT.PI/2.0) GO TO 120
      ZXNU=XNU*CONV(1,IUNIN)
      WRITE (IOUT,118) ZXNU
      GO TO 500
  120 IF(XNU.GT. 0.0) GO TO 150
      ZXNU=XNU*CONV(1,IUNIN)
      WRITE (IOUT,148) ZXNU
      GO TO 500
  150 EM1=1.0
      DELM=1.5
  200 EM2=EM1+DELM
      XNU1=PMNU(GAM,EM2,IERROR)
      IF(IERROR.EQ. 1) GO TO 600
      IF(XNU1 .GT.XNU) GO TO 300
      EM1=EM2
      GO TO 200
  300 GAMMA=GAM
      XNUX=XNU
      CALL PGEN(EMACH,VAL,FCTXM,EM1,EM2,1.0E-6,100,IER)
      IF(IER.EQ. 0) GO TO 400
      WRITE (IOUT,395) EMACH,VAL,IER
      GO TO 500
  400 XNMACH=EMACH
      GO TO 600
  500 IERROR=1
  600 RETURN
      END
C
C.....
C
      FUNCTION FCTXM(EMACH)
C THIS FUNCTION IS CALLED BY FUNCTION -XNMACH- ,VIA SUBROUTINE
C -PGEN- , TO ITERATIVELY FIND THE MACH NO. FROM THE GIVEN
C PRANDTL-MEYER ANGLE NU(XNU).
C
      COMMON/FCTA1/GAM,XNU,XX
C
  100 FORMAT('0THE ERROR IN THE PRANDTL-MEYER FUNCTION',
```

```
     1  ' WAS NOT TRANSMITTED, OUTPUT IS PROBALY NONSENSE',/)
C
        IOUT=8
        FCTXM=PMNU(GAM,EMACH,IERR)/XNU-1.0
        IF(IERR.EQ. 1) WRITE (IOUT,100)
        RETURN
        END
C
C.......................................................................
C
        FUNCTION WAVE(GAM,EMACH,ALF,IERROR)
C CALCULATES BY ITERATION THE TWO DIMENSIONAL OBLIQUE SHOCK WAVE
C ANGLE FROM THE MACH NO. AND WEDGE ANGLE.
C
        COMMON/CONFAC/CONV(10,4),UN(4),IUNIN,IUNOUT
        COMMON/FCTA1/GAMMA,EMX,ALPHA
        EXTERNAL FCTWV
C
  118   FORMAT('0THE OBLIQUE SHOCK-WAVE ANGLE IS NOT DEFINED FOR',
     1  ' MACH NO.=',1PE12.4,/)
  198   FORMAT('0CALCULATION FAILURE. THE OBLIQUE SHOCK WAVE ANGLE',
     1  1PE12.4,' IS GREATER THAN THE MAX. ANGLE=',E12.4,/)
  398   FORMAT('0CONVERGENCE FAILURE (WAVE ANGLE FROM MACH NO.).',
     1  ' WAVE ANGLE=',1PE12.4,'  FCTWV=',E12.4,'  IER=',I4,/)
C
        IOUT=8
        IF(EMACH.GT. 1.0) GO TO 120
        WRITE (IOUT,118) EMACH
        GO TO 500
  120   BET1=ASIN(1.0/EMACH)
C BET1 IS THE WAVE ANGLE FOR ZERO WEDGE ANGLE.
        GMP=GAM+1.0
        EMSQ=EMACH*EMACH
        SBAMAX=(GMP*EMSQ-4.0+SQRT(GMP)*SQRT(GMP*EMSQ*EMSQ
     1  +8.0*(GAM-1.0)*EMSQ+16.0))/(4.0*GAM*EMSQ)
        BAMAX=ASIN(SQRT(SBAMAX))
C BAMAX IS THE WAVE ANGLE FOR MAXIMUM WEDGE ANGLE AT THIS MACH NO.
        DELB=(BAMAX-BET1)/5.0
        DELX=1.10*DELB
  150   BET2=BET1+DELB
        IF(BET2 .GT.BAMAX-DELX) DELB=DELB/1.99
        IF(BET2 .LT.BAMAX) GO TO 200
        ZBET2=BET2*CONV(1,IUNIN)
        ZBAMAX=BAMAX*CONV(1,IUNIN)
        WRITE (IOUT,198) ZBET2,ZBAMAX
        GO TO 500
  200   EMSS=EMSQ*SIN(BET2)*SIN(BET2)
        TANB=TAN(BET2-ALF)*GMP*EMSS/((GAM-1.0)*EMSS+2.0)
        IF(TANB.GT.TAN(BET2)) GO TO 300
        BET1=BET2
        GO TO 150
  300   GAMMA=GAM
        EMX=EMACH
        ALPHA=ALF
        CALL PGEA(BETA,VAL,FCTWV,BET1,BET2,1.0E-6,100,IER)
        IF(IER.EQ. 0) GO TO 400
        ZBETA=BETA*CONV(1,IUNIN)
        WRITE (IOUT,398) ZBETA,VAL,IER
        GO TO 500
  400   WAVE=BETA
```

```
18610            GO TO 600
18620      500   IERROR=1
18630      600   RETURN
18640            END
18650      C
18660      C.....................................................................
18670      C
18680            FUNCTION FCTNV(BETA)
18690      C THIS FUNCTION IS CALLED BY FUNCTION  -WAVE- ,VIA SUBROUTINE
18700      C -PGEN- , TO ITERATIVELY FIND THE OBLIQUE SHOCK WAVE ANGLE
18710      C FROM THE GIVEN MACH NO, AND WEDGE ANGLE,
18720      C
18730            COMMON/FCTA1/GAM,EMACH,ALF
18740      C
18750            GMP=GAM+1.0
18760            EMSQ=EMACH*SIN(BETA)
18770            EMSQ=EMSQ*EMSQ
18780      C
18790            TANB=TAN(BETA-ALF)*GMP*EMSQ/((GAM-1.0)*EMSQ+2.0)
18800            FCTNV=TANB/TAN(BETA)-1.0
18810            RETURN
18820            END
18830      C
18840      C.....................................................................
18850      C
18860            FUNCTION CFMAX(GAM)
18870      C CALCULATES THE MAXIMUM VACUUM THRUST COEFFICENT, CF.
18880      C
18890            CFMAX=(2.0*GAM)/SQRT(GAM*GAM-1.0)
18900           1  *( (2.0/(GAM+1.0))**(1.0/(GAM-1.0)) )
18910            RETURN
18920            END
18930      C
18940      C.....................................................................
18950      C
18960            FUNCTION CFVAC(GAM,ARAT,PRAT,IERROR)
18970      C CALCULATES THE VACUUM THRUST COEFFICIENT CF, AND THE NOZZLE
18980      C EXIT TO TOTAL PRESSURE RATIO,
18990      C
19000            GMP=GAM+1.0
19010            GMN=GAM-1.0
19020            EM=AMACH(GAM,ARAT,1,IERROR)
19030            PRAT=1.0/PRATIO(GAM,EM)
19040            CFVAC=SQRT((2.0*GAM*GAM/GMN)*((2.0/GMP)**(GMP/GMN))*(1.0-(PRAT
19050           1  **(GMN/GAM))))+ARAT*PRAT
19060            RETURN
19070            END
19080      C
19090      C.....................................................................
19100      C
19110            FUNCTION PFIT(THET,PRAT)
19120      C CALCULATES THE LOCAL STATIC PRESSURE ON A BODY AT AN ANGLE THET
19130      C TO THE FREE STREAM BY A MODIFIED NEWTONIAN EQUATION.
19140      C P(INF,PITOT) IS THE PITOT PRESSURE, THAT IS THE TOTAL FREE STREAM
19150      C PRESSURE BEHIND A NORMAL SHOCK AT MACH(INF),
19160      C
19170            COMMON/CONSTS/PI,RUNIV
19180            COMMON/IDENT/IDEAD,INF,JET,JTERM,LAYER,MIX,MJBODY,M1INT,M2INT,
19190           1  IEXIT,IPITOT,IRATIO,ISTAT,ITOTAL,INFRAT,IPTRAT,JRETRN
19200            COMMON/AERO/A(10,7),CD,CDMC(10),CP(10),CT,EMACH(10),
```

```
19210          1  ENTHAL(10,7),GAMMA(10),P(10,7),Q(10),
19220          2  RHO(10,7),T(10,7),V(10),MOOT(10,7),WMOL(10)
19230      C
19240              IF(EMACH(INF).GT. 1.50) GO TO 40
19250              EM=PI*EMACH(INF)/2.0
19260              PRIT=(COS(THET)**2)+(SIN(THET)**2)*((COS(EM)**2)*0.380
19270          1  *(SIN(EM)**2))
19280              GO TO 50
19290         40   PRIT=(COS(THET)**2)+(SIN(THET)**2)*PRAT
19300         50   PRIT=PRIT*P(INF,IPITOT)
19310              RETURN
19320              END
19330      C
19340      C.....
19350      C
19360              FUNCTION GASRHO(P,WMOL,T)
19370      C CALCULATES THE GAS DENSITY FROM THE PERFECT GAS LAW.
19380      C
19390              COMMON/CONSTS/PI,RUNIV
19400      C
19410              GASRHO=P*WMOL/(RUNIV*T)
19420              RETURN
19430              END
19440      C
19450      C.....
19460      C
19470              FUNCTION SOUND(GAMMA,WMOL,T)
19480      C CALCULATES THE SOUND SPEED FOR A PERFECT GAS.
19490      C
19500              COMMON/CONSTS/PI,RUNIV
19510      C
19520              SOUND=SQRT(GAMMA*RUNIV*T/WMOL)
19530              RETURN
19540              END
19550      C
19560      C.....
19570      C
19580              FUNCTION FCTRK(X,Y)
19590      C THIS FUNCTION CALCULATES THE RIGHT HAND SIDE OF THE DY/DX
19600      C EQUATION. IT IS CALLED BY SUBROUTINE -RUNGK- .
19610      C
19620              COMMON/FCTA1/PHI,XX,YY
19630      C
19640              FCTRK=COTAN(PHI*(1.0-X*X))
19650              RETURN
19660              END
19670      C
19680      C.....
19690      C
19700              FUNCTION FCTPJ(RHOTRY)
19710      C THIS FUNCTION, SET UP IN THE FORM FCT(X)=0.0 , IS USED BY SUBROUTINE
19720      C -PGEN- ,WHICH ITERATIVELY FINDS THAT VALUE OF
19730      C CENTERLINE DENSITY, WHICH WILL RESULT IN MATCHING OF THE
19740      C JET PITOT PRESSURE WITH THE FREE STREAM PITOT PRESSURE.
19750      C
19760              COMMON/IDENT/IDEAD,INF,JET,JTERM,LAYER,MIX,MJBOY,M1INT,M2INT,
19770          1  IEXIT,IPITOT,IRATIO,ISTAT,ITOTAL,INFRAT,IPTRAT,JRETRN
19780              COMMON/AERO/A(10,7),CD,CONC(10),CP(10),CT,EMACH(10),
19790          1  ENTHAL(10,7),GAMMA(10),P(10,7),Q(10),
19800          2  RHO(10,7),T(10,7),V(10),MOOT(10,7),WMOL(10)
```

```
19810     C
19820           RHO(JTERM,ISTAT)=RHOTRY
19830           RHO(JTERM,IRATIO)=RHO(JET,ITOTAL)/RHO(JTERM,ISTAT)
19840           EMACH(JTERM)=RHMACH(GAMMA(JET),RHO(JTERM,IRATIO))
19850           P(JTERM,ISTAT)=P(JET,ITOTAL)/PRATIO(GAMMA(JET),EMACH(JTERM))
19860           P(JTERM,IPITOT)=P(JTERM,ISTAT)*PPITOT(GAMMA(JET),EMACH(JTERM))
19870           FCTPJ=P(JTERM,IPITOT)/P(INF,IPITOT)-1.0
19880           RETURN
19890           END
19900     C
19910     C.....
19920     C
19930           FUNCTION FCTCN(EMX)
19940     C THIS FUNCTION, SET UP IN THE FORM FCT(X)=0.0 , IS USED BY SUBROUTINE
19950     C -PGEW- ,WHICH ITERATIVELY FINDS THAT VALUE OF THETA(ND),
19960     C WHICH MAKES THE STATIC PRESSURE ON THE BLUNTING SPHERE EQUAL TO THE
19970     C STATIC PRESSURE AT THE INTERSECTION OF THE JET TERMINAL SHOCK WITH
19980     C THE JET BOUNDARY,
19990     C
20000           COMMON/CONSTS/PI,RUNIV
20010           COMMON/IDENT/IDEAD,INF,JET,JTERM,LAYER,MIX,MJBDY,M1INT,M2INT,
20020          1  IEXIT,IPITOT,IRATIO,ISTAT,ITOTAL,INFRAT,IPTRAT,JRETRN
20030           COMMON/JDENT/JBASE,JCENTR,JEXIT,JFACE,JSPHER,JSTAR,
20040          1  JTERSH,MAX,MERGE,MOD,ND,NPI,NS
20050           COMMON/AERO/A(10,7),CD,CONC(10),CP(10),CT,EMACH(10),
20060          1  ENTHAL(10,7),GAMMA(10),P(10,7),Q(10),
20070          2  RHO(10,7),T(10,7),V(10),WDOT(10,7),WMOL(10)
20080           COMMON/GEOM/ALPHA,AR(14,14),R(14,14),
20090          1  THETA(14),X(14,14),Y(14,14),XNO(14)
20100     C
20110           P1=P(INF,IPITOT)/PRATIO(GAMMA(JET),EMX)
20120           T1=T(JET,ITOTAL)/TRATIO(GAMMA(JET),EMX)
20130           B1=AR(JEXIT,JSPHER)*P(JET,IEXIT)*EMACH(JET)
20140          1  *SQRT(T1/T(JET,IEXIT))/(P1*EMX)
20150           Y(ND,JSPHER)=Y(ND,JEXIT)/R(JSPHER,JEXIT)
20160           C1=Y(ND,JSPHER)*Y(ND,JSPHER)
20170           SINTH=(B1*SQRT(B1*B1+4.0*C1))/2.0
20180           THETA(ND)=ASIN(SINTH)
20190           PTRY=PFIT(THETA(ND),P(INF,IPTRAT))
20200           FCTCN=PTRY/P1-1.0
20210           RETURN
20220           END
20230     C
20240     C.....
20250     C
20260           FUNCTION VEL2D1(Z)
20270     C CALCULATES THE TWO-DIMENSIONAL VELOCITY PROFILE,
20280     C
20290           COMMON/ROOT/NSSWCH,CAPPA,RHOES,UES,XBAR1,XK,XLAM,Y0,YSSL
20300     C
20310           VEL2D1=(1.0+ERF(XK*Z))/2.0 + XLAM/(COSH(Z)*COSH(Z))
20320           RETURN
20330           END
20340     C
20350     C.....
20360     C
20370           FUNCTION VEL2D2(Z)
20380     C CALCULATES THE SQUARE OF THE TWO-DIMENSIONAL VELOCITY PROFILE,
20390     C
20400           TEMP=VEL2D1(Z)
```

```
20410           VEL2D2=TEMP*TEMP
20420           RETURN
20430           END
20440   C
20450   C.....
20460   C
20470           FUNCTION ENT2D(Z)
20480   C CALCULATES THE PRODUCT OF THE TWO-DIMENSIONAL ENTHALPY TIMES
20490   C THE VELOCITY PROFILES.
20500   C
20510           COMMON/IDENT/IDEAD,INF,JEI,JTERM,LAYER,MIX,MJBDY,M1INT,M2INT,
20520        1  IEXIT,IPITOT,IRATIO,ISTAT,ITOTAL,INFRAT,IPTRAT,JRETRN
20530           COMMON/AERO/A(10,7),CO,CONC(10),CP(10),CT,EMACH(10),
20540        1  ENTHAL(10,7),GAMMA(10),P(10,7),Q(10),
20550        2  RHO(10,7),T(10,7),V(10),WDOT(10,7),WMOL(10)
20560           COMMON/ROOT/ASSWCH,CAPPA,RHOES,UES,XBARI,XK,XLAM,Y0,YSSL
20570           COMMON/ZZINT/ZNT1,ZNT2,ZNT3,ZNT4,XMU,XNU1,YK1,YK2,YK3,YSS(5)
20580   C
20590           TEMP=VEL2D1(Z)
20600           DUMMY=(1.0+ENTHAL(IDEAD,INF))/2.0 +(1.0-ENTHAL(IDEAD,INF))
20610        1  *ERF(XK*Z)/2.0 *XMU/(COSH(Z)*COSH(Z))
20620           ENT2D=TEMP*DUMMY
20630           RETURN
20640           END
20650   C
20660   C.....
20670   C
20680           FUNCTION CON2D(Z)
20690   C CALCULATES THE PRODUCT OF THE TWO-DIMENSIONAL CONCENTRATION TIMES
20700   C THE VELOCITY PROFILES.
20710   C
20720           COMMON/IDENT/IDEAD,INF,JEI,JTERM,LAYER,MIX,MJBDY,M1INT,M2INT,
20730        1  IEXIT,IPITOT,IRATIO,ISTAT,ITOTAL,INFRAT,IPTRAT,JRETRN
20740           COMMON/AERO/A(10,7),CO,CONC(10),CP(10),CT,EMACH(10),
20750        1  ENTHAL(10,7),GAMMA(10),P(10,7),Q(10),
20760        2  RHO(10,7),T(10,7),V(10),WDOT(10,7),WMOL(10)
20770           COMMON/ROOT/ASSWCH,CAPPA,RHOES,UES,XBARI,XK,XLAM,Y0,YSSL
20780           COMMON/ZZINT/ZNT1,ZNT2,ZNT3,ZNT4,XMU,XNU1,YK1,YK2,YK3,YSS(5)
20790   C
20800           TEMP=VEL2D1(Z)
20810           DUMMY=CONC(IDEAD)*(1.0-ERF(XK*Z))/2.0 +XNU1/(COSH(Z)*COSH(Z))
20820           CON2D=TEMP*DUMMY
20830           RETURN
20840           END
20850   C
20860   C.....
20870   C
20880           FUNCTION FCTLAM(XLAMX)
20890   C THIS FUNCTION, SET UP IN THE FORM FCT(X)=0.0, IS CALLED BY
20900   C SUBROUTINE -PGEW- TO ITERATIVELY FIND THE VALUE OF LAMDA
20910   C IN THE TWO-DIMENSIONAL CASE.
20920   C
20930           COMMON/ROOT/ASSWCH,CAPPA,RHOES,UES,XBARI,XK,XLAM,Y0,YSSL
20940           COMMON/ZZINT/ZNT1,ZNT2,ZNT3,ZNT4,XMU,XNU1,YK1,YK2,YK3,YSS(5)
20950           EXTERNAL VEL2D1,VEL2D2
20960   C
20970           XLAM=XLAMX
20980           CALL DGS(-Y0,Y0,VEL2D1,ZNT1)
20990           CALL DGS(-Y0,Y0,VEL2D2,ZNT2)
21000           FCTLAM=YSS(2)/UES-YK1-ZNT2/ZNT1
```

```
21010            RETURN
21020            END
21030    C
21040    C.....
21050    C
21060            FUNCTION FCTMU(XMX)
21070    C THIS FUNCTION, SET UP IN THE FORM FCT(X)=0.0, IS CALLED BY
21080    C SUBROUTINE -PGEW- TO ITERATIVELY FIND THE VALUE OF MU
21090    C IN THE TWO-DIMENSIONAL CASE.
21100    C
21110            COMMON/IDENT/IDEAD,INF,JET,JTERM,LAYER,MIX,MJBDY,M1INT,M2INT,
21120         1  IEXIT,IPITOT,IRATIO,ISTAT,ITOTAL,INFRAT,IPTRAT,JRETRN
21130            COMMON/AERO/A(10,7),CD,CONC(10),CP(10),CT,EMACH(10),
21140         1  ENTHAL(10,7),GAMMA(10),P(10,7),Q(10),
21150         2  RHO(10,7),T(10,7),V(10),WDOT(10,7),WMOL(10)
21160            COMMON/ROOT/ISSWCH,CAPPA,RHOES,UES,XBARI,XK,XLAM,Y0,YSSL
21170            COMMON/ZZINT/ZNT1,ZNT2,ZNT3,ZNT4,XMU,XNU1,YK1,YK2,YK3,YSS(5)
21180            EXTERNAL ENT2D
21190    C
21200            XMU=XMX
21210            CALL QG6(-Y0,Y0,ENT2D,ZNT3)
21220            FCTMU=YSS(3)-YK2*(1.0-ENTHAL(IDEAD,INF))-ZNT3/ZNT1
21230            RETURN
21240            END
21250    C
21260    C.....
21270    C
21280            FUNCTION FCTNU(XNUX)
21290    C THIS FUNCTION, SET UP IN THE FORM FCT(X)=0.0, IS CALLED BY
21300    C SUBROUTINE -PGEW- TO ITERATIVELY FIND THE VALUE OF NU
21310    C IN THE TWO-DIMENSIONAL CASE.
21320    C
21330            COMMON/IDENT/IDEAD,INF,JET,JTERM,LAYER,MIX,MJBDY,M1INT,M2INT,
21340         1  IEXIT,IPITOT,IRATIO,ISTAT,ITOTAL,INFRAT,IPTRAT,JRETRN
21350            COMMON/AERO/A(10,7),CD,CONC(10),CP(10),CT,EMACH(10),
21360         1  ENTHAL(10,7),GAMMA(10),P(10,7),Q(10),
21370         2  RHO(10,7),T(10,7),V(10),WDOT(10,7),WMOL(10)
21380            COMMON/ROOT/ISSWCH,CAPPA,RHOES,UES,XBARI,XK,XLAM,Y0,YSSL
21390            COMMON/ZZINT/ZNT1,ZNT2,ZNT3,ZNT4,XMU,XNU1,YK1,YK2,YK3,YSS(5)
21400            EXTERNAL CON2D
21410    C
21420            XNU1=XNUX
21430            CALL QG6(-Y0,Y0,CON2D,ZNT4)
21440            FCTNU=YSS(4)-YK3*CONC(IDEAD)-ZNT4/ZNT1
21450            RETURN
21460            END
21470    C
21480    C.....
21490    C
21500            FUNCTION FCTYSS(YSSX)
21510    C THIS FUNCTION, SET UP IN THE FORM FCT(X)=0.0, IS CALLED BY
21520    C SUBROUTINE -PGEW- TO ITERATIVELY FIND THE VALUE OF THE SEPARATION
21530    C STREAMLINE IN THE TWO-DIMENSIONAL CASE.
21540    C
21550            COMMON/IDENT/IDEAD,INF,JET,JTERM,LAYER,MIX,MJBDY,M1INT,M2INT,
21560         1  IEXIT,IPITOT,IRATIO,ISTAT,ITOTAL,INFRAT,IPTRAT,JRETRN
21570            COMMON/AERO/A(10,7),CD,CONC(10),CP(10),CT,EMACH(10),
21580         1  ENTHAL(10,7),GAMMA(10),P(10,7),Q(10),
21590         2  RHO(10,7),T(10,7),V(10),WDOT(10,7),WMOL(10)
21600            COMMON/ROOT/ISSWCH,CAPPA,RHOES,UES,XBARI,XK,XLAM,Y0,YSSL
```

```
      COMMON/ZZINT/ZNT1,ZNT2,ZNT3,ZNT4,XMU,XNU1,YK1,YK2,YK3,YSS(5)
      EXTERNAL VEL2D1
C
      YSSL=YSSX
      CALL QGB(0.Y0,YSSL,VEL2D1,ZNT2)
      FCTYSS=ROOT(JRETRN,1)/YSS(1)-ZNT2/ZNT1
      RETURN
      END
C
C.....
C
      FUNCTION VEL3D1(Z)
C CALCULATES THE THREE-DIMENSIONAL VELOCITY PROFILE,
C
      COMMON/ROOT/XSSXCH,CAPPA,RHOES,UES,XBARI,XK,XLAM,R0,RSSL
C
      VEL3D1=Z*VEL2D1(Z-R0)
      RETURN
      END
C
C.....
C
      FUNCTION VEL3D2(Z)
C CALCULATES THE SQUARE OF THE THREE-DIMENSIONAL VELOCITY PROFILE,
C
      COMMON/ROOT/XSSXCH,CAPPA,RHOES,UES,XBARI,XK,XLAM,R0,RSSL
C
      VEL3D2=Z*VEL2D2(Z-R0)
      RETURN
      END
C
C.....
C
      FUNCTION ENT3D(Z)
C CALCULATES THE PRODUCT OF THE THREE-DIMENSIONAL ENTHALPY TIMES
C THE VELOCITY PROFILES,
C
      COMMON/ROOT/XSSXCH,CAPPA,RHOES,UES,XBARI,XK,XLAM,R0,RSSL
C
      ENT3D=Z*ENT2D(Z-R0)
      RETURN
      END
C
C.....
C
      FUNCTION CON3D(Z)
C CALCULATES THE PRODUCT OF THE THREE-DIMENSIONAL CONCENTRATION TIMES
C THE VELOCITY PROFILES,
C
      COMMON/ROOT/XSSXCH,CAPPA,RHOES,UES,XBARI,XK,XLAM,R0,RSSL
C
      CON3D=Z*CON2D(Z-R0)
      RETURN
      END
C
C.....
C
      FUNCTION FCT3LM(XLAMX)
C THIS FUNCTION, SET UP IN THE FORM FCT(X)=0.0, IS CALLED BY
C SUBROUTINE -PGEN- TO ITERATIVELY FIND THE VALUE OF LAMDA
```

```
C IN THE THREE-DIMENSIONAL CASE,
C
      COMMON/ROOT/NSSWCH,CAPPA,RHOES,UES,XBARI,XK,XLAM,R0,RSSL
      COMMON/ZZINT/ZNT1,ZNT2,ZNT3,ZNT4,XMU,XNU1,YK1,YK2,YK3,YSS(5)
      EXTERNAL VEL3D1,VEL3D2
C
      XLAM=XLAMX
      CALL GG8(0,0,2,2*R0,VEL3D1,ZNT1)
      CALL GG8(0,0,2,2*R0,VEL3D2,ZNT2)
      FCT3LM=YSS(2)/UES-YK1-ZNT2/ZNT1
      RETURN
      END
C
C.....
C
      FUNCTION FCT3MU(XMX)
C THIS FUNCTION, SET UP IN THE FORM FCT(X)=0.0, IS CALLED BY
C SUBROUTINE -PGEN- TO ITERATIVELY FIND THE VALUE OF MU
C IN THE THREE-DIMENSIONAL CASE,
C
      COMMON/IDENT/IDEAD,INF,JET,JTERM,LAYER,MIX,MJBDY,M1INT,M2INT,
     1  IEXIT,IPITOT,IRATIO,ISTAT,ITOTAL,INFRAT,IPTRAT,JRETRN
      COMMON/AERO/A(10,7),CD,CONC(10),CP(10),CT,EMACH(10),
     1  ENTHAL(10,7),GAMMA(10),P(10,7),Q(10),
     2  RHO(10,7),T(10,7),V(10),WDOT(10,7),WMOL(10)
      COMMON/ROOT/NSSWCH,CAPPA,RHOES,UES,XBARI,XK,XLAM,R0,RSSL
      COMMON/ZZINT/ZNT1,ZNT2,ZNT3,ZNT4,XMU,XNU1,YK1,YK2,YK3,YSS(5)
      EXTERNAL ENT3D
C
      XMU=XMX
      CALL GG8(0,0,2,2*R0,ENT3D,ZNT3)
      FCT3MU=YSS(3)-YK2*(1.4-ENTHAL(IDEAD,INF))-ZNT3/ZNT1
      RETURN
      END
C
C.....
C
      FUNCTION FCT3NU(XNUX)
C THIS FUNCTION, SET UP IN THE FORM FCT(X)=0.0, IS CALLED BY
C SUBROUTINE -PGEN- TO ITERATIVELY FIND THE VALUE OF NU
C IN THE THREE-DIMENSIONAL CASE,
C
      COMMON/IDENT/IDEAD,INF,JET,JTERM,LAYER,MIX,MJBDY,M1INT,M2INT,
     1  IEXIT,IPITOT,IRATIO,ISTAT,ITOTAL,INFRAT,IPTRAT,JRETRN
      COMMON/AERO/A(10,7),CD,CONC(10),CP(10),CT,EMACH(10),
     1  ENTHAL(10,7),GAMMA(10),P(10,7),Q(10),
     2  RHO(10,7),T(10,7),V(10),WDOT(10,7),WMOL(10)
      COMMON/ROOT/NSSWCH,CAPPA,RHOES,UES,XBARI,XK,XLAM,R0,RSSL
      COMMON/ZZINT/ZNT1,ZNT2,ZNT3,ZNT4,XMU,XNU1,YK1,YK2,YK3,YSS(5)
      EXTERNAL CON3D
C
      XNU1=XNUX
      CALL GG8(0,0,2,2*R0,CON3D,ZNT4)
      FCT3NU=YSS(4)-YK3*CONC(IDEAD)-ZNT4/ZNT1
      RETURN
      END
C
C.....
C
      FUNCTION RHO3D(Z)
```

```
C CALCULATES THE THREE-DIMENSIONAL DENSITY PROFILE,
C
      COMMON/IDENT/IDEAD,INF,JET,JTERM,LAYER,MIX,MJBDY,M1INT,M2INT,
     1  IEXIT,IPITOT,IRATIO,ISTAT,ITOTAL,INFRAT,IPTRAT,JRETRN
      COMMON/AERO/A(12,7),CD,CONC(10),CP(10),CT,EMACH(10),
     1  ENTHAL(10,7),GAMMA(10),P(10,7),Q(10),
     2  RHO(10,7),T(10,7),V(10),WDOT(10,7),WMOL(10)
      COMMON/ROOT/SSMCH,CAPPA,RHOES,UES,XBARI,XK,XLAM,R0,RSSL
C
      UER=VEL2D1(Z-R0)
      HR=ENT2D(Z-R0)/UER
      CONR=CON2D(Z-R0)/UER
C
      USSR=UER*UES*V(INF)
      HSTR=HR*ENTHAL(INF,1)-0.5*USSR*USSR
      CPR=CONR*CP(JET)+(1.0-CONR)*CP(INF)
      WMR=1.0/( CONR/WMOL(JET)+(1.0-CONR)/WMOL(INF) )
      TR=HSTR/CPR
      RHOR=GASRHO(P(IDEAD,ISTAT),WMR,TR)
      RHO3D=Z*RHOES*RHO(INF,ISTAT)/RHOR
      RETURN
      END
C
C.....
C
      FUNCTION FCTRSS(RSSX)
C THIS FUNCTION, SET UP IN THE FORM FCT(X)=0.0, IS CALLED BY
C SUBROUTINE -PGER- TO ITERATIVELY FIND THE VALUE OF THE SEPARATION
C STREAMLINE IN THE THREE-DIMENSIONAL CASE,
C
      COMMON/IDENT/IDEAD,INF,JET,JTERM,LAYER,MIX,MJBDY,M1INT,M2INT,
     1  IEXIT,IPITOT,IRATIO,ISTAT,ITOTAL,INFRAT,IPTRAT,JRETRN
      COMMON/AERO/A(12,7),CD,CONC(10),CP(10),CT,EMACH(10),
     1  ENTHAL(10,7),GAMMA(10),P(10,7),Q(10),
     2  RHO(10,7),T(10,7),V(10),WDOT(10,7),WMOL(10)
      COMMON/ROOT/SSMCH,CAPPA,RHOES,UES,XBARI,XK,XLAM,R0,RSSL
      COMMON/ZINT/ZNT1,ZNT2,ZNT3,ZNT4,XNU,XNU1,YK1,YK2,YK3,YSS(5)
      EXTERNAL VEL3D1
C
      RSSL=RSSX
      CALL NG8(0.0,RSSL,VEL3D1,ZNT2)
      FCTRSS=WDOT(JRETRN,1)/YSS(1)-ZNT2/ZNT1
      RETURN
      END
C
C.....
C
      SUBROUTINE DERIV(NI,NO,H,Y,Z)
C CALCULATES THE DERIVATIVE OF A VECTOR Y AND STORES IT IN ANOTHER
C VECTOR Z. (BASED ON IBM SCIENTIFIC SUBROUTINE -DET3- ),
C
      DIMENSION Y(200),Z(200)
C
      HH=0.5/H
      Z(NI)=HH*(-3.0*Y(NI)+4.0*Y(NI+1)-Y(NI+2))
      NIS=NI+1
      NOS=NO-1
      DO 100 I=NIS,NOS
  100 Z(I)=HH*(Y(I+1)-Y(I-1))
      Z(NO)=HH*(Y(NO-2)-4.0*Y(NO-1)+3.0*Y(NO))
```

```
      RETURN
      END
C
C.......................................................................
C
      SUBROUTINE SIMPS(NI,NO,H,Y,YI,YOUT)
C CALCULATES THE INTEGRAL OF A VECTOR Y OVER THE INTERVAL NI TO NO
C (WHICH MUST BE EVEN) AND RETURNS THE FINAL VALUE ONLY.
C (BASED ON IBM SCIENTIFIC SUBROUTINE -QSF2- ).
C
      DIMENSION Y(200)
C
      HH=H/3.0
      YOUT=YI
      NOS=NO-2
      DO 100 I=NI,NOS,2
  100 YOUT=YOUT+HH*(Y(I)+4.0*Y(I+1)+Y(I+2))
      RETURN
      END
C
C.......................................................................
C
      SUBROUTINE RUNGK(FCT,H,XI,YI,K,N,XOUT,YOUT)
C A FOURTH ORDER RUNGE-KUTTA INTEGRATION SUBROUTINE. IT USES A
C FUNCTION FCT(X,Y) WHERE FCT=DY/DX=F(X,Y).
C (BASED ON THE IBM SCIENTIFIC SUBROUTINE -RK1- ).
C
      COMMON/FCTA1/PHI,XX,YY
      DIMENSION XOUT(N),YOUT(N)
C
      H2=H/2.0
      Y=YI
      X=XI
      DO 20 I=1,N
      DO 10 J=1,K
      T1=H*FCT(X,Y)
      T2=H*FCT(X+H2,Y+T1/2.0)
      T3=H*FCT(X+H2,Y+T2/2.0)
      T4=H*FCT(X+H,Y+T3)
      Y=Y+(T1+2.0*T2+2.0*T3+T4)/6.0
   10 X=X+H
      YOUT(I)=Y
   20 XOUT(I)=X
      RETURN
      END
C
C.......................................................................
C
      SUBROUTINE FCTSS(SSTAR,YSSTAR,DERY,IERROR)
C THIS SUBROUTINE IS CALLED BY SUBROUTINE -HPCG-. THE FIRST TIME
C IT IS CALLED, IT CALCULATES THE INITIAL VALUES. THEREAFTER
C IT SKIPS TO AND CALCULATES THE RIGHT HAND SIDE OF THE DIFFERENTIAL
C EQUATIONS.
C
      COMMON/CONSTS/PI,RUNIV
      COMMON/IDENT/IDEAD,INF,JET,JTERM,LAYER,MIX,MJBDY,M1INT,M2INT,
     1 IEXIT,IPITOT,IRATIO,ISTAT,ITOTAL,INFRAT,IPIRAT,JRETRN
      COMMON/JDENT/JBASE,JCENTR,JEXIT,JFACE,JSPHER,JSTAR,
     1 JTERSH,MAX,MERGE,MOD,ND,NPI,NS
      COMMON/AERO/A(10,7),CD,CNC(10),CP(10),CT,EMACH(10),
```

```
24010          1  ENTHAL(10,7),GAMMA(10),P(10,7),Q(10),
24020          2  RHO(10,7),T(10,7),V(10),WDOT(10,7),WMOL(10)
24030             COMMON/GLOB/ALPHA,AR(14,14),R(14,14),
24040          1  THETA(14),X(14,14),Y(14,14),XNU(14)
24050             COMMON/ROOT/NSSWCH,CAPPA,RHOES,UES,XBARI,XK,XLAM,Y0,YSSL
24060             DIMENSION YSSTAR(5),DERY(5)
24070       C
24080       C NOTE THAT THE FIRST TIME -FCTSS- IS CALLED, NSSWCH=1 , THEREAFTER,
24090       C NSSWCH=2 IF THET IS LESS THAN THETA(NS), AND NSSWCH=3 IF
24100       C THET IS GREATER THAN THETA(NS).
24110       C
24120       C SSTAR=XBAR-XBARI, XBARI=INITIAL VALUE OF XBAR, CORRESPONDING
24130       C TO THETA(MERGE),
24140             XBAR=SSTAR+XBARI
24150             IF(XBAR.GT.THETA(NS)) GO TO 60
24160       C THET IS LESS THAN THETA(NS),
24170             THET=XBAR
24180             RSTAR=SIN(THET)
24190             GO TO 70
24200       C THET IS GREATER THAN OR EQUAL TO THETA(NS),
24210        60   THET=THETA(NS)+ATAN(XBAR-THETA(NS))
24220             RSTAR=SIN(THET)/COS(THET-THETA(NS))
24230       C THE FLAG NSSWCH INSURES THAT THE INITIAL CONDITIONS ARE
24240       C CALCULATED ONLY ONCE, IF THETA(MERGE) IS GREATER THAN THETA(NS),
24250       C PARAMETERS ARE CALCULATED AT THETA(NS) AND USED TO CALCULATE
24260       C THE INITIAL CONDITIONS.
24270        70   IF(NSSWCH.EQ. 3) GO TO 160
24280       C
24290          110  IF(THET.GT. PI/2.0) GO TO 130
24300          120  PE=PFIT(THET,P(INF,IPIRAT))
24310               PTS=P(INF,IPITOT)/PE
24320               EME=PMACH(GAMMA(INF),PTS)
24330               GO TO 140
24340          130  XNU1=XNU(NPI)+THET-PI/2.0
24350               EME=XNMACH(GAMMA(INF),XNU1,IERROR)
24360               IF(IERROR.EQ. 1) GO TO 300
24370               PTS=PRATIO(GAMMA(INF),EME)
24380               PE=P(INF,IPITOT)/PTS
24390          140  RHOES=RHO(INF,IRATIO)*P(INF,IPITOT)/P(INF,ITOTAL)
24400             1  /(PTS**(1.0/GAMMA(INF)))
24410               UES=EME/EMACH(INF)*SQRT(T(INF,IRATIO))
24420             1  /(PTS**((GAMMA(INF)-1.0)/(2.0*GAMMA(INF))))
24430       C
24440               IF(NSSWCH.GT. 1) GO TO 150
24450       C CALCULATION OF THE INITIAL VALUES,
24460               YSSTAR(1)=2.0*WDOT(JET,1)/WDOT(INF,1)
24470               YSSTAR(2)=UES*WDOT(M1INT,JET)/2.0+V(MIX)/(2.0*V(INF))
24480               YSSTAR(3)=WDOT(M1INT,JET)*(1.0-ENTHAL(IDEAD,INF))/2.0
24490             1  +(ENTHAL(JET,INF)+ENTHAL(IDEAD,INF))/2.0
24500               YSSTAR(4)=(1.0*CONC(IDEAD)*(1.0-WDOT(M1INT,JET)))/2.0
24510               YSSTAR(5)=0.0
24520       C
24530       C EVALUATE THE PSEUDO-CONSTANTS.
24540          150  B=UES*SQRT(RHOES*RHO(IDEAD,INFRAT))/2.0
24550               C=1.0+RHO(IDEAD,INFRAT)/RHOES
24560          160  AA=RHOES*(YSSTAR(2)-UES/2.0)
24570       C
24580       C CALCULATION OF THE RIGHT HAND SIDE OF THE DIFFERENTIAL EQUATIONS.
24590               DERY(1)=0.20*RSTAR*(AA*C+2.0*B)
24600               DERY(2)=( 0.20*RSTAR*UES*(AA+B)-YSSTAR(2)*DERY(1) )/YSSTAR(1)
```

```
24610           DERY(3)=( 3,20*RSTAR*(AA*(1,0+(C-1,0)*ENTHAL(IDEAD,INF))
24620         1 +B*(1,0+ENTHAL(IDEAD,INF)))-YSSTAR(3)*DERY(1) )/YSSTAR(1)
24630           DERY(4)=( 3,20*RSTAR*CONC(IDEAD)*(B+AA*(C-1,0))
24640         1 -YSSTAR(4)*DERY(1) )/YSSTAR(1)
24650           DERY(5)=0,20*RSTAR*(B+AA*(C-1,0))
24660       300 RETURN
24670           END
24680     C
24690     C.....................................................................
24700     C
24710           SUBROUTINE OUTP(SSTAR,YSSTAR,DERY,IHLF,NDIM,PRMT,IERROR)
24720     C THIS SUBROUTINE IS REQUIRED BY THE INTEGRATION SUBROUTINE -HPCG- ,
24730     C IF THE BLUNTING SPHERE DIAMETER IS LESS THAN THE BASE DIAMETER,
24740     C ITS ONLY ACTION IS TO PRESERVE THE CURRENT VALUE OF SSTAR, AS
24750     C A CHECK ON INTEGRATION FAILURE,
24760     C
24770     C IF THE BLUNTING SPHERE DIAMETER IS GREATER THAN THE BASE DIAMETER,
24780     C AND THEI IS GREATER THAN THETA(NS),(I.E, THE INTEGRATION HAS REACHED
24790     C THE CONICAL PORTION), IT CALCULATES LAMDA,KAPPA AND THE
24800     C PHYSICAL LENGTHS, BOTH FROM GEOMETRIC CONSIDERATIONS AND A
24810     C MASS BALANCE, AND TERMINATES INTEGRATION WHEN THE LATTER
24820     C EXCEEDS THE FORMER,
24830     C
24840           COMMON/CONSTS/PI,RUNIV
24850           COMMON/IDENT/IDEAD,INF,JET,JTERM,LAYER,MIX,MJBUY,M1INT,M2INT,
24860         1 IEXIT,IPITOT,IRATIO,ISTAT,ITOTAL,INFRAT,IPTRAT,JRETRN
24870           COMMON/JDENT/JBASE,JCENTR,JEXIT,JFACE,JSPHER,JSTAR,
24880         1 JTERSH,MAX,MERGE,MOD,ND,NPI,NS
24890           COMMON/AERO/A(10,7),CD,CONC(10),CP(10),CT,EMACH(10),
24900         1 ENTHAL(10,7),GAMMA(10),P(10,7),Q(10),
24910         2 RHO(10,7),T(10,7),V(10),WDOT(10,7),WMOL(10)
24920           COMMON/GEOM/ALPHA,AR(14,14),R(14,14),
24930         1 THETA(14),X(14,14),Y(14,14),XNU(14)
24940           COMMON/ROOT/NSWCH,CAPPA,RHOES,UES,XBARI,XK,XLAM,R0,RSSL
24950           COMMON/ZZINT/ZNT1,ZNT2,ZNT3,ZNT4,XMU,XNU1,YK1,YK2,YK3,YSS(5)
24960           DIMENSION PRMT(6),YSSTAR(5),DERY(5)
24970           EXTERNAL FCT3LM,FCT3MU,FCT3NU,FCTRSS,RHO3D
24980     C
24990       228 FORMAT('0CONVERGENCE FAILURE, LAMDA=',1PE12.4,'  FCT3LM=',
25000         1 E12.4,'  IER=',I4,/)
25010       248 FORMAT('0CONVERGENCE FAILURE, MU=',1PE12.4,'  FCT3MU=',
25020         1 E12.4,'  IER=',I4,/)
25030       268 FORMAT('0CONVERGENCE FAILURE, NU=',1PE12.4,'  FCT3NU=',
25040         1 E12.4,'  IER=',I4,/)
25050       308 FORMAT('0CONVERGENCE FAILURE, RSSL=',1PE12.4,'  FCTRSS=',
25060         1 E12.4,'  IER=',I4,/)
25070     C
25080           IOUT=6
25090           PRMT(6)=SSTAR
25100           IF(THETA(NS),LT,PI/2,0) GO TO 960
25110     C
25120     C DELSST IS THE NONDIMENSIONAL DISTANCE FROM THE SPHERE-CONE
25130     C INTERSECTION POINT, ALONG THE CONE,
25140           DELSST=SSTAR-(THETA(NS)-XBARI)
25150           IF(DELSST,LT, 0,0) GO TO 960
25160     C
25170           IF(NSWCH,EQ, 1) GO TO 400
25180           YGEOM=(1,4-DELSST*TAN(ALPHA))*R(JSPHER,1)*COS(ALPHA)
25190           DELL=DELSST*TAN(ALPHA)
25200     C
```

```
25210           DO 200 I=1,NDIM
25220     200   YSS(I)=YSSTAR(I)
25230 C
25240 C FIND LAMDA BY AN ITERATIVE PROCEDURE,
25250           CALL PGEN(XLAM,VAL,FCT3LM,0,50,1,0,1.0E-6,100,IER)
25260           IF(IER.EQ. 0) GO TO 230
25270           WRITE (IOUT,220) XLAM,VAL,IER
25280           GO TO 900
25290 C
25300 C FIND MU BY AN ITERATIVE PROCEDURE,
25310     230   CALL PGEN(XMU,VAL,FCT3MU,0,0,0,50,1.0E-6,100,IER)
25320           IF(IER.EQ. 0) GO TO 250
25330           WRITE (IOUT,240) MU,VAL,IER
25340           GO TO 900
25350 C
25360 C FIND NU BY AN ITERATIVE PROCEDURE,
25370     250   CALL PGEN(XNU1,VAL,FCT3NU,0,0,0,50,1.0E-6,100,IER)
25380           IF(IER.EQ. 0) GO TO 270
25390           WRITE (IOUT,260) NU,VAL,IER
25400           GO TO 900
25410 C
25420     270   CAPPA=2.0*PI*RHOES*UES*ZNT1/(YSSTAR(1)*AR(JSPHER,1))
25430 C
25440 C THE TOTAL ENTRAINED AND THE RECIRCULATED MASS FLOW IS NOW MADE
25450 C DIMENSIONAL ONCE AGAIN,
25460           YSS(1)=YSS(1)*WDOT(INF,1)
25470           YSS(5)=YSS(5)*WDOT(INF,1)
25480 C
25490 C CALCULATE THE MASS RETURNED TO THE DEAD AIR REGION,
25500           WDOT(JRETRN,1)=WDOT(MJBDY,1)+WDOT(M2INT,1)+YSS(5)
25510 C FIND THE SEPARATION STREAMLINE BY AN ITERATIVE PROCEDURE,
25520           CALL PGEN(RSSL,VAL,FCTRSS,2.0,2,5,1.0E-6,100,IER)
25530           IF(IER.EQ. 0) GO TO 310
25540           WRITE (IOUT,300) RSSL,VAL,IER
25550           GO TO 900
25560 C
25570     310   CALL UGB(0,0,RSSL,RHOSD,ZNT5)
25580 C
25590           YMASS=SQRT(2.0*ZNT5/CAPPA)
25600 C
25610           DELENG=(YGEOM-YMASS)/(2.0*R(JSPHER,1)*SIN(ALPHA)) +DELSST
25620           TYPE 41,SSTAR,DELL,DELENG,CAPPA,XLAM,YGEOM,YMASS
25630      41   FORMAT(' S*,DELS/L,NEW DEL=',5F10.5,
25640        1  /' KAPPA,LAMDA,YG,YM*=',1P4E12.4)
25650           NSWCH=1
25660     400   IF(DELSST.GT.DELENG) NSWCH=0
25670           IF(YGEOM.LT. 1.050*YMASS) NSWCH=0
25680           IF(YGEOM.GT.YMASS) GO TO 960
25690           GO TO 930
25700     900   IERROR=1
25710     930   PRNT(5)=1.0
25720     960   RETURN
25730           END
25740 C
25750 C.....
25760 C
25770           SUBROUTINE PGEN(X,VAL,FCT,XG1,XG2,EPS,IEND,IER)
25780 C THIS SUBROUTINE USES THE TECHNIQUE OF FALSE POSITION WITH
25790 C UPDATING ANCHORS, THE FUNCTION THAT IT CALLS MUST BE IN THE
25800 C FORM FCT(X)=0 ,X IS THE VALUE OF THE ROOT, VAL IS THE VALUE
```

```
C OF FCT(X), XG1,XG2 ARE THE INITIAL GUESSES OF X, EPS IS THE ERROR
C BOUND, IEND IS THE MAX, NUMBER OF ITERATIONS, AND IER IS AN
C ERROR RETURN.
C
      IER=0
      X1=XG1
      F1=FCT(X1)
      VAL=F1
      X2=XG2
C
      DO 100 I=1,IEND
      F2=FCT(X2)
      VAL=F2
      DIFF=F2-F1
      IF(ABS(DIFF),LT, 1.0E-35) GO TO 200
      X=X2-F2*(X2-X1)/DIFF
      IF(ABS(X/X2-1.0),LT,EPS) GO TO 300
      F1=F2
      X1=X2
      X2=X
  100 CONTINUE
C
C NO CONVERGENCE AFTER IEND ITERATIONS,
      IER=1
      GO TO 300
C
C DENOMINATOR IS TOO SMALL,
  200 IER=2
  300 RETURN
      END
C
C.....
C
      SUBROUTINE QG8(XL,XU,FCT,Y)
C CALCULATES THE INTEGRAL OF THE FUNCTION FCT(X), BY SUMMING OVER X
C FROM XL TO XU,BY MEANS OF A FOURTH ORDER GAUSSIAN FORMULA,
C (TAKEN DIRECTLY FROM THE IBM SCIENTIFIC SUBROUTINES, -QG8- ),
C
C
      A=.5*(XU+XL)
      B=XU-XL
      C=.4801449*B
      Y=.2261427*(FCT(A+C)+FCT(A-C))
      C=.3983332*B
      Y=Y+.1111905*(FCT(A+C)+FCT(A-C))
      C=.2627662*B
      Y=Y+.1568533*(FCT(A+C)+FCT(A-C))
      C=.0971732*B
      Y=B*(Y+.1013419*(FCT(A+C)+FCT(A-C)))
      RETURN
      END
C
C.....
C
      SUBROUTINE HPCG(PRMT,Y,DERY,NDIM,IHLF,FCT,OUTP,AUX,IERROR)
C SOLVES A SYSTEM OF FIRST ORDER ORDINARY GENERAL DIFFERENTIAL
C EQUATIONS WITH GIVEN INITIAL VALUES, BY USING A FOURTH ORDER
C HAMMING-S MODIFIED PREDICTOR-CORRECTOR METHOD. A FOURTH
C ORDER RUNGE-KUTTA METHOD IS USED TO GENERATE THE NECESSARY
C INITIAL VALUES,
```

```
C (TAKEN DIRECTLY AND SLIGHTLY MODIFIED FROM THE IBM SCIENTIFIC
C SUBROUTINES, -HPCG- ).
C
      DIMENSION PRMT(6),Y(5),DERY(5),AUX(16,5)
C
      N=1
      IHLF=0
      X=PRMT(1)
      H=PRMT(3)
      PRMT(5)=0.
      DO 1 I=1,NDIM
      AUX(16,I)=0.
      AUX(15,I)=DERY(I)
    1 AUX(1,I)=Y(I)
      IF(H*(PRMT(2)-X))3,2,4
C
C ERROR RETURNS
    2 IHLF=12
      GO TO 4
    3 IHLF=13
C
C COMPUTATION OF DERY FOR STARTING VALUES
    4 CALL FCT(X,Y,DERY,IERROR)
      IF(IERROR.EQ. 1) GO TO 230
C
C RECORDING OF STARTING VALUES
      CALL OUTP(X,Y,DERY,IHLF,NDIM,PRMT,IERROR)
      IF(IERROR.EQ. 1) GO TO 230
      IF(PRMT(5))6,5,6
    5 IF(IHLF)7,7,6
    6 RETURN
    7 DO 8 I=1,NDIM
    8 AUX(0,I)=DERY(I)
C
C COMPUTATION OF AUX(2,I)
      ISW=1
      GO TO 100
C
    9 X=X+H
      DO 10 I=1,NDIM
   10 AUX(2,I)=Y(I)
C
C INCREMENT H IS TESTED BY MEANS OF BISECTION
   11 IHLF=IHLF+1
      X=X-H
      DO 12 I=1,NDIM
   12 AUX(4,I)=AUX(2,I)
      H=.5*H
      N=1
      ISW=2
      GO TO 100
C
   13 X=X+H
      CALL FCT(X,Y,DERY,IERROR)
      IF(IERROR.EQ. 1) GO TO 230
      N=2
      DO 14 I=1,NDIM
      AUX(2,I)=Y(I)
   14 AUX(3,I)=DERY(I)
      ISW=3
```

```
27010          GO TO 100
27020    C
27030    C COMPUTATION OF TEST VALUE DELT
27040       15 DELT=0.
27050          DO 16 I=1,NDIM
27060       16 DELT=DELT+AUX(15,I)*ABS(Y(I)-AUX(4,I))
27070          DELT=.06666667*DELT
27080          IF(DELT-PRMT(4))19,19,17
27090       17 IF(IHLF-10)11,18,18
27100    C
27110    C NO SATISFACTORY ACCURACY AFTER 10 BISECTIONS. ERROR MESSAGE.
27120       18 IHLF=11
27130          X=X+H
27140          GO TO 4
27150    C
27160    C THERE IS SATISFACTORY ACCURACY AFTER LESS THAN 11 BISECTIONS.
27170       19 X=X+H
27180          CALL FCT(X,Y,DERY,IERROR)
27190          IF(IERROR.EQ. 1) GO TO 230
27200          DO 20 I=1,NDIM
27210          AUX(3,I)=Y(I)
27220       20 AUX(10,I)=DERY(I)
27230          N=3
27240          ISW=4
27250          GO TO 100
27260    C
27270       21 N=1
27280          X=X+H
27290          CALL FCT(X,Y,DERY,IERROR)
27300          IF(IERROR.EQ. 1) GO TO 230
27310          X=PRMT(1)
27320          DO 22 I=1,NDIM
27330          AUX(11,I)=DERY(I)
27340       22 Y(I)=AUX(1,I)+H*(.375*AUX(8,I)+.7916667*AUX(9,I)
27350         1-.2083333*AUX(10,I)+.0416667*DERY(I))
27360       23 X=X+H
27370          N=N+1
27380          CALL FCT(X,Y,DERY,IERROR)
27390          IF(IERROR.EQ. 1) GO TO 230
27400          CALL OUTP(X,Y,DERY,IHLF,NDIM,PRMT,IERROR)
27410          IF(IERROR.EQ. 1) GO TO 230
27420          IF(PRMT(5))6,24,6
27430       24 IF(N-4)25,200,200
27440       25 DO 26 I=1,NDIM
27450          AUX(N,I)=Y(I)
27460       26 AUX(N+7,I)=DERY(I)
27470          IF(N-3)27,29,200
27480    C
27490       27 DO 28 I=1,NDIM
27500          DELT=AUX(9,I)+AUX(9,I)
27510          DELT=DELT+DELT
27520       28 Y(I)=AUX(1,I)+.3333333*H*(AUX(8,I)+DELT+AUX(10,I))
27530          GO TO 23
27540    C
27550       29 DO 30 I=1,NDIM
27560          DELT=AUX(9,I)+AUX(10,I)
27570          DELT=DELT+DELT+DELT
27580       30 Y(I)=AUX(1,I)+.375*H*(AUX(8,I)+DELT+AUX(11,I))
27590          GO TO 23
27600    C
```

```
C
C THE FOLLOWING PART OF SUBROUTINE HPCG COMPUTES BY MEANS OF
C RUNGE-KUTTA METHOD STARTING VALUES FOR THE NOT SELF-STARTING
C PREDICTOR-CORRECTOR METHOD.
  102 DO 101 I=1,NDIM
      Z=H*AUX(N+7,I)
      AUX(5,I)=Z
  101 Y(I)=AUX(N,I)+.4*Z
C Z IS AN AUXILIARY STORAGE LOCATION
C
      Z=X+.4*H
      CALL FCT(Z,Y,DERY,IERROR)
      IF(IERROR.EQ. 1) GO TO 230
      DO 102 I=1,NDIM
      Z=H*DERY(I)
      AUX(6,I)=Z
  102 Y(I)=AUX(N,I)+.2969776*AUX(5,I)+.1587596*Z
C
      Z=X+.4557672*H
      CALL FCT(Z,Y,DERY,IERROR)
      IF(IERROR.EQ. 1) GO TO 230
      DO 103 I=1,NDIM
      Z=H*DERY(I)
      AUX(7,I)=Z
  103 Y(I)=AUX(N,I)+.2181004*AUX(5,I)-3.050965*AUX(6,I)+3.832865*Z
C
      Z=X+H
      CALL FCT(Z,Y,DERY,IERROR)
      IF(IERROR.EQ. 1) GO TO 230
      DO 104 I=1,NDIM
  104 Y(I)=AUX(N,I)+.1747603*AUX(5,I)-.5514807*AUX(6,I)
     1+1.255556*AUX(7,I)+.1711848*H*DERY(I)
      GO TO(9,13,15,21),ISW
C
C POSSIBLE BREAK-POINT FOR LINKAGE
C
C STARTING VALUES ARE COMPUTED,
C NOW START HAMMINGS MODIFIED PREDICTOR-CORRECTOR METHOD.
  200 ISTEP=3
  201 IF(N-8)204,202,204
C
C N=8 CAUSES THE ROWS OF AUX TO CHANGE THEIR STORAGE LOCATIONS
  202 DO 203 N=2,7
      DO 203 I=1,NDIM
      AUX(N-1,I)=AUX(N,I)
  203 AUX(N+6,I)=AUX(N+7,I)
      N=7
C
C N LESS THAN 8 CAUSES N+1 TO GET N
  204 N=N+1
C
C COMPUTATION OF NEXT VECTOR Y
      DO 205 I=1,NDIM
      AUX(N-1,I)=Y(I)
  205 AUX(N+6,I)=DERY(I)
      X=X+H
  206 ISTEP=ISTEP+1
      DO 207 I=1,NDIM
      DELT=AUX(N-4,I)+1.333333*H*(AUX(N+6,I)+AUX(N+6,I)-AUX(N+5,I)+
     1AUX(N+4,I)+AUX(N+4,I))
      Y(I)=DELT-.9256198*AUX(16,I)
```

```
28210      207 AUX(16,I)=DELT
28220    C PREDICTOR IS NOW GENERATED IN ROW 16 OF AUX, MODIFIED PREDICTOR
28230    C IS GENERATED IN Y, DELT MEANS AN AUXILIARY STORAGE,
28240    C
28250          CALL FCT(X,Y,DERY,IERROR)
28260          IF(IERROR,EQ, 1) GO TO 230
28270    C DERIVATIVE OF MODIFIED PREDICTOR IS GENERATED IN DERY
28280    C
28290          DO 208 I=1,NDIM
28300          DELT=.125*(9.*AUX(N-1,I)-AUX(N-3,I)+3.*H*(DERY(I)+AUX(N+6,I)*
28310         1AUX(N+6,I)-AUX(N+5,I)))
28320          AUX(16,I)=AUX(16,I)-DELT
28330      208 Y(I)=DELT+.07438417*AUX(16,I)
28340    C
28350    C TEST WHETHER H MUST BE HALVED OR DOUBLED
28360          DELT=0.
28370          DO 209 I=1,NDIM
28380      209 DELT=DELT+AUX(15,I)*ABS(AUX(16,I))
28390          IF(DELT-PRMT(4))210,222,222
28400    C
28410    C H MUST NOT BE HALVED, THAT MEANS Y(I) ARE GOOD,
28420      210 CALL FCT(X,Y,DERY,IERROR)
28430          IF(IERROR,EQ, 1) GO TO 230
28440          CALL OUTP(X,Y,DERY,IHLF,NDIM,PRMT,IERROR)
28450          IF(IERROR,EQ, 1) GO TO 230
28460          IF(PRMT(5))212,211,212
28470      211 IF(IHLF-11)213,212,212
28480      212 RETURN
28490      213 IF(H*(X-PRMT(2)))214,212,212
28500      214 IF(ABS(X-PRMT(2))-.1*ABS(H))212,215,215
28510      215 IF(DELT-.02*PRMT(4))216,216,201
28520    C
28530    C
28540    C H COULD BE DOUBLED IF ALL NECESSARY PRECEEDING VALUES ARE
28550    C AVAILABLE
28560      216 IF(IHLF)201,201,217
28570      217 IF(N-7)201,218,218
28580      218 IF(ISTEP-4)221,219,219
28590      219 IMOD=ISTEP/2
28600          IF(ISTEP-IMOD-IMOD)201,220,201
28610      220 H=H+H
28620          IHLF=IHLF-1
28630          ISTEP=0
28640          DO 221 I=1,NDIM
28650          AUX(N-1,I)=AUX(N-2,I)
28660          AUX(N-2,I)=AUX(N-4,I)
28670          AUX(N-3,I)=AUX(N-6,I)
28680          AUX(N+6,I)=AUX(N+5,I)
28690          AUX(N+5,I)=AUX(N+3,I)
28700          AUX(N+4,I)=AUX(N+1,I)
28710          DELT=AUX(N+6,I)+AUX(N+5,I)
28720          DELT=DELT+DELT+DELT
28730      221 AUX(16,I)=8.962963*(Y(I)-AUX(N-3,I))-3.361111*H*(DERY(I)+DELT
28740         1*AUX(N+4,I))
28750          GO TO 201
28760    C
28770    C
28780    C H MUST BE HALVED
28790      222 IHLF=IHLF+1
28800          IF(IHLF-10)223,223,210
```

```
C
      223 H=.5*H
          ISTEP=0
C         DO 224 I=1,NDIM
          Y(I)=.2039E625*(80.*AUX(N-1,I)+135.*AUX(N-2,I)+40.*AUX(N-3,I)+
         1AUX(N-4,I))-.1171875*(AUX(N+6,I)-6.*AUX(N+5,I)-AUX(N+4,I))*H
C         AUX(N-4,I)=.2039E625*(12.*AUX(N-1,I)+135.*AUX(N-2,I)+
         1108.*AUX(N-3,I)+AUX(N-4,I))-.234375*(AUX(N+6,I)+18.*AUX(N+5,I)-
         29.*AUX(N+4,I))*H
C         AUX(N-3,I)=AUX(N-2,I)
      224 AUX(N+4,I)=AUX(N+5,I)
          X=X-H
C         DELI=X-(H+H)
          CALL FCT(DELT,Y,DERY,IERROR)
          IF(IERROR.EQ. 1) GO TO 230
C         DO 225 I=1,NDIM
          AUX(N-2,I)=Y(I)
          AUX(N+5,I)=DERY(I)
C     225 Y(I)=AUX(N-4,I)
          DELI=DELT-(H+H)
          CALL FCT(DELT,Y,DERY,IERROR)
C         IF(IERROR.EQ. 1) GO TO 230
          DO 226 I=1,NDIM
          DELI=AUX(N+5,I)*AUX(N+4,I)
C         DELI=DELT+DELT+DELT
          AUX(16,I)=8.962963*(AUX(N-1,I)-Y(I))-3.361111*H*(AUX(N+6,I)+DELI
         1+DERY(I))
C     226 AUX(N+3,I)=DERY(I)
          GO TO 206
C
C ERROR RETURN BECAUSE OF TROUBLES IN SUBROUTINES -FCT- OR -OUTP- .
      230 IHLF=14
          RETURN
C         END
C
C.....
C
          SUBROUTINE RTWI(X,VAL,FCT,XST,EPS,IEND,IER)
C SOLVES THE GENERAL NONLINEAR EQUATION OF THE FORM X=FCT(X) BY MEANS
C OF WEGENSTEIN-S MODIFICATION OF THE SECANT METHOD,
C (TAKEN DIRECTLY FROM THE IBM SCIENTIFIC SUBROUTINES, -RTWI- ),
C
C PREPARE ITERATION
          IER=0
          TOL=XST
          X=FCT(TOL)
          A=X-XST
          B=-A
          TOL=X
          VAL=X-FCT(TOL)
C
C START ITERATION LOOP
          DO 6 I=1,IEND
          IF(VAL)1,7,1
C
C     EQUATION IS NOT SATISFIED BY X
        1 B=B/VAL-1.
          IF(B)2,8,2
C
C ITERATION IS POSSIBLE
        2 A=A/B
```

```
29410           X=X+A
29420           B=VAL
29430           TOL=X
29440           VAL=X-FCT(TOL)
29450     C
29460     C TEST ON SATISFACTORY ACCURACY
29470           TOL=EPS
29480           D=ABS(X)
29490           IF(D-1.)4,4,3
29500         3 TOL=TOL*D
29510         4 IF(ABS(A)-TOL)5,5,6
29520         5 IF(ABS(VAL)-10.*TOL)7,7,6
29530         6 CONTINUE
29540     C END OF ITERATION LOOP
29550     C
29560     C NO CONVERGENCE AFTER IEND ITERATION STEPS, ERROR RETURN.
29570           IER=1
29580         7 RETURN
29590     C
29600     C ERROR RETURN IN CASE OF ZERO DIVISOR
29610         8 IER=2
29620           RETURN
29630           END
29640     1 ENGL,ENGL.
29650     10
29660     1,40,28,967,0,1,540,0,2847,81
29670     1,40,28,967,125,319,1458,00
29680     1,0,4,2350,0,0
29690     26,46875,0,0,60,0
29700     0 ENGL,ENGL.
```

APPENDIX B

DISTRIBUTION LIST FOR FINAL REPORT

Contract NAS7-567

Copies	Recipient	Designee
	Ames Research Center NASA Moffett Field, California 94035	
1	A. S. Hertzog, Director of Procurement	(x)
1	Patents and Contracts Management	(x)
	Jet Propulsion Laboratory 4800 Oak Grove Dr. Pasadena, Calif. 91103	
10	Mr. Hartwell R. Long (Technical Manager)	(x)
3	Chief, Liq. Propulsion Technology RPL Office of Advanced Research and Technology NASA Headquarters Washington, D. C. 20546	(x)
1	Director, Technology Utilization Division Office of Technology Utilization NASA Headquarters Washington, D. C. 20546	(x)
20	NASA Scientific & Technical Info. Facility P. O. Box 33 College Park, Maryland 20740	(x)
1	Director, Launch Vehicles & Propulsion, SV Office of Space Science and Applications NASA Headquarters Washington, D. C. 20546	(x)
1	Director, Advanced Manned Missions, MT Office of Manned Space Flight NASA Headquarters Washington, D. C. 20546	(x)
1	Mission Analysis Division NASA Ames Research Center Moffett Field, California 94035	(x)

Copies	Recipient	Designee
	NASA Field Centers	
2	Ames Research Center Moffett Field, California 94035	Hans M. Mark V. D. Reed
1	Goddard Space Flight Center Greenbelt, Maryland 20771	Merland L. Moseson Code 620
2	Jet Propulsion Laboratory California Institute of Technology 4800 Oak Grove Drive Pasadena, California 91103	Henry Burlage,Jr. Propulsion Div. 38
2	Langley Research Center Langley Station Hampton, Virginia 23365	Ed Cortwright, Director D. J. Carter P. K. Pierpont
2	Lewis Research Center 21000 Brookpark Road Cleveland, Ohio 44135	B. T. Lundin, Director Dr. H. Mark
2	Marshall Space Flight Center Huntsville, Alabama 35812	Hans G. Paul Code R-P+VED V. F. Henson, S&E,AERO-AA
2	Manned Spacecraft Center Houston, Texas 77058	J.G. Thibodaux, Jr. Chief, Prop. + Power Div. B. Redd
2	John F. Kennedy Space Center, NASA Cocoa Beach, Florida 32931	Dr. Kurt H. Debus
	Government Installations	
1	Aeronautical Systems Division Air Force Systems Command Wright-Patterson Air Force Base Dayton, Ohio 45433	D. L. Schmidt Code ASRCNC-2 V. Dahlem, Code FDMG
1	Air Force Missile Development Center Holloman Air Force Base New Mexico 88330	
1	Air Force Missile Test Center Patrick Air Force Base, Florida	L. J. Ullian
1	Space and Missile Systems Organization Air Force Unit Post Office Los Angeles, Calif. 90045	Col. Clark Technical Data Center Lt. J. F. Turk

Copies	Recipient	Designee
1	Arnold Engineering Development Center Arnold Air Force Station Tullahoma, Tennessee 37388	Dr. H. K. Doetsch
1	Bureau of Naval Weapons Department of the Navy Washington, D. C. 20546	J. Kay RTMS-41
1	Defense Documentation Center Hdqrs. Cameron Station, Building 5 5010 Duke Street Alexandria, Virginia 22314 ATTN: TISIA	
1	Headquarters, U.S. Air Force Washington, D. C. 20546	Col. C.K. Stambaugh AFRST
1	Picatinny Arsenal Dover, New Jersey 07801	I. Forsten, Chief Liq. Propulsion Lab.
2	Air Force Rocket Propulsion Lab. Research and Technology Division Air Force Systems Command Edwards, California 93523	RPRPD/Mr. H. Main Dr. L. Quinn C. H. Allen
1	U. S. Army Missile Command Redstone Arsenal Alabama 35809	Mr. Walter Wharton Dr. S.P.D. Smith
1	U. S. Naval Ordnance Test Station China Lake California 93557	Code 4562 Chief, Missile Propulsion Div.
	CPIA	
1	Chemical Propulsion Information Agency Applied Physics Laboratory 8621 Georgia Avenue Silver Spring, Maryland 20910	Tom Reedy T. M. Gilliland
	Industry Contractors	
1	Aerojet-General Corporation P. O. Box 296 Azusa, California 91703	W. L. Rogers
1	Aerojet-Liquid Rocket Company P. O. Box 13222 Technical Library, Bldg, 2015, Dept.2410 Sacramento, Calif. 95813	R. Stiff Dr. V. H. Ransom

Copies	Recipient	Designee
1	Space Division Aerojet-General Corporation 9200 East Flair Dr. El Monte, California 91734	S. Machlawski
1	Aerospace Corporation 2400 East El Segundo Boulevard P. O. Box 95085 Los Angeles, Calif. 90045	John G. Wilder MS-2293
1	Atlantic Research Corporation Edsall Road and Shirley Highway Alexandria, Virginia 22314	Dr. Ray Friedman
1	AVCO Systems Division Wilmington, Massachusetts	Howard B. Winkler
1	Beech Aircraft Corporation Boulder Division Box 631 Boulder, Colorado	J. H. Rodgers
1	Bell Aerosystems Company P. O. Box 1 Buffalo, N. Y. 14240	W. M. Smith
1	BELLCOMM 955 L-Enfant Plaza, S. W. Washington, D. C.	H. S. London
1	Bendix Systems Division Bendix Corporation 3300 Plymouth Road Ann Arbor, Michigan 48105	John M. Brueger
1	Boeing Company P. O. Box 3999 Seattle, Washington 98124	J. D. Alexander E. D. Simon
1	Boeing Company 1625 K Street N. W. Washington, D. C. 20006	Library
1	Boeing Company P. O. Box 1680 Huntsville, Alabama 35801	Ted Snow
1	Missile Division Chrysler Corporation P. O. Box 2628 Detroit, Michigan 48231	Mr. John Gates

Copies	Recipient	Designee
1	Wright Aeronautical Division Curtiss-Wright Corporation Wood-Ridge, New Jersey 07075	G. Kelley
1	Research Center Fairchild Hiller Corporation Germantown, Maryland	Ralph Hall
1	Republic Aviation Corporation Fairchild Hiller Corporation Farmingdale, Long Island, N. Y.	Library
1	General Dynamics, Convair Division Library + Info. Services (128-00) P. O. Box 1128 San Diego, Calif. 92112	Library
1	Missile and Space Systems Center General Electric Company Valley Forge Space Technology Center P. O. Box 8555 Philadelphia, Pa.	F. Mezger F. E. Schultz J. R. Rausch
1	Grumman Aircraft Engineering Corp. Bethpage, Long Island New York 11714	Joseph Gavin R. Haslet
1	Honeywell, Inc. Aerospace Division 2600 Ridgway Rd. Minneapolis, Minn.	Mr. Gordon Harms
1	Hughes Aircraft Co. Aerospace Group Centinela and Teale Streets Culver City, Calif. 90230	E. H. Meier V. P. and Div. Mgr., Research + Dev. Div.
1	Walter Kidde and Company, Inc. Aerospace Operations 567 Main Street Belleville, New Jersey	R. J. Hanville Dir. of Research Engr.
1	Ling-Temco-Vought Corporation P. O. Box 5907 Dallas, Texas 75222	Library
1	Arthur D. Little, Inc. 20 Acorn Park Cambridge, Mass. 02140	Library
1	Lockheed Missiles and Space Co. Attn-Technical Information Center P. O. Box 504 Sunnyvale, Calif. 94088	J. Guill C. F. Ehrlich

Copies	Recipient	Designee
1	Lockheed Propulsion Company P. O. Box 111 Redlands, Calif. 92374	Library
1	The Marquardt Corporation 16555 Saticoy Street Van Nuys, Calif. 91409	R. C. Stechman
1	Baltimore Division Martin Marietta Corporation Baltimore, Maryland 21203	Mr. J. Calathes (3214)
1	Denver Division Martin Marietta Corporation P. O. Box 179 Denver, Colorado 80201	Dr. Morganthaler A. J. Kullas L. E. Fidler
1	Orlando Division Martin Marietta Corporation Box 5837 Orlando, Florida	J. Ferm
1	Astropower Laboratory Mc Donnell-Douglas Aircraft Company 2121 Paularimo Newport Beach, Calif. 92663	Dr. George Moc Director, Research
1	Mc Donnel-Douglas Aircraft Corp. P. O. Box 516 Municipal Airport St. Louis, Missouri 63166	R. A. Herzmark
1	Mc Donnell-Douglas Astronautics Co. 5301 Bolsa Avenue Huntington Beach, Calif. 92647	J. L. Waisman
1	Missile and Space Systems Division Mc Donnell-Douglas Aircraft Company 3000 Ocean Park Boulevard Santa Monica, Calif 90406	Mr. R. W. Hallet Chief Engineer Adv. Space Tech.
1	Space + Information Systems Division North American Rockwell 12214 Lakewood Boulevard Downey, California 90241	F. G. Etheridge
1	Rocketdyne (Library 586-306) 6633 Canoga Avenue Canoga Park, Calif. 91304	Dr. R. J. Thompson S. F. Iacobellis J. C. Hyde

Copies	Recipient	Designee
1	Northrop Space Laboratories 3401 West Broadway Howthorne, Calif. 90250	Dr. William Howard
1	Aeronautronic Division Philco Corporation Ford Road Newport Beach, Calif. 92663	Library
1	Astro-Electronics Division Radio Corporation of America Princeton, New Jersey 08540	Y. Brill
1	Rocket Research Corporation York Center Redmond, Washington 98052	Foy McCullough, Jr. T. A. Groudle
1	Scientific Service Bureau, Inc. P. O. Box 375 Morrisplains, New Jersey 07950	T. F. Seamans
1	Sunstrand Aviation 4747 Harrison Avenue Rockford, Illinois 61101	R. W. Reynolds
1	Stanford Research Institute 333 Ravenswood Avenue Menlo Park, Calif. 94025	Dr. Gerald Marksman
1	TRW Systems Group TRW Incorporated One Space Park Redondo Park, Calif. 90278	G. W. Elverum S. S. Cherry
1	Tapco Division TRW, Incorporated 23555 Euclid Avenue Cleveland, Ohio 44117	P. T. Angell
1	Thiokol Chemical Corp. Aerospace Services Elkton Division Bristol, Pennsylvania	Library
1	Thiokol Chemical Corp. Huntsville Division Huntsville, Alabama 35807	John Goodloe

Copies	Recipient	Designee
1	Research Laboratories United Aircraft Corp. 400 Main Street East Hartford, Conn. 06108	Erle Martin
1	Hamilton Standard Division United Aircraft Corp. Windsor Locks, Conn. 06096	Mr. R. Hatch
1	United Technology Center 587 Methilda Avenue P. O. Box 358 Sunnyvale, Calif. 94088	Dr. David Altman
1	Florida Research and Development Pratt and Whitney Aircraft United Aircraft Corporation P. O. Box 2691 West Palm Beach, Florida 33402	R. J. Coar L. E. Ruby
1	Vickers, Inc. Box 302 Troy, Michigan	
1	Sandia Corporation P. O. Box 5000 Albuquerque, New Mexico	Dr. J. K. Cole
1	AVCO Corporation AVCO Space Systems Div. Lowell Industrial Park Lowell, Mass. 01851	Dr. B. L. Reeves
1	Consolidated Eng. Technology Corp. 188 Whisman Road Mountain View, Calif. 94040	Dr. R. Anderson
1	G.V.R. Rao and Associates 14827 Ventura Boulevard Sherman Oaks, Calif. 91403	G. V. R. Rao
1	Lockheed Missiles and Space Co. Huntsville Research and Eng. Center 4800 Bradford Drive Huntsville, Alabama	J. W. Benefield R. J. Prozan
1	Cornell Aeronautical Laboratory, Inc. Buffalo, New York 14221	Dr. J. G. Hall K. Hendershot